Giuseppe Querques
Eric H. Souied
Editors

Macular Dystrophies

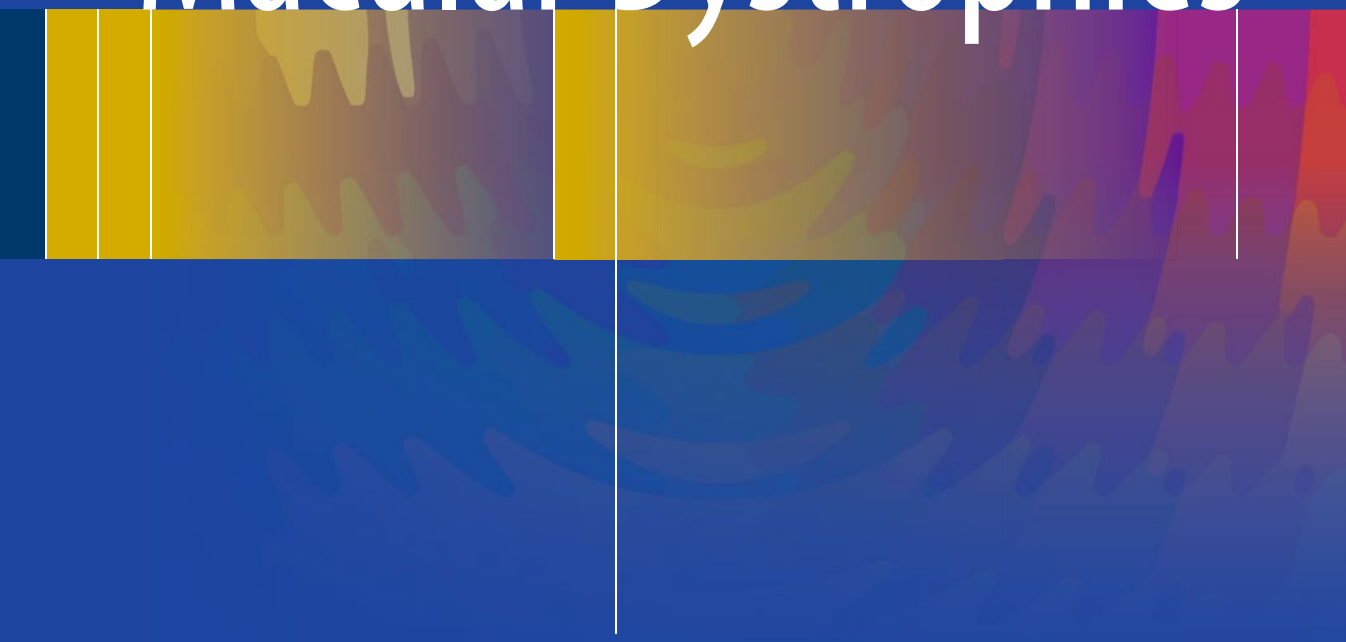

Springer

Macular Dystrophies

Giuseppe Querques • Eric H. Souied
Editors

Macular Dystrophies

Springer

Editors
Giuseppe Querques
University Paris Est Créteil
Créteil
France

Eric H. Souied
Ophthalmology
University Paris Est Créteil
Créteil
France

ISBN 978-3-319-26619-0 ISBN 978-3-319-26621-3 (eBook)
DOI 10.1007/978-3-319-26621-3

Library of Congress Control Number: 2016931372

Springer Cham Heidelberg New York Dordrecht London

Printed on acid-free paper

Springer International Publishing AG Switzerland is part of Springer Science+Business Media (www.springer.com)

Editors' Brief Bios

Giuseppe Querques, MD, PhD, is an associate professor at the University Vita-Salute San Raffaele in Milan, Italy. He earned his medical degree from the University of Bari and completed his ophthalmology residency at the University of Foggia, Italy. During his ophthalmology residency, Dr. Querques completed a medical fellowship at Retina Associates of New Jersey, USA; at Creteil Eye Clinic, University of Paris XII, France; and at Inselspital Eye Clinic, University of Bern, Switzerland. He obtained his doctoral degree from the University of Foggia and completed a postdoctoral fellowship at Creteil Eye Clinic. Dr. Querques's main interests are medical retina (age-related macular degeneration, retinal vascular diseases, and inherited macular and retinal dystrophies) and ophthalmic surgery (retina and cataract).

Dr. Querques has contributed to more than 200 peer-reviewed articles, and his current main areas of both clinical and laboratory researches are the diagnosis (imaging) and treatment of age-related macular degeneration, retinal vascular diseases, and hereditary retinal diseases.

Eric H. Souied, MD, PhD, is the head of the Department of Ophthalmology at Centre Hospitalier Intercommunal de Creteil, University Paris Est Creteil, and L'hôpital Henri Mondor, Creteil, France. He earned his medical and doctoral degrees at the University of Paris Est Creteil, where he also completed his ophthalmology residency with Professor Gabriel Coscas. He completed a medical fellowship at the Creteil University Eye Clinic and a postdoctoral fellowship at the Jules Stein Eye Institute, University of California, Los Angeles (UCLA), USA. His main topics are medical retina (age-related macular degeneration, inherited macular and retinal dystrophies) and ophthalmic surgery (retina and cataract).

Professor Souied has contributed to more than 200 peer-reviewed articles published in the areas of age-related macular degeneration, hereditary retinal diseases, ophthalmic genetics, and gene therapy of retinal dystrophies. He is a member of the Macula Society, the Club Jules Gonin, the American Academy of Ophthalmology, and the Association for Research in Vision and Ophthalmology. He was the founder and president of the association DMLA, La Dégénérescence Maculaire Liée à l'Age, and is the founder and president of La Fédération France Macula, which held its first congress, MaculArt, in Paris in June 2015.

Preface

Macular dystrophy defines many different inherited or sporadic rare eye conditions, linked by a problem with photoreceptors or other structures of the central retina. Macular dystrophies may have early or late onset and may be stationary or progressive. Basic scientists, guided by clinical research retinal specialists, have developed meaningful imaging modalities that have led to a better understanding of known macular dystrophies, as well as clinically distinct entities, and their management.

This book collects chapters authored by internationally recognized experts in the field of macular dystrophies. The authors bring latest evidences together with their personal experience and full teaching acumen to each chapter, culminating in a book on current management, new diagnostic techniques, and experimental therapies for principal macular dystrophies.

As a multiauthored text, there are multiple literary styles; for this reason, the editors have worked to provide a level of conformity without sacrificing the originality of the individual authors. Chapter topics range from molecular biology to state-of-the-art diagnostic techniques and newest treatment options.

In summary, this book provides the ophthalmologist with most recent data on macular dystrophies and experimental approach, while also including the multiple areas still debated.

Creteil, France — Giuseppe Querques
Milan, Italy
Creteil, France — Eric Haim Souied

Contents

1 Best Vitelliform Macular Dystrophy 1
Jennyfer Zerbib, Eric H. Souied, and Giuseppe Querques

2 The Pattern Dystrophies 11
Itay Chowers and Camiel J.F. Boon

3 Stargardt Disease 25
Carel B. Hoyng, Stanley Lambertus, and Nathalie M. Bax

4 Macular Changes in Generalized Retinal Dystrophies and in Cone Dystrophies 31
Carel B. Hoyng and Ramon A.C. van Huet

5 Malattia Leventinese (Autosomal Dominant Drusen) 39
Veronika Vaclavik and Francis L. Munier

6 North Carolina Macular Dystrophy and North Carolina Macular Dystrophy-Like Disorders 53
Michel Michaelides and Anthony Moore

7 Sorsby Fundus Dystrophy 59
Michel Michaelides and Anthony Moore

8 Mitochondrial Retinal Dystrophy Associated with the (m.3243A>G) Mutation 63
Camiel J.F. Boon and Pascale Massin

9 X-Linked Retinoschisis 71
Isabelle Audo, José-Alain Sahel, Saddek Mohand-Saïd, Graham Holder, and Anthony Moore

10 Miscellaneous Rare Macular Dystrophies 83
M. Dominik Fischer and Camiel J.F. Boon

11 Macular Dystrophies: Management and Interventions 101
Katia Marazova and José-Alain Sahel

Index 117

Contributors

Editors

Giuseppe Querques, MD, PhD Department of Ophthalmology, Centre Hospitalier Intercommunal de Creteil, University Paris Est Creteil, Creteil, France

Department of Ophthalmology, IRCCS San Raffaele Scientific Institute, University Vita-Salute San Raffaele, Milan, Italy

Eric H. Souied, MD, PhD Department of Ophthalmology, Centre Hospitalier Intercommunal de Creteil, University Paris Est Creteil, Creteil, France

Authors

Isabelle Audo, MD, PhD Département de génétique, Institut de la Vision, Paris, France

Institut de la Vision, Sorbonne Universités, UPMC University Paris 06, UMR_S 968, Paris, France

Centre Hospitalier National d'Ophtalmologie des Quinze-Vingts, DHU View Maintain, INSERM-DHOS CIC 1423, Paris, France

INSERM, U968, Paris, France

CNRS, UMR_7210, Paris, France

University College of London Institute of Ophthalmology, London, UK

Nathalie M. Bax, MD Department of Ophthalmology, Radboud University Medical Center, Nijmegen, Netherlands

Camiel J.F. Boon, MD, PhD, FEB Ophth Department of Ophthalmology, Leiden University Medical Center, Leiden, The Netherlands

Itay Chowers, MD Department of Ophthalmology, Hadassah-Hebrew University Medical Center, Jerusalem, Israel

M. Dominik Fischer, MD, FEBO Department of Ophthalmology, Centre for Ophthalmology Tubingen, University Eye Hospital Tubingen, Tubingen, Germany

Graham Holder, PhD Moorfields Eye Hospital, University College London Institute of Ophthalmology, London, UK

Carel B. Hoyng, MD, PhD Department of Ophthalmology, Radboud University Medical Center, Nijmegen, The Netherlands

Stanley Lambertus, MD Department of Ophthalmology, Radboud University Medical Center, Nijmegen, The Netherlands

Katia Marazova, PhD Institut de la Vision, Sorbonne Universités, UPMC University Paris 06, CNRS UMR_7210, Paris, France

Pascale Massin, MD, PhD Department of Ophthalmology, Lariboisière Hospital, Paris, France

Michel Michaelides, BSc, MBBS, MD, FRC Ophth, FACS Departments of Inherited Eye Disease, Medical Retina, and Paediatric Ophthalmology, Moorfields Eye Hospital, London, UK

Department of Genetics, UCL Institute of Ophthalmology, London, UK

Saddek Mohand-Saïd, MD, PhD Institut de la Vision, Sorbonne Universités, UPMC University Paris 06, UMR_S 968, Paris, France

Centre Hospitalier National d'Ophtalmologie des Quinze-Vingts, DHU View Maintain, INSERM-DHOS CIC 1423, Paris, France

INSERM, U968, Paris, France

CNRS, UMR_7210, Paris, France

Anthony Moore, MA, FRCS, FRC Ophth, FMed, Sci Department of Ophthalmology, University of California School of Medicine, San Francisco, California

Francis L. Munier, MD Retinoblastoma and Oculogenetic Units, Department of Ophthalmology, Jules-Gonin Eye Hospital, University of Lausanne, Lausanne, Switzerland

José-Alain Sahel, MD Institut de la Vision, Sorbonne Universités, UPMC University Paris 06, CNRS UMR_7210, Paris, France

Centre Hospitalier National d'Ophtalmologie des Quinze-Vingts, DHU Sight Again, INSERM-DHOS CIC 1423, Paris, France

Veronika Vaclavik, MD Oculogenetic Unit, Jules-Gonin Eye Hospital, Unviersity of Lausanne, Lausanne, Switzerland

Medical Retina, Hospital Cantonal Fribourg, Fribourg, Switzerland

Ramon A.C. van Huet, MD Department of Ophthalmology, Radboud University Medical Center, Nijmegen, The Netherlands

Jennyfer Zerbib, MD Department of Ophthalmology, Centre Hospitalier Intercommunal de Creteil, University Paris Est Creteil, Creteil, France

Best Vitelliform Macular Dystrophy

1

Jennyfer Zerbib, Eric H. Souied, and Giuseppe Querques

Abstract

Best vitelliform macular dystrophy (Best VMD) also called Best disease is a clinically heterogeneous and pleomorphic disease, in most cases showing an autosomal dominant pattern of inheritance with extremely variable penetrance and expressivity. In most cases, patients harbour heterozygous mutation in *BEST1* gene, coding for a protein acting as a Ca^{2+}-activated Cl^- channel. In most cases the disease begins in the first decade of life. Five stages based on fundus examination have been described: each stage is also characterized by typical spectral-domain optical coherence tomography (SD-OCT) and fundus autofluorescence (FAF) signs. *BEST1* gene is also related to other diseases, called bestrophinopathies.

Keywords

Best disease • Choroidal neovascularization • Dystrophy • Macula • Vitelliform

1.1 Introduction

Vitelliform macular dystrophy (VMD; OMIM #153700), also called Best disease [1], is a clinically heterogeneous and pleomorphic disease, in most cases showing an autosomal dominant pattern of inheritance with extremely variable penetrance and expressivity. Best VMD has often an early-onset characterized by large deposits of lipofuscin-like material in the subretinal space, which creates characteristic macular lesions resembling the yolk of an egg (‘vitelliform’).

J. Zerbib, MD • E.H. Souied, MD, PhD
Department of Ophthalmology, Centre Hospitalier Intercommunal de Creteil, University Paris Est Creteil, Creteil, France

G. Querques, MD, PhD (✉)
Department of Ophthalmology, Centre Hospitalier Intercommunal de Creteil, University Paris Est Creteil, Creteil, France

Department of Ophthalmology, IRCCS San Raffaele Scientific Institute, University Vita-Salute San Raffaele, Milan, Italy
e-mail: giuseppe.querques@hotmail.it

G. Querques, E.H. Souied (eds.), *Macular Dystrophies*, DOI 10.1007/978-3-319-26621-3_1

1.2 Genetics

BEST1 (chromosome 11q12–q13) [2], is the gene mainly involved in Best VMD cases, which encodes a 68 kDa protein called bestrophin-1 [3] that is localized to the basolateral plasma membrane of the retinal pigment epithelium (RPE) and appears to exhibit properties of Ca -activated Cl channels [4]. In Best VMD, linked to the *BEST1* gene, individuals harbour in most cases an heterozygous mutation. More than 100 different *BEST1* mutations have been reported, mainly missense mutations [5]. Several diseases have been linked to mutations in the *BEST1* gene, including autosomal recessive VMD, autosomal recessive bestrophinopathy, adult-onset foveomacular vitelliform dystrophy, autosomal dominant vitreoretinochoroidopathy, and retinitis pigmentosa [6–12]. *BEST1* gene mutations do not explain all Best VMD cases. Another gene has also been implicated recently in typical Best VMD, the *IMPG1* gene [13].

1.3 Clinical Description

Best VMD has a bimodal onset distribution with one maximum peak before puberty and a second following puberty and extending through the fifth decade of life [14, 15]. Prior to the identification of the *BEST1* gene, a diagnosis of Best VMD was based on the presence of a clinically identifiable fundus lesion, family history of the disease, and a decreased electrooculogram (EOG) Arden ratio (light peak/dark trough) with an otherwise normal clinical electroretinogram (ERG) [16, 17].

1.4 Fundus Findings

Five progressive stages can be defined on the basis of fundus examination. These stages do not always occur consecutively nor do they occur inevitably in all patients [5, 18]. The previtelliform stage represents the first stage and is characterized by absence of symptoms and normal macula or subtle RPE alterations [19, 20]. However, small signs on SD-OCT or EOG can be detected. On SD-OCT a thicker and more reflective appearance of the layer between the RPE and the ellipsoid zone (EZ) (formerly known as the interface of inner segments [IS] and outer segments [OS] of the photoreceptors), namely, the interdigitation zone (also known as the Verhoeff membrane), could be observed [20–22]. On electrooculogram, a reduced light peak/dark trough can be detected [22].

The second stage of Best VMD, the vitelliform stage, is characterized by a well-circumscribed 0.5- to 2-disc-diameter "egg-yolk" lesion within the macula and by variable symptoms including metamorphopsia, blurred vision, and a decrease of central vision [19, 20]. The third stage is characterized by the yellow material that accumulates inferiorly (the pseudohypopyon stage) and is followed by partial reabsorption of the material (scrambled-egg lesion) in the vitelliruptive fourth stage and by final macular atrophy or fibrosis development in the atrophic/fibrotic fifth stage [19, 20].

Unilateral lesion, or multifocal vitelliform macular dystrophy associated to mutation in the *BEST1* gene, has been reported [23, 24].

1.5 Fundus Autofluorescence (FAF)

Macular autofluorescence may originate from lipofuscin accumulation in the RPE but also from debris (unphagocytosed photoreceptor OS) and lipofuscin accumulation in the subretinal space [25].

The yellowish subretinal material, as seen during the vitelliform stage, is intensely hyperautofluorescent (Fig. 1.1) [18]. More advanced lesions show loss of autofluorescence, particularly in the upper part of the lesion in the pseudohypopyon stage and centrally with an increased amount of the autofluorescence at the outer border of the lesion in the vitelliruptive stage.

1.6 Fluorescein and Indocyanine Angiography

The yellowish material in the vitelliform and the pseudohypopyon stages causes blocking effect on fluorescein angiography. Fluorescein

angiography also shows hyperfluorescence in the early phase due to transmission defects linked to RPE and chorioretinal atrophy and on the late phase due to material staining.

Indocyanine green angiography can be helpful when choroidal neovascularization is suspected because neovascularization is often difficult to identify on fluorescein angiography. In addition, indocyanine green angiography may show hyperfluorescent spots in the peripheral retina that are not seen on fundus examination and fluorescein angiography [26].

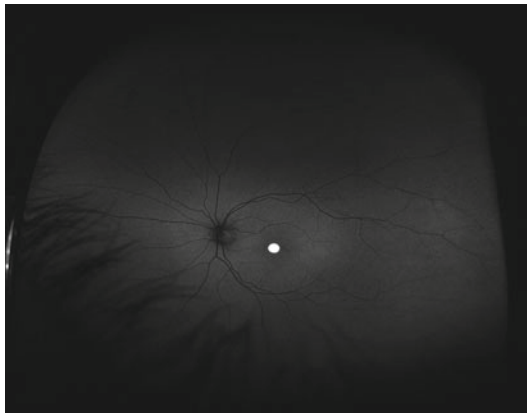

Fig. 1.1 Fundus autofluorescence using ultra-wide-field imaging in a patient with vitelliform stage. The lesion is intensively hyperautofluorecent

1.7 Optical Coherence Tomography

With the advent of optical coherence tomography (OCT), it has been possible to anatomically investigate, in vivo, the vitelliform lesions. Spectral-domain (SD) OCT findings have been reported in all of the progressive stages of the disease, including the previtelliform stage [20], and proposed that early changes in Best VMD may involve the layer between the RPE and the EZ, first with accumulation of material beneath the sensory retina and then with disruption. The RPE is also affected in the disease course, with hypertrophy, disruption, and attenuation [20].

The previtelliform stage can show a thicker and more reflective appearance of the interdigitation zone (the layer between the RPE and EZ) (Figs. 1.2 and 1.3) [18, 20]. Vitelliform lesions are highly reflective, located between the EZ and the RPE (Figs. 1.3 and 1.4) [18, 20]. Pseudohypopyon lesions are characterized by two different zones: in the upper part of the lesion, the SD-OCT scans show an hyporeflectivity located between the RPE and the EZ, with clumping of hyperreflective material on the posterior retinal surface; in the lower part of the lesion, where the material is still visible, the SD-OCT scan shows the yellowish material that, similarly to the typical vitelliform lesion, appears

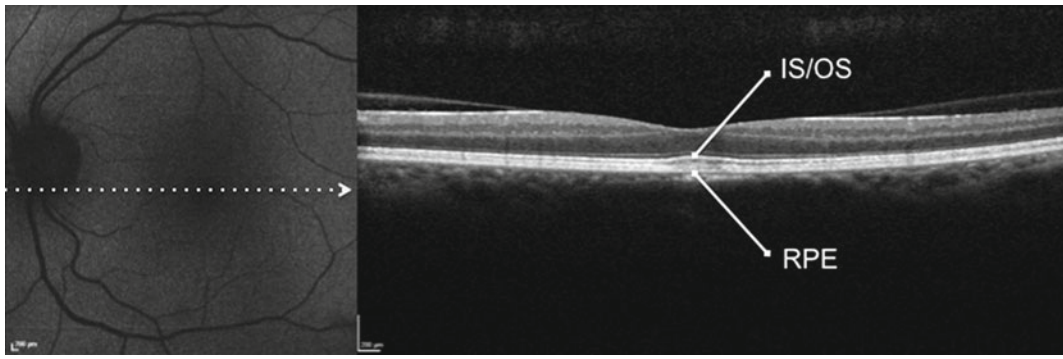

Fig. 1.2 Blue fundus autofluorescence (FAF) and spectral-domain optical coherence tomography (SD-OCT) from a patient affected with previtelliform lesion. Blue FAF frame shows no increased macular autofluorescence. SD-OCT scans show a slight thickening of the hyperreflective band located between the hyperreflective photoreceptor inner segment (IS) ellipsoid portion (ellipsoid zone, *EZ*) and the hyperreflective retinal pigment epithelium (*RPE*)/Bruch's membrane complex (Adapted from Querques et al. [18] with the kind permission of *Molecular Vision,* Department of Ophthalmology, Emory University)

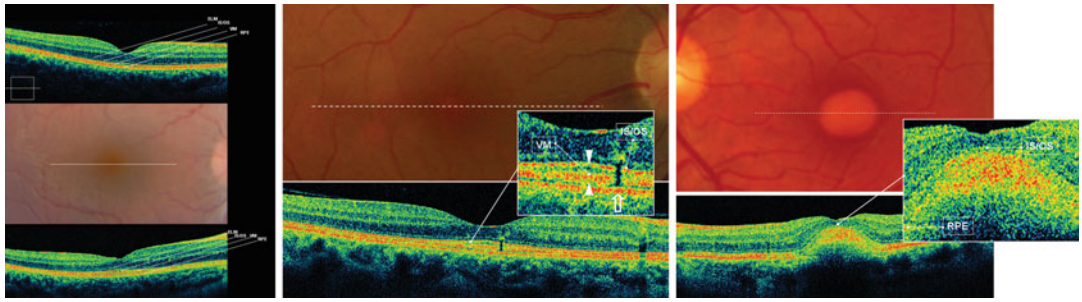

Fig. 1.3 Spectral-domain optical coherence tomography (SD-OCT) images from a normal subject, a patient with the previtelliform stage, and a patient with the vitelliform stage of vitelliform macular dystrophy. (*Top left*) SD-OCT scan of normal macula. Colour fundus photographs of the right eye of two patients (*middle left)* Case 1 and (*top middle*) Case 2 showing no major alterations except for foveal granularity. SD-OCT scans from (*bottom left*) Case 1 and (*bottom middle*) Case 2 showing a thicker and more reflective appearance of the interdigitation zone/Verhoeff membrane [*VM*] (enlarged view, *arrowheads*) in the central region compared with the normal human macula. (*Bottom left*) Normal appearance of all major intraretinal layers for Case 1. (*Bottom middle*) Focal disruption of ellipsoid zone and VM (*open arrow*) for Case 2. (*Top right*) Colour fundus photograph of the left eye macula of a third patient showing the typical well-circumscribed yellow lesion, which looks like the yolk of an egg. (*Bottom right*) SD-OCT scan showing a highly reflective area, located between the hyporeflective outer nuclear layer and the hyperreflective retinal pigment epithelium (*RPE*) layer. Focal disruption of the ellipsoid zone/interface of inner segment – outer segment (*IS/OS*) over the lesion and an almost normal appearance of all major intraretinal layers can be detected, although the macular retina is raised by the material, resulting in the partial disappearance of the foveal depression (enlarged view). *ELM* external limiting membrane (From Querques et al. [20], with the kind permission of Elsevier)

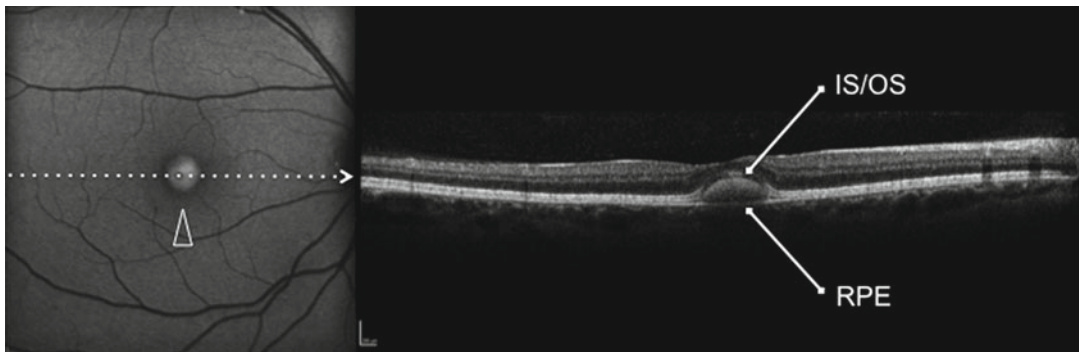

Fig. 1.4 Blue fundus autofluorescence (FAF) and spectral-domain optical coherence tomography (SD-OCT) from a patient affected with vitelliform lesion. Blue FAF frames show a highly autofluorescent macular lesion (*left panel, arrowhead*). SD-OCT scans show a hyperreflective dome-shaped lesion located in the subretinal space, between the hyperreflective photoreceptor inner segment (IS) ellipsoid portion (ellipsoid zone, *EZ*) and the hyperreflective retinal pigment epithelium (RPE)/Bruch's membrane complex (*right panel*) (Adapted from Querques et al. [18] with the kind permission of *Molecular Vision,* Department of Ophthalmology, Emory University)

as a highly reflective area located in the subretinal space (Figs. 1.5 and 1.6) [18, 20]. Vitelliruptive lesions are characterized by an optically empty lesion between the RPE and the EZ, with clumping of hyperreflective material on the posterior retinal surface (similar to the upper part of the pseudohypopyon) (Fig. 1.7) [20]. Furthermore, on some parts, the OCT scan may reveal hyperreflective mottling on the RPE layer (see Fig. 1.7), probably representing areas of focal hypertrophy. Atrophic lesions are characterized by thinning of all the retinal layers and diffuse loss of the EZ within the macular area, with enhanced RPE reflectivity (Fig. 1.8) [20]. Fibrotic lesions are

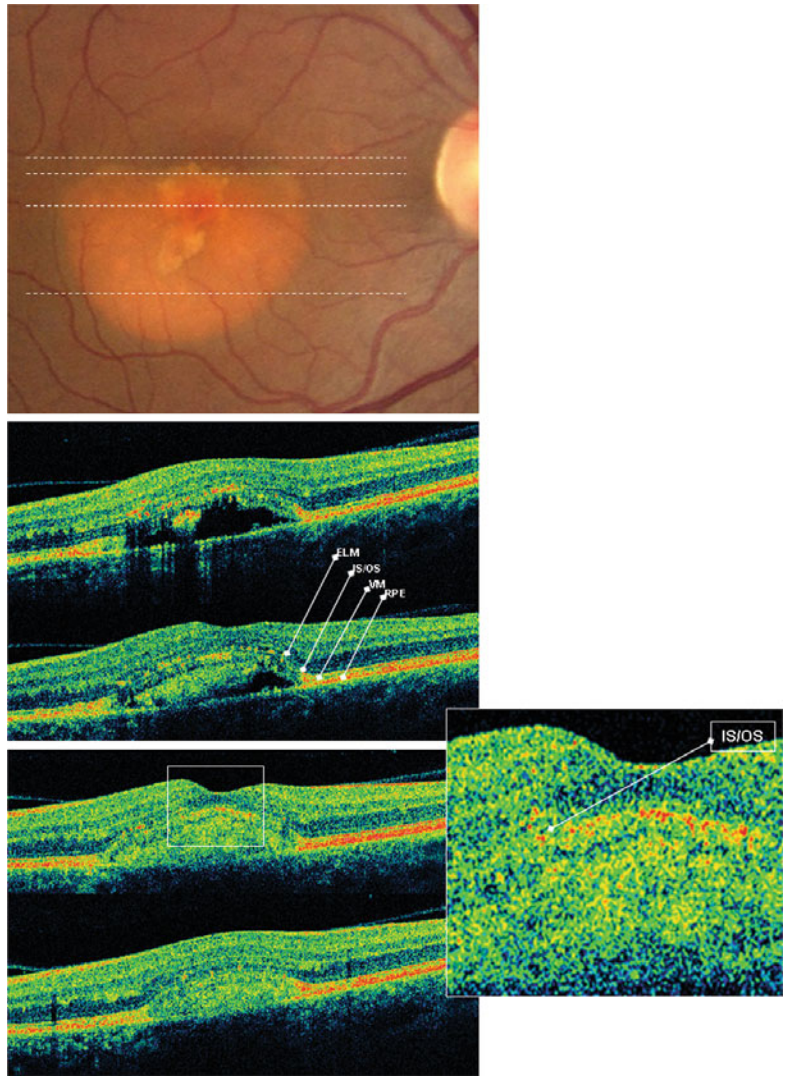

Fig. 1.5 Spectral-domain optical coherence tomography (SD-OCT) scans of a pseudohypopyon-stage vitelliform macular dystrophy patient. Colour fundus photograph (*top*) of the right eye of a patient showing the yellow material that accumulates inferiorly to form a pseudohypopyon appearance, characterized by two different zones (*upper* and *lower*). (*Middle*) In the upper part of the lesion, SD-OCT scans show a hyporeflective zone with clumping of hyperreflective material on the posterior retinal surface, located between the RPE and the ellipsoid zone/the interface of inner segment – outer segment (*IS/OS*) of the photoreceptors (corresponding to the interdigitation zone/VM). *(Bottom*) In the lower part of the lesion, where the material is still visible, the SD-OCT scans show the yellowish material that appears as a highly reflective area located between the hyporeflective outer nuclear layer and the hyperreflective RPE layer, consistent with the vitelliform lesion. A focal disruption of the ellipsoid zone (i.e. the IS/OS) over the lesion (enlarged view), and an almost normal appearance of all major intraretinal layers can be detected in both the upper and the lower part of the lesion (From Querques et al. [20], with the kind permission of Elsevier)

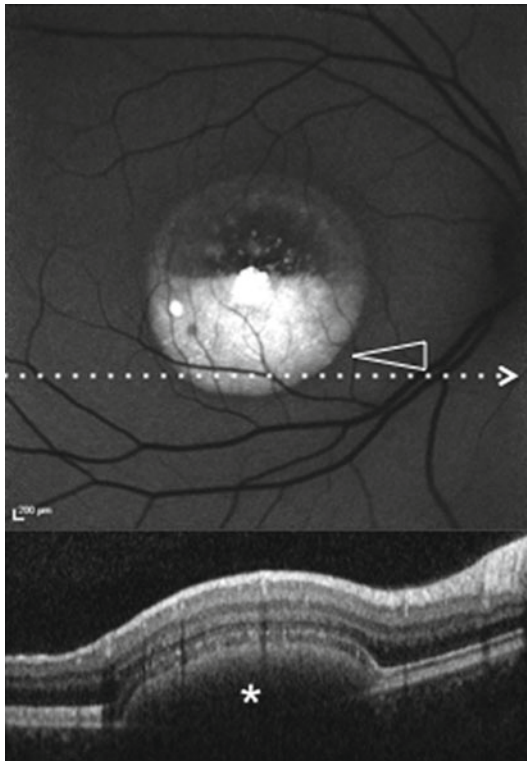

Fig. 1.6 Blue fundus autofluorescence (FAF) and spectral-domain optical coherence tomography (SD-OCT) from a patient affected with pseudohypopyon lesion. Blue FAF frame and SD-OCT scan (*top* and *bottom panels, respectively*) show a partial reabsorption of the hyperautofluorescent (*arrowhead*)/hyperreflective material (*asterisk*) and replacement by a fluid component (Adapted from Querques et al. [18] with the kind permission of *Molecular Vision,* Department of Ophthalmology, Emory University)

characterized by a prominent, highly hyperreflective thickening at RPE level often associated to hyporeflective spaces part above the hyperreflective lesion (see Fig. 1.8).

1.8 Multimodal Imaging

Blue FAF and SD-OCT represent noninvasive imaging techniques to monitor Best VMD [5, 18]. The previtelliform lesions are characterized on blue FAF by absence or only slight autofluorescence and on SD-OCT by a slight thickening of the hyperreflective band located between the RPE and EZ (the interdigitation zone). The vitelliform lesion is characterized on blue FAF by a well-circumscribed high autofluorescence within the macula and on SD-OCT by a dome-shaped hyperreflectivity located in the subretinal space. Pseudohypopyon lesions are characterized on blue FAF by a well-circumscribed high autofluorescence within the inferior macula and on SD-OCT by a hyperreflectivity located in the inferior-macula subretinal space; the partial reabsorption of the hyperautofluorescent (FAF) and hyperreflective (SD-OCT) material is replaced by a fluid component, showing no increased fluorescence on FAF or reflectivity on SD-OCT examination and sedimentation of residual material according to the laws of gravity (the hyperautofluorescent [FAF] and hyperreflective [SD-OCT] material located in the inferior macula). Vitelliruptive lesions are characterized by no increased autofluorescence and reflectivity on blue FAF and SD-OCT; however, some residual dispersed autofluorescent material, and clumping of hyperreflective material on the posterior retinal surface, may be detected on FAF and SD-OCT, respectively. Atrophic lesions appear with a decreased autofluorescence on blue FAF and by diffuse loss of photoreceptor and other sensory retina layers on SD-OCT. Fibrotic lesions are characterized by inhomogeneous areas of absolute hypoautofluorescence mixed with hyperautofluorescence (due to some residual dispersed autofluorescent material) on blue FAF and by a prominent, highly hyperreflective thickening at the RPE level.

1.9 Electrophysiology

In Best VMD, a decreased to absent light rise on the EOG is typically observed [27]. However, several studies indicate that the EOG can be sometimes normal in *BEST1* mutation carriers [28]. An Arden ratio (light peak/dark trough) of 1.5 or lower is typically the threshold for diagnosis

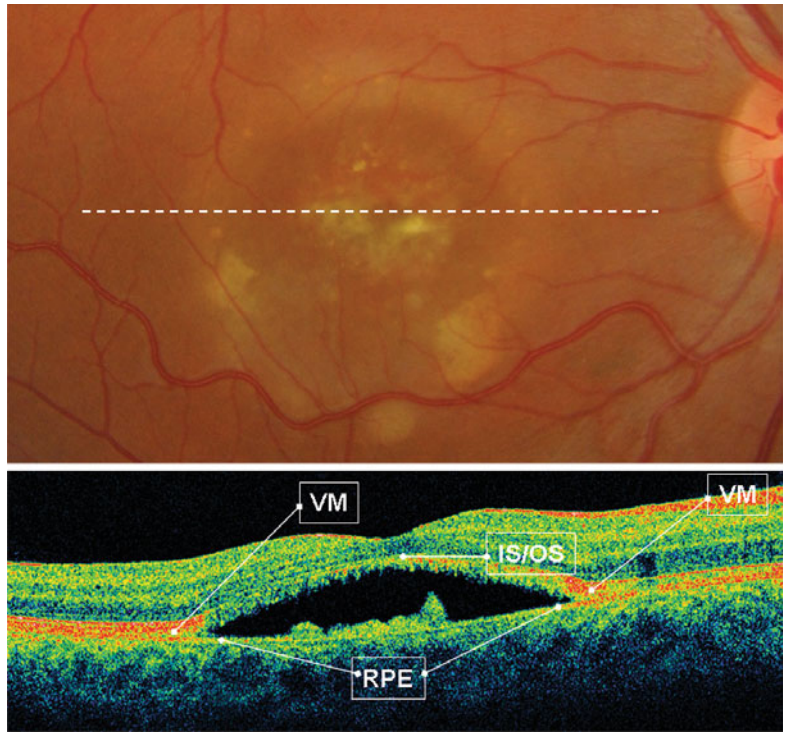

Fig. 1.7 Spectral-domain optical coherence tomography (SD-OCT) scans obtained from a vitelliruptive stage vitelliform macular dystrophy patient. (*Top*) Colour fundus photograph of the right eye of a patient showing the vitelliruptive lesion characterized by a scrambled-egg appearance with dispersion of the vitelliform material without any signs of atrophy or fibrosis. (*Bottom*) SD-OCT scan showing an optically empty lesion between the RPE and the photoreceptor ellipsoid zone (i.e. the IS/OS), comparable with the upper part of the pseudohypopyon, with clumping of hyperreflective material on the posterior retinal surface. In some parts, the SD-OCT scan reveals hyperreflective mottling on the RPE layer. Focal disruption of the ellipsoid zone (i.e. the IS/OS) over the lesion and almost normal appearance of all major intraretinal layers can be observed (From Querques et al. [20], with the kind permission of Elsevier)

of Best VMD [29, 30], though there have been several cases with Arden ratios >1.5 reported [31, 32]. The low Arden ratio helps differentiating Best VMD from all other bestrophinopathies, other diseases that may present with an apparent vitelliform lesion and all other inherited maculopathies.

Photopic and scotopic full-field ERG is generally normal in Best VMD patients, although the 30 Hz flicker and dark-adapted ERG may be abnormal, particularly in the advanced stages of the disease. The multifocal ERG is abnormal in the majority of Best VMD patients.

1.10 Progression

With respect to the functional aspects of the disease, Best VMD patients experience a progressive decrease of vision over time, even though about 30 % of patients carrying a *BEST1* mutation retain 20/40 or better visual acuity into the five and six decades [33]. Among individuals with visible clinical manifestations of the disease at any point in time, 61 % have 20/40 or better vision and only 10 % are legally blind [34].

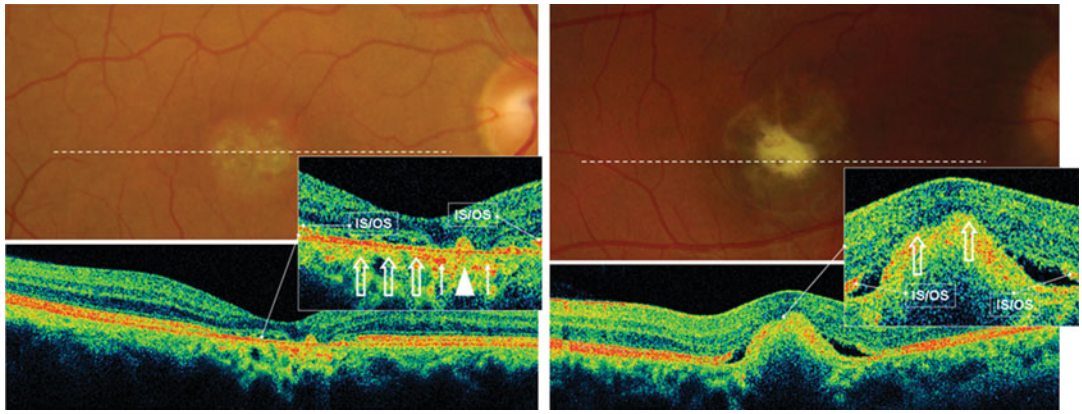

Fig. 1.8 Spectral-domain optical coherence tomography (SD-OCT) scans obtained from atrophic and fibrotic stage vitelliform macular dystrophy patients. Colour fundus photographs of the right eye of (*top left*) a patient and (*top right*) of another patient showing, respectively, the atrophic lesion, characterized by atrophy with or without residual dispersed material, and the fibrotic lesion, characterized by the appearance of macular fibrosis, without any detectable active choroidal neovascularization. (*Bottom left*) SD-OCT scans showing the atrophic lesion characterized by thinning of all the retinal layers (*enlarged view, thin arrows*) and diffuse loss of the ellipsoid zone (i.e. the IS/OS) (*enlarged view, open arrows*), with enhanced reflectivity of the RPE, which seems to spread far behind it, and still some hyperreflective mottling on the RPE layer (*arrowhead*) associated with areas of focal RPE loss. (*Bottom right*) On SD-OCT, the fibrotic lesion is characterized by a prominent highly hyperreflective thickening at RPE level, inducing marked anterior bulging, accompanied by thinning of the sensory retina and diffuse loss of the ellipsoid zone above it (*enlarged view, open arrows*) (From Querques et al. [20], with the kind permission of Elsevier)

With respect to the morphological aspects of the disease, Best VMD is characterized by a dynamic-alternating phase of material accumulation and reabsorption, ending with atrophy or fibrosis (with or without choroidal neovascularization). The five different stages of the disease do not always occur consecutively and it has been shown that the typical stage progression could be reverted (i.e. from vitelliruptive to pseudophypopyon) [18].

Choroidal neovascularization is a complication that can virtually occur in any stage during the disease progression; anti-vascular endothelial growth (VEGF) therapies have shown to be effective and safe even in children [35, 36].

1.11 Genotype-Phenotype Correlations

BEST1 mutations are not correlated with the severity of the functional and clinical data in Best VMD. Even with the same mutation, the age of onset and the disease progression (stage of the disease and visual function) show very high variability interfamilially and intrafamilially [23, 37].

1.12 Differential Diagnosis

Depending from the different stages of the disease, and because of the variability of the lesions, the clinical diagnosis can be challenging and different pathologies should be distinguished from Best VMD. This is true for mild cases with some RPE alterations and small vitelliform lesions but also for later stages with atrophy or fibrosis. Vitelliform lesions can be seen in adult-onset foveomacular vitelliform dystrophy but also secondary to other diseases characterized by "pseudovitelliform" material accumulation, such as central serous chorioretinopathy, and RPE detachments due to confluence of macular drusen (in basal laminar drusen and AMD) [17, 38, 39] or in acute exudative polymorphous vitelliform maculopathy [40] and vitelliform paraneoplastic retinopathy [41]. Advanced cases with macular

atrophy can be mistaken for atrophic AMD in elderly patients; in these cases, both familial history and electrophysiology can help make correct diagnosis. Diagnosis of choroidal neovascularization can be challenging in vitelleruptive stages, because serous retinal detachment on OCT and leakage on fluorescein angiography are often observed.

1.13 Other Bestrophinopathies

BEST1 gene is also implicated in other retinal diseases such as adult-onset foveomacular vitelliform dystrophy, autosomal dominant vitreoretinochoroidopathy (ADVIRC) [6, 42, 43], MRSC syndrome [44] (characterized by microcornea, rod-cone dystrophy, early-onset pulverulent cataract, and posterior staphyloma), and autosomal recessive bestrophinopathy [12].

References

1. Best F. Uber eine hereditare maculaafektion; Beitrage zur verergslehre. Zschr Augenheilkd. 1905;13: 199–212.
2. Stone EM, Nichols BE, Streb LM, Kimura AE, Sheffield VC. Genetic linkage of vitelliform macular degeneration (Best's disease) to chromosome 11q13. Nat Genet. 1992;1(4):246–50.
3. Petrukhin K, Koisti MJ, Bakall B, Li W, Xie G, Marknell T, et al. Identification of the gene responsible for Best macular dystrophy. Nat Genet. 1998; 19(3):241–7.
4. Sun H, Tsunenari T, Yau KW, Nathans J. The vitelliform macular dystrophy protein defines a new family of chloride channels. Proc Natl Acad Sci U S A. 2002;99:4008–13.
5. Boon CJ, Klevering BJ, Leroy BP, Hoyng CB, Keunen JE, den Hollander AI. The spectrum of ocular phenotypes caused by mutations in the *BEST1* gene. Prog Retin Eye Res. 2009;28(3):187–205.
6. Kaufman SJ, Goldberg MF, Orth DH, Fishman GA, Tessler H, Mizuno K. Autosomal dominant vitreoretinochoroidopathy. Arch Ophthalmol. 1982;100: 272–8.
7. Lotery AJ, Munier FL, Fishman GA, Weleber RG, Jacobson SG, Affatigato LM, et al. Allelic variation in the *VMD2* gene in best disease and age-related macular degeneration. Invest Ophthalmol Vis Sci. 2000;41(6):1291–6.
8. Bakall B, Radu RA, Stanton JB, Burke JM, McKay BS, Wadelius C, et al. Enhanced accumulation of A2E in individuals homozygous or heterozygous for mutations in *BEST1* (*VMD2*). Exp Eye Res. 2007;85(1): 34–43.
9. Gass JD. A clinicopathologic study of a peculiar foveomacular dystrophy. Trans Am Ophthalmol Soc. 1974;72:139–56.
10. Patrinely JR, Lewis RA, Font RL. Foveomacular vitelliform dystrophy, adult type: a clinicopathologic study including electron microscopic observations. Ophthalmology. 1985;92:1712–8.
11. Davidson AE, Millar ID, Urquhart JE, Burgess-Mullan R, Shweikh Y, Parry N, et al. Missense mutations in a retinal pigment epithelium protein, bestrophin-1, cause retinitis pigmentosa. Am J Hum Genet. 2009;85(5):581–92.
12. Burgess R, Millar ID, Leroy BP, Urquhart JE, Fearon IM, De Baere E, et al. Biallelic mutation of *BEST1* causes a distinct retinopathy in humans. Am J Hum Genet. 2008;82(1):19–31.
13. Manes G, Meunier I, Avila-Fernndez A, Banfi S, Le Meur G, Zanlonghi X, et al. Mutations in *IMPG1* cause vitelliform macular dystrophies. Am J Hum Genet. 2013;93(3):571–8.
14. Nordstrom S, Barkman Y. Hereditary macular degeneration (HMD) in 246 cases traced to one gene-source in central Sweden. Hereditas. 1977;84:163–76.
15. Deutman AF, Hoyng CB. Macular dystrophies. In: Ryan SJ, editor. Retina. 3rd ed. St. Louis: Mosby; 2001. p. 1210–57.
16. Thorburn W, Nordström S. EOG in a large family with hereditary macular degeneration. (Best's vitelliform macular dystrophy) identification of gene carriers. Acta Ophthalmol (Copenh). 1978;56(3):455–64.
17. Marmor MF. "Vitelliform" lesions in adults. Ann Ophthalmol. 1979;11(11):1705–12.
18. Querques G, Zerbib J, Georges A, Massamba N, Forte R, Querques L, et al. Multimodal analysis of the progression of Best vitelliform macular dystrophy. Mol Vis. 2014;20:575–92.
19. Mohler CW, Fine SL. Long-term evaluation of patients with Best's vitelliform dystrophy. Ophthalmology. 1981;88:688–92.
20. Querques G, Regenbogen M, Quijano C, Delphin N, Soubrane G, Souied EH. High definition optical coherence tomography features in vitelliform macular dystrophy. Am J Ophthalmol. 2008;146:501–7.
21. Spaide RF, Curcio CA. Anatomical correlates to the bands seen in the outer retina by optical coherence tomography: literature review and model. Retina. 2011;31(8):1609–19.
22. Querques G, Zerbib J, Santacroce R, Margaglione M, Delphin N, Querques L, et al. The spectrum of subclinical Best vitelliform macular dystrophy in subjects with mutations in *BEST1* gene. Invest Ophthalmol Vis Sci. 2011;52(7):4678–84.
23. Querques G, Zerbib J, Santacroce R, Margaglione M, Delphin N, Rozet JM, et al. Functional and clinical data of Best vitelliform macular dystrophy patients with mutations in the *BEST1* gene. Mol Vis. 2009; 15:2960–72.

24. Querques G, Regenbogen M, Soubrane G, Souied EH. High-resolution spectral domain optical coherence tomography findings in multifocal vitelliform macular dystrophy. Surv Ophthalmol. 2009;54(2): 311–6.
25. Arnold JJ, Sarks JP, Killingsworth MC, Kettle EK, Sarks SH. Adult vitelliform macular degeneration: a clinicopathological study. Eye (Lond). 2003;17(6): 717–26.
26. Maruko I, Iida T, Spaide RF, Kishi S. Indocyanine green angiography abnormality of the periphery in vitelliform macular dystrophy. Am J Ophthalmol. 2006;141(5):976–8.
27. Deutman AF. Electro-oculography in families with vitelliform dystrophy of the fovea. Detection of the carrier state. Arch Ophthalmol. 1969;81(3):305–16.
28. Meunier I, Sénéchal A, Dhaenens CM, Arndt C, Puech B, Defoort-Dhellemmes S, et al. Systematic screening of *BEST1* and *PRPH2* in juvenile and adult vitelliform macular dystrophies: a rationale for molecular analysis. Ophthalmology. 2011;118(6):1130–6.
29. Blodi CF, Stone EM. Best's vitelliform dystrophy. Ophthalmic Paediatr Genet. 1990;11(1):49–59.
30. Cross HE, Bard L. Electro-oculography in Best's macular dystrophy. Am J Ophthalmol. 1974;77(1): 46–50.
31. Caldwell GM, Kakuk LE, Griesinger IB, Simpson SA, Nowak NJ, Small KW, et al. Bestrophin gene mutations in patients with Best vitelliform macular dystrophy. Genomics. 1999;58(1):98–101.
32. Wabbels B, Preising MN, Kretschmann U, Demmler A, Lorenz B. Genotype-phenotype correlation and longitudinal course in ten families with best vitelliform macular dystrophy. Graefes Arch Clin Exp Ophthalmol. 2006;244(11):1453–66.
33. Fishman GA, Baca W, Alexander KR, Derlacki DJ, Glenn AM, Viana M. Visual acuity in patients with best vitelliform macular dystrophy. Ophthalmology. 1993;100(11):1665–70.
34. Booij JC, Boon CJ, van Schooneveld MJ, ten Brink JB, Bakker A, de Jong PT, et al. Course of visual decline in relation to the *BEST1* genotype in vitelliform macular dystrophy. Ophthalmology. 2010;117(7): 1415–22.
35. Leu J, Schrage NF, Degenring RF. Choroidal neovascularisation secondary to Best's disease in a 13-year-old boy treated by intravitreal bevacizumab. Graefes Arch Clin Exp Ophthalmol. 2007;245(11):1723–5.
36. Querques G, Bocco MC, Soubrane G, Souied EH. Intravitreal ranibizumab (Lucentis) for choroidal neovascularization associated with vitelliform macular dystrophy. Acta Ophthalmol. 2008;86(6):694–5.
37. Boon CJ, Theelen T, Hoefsloot EH, van Schooneveld MJ, Keunen JE, Cremers FP, et al. Clinical and molecular genetic analysis of best vitelliform macular dystrophy. Retina. 2009;29(6):835–47.
38. Burgess DB, Olk RJ, Uniat LM. Macular disease resembling adult foveomacular vitelliform dystrophy in older adults. Ophthalmology. 1987;94(4):362–6.
39. Boon CJ, Klevering BJ, Hoyng CB, Zonneveld-Vrieling MN, Nabuurs SB, Blokland E, et al. Basal laminar drusen caused by compound heterozygous variants in the *CFH* gene. Am J Hum Genet. 2008;82(2):516–23.
40. Gass JD, Chuang EL, Granek H. Acute exudative polymorphous vitelliform maculopathy. Trans Am Ophthalmol Soc. 1988;86:354–66.
41. Eksandh L, Adamus G, Mosgrove L, Andréasson S. Autoantibodies against bestrophin in a patient with vitelliform paraneoplastic retinopathy and a metastatic choroidal malignant melanoma. Arch Ophthalmol. 2008;126(3):432–5.
42. Yardley J, Leroy BP, Hart-Holden N, Lafaut BA, Loeys B, Messiaen LM, et al. Mutations of *VMD2* splicing regulators cause nanophthalmos and autosomal dominant vitreoretinochoroidopathy (ADVIRC). Invest Ophthalmol Vis Sci. 2004;45(10):3683–9.
43. Burgess R, MacLaren RE, Davidson AE, Urquhart JE, Holder GE, Robson AG, et al. ADVIRC is caused by distinct mutations in BEST1 that alter pre-mRNA splicing. J Med Genet. 2009;46(9):620–5.
44. Reddy MA, Francis PJ, Berry V, Bradshaw K, Patel RJ, Maher ER, Kumar R, Bhattacharya SS, Moore AT. A clinical and molecular genetic study of a rare dominantly inherited syndrome (MRCS) comprising of microcornea, rod-cone dystrophy, cataract, and posterior staphyloma. Br J Ophthalmol. 2003;87(2): 197–202.

The Pattern Dystrophies

2

Itay Chowers and Camiel J.F. Boon

Abstract

The pattern dystrophies form a clinically and genetically heterogeneous group of retinal phenotypes including adult-onset foveomacular vitelliform dystrophy (AFVD), butterfly-shaped pigment dystrophy (BPD), reticular dystrophy of the retinal pigment epithelium, pseudo-Stargardt pattern dystrophy (multifocal pattern dystrophy simulating Stargardt disease/fundus flavimaculatus), and fundus pulverulentus. The pattern dystrophies constitute a group of retinal disorders characterized by a variety of deposits of yellow, orange, or gray pigment, predominantly in the macular area. The age at onset in pattern dystrophies is highly variable, but patients tend to remain asymptomatic until the 5th decade or may even remain asymptomatic throughout life. The course of pattern dystrophies is often benign, although severe vision loss occurs in up to 50 % of the affected individuals after the age of 70, as a result of chorioretinal atrophy and/or the development of choroidal neovascularization.

Keywords

Pattern dystrophy • Adult-onset foveomacular vitelliform dystrophy • Butterfly-shaped pigment dystrophy • Reticular dystrophy of the retinal pigment epithelium • Pseudo-Stargardt pattern dystrophy • Fundus pulverulentus

2.1 The Pattern Dystrophies: Introduction

The clinically and genetically heterogeneous group of pattern dystrophies (PD) is characterized broadly by a variety of deposits of yellow, orange, or dark pigment, predominantly in the macular area. The term was originally suggested by Hsieh and colleagues [1] and Marmor and

I. Chowers, MD (✉)
Department of Ophthalmology, Hadassah-Hebrew University Medical Center, Jerusalem, Israel
e-mail: chowers@hadassah.org.il

C.J.F. Boon, MD, PhD, FEBOphth
Department of Ophthalmology, Leiden University Medical Center, Leiden, The Netherlands

G. Querques, E.H. Souied (eds.), *Macular Dystrophies*, DOI 10.1007/978-3-319-26621-3_2

colleagues [2]. A wide variety of clinical presentations and patterns has been included in the group of PD, and Gass has classified PD into five major subgroups [3]: adult-onset foveomacular vitelliform dystrophy (AFVD), butterfly-shaped pigment dystrophy (BPD), reticular dystrophy of the retinal pigment epithelium, multifocal pattern dystrophy simulating Stargardt disease/fundus flavimaculatus, and fundus pulverulentus. Yet, Gass and others also noted that additional forms of PD are observed and that even the eyes of the same patient may manifest different forms of PD.

Since Gass description of the classification more than three decades ago, important insights into PD were obtained. Among these insights, which will be discussed in this chapter, were the identification of various genetic defects associated with some of these phenotypes and a more detailed understanding of the lesion composition and their pathogenesis based on multimodal imaging, histological, and laboratory studies.

2.2 Adult-Onset Foveomacular Vitelliform Dystrophy

2.2.1 Background

Adult-onset foveomacular vitelliform dystrophy (AFVD) is the most common form of PD. AFVD was first described by Gass in 1974 and was initially termed "peculiar foveomacular dystrophy" [4], and later adult-onset foveomacular vitelliform dystrophy (AFVD). Following Gass' description, multiple authors have described this phenotype, and multiple terms were utilized to describe the phenotype [5–19]. Among the terms used were adult macular vitelliform degeneration [10], adult vitelliform macular degeneration [8, 11, 17], pseudovitelliform macular degeneration [16], adult-onset foveomacular pigment epithelial dystrophy [18], adult foveomacular vitelliform dystrophy [5, 7], and adult vitelliform macular dystrophy [6, 15]. This conflicting terminology generated confusion in the field and hampered accurate diagnosis and study of the phenotype [15].

While AFVD was initially described as an autosomal-dominant trait, it was later reported that most cases are sporadic. Mutations in *PRPH2*, *BEST1*, and *IMPG1* and *IMPG2* genes were associated with this phenotype [20–23]. Mutations in these genes can cause a spectrum of clinical pictures, including other maculopathies or panretinal dystrophies. Furthermore, most AFVD patients do not carry mutations in the *PRPH2*, *BEST1*, and *IMPG1* and *IMPG2* gene. Sporadic AFVD was associated with an *HTRA1* single nucleotide polymorphism (SNP) which is also associated with age-related macular degeneration [24].

Interestingly, *PRPH2* is expressed in rods and cones, whereas *IMPG1* and *IMPG2* are components of the interphotoreceptor matrix, and *BEST1* is expressed exclusively in the RPE. Since mutations in each of these genes can result in the AFVD phenotype, it is conceivable that altered photoreceptor outer segments, intercellular matrix, or RPE function can each lead to formation of vitelliform lesions which characterize AFVD. Thus, AFVD may be the result of altered RPE-photoreceptor complex function, probably due to defective photoreceptor intake by the RPE leading to the buildup of the subretinal vitelliform material. Currently, there is no treatment for AFVD.

2.2.2 Clinical Findings

Gass, in his original description of nine cases, has suggested that AFVD usually manifests between 30 and 50 years of age and shows bilateral subfoveal vitelliform yellowish deposit at an average size of one-third disc area with a central pigmented spot (Fig. 2.1) [4]. In fact, AFVD often manifest in elderly individuals and the vitelliform lesion is often considerably larger. Vitelliform lesions in AFVD can also demonstrate characteristics and stages such as a pseudohypopyon or a vitelliruptive lesion which can also be seen in Best vitelliform macular dystrophy. In some cases, multifocal vitelliform lesions are present [25]. With time, lesions can show more pigment changes, progressive atrophy and/or choroidal neovascularization with corresponding vision loss. Some older patients may show drusen in

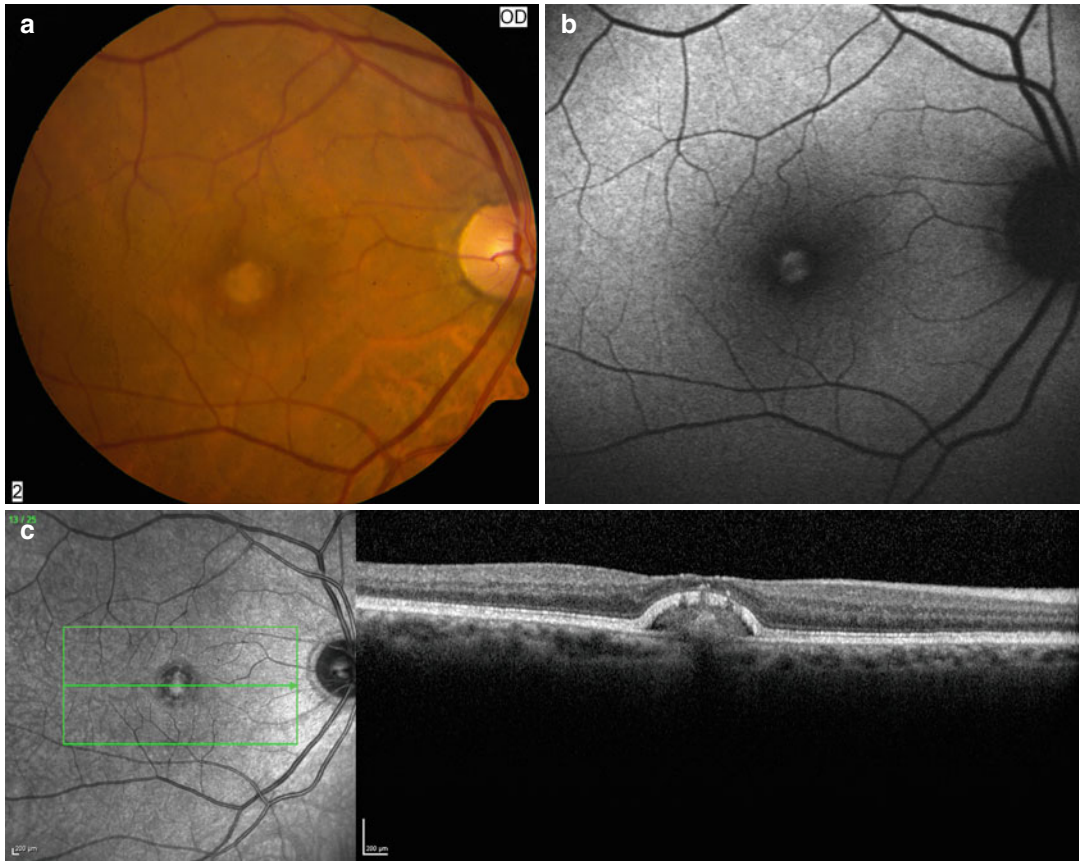

Fig. 2.1 Adult-onset foveomacular vitelliform dystrophy (AFVD). (**a**) Color fundus photograph of a 69-year-old male diagnosed with AFVD. The visual acuity was 0.8 in each eye. Patient was negative for *PRPH2*, *BEST1*, and *IMPG1/2* gene mutations. A vitelliform lesion of approximately one-third disc diameter in size is evident. Few drusen are also seen. (**b**) Fundus autofluorescence shows a hyperautofluorescent signal from the vitelliform lesion. (**c**) Spectral-domain optical coherence tomography (SD-OCT) demonstrates a dome-shape subretinal vitelliform lesion

combination with vitelliform lesions, a phenotype that apparently overlaps with age-related macular degeneration, and may therefore be different from "classical" AVFD with isolated vitelliform lesions without drusen. Data from multiple cohorts suggested that the majority of AFVD cases actually manifest in elderly individuals and that vitelliform lesions are often up to one disc diameter in size. In addition, AFVD is commonly accompanied by RPE atrophy or hyperpigmentation [5–7, 10, 11, 15–18] and by pigment epithelium detachment (PED) [14, 19, 26].

On fluorescein angiography (FA), vitelliform lesions in AFVD show blockage of fluorescence in the early phase of the angiogram, with late staining that can be difficult to distinguish from occult choroidal neovascularization (CNV). Optical coherence tomography (OCT) shows a hyperreflective dome-shape subretinal lesion in the vitelliform stage (see Fig. 2.1). This may be replaced by heterogeneous lesion reflectance in the pseudohypopyon and vitelliruptive stages of the lesion, with photoreceptor and RPE cell loss in the atrophic stage. On fundus autofluorescence (FAF; see Fig. 2.1), the vitelliform material demonstrates hyperautofluorescence, with progressive hypo-autofluorescence with advancing atrophy of the lesion [4, 5, 12, 14, 27]. Electrophysiology and color vision studies are generally normal except for a slightly subnormal electro-oculogram (EOG) in some of the cases of AFVD. Multifocal ERG may show suppressed

central amplitudes, and microperimetry demonstrates reduced sensitivity over the vitelliform lesion which may extend to surrounding seemingly unaffected retina [4, 12, 15, 19, 28].

Histological studies have demonstrated the subretinal location of the vitelliform lesion. The lesion is composed of photoreceptor outer segment remnants, lipofuscin components (corresponding to increased fundus autofluorescence), pigment-containing macrophages, and RPE cells. Outer photoreceptor segment disruption and outer nuclear layer loss are observed over the vitelliform lesion. RPE cells at the base of the lesion are initially hypertrophic and are later hypopigmented at the lesion center and hyperpigmented at its circumference. RPE cell loss occurs at later stage of the disease [4, 29–31].

2.2.3 Disease Course

AFVD may be diagnosed while the patient is asymptomatic or when it is associated with variable visual symptoms including reduced visual acuity or metamorphopsia. Often, the visual acuity is well preserved at diagnosis. Disease progression in AFVD is usually associated with slow visual deterioration which occurs over years [10, 11, 16]. For example, Renner and colleagues evaluated 120 eyes of 61 patients with a mean age of 55 years having a central, yellow, subretinal lesion smaller than one disc diameter in at least one eye. Approximately half of the eyes showed disease progression with vision loss in many cases and other visual symptoms such as metamorphopsia, central scotoma, and visual disturbance [15]. Ten cases had follow-up of longer than 5 years and preserved 20/50 in at least one eye.

Querques et al. described the natural course of AFVD using SD-OCT in 46 eyes of 31 patients with a mean age of 75 years and a mean follow-up of 16 months (range 12–30 months) [14]. The authors classified the lesions based on OCT characteristics into vitelliform, pseudohypopyon, vitelliruptive, and atrophic stages. During follow-up, the mean visual acuity reduced from 0.32 logMAR to 0.39 logMAR. Visual decline was associated with progression of the vitelliform lesion stage and disruption of the ellipsoid zone. Overall, 61 % of the lesions remained vitelliform during the course of the study while 11 % became atrophic during follow-up. Vision loss was also associated with thinning of the outer nuclear layer over the vitelliform lesion, probably reflecting photoreceptor cell loss [9].

AFVD eyes can also develop CNV which by itself can lead to visual loss [10, 18, 26, 32–35]. If CNV develops, anti-vascular endothelial growth factor therapy may be helpful in reducing exudation and limiting the angiogenic process [33, 35]. Yet, the visual outcome is usually limited by the presence of the vitelliform foveal lesion and its progression.

2.2.4 Differential Diagnosis

Vitelliform foveal lesions similar to those observed in AFVD can be seen in several ophthalmic and systemic conditions. Often, AFVD is confused with AMD. Both diseases may develop sporadically in aged individuals. Drusen were described in some AFVD cases and are also the hallmark of AMD, and CNV may develop in both. Both AFVD and AMD also share an *HTRA1* risk SNP. In fact, there is no consensus where the line of distinction between AMD complicated with a vitelliform lesion and AFVD with drusen should be drawn. Some have suggested that AFVD may be a specific phenotype of AMD [10]. Others consider typical AFVD as a phenotype without drusen and would classify cases with adult vitelliform lesions associated with drusen as a form of AMD. Further insights into the pathogenesis of this phenotype are required to resolve this issue.

Vitelliform lesions in Best vitelliform macular dystrophy, an autosomal-dominant condition which is associated with *BEST1* mutations, develop at childhood, and a diagnosis of genetically confirmed Best disease over the age of 40 years is uncommon. Vitelliform foveal lesions can also develop secondary to vitreomacular traction and epiretinal membrane, both of which are readily recognized on OCT. Chronic presence of subfoveal fluid in conditions such as central

serous choroidopathy (CSC) or following retinal detachment repair can also result in lesions with a vitelliform aspect. Systemic conditions associated with vitelliform lesions include pseudoxanthoma elasticum maculopathy [9], mitochondrial retinal dystrophy associated with the m.3243A>G mutation [36], Kearns-Sayre syndrome [37], desferrioxamine-related retinopathy [38, 39], and binimetinib treatment [40]. Vitelliform lesions can also appear as multifocal and acute in acute exudative polymorphous vitelliform maculopathy [41]; this may be a paraneoplastic manifestation of variety of cancers with potential association with anti-RPE antibodies [42–47].

2.2.5 Conclusion

AFVD, the most common form of PD, is associated with mutations in several genes, but most cases are sporadic. AFVD is characterized by vitelliform lesions in the fovea, in association with a usually normal EOG. The disease is diagnosed in adults and generally follows a course of slow visual decline, which may eventually be accelerated because of the development of foveal atrophy or CNV.

2.3 Butterfly-Shaped Pigment Dystrophy

2.3.1 Background

Butterfly-shaped pigment dystrophy (BPD) was first described by Deutman and colleagues [48]. In this autosomal-dominantly inherited macular dystrophy, a spoke-like pigment pattern that may resemble the shape of a butterfly is observed in the macula [49]. Other phenotypes of the pattern dystrophy group that can be caused by *PRPH2* mutations include AFVD and pseudo-Stargardt pattern dystrophy (multifocal pattern dystrophy simulating Stargardt disease/fundus flavimaculatus) [49]. BPD is genetically heterogeneous: besides mutations in the *PRPH2* gene and the *CTNNA1* gene, a locus on 5q21.2–q33.2 is also associated with autosomal-dominant BPD [49–54].

2.3.2 Clinical Findings

Patients can present with mild loss of visual acuity and/or metamorphopsia after the age of 40, but BPD patients are often asymptomatic. Patient with BPD caused by mutations in the *PRPH2* gene has yellowish lesions in the macula at the level of the outer retina and retinal pigment epithelium (RPE) [49]. The lesions have three or more branches that can resemble wings of a butterfly (Fig. 2.2a). The butterfly-shaped lesions can evolve from lesions similar to adult-onset foveomacular vitelliform dystrophy. Some patients with *PRPH2* mutations show a BPD lesion in the macula together with multiple flavimaculatus-like yellow flecks in the posterior pole (Fig. 2.2) [55]. These cases can be regarded as pseudo-Stargardt pattern dystrophy. On fluorescein angiography, the pigmented regions of the lesion are hypofluorescent, whereas surrounding depigmented zones and areas of chorioretinal atrophy are hyperfluorescent (see Fig. 2.2) [49, 56]. On FAF, lesions show variably increased and decreased autofluorescence (see Fig. 2.2) [57]. On optical coherence tomography, the lesions correspond to hyperreflective granular changes at the photoreceptor-RPE interface. The central visual field is normal or shows slightly decreased central sensitivity in cases without profound chorioretinal atrophy. The peripheral visual field is normal. Full-field electroretinography (ERG) is normal, except in cases that advance to extensive pseudo-Stargardt pattern dystrophy [49, 56, 58, 59]. The electrooculogram (EOG) in BPD is normal to slightly subnormal.

2.3.3 Disease Course

Most patients with BPD have a good visual acuity in at least one eye for many decades. The development of choroidal neovascularization is very rare [60]. However, a marked decline in visual acuity can develop after the seventh decade by progressive photoreceptor and RPE atrophy in the macula [32, 61].

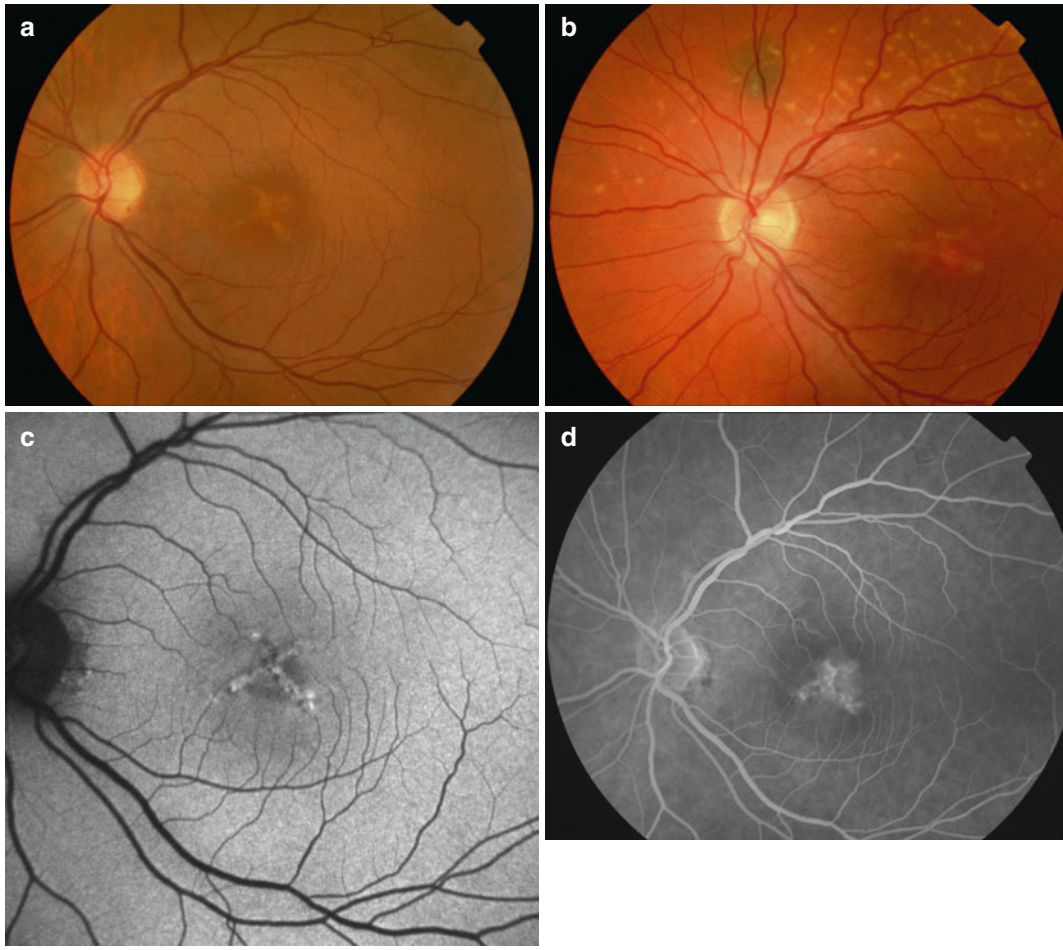

Fig. 2.2 Butterfly-shaped pigment dystrophy (BPD). (**a**) Color fundus photograph of a butterfly-shaped hypopigmented lesion in a 62-year-old patient carrying an autosomal-dominant mutation in the *PRPH2* gene. In some patients with BPD, more darkly pigmented, branching lesions can be seen in the macula, but such cases are usually not associated with *PRPH2* gene mutations. (**b**) Butterfly-shaped lesions can be associated with irregular yellowish flavimaculatus flecks, in association with *PRPH2* mutations, thus showing overlap with pseudo-Stargardt pattern dystrophy. (**c**) Fundus autofluorescence shows relatively marked autofluorescence changes typical of hereditary macular conditions. (**d**) Fluorescein angiography in this case shows hyperfluorescence due to a retinal pigment epithelium (RPE) window defect but can also show blockage in cases of hyperpigmentation at the level of the RPE

2.3.4 Differential Diagnosis

BPD should be differentiated from the other *PRPH2*-associated macular dystrophies, long-standing atrophic RPE detachments, atrophic age-related macular degeneration, and atrophic central serous chorioretinopathy. Pattern dystrophies can also be observed in association with maternally inherited diabetes and deafness (mitochondrial retinal dystrophy; see Chap. 8), myotonic dystrophy, pseudoxanthoma elasticum, and Crohn's disease.

2.3.5 Conclusion

BPD is an autosomal-dominantly inherited macular dystrophy at the mild end of the clinical

spectrum of dystrophies. However, central vision loss can still become more pronounced in the elderly population due to progressive atrophy and/or neovascularization.

2.4 Pseudo-Stargardt Pattern Dystrophy (Multifocal Pattern Dystrophy Simulating Stargardt Disease/Fundus Flavimaculatus)

2.4.1 Background

The human *PRPH2* gene causes a broad spectrum of retinal dystrophies, ranging from purely macular phenotypes to retinitis pigmentosa [49]. The PRPH2 protein localizes to the rim region of rod and cone outer segment discs and lamellae and plays an important role in photoreceptor outer segment morphogenesis [49]. *PRPH2*-associated phenotypes are inherited autosomal dominantly with the exception of digenic retinitis pigmentosa, which also requires a mutation in the *ROM1* gene.

Identical *PRPH2* mutations are associated with decreased penetrance and variable expression, which can result in a markedly variable spectrum of clinical pictures even in families carrying the same mutation [55]. A *PRPH2*-associated dystrophy that appears purely macular at first may eventually evolve into a clinical picture with widespread retinal involvement. The pseudo-Stargardt pattern dystrophy phenotype, as the name coined by Boon et al. [62] indicates, can closely mimic autosomal recessive Stargardt disease (*STGD1*). Up to 20 % of patients with presumed autosomal recessive Stargardt disease of the fundus flavimaculatus subtype, in whom no *ABCA4* gene mutation is found, actually carry an autosomal-dominant *PRPH2* mutation. This finding underscores the importance of genetic testing, as such findings greatly influence the visual prognosis, genetic counseling, and possible future therapeutic perspectives.

2.4.2 Clinical Findings

Most pseudo-Stargardt pattern dystrophy patients start to notice vision loss in their fifth decade, but some patients can remain asymptomatic [55]. Initial symptoms can include metamorphopsia, central vision loss, and/or scotoma. There are varying degrees of night blindness in up to half of the patients, generally with more advanced disease. On funduscopy, patients show irregular yellowish flecks in the posterior pole (Fig. 2.3), and these flecks closely resemble flavimaculatus flecks that can be seen in Stargardt disease. The flecks can gradually become confluent to form a mildly atrophic oval zone that encircles the macula and optic disc (see Fig. 2.3). The aspect of macular lesions in pseudo-Stargardt pattern dystrophy is variable: some lesions consist of a few clustered yellowish or slightly pigmented spots or have the aspect of butterfly-shaped pigment dystrophy [55]. In other cases, macular lesions can show large confluent and irregular flecks or spots.

On fluorescein angiography, the Stargardt-like flecks and the macular lesions are hyperfluorescent, sometimes with a central hypofluorescent spot (see Fig. 2.3). In contrast to most cases of Stargardt disease, there is no blockage of choroidal background fluorescence ("dark choroid"). On FAF, the Stargardt-like flecks are initially highly increased autofluorescent (see Fig. 2.3). The flecks are often bordered by small zones of decreased autofluorescence. When these flecks merge, the resulting oval zone is visible as a band of generally increased autofluorescence with granular zones of decreased autofluorescence (see Fig. 2.3) [55]. The macular lesions correspond to various patterns of increased and decreased autofluorescence. OCT shows that the Stargardt-like flecks and macular lesions correspond to abnormalities on the photoreceptor outer segment-RPE level (Fig. 2.3).

The full-field ERG is normal in early pseudo-Stargardt pattern dystrophy, when the Stargardt-like flecks are still well defined and principally located in the posterior pole. With disease progression, full-field ERG can reveal generalized cone and/or rod dysfunction [55]. In

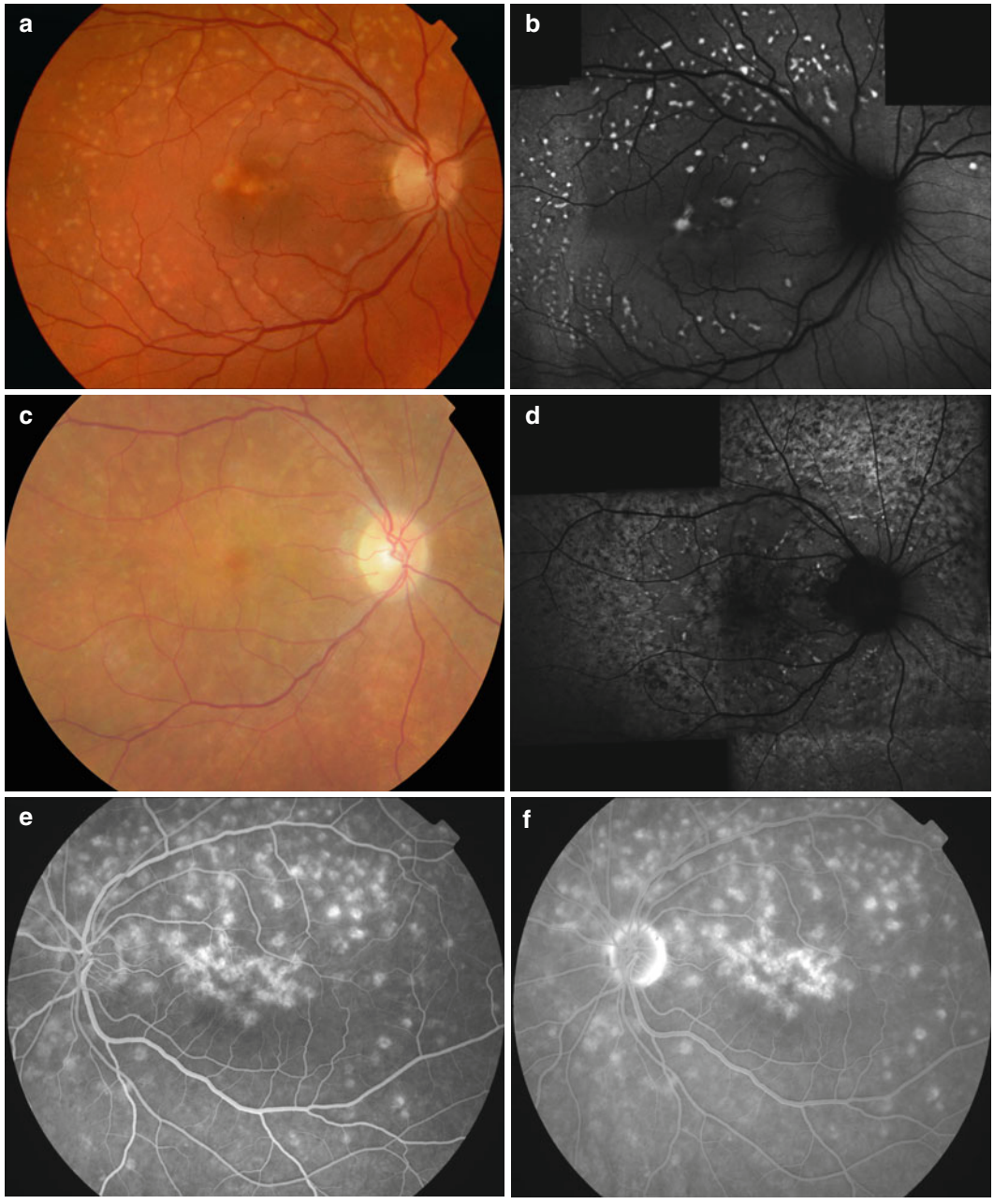

Fig. 2.3 Pseudo-Stargardt pattern dystrophy. (**a**) Color fundus photography of typical pseudo-Stargardt pattern dystrophy (caused by autosomal-dominantly inherited mutations in the *PRPH2* gene) with Stargardt-like flavimaculatus flecks in combination with multifocal pigmentary changes in the macula. (**b**) These lesions are typically markedly hyperautofluorescent in the earlier stages of the disease. (**c**) With advancing disease, lesions in the macula and flecks around the arcade become confluent and mildly atrophic, which is also reflected on fundus autofluorescence (FA) (**d**). Still, visual acuity at this stage, which is reached beyond the age of 45–50, can be fairly good (>20/30). On fluorescein angiography, lesions are hyperfluorescent in the early (**e**) and late (**f**) phase, compatible with mild retinal pigment epithelium (RPE) atrophy and possibly some late staining. Unlike in many Stargardt disease cases, the angiogram in pseudo-Stargardt pattern dystrophy does not show marked masking of choroidal background fluorescence ("dark choroid"). (**g**) Spectral-domain optical coherence tomography in pseudo-Stargardt pattern dystrophy shows irregularities at the outer photoreceptor-RPE level. (**h**) In some elderly patients, the disease can eventually progress to profound chorioretinal atrophy of the posterior pole, which is clearly reflected on FAF as black areas corresponding to RPE atrophy (**i**)

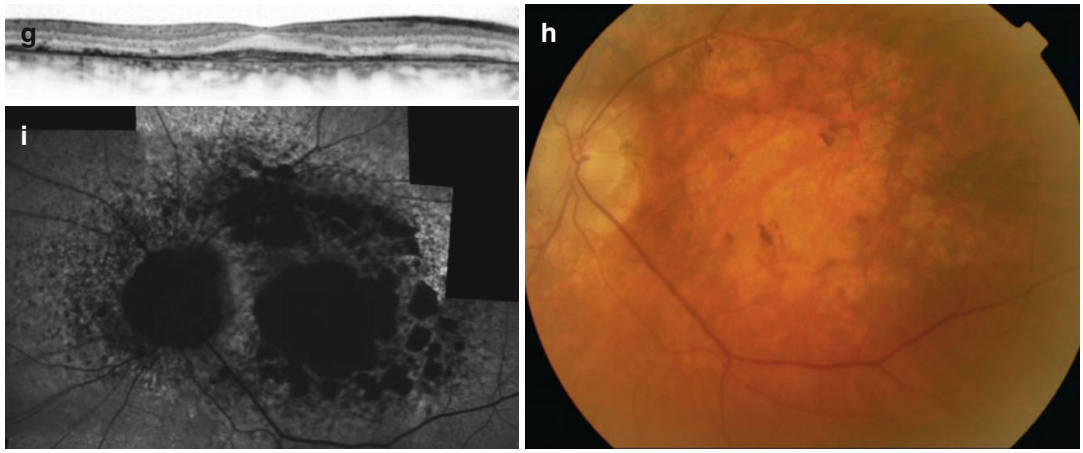

Fig. 2.3 (continued)

advanced cases, the photopic and scotopic full-field ERG responses become severely abnormal to non-recordable. These ERG findings indicate that pseudo-Stargardt pattern dystrophy can evolve from a dystrophy that initially appears localized to the macula—both functionally and anatomically—to widespread panretinal photoreceptor dystrophy. The EOG results vary widely but may show a subnormal to absent light rise in more than half of advanced cases [55].

2.4.3 Disease Course

In advancing disease, the retinal abnormalities extend beyond the posterior pole and do not tend to spare the peripapillary retina in contrast to Stargardt disease (see Fig. 2.3). Profound macular atrophy and marked vision loss (to as low as finger counting) generally do not develop before the age of 55. In advanced disease, patients may also show slight retinal arteriolar attenuation, perivascular and retinal hyperpigmented clumping, and temporal pallor of the optic disc [55].

2.4.4 Differential Diagnosis

In contrast to typical Stargardt disease, see Chap. 3, pseudo-Stargardt pattern dystrophy has an autosomal-dominant pattern of inheritance, a relatively late age at onset, a comparatively good visual acuity, and no dark choroid on fluorescein angiography. Other differential diagnostic entities that should be considered include autosomal-dominant Stargardt-like dystrophies such as STGD3 (caused by mutations in the *ELOVL4* gene), STGD4, and pattern dystrophy associated with maternally inherited diabetes and deafness (m.3243A>G mitochondrial retinal dystrophy, see Chap. 8).

2.4.5 Conclusion

Pseudo-Stargardt pattern dystrophy is a progressive autosomal-dominant retinal dystrophy caused by mutations in the *PRPH2* gene. This phenotype is characterized by multifocal irregular yellowish flecks in the posterior pole and should be differentiated mainly from autosomal recessive Stargardt disease.

2.5 Reticular Pattern Dystrophy

2.5.1 Background

In 1950, Sjögren described a new form of retinal degenerations which he termed "dystrophia reticularis laminae pigmentosae retinae" [63]. The phenotype was later termed reticular dystrophy and was classified as one of the pattern dystrophies

[2, 3]. Autosomal-dominant and autosomal recessive inheritance patterns have been described in association with this phenotype.

2.5.2 Clinical Findings

In reticular pattern dystrophy, a network of (hyper) pigmentary abnormalities extends to the periphery of the macula in forms resembling a chicken wire or fishnet with knots. The patterns are more readily detected on fluorescein angiography, on which a network of hypofluorescent patterns surrounded by hyperfluorescent lines is evident.

OCT may demonstrate small RPE elevations in over half of patients. An altered ellipsoid zone and outer limiting membrane (OLM) are also observed in approximately half of the eyes. The subretinal material appears densely hyperreflective in most eyes, while some may show hypo-reflective areas [64, 65]. Electrophysiology including ERG and EOG testing and psychophysical tests such as color vision and dark adaptation may be unaffected or impaired [66]. A mild, relatively common, asymptomatic, and relatively stable form of reticular hyperpigmentation in the (mid)peripheral retina can also be seen in elderly patients. Thus far, this variant of reticular retinal changes has not been associated with any genetic abnormalities.

Ocular features which may be associated with reticular dystrophy include spherophakia with myopia and luxated lenses, partial atrophy of the iris, scleral staphyloma, convergent strabismus, and choroidal neovascularization [63, 67]. Deafmutism and choreatiform behavior was also described in association with reticular dystrophy in the original description of Sjögren [63].

2.5.3 Disease Course

The pigmentary changes often first appear in proximity to the fovea center; they later extend to the macula periphery manifesting an oval pattern which may encompass the entire posterior pole. The hyperpigmented areas gradually fade, leaving corresponding areas of RPE atrophy.

2.5.4 Differential Diagnosis

The differential diagnosis of reticular pattern dystrophy mainly includes maculopathies with RPE pigmentation and atrophy involving deposition of subretinal material. The combination of ophthalmoscopy, fluorescein angiography, OCT, and genetic tests can readily distinct reticular dystrophy from Stargardt disease, Best vitelliform macular dystrophy, other pattern dystrophies, and dominant drusen.

2.5.5 Conclusions

Reticular dystrophy is an uncommon form of pattern dystrophy. Lesion location between the RPE and photoreceptors is similar to other pattern dystrophies. Yet, material deposition images in OCT are more similar to the ones observed in fundus flavimaculatus than the ones seen in adult-onset foveomacular vitelliform dystrophy [64]. Eventually, vision loss may occur secondary to the development of choroidal neovascularization and macular atrophy.

2.6 Fundus Pulverulentus (Coarse Pigment Mottling of the Macula)

2.6.1 Background

Fundus pulverulentus is an uncommon macular phenotype that was first described by Slezak and Hommer in 1969 [68]. It was later suggested to group with other RPE dystrophies [69]. An autosomal-dominant inheritance pattern may be present [68, 69], but affected family members may also manifest other forms of PD [70, 71]. Association with *PRPH2* gene mutation has also been described [71].

2.6.2 Clinical Findings

Gass has described the phenotype rather aspecifically as a coarse mottling of the RPE in the macula

area [3]. The visual field, color vision, full-field ERG, and dark adaptation are normal, but the EOG can in some cases be subnormal [70].

2.6.3 Disease Course

Little is known on the disease progression of this subtype of PD, but mild visual loss has been described. Fundus pulverulentus can also be associated with the development of CNV [72].

2.6.4 Differential Diagnosis

This phenotype shows similarities to the other forms of PDs. It was also associated with pseudoxanthoma elasticum where progression from fundus pulverulentus to BPD was reported [73]. Mitochondrial retinal dystrophy (maternally inherited diabetes and deafness and MELAS syndrome) [36] and toxic maculopathies such as desferrioxamine retinopathy can have a similar phenotype [74].

2.6.5 Conclusions

Fundus pulverulentus is an uncommon and nonspecific form of PD that can be seen in association with pseudoxanthoma elasticum. The disease is more a description of an atypical macular pigmentation pattern rather than an isolated clinical entity.

References

1. Hsieh RC, Fine BS, Lyons JS. Patterned dystrophies of the retinal pigment epithelium. Arch Ophthalmol. 1977;95(3):429–35.
2. Marmor MF, Byers B. Pattern dystrophy of the pigment epithelium. Am J Ophthalmol. 1977;84(1):32–44.
3. Gass J. Stereoscopic atlas of macular diseases, vol. 2. 4th ed. St Louis: Mosby; 1997.
4. Gass J. A clinicopathologic study of a peculiar foveomacular dystrophy. Trans Am Ophthalmol Soc. 1974;72:139–56.
5. Benhamou N, Souied EH, Zolf R, Coscas F, Coscas G, Soubrane G. Adult-onset foveomacular vitelliform dystrophy: a study by optical coherence tomography. Am J Ophthalmol. 2003;135(3):362–7.
6. Brecher R, Bird A. Adult vitelliform macular dystrophy. Eye (Lond). 1990;4(Pt 1):210–5.
7. Burgess D, Olk R, Uniat L. Macular disease resembling adult foveomacular vitelliform dystrophy in older adults. Ophthalmology. 1987;94:362–6.
8. Epstein G, Rabb M. Adult vitelliform macular degeneration: diagnosis and natural history. Br J Ophthalmol. 1980;64:733–40.
9. Freund KB, Laud K, Lima LH, Spaide RF, Zweifel S, Yannuzzi LA. Acquired vitelliform lesions: correlation of clinical findings and multiple imaging analyses. Retina. 2011;31(1):13–25.
10. Glacet-Bernard A, Soubrane G, Coscas G. Macular vitelliform degeneration in adults. Retrospective study of a series of 85 patients. J Fr Ophtalmol. 1990;13:407–20.
11. Greaves A, Sarks J, Sarks S. Adult vitelliform macular degeneration: a clinical spectrum. Aust N Z J Ophthalmol. 1990;18:171–8.
12. Parodi MB, Iacono P, Pedio M, Pece A, Isola V, Fachin A, et al. Autofluorescence in adult-onset foveomacular vitelliform dystrophy. Retina. 2008;28(6):801–7.
13. Pierro L, Tremolada G, Introini U, Calori G, Brancato R. Optical coherence tomography findings in adult-onset foveomacular vitelliform dystrophy. Am J Ophthalmol. 2002;134(5):675–80.
14. Querques G, Forte R, Querques L, Massamba N, Souied EH. Natural course of adult-onset foveomacular vitelliform dystrophy: a spectral-domain optical coherence tomography analysis. Am J Ophthalmol. 2011;152(2):304–13.
15. Renner AB, Tillack H, Kraus H, Kohl S, Wissinger B, Mohr N, et al. Morphology and functional characteristics in adult vitelliform macular dystrophy. Retina. 2004;24(6):929–39.
16. Sabates R, Pruett R, Hirose T. Pseudovitelliform macular degeneration. Retina. 1982;2:197–205.
17. Theischen M, Schilling H, Steinhorst U. EOG in adult vitelliform macular degeneration, butterfly-shaped pattern dystrophy and Best disease. Ophthalmologe. 1997;94(3):230–3 [article in German].
18. Vine A, Schatz H. Adult-onset foveomacular pigment epithelial dystrophy. Am J Ophthalmol. 1980;89:680–91.
19. Puche N, Querques G, Benhamou N, Tick S, Mimoun G, Martinelli D, et al. High-resolution spectral domain optical coherence tomography features in adult onset foveomacular vitelliform dystrophy. Br J Ophthalmol. 2010;94(9):1190–6.
20. Wells J, Wroblewski J, Keen J, Inglehearn C, Jubb C, Eckstein A, et al. Mutations in the human retinal degeneration slow (RDS) gene can cause either retinitis pigmentosa or macular dystrophy. Nat Genet. 1993;3(3):213–8.
21. Bandah-Rozenfeld D, Collin RW, Banin E, van den Born LI, Coene KL, Siemiatkowska AM, et al. Mutations in *IMPG2*, encoding interphotoreceptor matrix proteoglycan 2, cause autosomal-recessive retinitis pigmentosa. Am J Hum Genet. 2010;87(2):199–208.

22. Manes G, Meunier I, Avila-Fernández A, Banfi S, Le Meur G, Zanlonghi X, et al. Mutations in *IMPG1* cause vitelliform macular dystrophies. Am J Hum Genet. 2013;93(3):571–8.
23. Kramer F, White K, Pauleikhoff D, Gehrig A, Passmore L, Rivera A, et al. Mutations in the *VMD2* gene are associated with juvenile-onset vitelliform macular dystrophy (Best disease) and adult vitelliform macular dystrophy but not age-related macular degeneration. Eur J Hum Genet. 2000;8(4):286–92.
24. Jaouni T, Averbukh E, Burstyn-Cohen T, Grunin M, Banin E, Sharon D, Chowers I. Association of pattern dystrophy with an HTRA1 single-nucleotide polymorphism. Arch Ophthalmol. 2012;130(8):987–91.
25. Boon CJ, Klevering BJ, den Hollander AI, Zonneveld MN, Theelen T, Cremers FP, Hoyng CB. Clinical and genetic heterogeneity in multifocal vitelliform dystrophy. Arch Ophthalmol. 2007;125(8):1100–6.
26. Battaglia Parodi M, Di Crecchio L, Ravalico G. Vascularized pigment epithelial detachment in adult-onset foveomacular vitelliform dystrophy. Eur J Ophthalmol. 2000;10(3):266–9.
27. Querques G, Bux AV, Prato R, Iaculli C, Souied EH, Delle Noci N. Correlation of visual function impairment and optical coherence tomography findings in patients with adult-onset foveomacular vitelliform macular dystrophy. Am J Ophthalmol. 2008;146(1):135–42.
28. Furino C, Boscia F, Cardascia N, Sborgia L, Sborgia C. Fundus autofluorescence, optical coherence tomography and visual acuity in adult-onset foveomacular dystrophy. Ophthalmologica. 2008;222(4):240–4.
29. Jaffe GJ, Schatz H. Histopathologic features of adult-onset foveomacular pigment epithelial dystrophy. Arch Ophthalmol. 1988;106(7):958–60.
30. Dubovy SR, Hairston RJ, Schatz H, Schachat AP, Bressler NM, Finkelstein D, Green WR. Adult-onset foveomacular pigment epithelial dystrophy: clinicopathologic correlation of three cases. Retina. 2000;20(6):638–49.
31. Arnold JJ, Sarks JP, Killingsworth MC, Kettle EK, Sarks SH. Adult vitelliform macular degeneration: a clinicopathological study. Eye (Lond). 2003;17(6):717–26.
32. Francis P, Schultz D, Gregory AM, Schain MB, Barra R, Majewski J, et al. Genetic and phenotypic heterogeneity in pattern dystrophy. Br J Ophthalmol. 2005;89:115–9.
33. Mimoun G, Caillaux V, Querques G, Rothschild P, Puche N, Souied E. Ranibizumab for choroidal neovascularization associated with adult-onset foveomacular vitelliform dystrophy: one-year results. Retina. 2013;33:513–21.
34. Da Pozzo S, Parodi MB, Toto L, Ravalico G. Occult choroidal neovascularization in adult-onset foveomacular vitelliform dystrophy. Ophthalmologica. 2001;215(6):412–4.
35. Tiosano L, Jaouni T, Averbukh E, Grunin M, Banin E, Chowers I. Bevacizumab treatment for choroidal neovascularization associated with adult-onset foveomacular vitelliform dystrophy. Eur J Ophthalmol. 2014;24(5):890–6.
36. de Laat P, Smeitink JA, Janssen MC, Keunen JE, Boon CJ. Mitochondrial retinal dystrophy associated with the m.3243A>G mutation. Ophthalmology. 2013;120(12):2684–96.
37. Ascaso FJ, Lopez-Gallardo E, Del Prado E, Ruiz-Pesini E, Montoya J. Macular lesion resembling adult-onset vitelliform macular dystrophy in Kearns-Sayre syndrome with multiple mtDNA deletions. Clin Exp Ophthalmol. 2010;38(8):812–6.
38. Gonzales C, Lin A, Engstrom R, Kreiger A. Bilateral vitelliform maculopathy and deferoxamine toxicity. Retina. 2004;24:464–7.
39. Genead M, Fishman G, Anastasakis A, Lindeman M. Macular vitelliform lesion in desferrioxamine-related retinopathy. Doc Ophthalmol. 2010;121:161–6.
40. Urner-Bloch U, Urner M, Stieger P, Galliker N, Winterton N, Zubel A, et al. Transient MEK inhibitor-associated retinopathy in metastatic melanoma. Ann Oncol. 2014;25(7):1437–41.
41. Gass J, Chuang E, Granek H. Acute exudative polymorphous vitelliform maculopathy. Trans Am Ophthalmol Soc. 1988;86:354–66.
42. Al-Dahmash SA, Shields CL, Bianciotto CG, Witkin AJ, Witkin SR, Shields JA. Acute exudative paraneoplastic polymorphous vitelliform maculopathy in five cases. Ophthalmic Surg Lasers Imaging. 2012;43(5):366–73.
43. Grunwald L, Kligman BE, Shields CL. Acute exudative polymorphous paraneoplastic vitelliform maculopathy in a patient with carcinoma, not melanoma. Arch Ophthalmol. 2011;129(8):1104–6.
44. Koreen L, He SX, Johnson MW, Hackel RE, Khan NW, Heckenlively JR. Anti-retinal pigment epithelium antibodies in acute exudative polymorphous vitelliform maculopathy: a new hypothesis about disease pathogenesis. Arch Ophthalmol. 2011;129(1):23–9.
45. Khan J, McBain V, Santiago C, Lois N. Bilateral 'vitelliform-like' macular lesions in a patient with multiple myeloma. BMJ Case Rep. 2010;23:2010.
46. Sotodeh M, Paridaens D, Keunen J, van Schooneveld M, Adamus G, Baarsma S. Paraneoplastic vitelliform retinopathy associated with cutaneous or uveal melanoma and metastases. Klin Monatsbl Augenheilkd. 2005;222(11):910–4.
47. Eksandh L, Adamus G, Mosgrove L, Andreasson S. Autoantibodies against bestrophin in a patient with vitelliform paraneoplastic retinopathy and a metastatic choroidal malignant melanoma. Arch Ophthalmol. 2008;126(3):432–5.
48. Deutman AF, van Blommestein JD, Henkes HE, Waardenburg PJ, Solleveld-van Driest E. Butterfly-shaped pigment dystrophy of the fovea. Arch Ophthalmol. 1970;83(5):558–69.
49. Boon CJ, den Hollander AI, Hoyng CB, Cremers FP, Klevering BJ, Keunen JE. The spectrum of retinal

dystrophies caused by mutations in the peripherin/RDS gene. Prog Retin Eye Res. 2008;27(2):213–35.
50. Nichols BE, Drack AV, Vandenburgh K, Kimura AE, Sheffield VC, Stone EM. A 2 base pair deletion in the RDS gene associated with butterfly-shaped pigment dystrophy of the fovea. Hum Mol Genet. 1993;2(5):601–3.
51. Nichols BE, Sheffield VC, Vandenburgh K, Drack AV, Kimura AE, Stone EM. Butterfly-shaped pigment dystrophy of the fovea caused by a point mutation in codon 167 of the RDS gene. Nat Genet. 1993;3(3):202–7.
52. van Lith-Verhoeven JJ, Cremers FP, van den Helm B, Hoyng CB, Deutman AF. Genetic heterogeneity of butterfly-shaped pigment dystrophy of the fovea. Mol Vis. 2003;9:138–43.
53. den Hollander AI, van Lith-Verhoeven JJ, Kersten FF, Heister JG, de Kovel CG, Deutman AF, et al. Identification of novel locus for autosomal dominant butterfly shaped macular dystrophy on 5q21.2–q33.2. J Med Genet. 2004;41:699–702.
54. Saksens NT, Krebs MP, Schoenmaker-Koller FE, Hicks W, Yu M, Shi L. et al. Mutations in CTNNA1 cause butterfly-shaped pigment dystrophy and perturbed retinal pigment epithelium integrity. Nat Genet. 2015. [Published ahead of print].
55. Boon CJ, van Schooneveld MJ, den Hollander AI, van Lith-Verhoeven JJ, Zonneveld-Vrieling MN, Theelen T, et al. Mutations in the peripherin/RDS gene are an important cause of multifocal pattern dystrophy simulating STGD1/fundus flavimaculatus. Br J Ophthalmol. 2007;91(11):1504–11.
56. Fossarello M, Bertini C, Galantuomo MS, Cao A, Serra A, Pirastu M. Deletion in the peripherin/RDS gene in two unrelated Sardinian families with autosomal dominant butterfly-shaped macular dystrophy. Arch Ophthalmol. 1996;114(4):448–56.
57. Boon CJ, Jeroen Klevering B, Keunen JE, Hoyng CB, Theelen T. Fundus autofluorescence imaging of retinal dystrophies. Vis Res. 2008;48(26):2569–77.
58. Pinckers A. Patterned dystrophies of the retinal pigment epithelium. A review. Ophthalmic Paediatr Genet. 1988;9:77–114.
59. Prensky J, Bresnick G. Butterfly-shaped macular dystrophy in four generations. Arch Ophthalmol. 1983;101:1198–203.
60. DA Marano F, Aandekerk AL. Butterfly-shaped pigment dystrophy of the fovea associated with subretinal neovascularization. Graefes Arch Clin Exp Ophthalmol. 1996;234:270–4.
61. Marmor MF, McNamara JA. Pattern dystrophy of the retinal pigment epithelium and geographic atrophy of the macula. Am J Ophthalmol. 1996;122(3):382–92.
62. Boon CJ. Retinal dystrophies associated with the *PRPH2* gene. In: Puech B, De Laey J-J, Holder GE, editors. Inherited chorioretinal dystrophies. Berlin: Springer; 2014. p. 218–20.
63. Sjogren H. Dystrophia reticularis laminae pigmentosae retinae, an earlier not described hereditary eye disease. Acta Ophthalmol (Copenh). 1950;28(3):279–95.
64. Zerbib J, Querques G, Massamba N, Puche N, Tilleul J, Lalloum F, et al. Reticular pattern dystrophy of the retina: a spectral-domain optical coherence tomography analysis. Am J Ophthalmol. 2013;156(6):1228–37.
65. Hannan SR, de Salvo G, Stinghe A, Shawkat F, Lotery AJ. Common spectral domain OCT and electrophysiological findings in different pattern dystrophies. Br J Ophthalmol. 2013;97(5):605–10.
66. Chen MS, Chang CC, Tsai TH, Fan IM, Hou PK. Reticular dystrophy of the retinal pigment epithelium. J Formos Med Assoc. 2007;106(6):490–4.
67. Parodi MB, Liberali T, Pedio M, Francis PJ, Piccolino FC, Fiotti N, et al. Photodynamic therapy of subfoveal choroidal neovascularization secondary to reticular pattern dystrophy: three-year results of an uncontrolled, prospective case series. Am J Ophthalmol. 2006;141(6):1152–4.
68. Slezak H, Hommer K. Fundus pulverulentus. Albrecht von Graefes Arch Klin Exp Ophthalmol. 1969;178(2):176–82 [article in German].
69. O'Donnell FE, Schatz H, Reid P, Green WR. Autosomal dominant dystrophy of the retinal pigment epithelium. Arch Ophthalmol. 1979;97(4):680–3.
70. de Jong PT, Delleman JW. Pigment epithelial pattern dystrophy. Four different manifestations in a family. Arch Ophthalmol. 1982;100(9):1416–21.
71. Vaclavik V, Tran HV, Gaillard MC, Schorderet DF, Munier FL. Pattern dystrophy with high intrafamilial variability associated with Y141C mutation in the peripherin/RDS gene and successful treatment of subfoveal CNV related to multifocal pattern type with anti-VEGF (ranibizumab) intravitreal injections. Retina. 2012;32(9):1942–9.
72. Battaglia Parodi M. Choroidal neovascularization in fundus pulverulentus. Acta Ophthalmol Scand. 2002;80(5):559–60.
73. Agarwal A, Patel P, Adkins T, Gass JD. Spectrum of pattern dystrophy in pseudoxanthoma elasticum. Arch Ophthalmol. 2005;123(7):923–8.
74. Viola F, Barteselli G, Dell'Arti L, Vezzola D, Mapelli C, Villani E, Ratiglia R. Multimodal imaging in deferoxamine retinopathy. Retina. 2014;34(7):1428–38.

Stargardt Disease

3

Carel B. Hoyng, Stanley Lambertus, and Nathalie M. Bax

Abstract

Stargardt disease is the most prevalent inherited disease that causes visual impairment in childhood and young adults. Stargardt disease is caused by mutations in the ABCA4 gene. Although Stargardt disease was originally considered a juvenile macular degeneration, initial abnormalities may develop at early childhood until late adulthood and include a wide range of clinical, psychophysical, and imaging findings. In recent years, considerable advances have been made in our understanding of the clinical phenotypes, natural history, and molecular genetics of Stargardt disease and have led to the first steps in developing therapies.

Keywords

Retinal dystrophy • Stargardt • Fundus flavimaculatus • Flecks • *ABCA4* • STGD1 • Macula • Ophthalmogenetics • Juvenile macular degeneration

3.1 Introduction

Stargardt disease, also known as Stargardt 1 (STGD1), forms part of a heterogeneous group of inherited retinal dystrophies [1]. In fact, it is the most prevalent inherited disease that causes visual impairment in childhood, affecting 1: 8000–1:10,000 people worldwide [2]. It is an autosomal recessive retinal dystrophy and has been linked to mutations in the *ABCA4* gene [3]. Both sexes are equally affected. The disease typically presents within the first two decades of life, even though symptoms can also appear at adulthood or as late as the seventh decade. The age at onset has a trimodal distribution with means at about 7, 23 and 55 years with various abnormalities [4, 5 and unpublished data].

It is typically characterized by a progressive bilateral loss of central vision causing blurry vision [6]. Peripheral vision is usually unaffected. Most patients also have impaired color vision. Photophobia may be present.

The clinical diagnosis is based on ophthalmological examinations consisting of visual acuity, visual field testing, ophthalmoscopy, electroretinography, fluorescein angiography, fundus autofluorescence,

C.B. Hoyng, MD, PhD (✉) • S. Lambertus, MD
N.M. Bax, MD
Department of Ophthalmology, Radboud University Medical Center, Nijmegen, The Netherlands
e-mail: Carel.Hoyng@Radboudumc.nl

G. Querques, E.H. Souied (eds.), *Macular Dystrophies*, DOI 10.1007/978-3-319-26621-3_3

and optical coherence tomography. On ophthalmoscopy, progressive macular atrophy surrounded by irregular or pisciform yellow-white flecks is seen and may extend beyond the vascular arcades [7]. Fluorescein angiography may show a characteristic absence of choroidal background fluorescence, the so-called dark choroid. However, there is considerable clinical heterogeneity.

3.2 Early-Onset Stargardt

The mean age at onset of early-onset Stargardt is about 7 years. These patients all notice a fast decline in visual acuity, either by themselves, their parents, or school physicians. Therefore, the visual acuity is already severely decreased at the first visit to the ophthalmologist. This decrease in visual acuity may be initially unexplained, as ophthalmoscopy may not reveal any abnormalities or only minor central retinal pigment epithelium (RPE) alterations. Additional technical and genetic examinations are therefore required to exclude the diagnosis of early-onset Stargardt [4, 8].

3.2.1 Technical Examinations

Spectral-domain optical coherence tomography Thickening of the external limiting membrane (ELM) has been suggested as an early sign in the absence of other functional and structural changes to the retina. It may reflect a gliotic response to cellular stress at the photoreceptor level. Edges of the inner segment ellipsoid band appear to recede earlier than the ELM band in active lesions [9].

Fundus autofluorescence Atrophic foveal changes (sometimes as a bull's-eye lesion) appear as hypoautofluorescent lesions, surrounded by a hyperautofluorescent perifoveal ring and/or very subtle hyperautofluorescent flecks/dots. Hyperautofluorescence may precede the apparent atrophic changes.

Fluorescein angiography The dark choroid sign is present in approximately 75 % of patients.

Multifocal electroretinography A central decrease in sensitivity indicates early foveal dysfunction. Full-field electroretinography may not be informative, as this may indicate normal retinal function.

3.2.2 Natural Course

Apparent central atrophy and the hallmark of Stargardt disease, yellow-white flecks, may appear later. Flecks may not be limited to the posterior pole and tend to expand beyond the vascular arcades over time. Moreover, the atrophic RPE lesions also expand centrifugally throughout the posterior pole and thus not limited to the macula. This progressive retinal degeneration eventually results in profound chorioretinal atrophy with retinal pigmentations. At this stage, traces of yellow-white flecks may only be seen in the far periphery.

This rapid and severe retinal degeneration results in a severe visual impairment (20/200), which is usually reached before adulthood, and eventually, a visual acuity of about 20/500 or lower is expected at the age of about 40 years.

3.3 Intermediate-Onset Stargardt

The mean age at onset of intermediate-onset Stargardt is about 23 years (unpublished data). At presentation, the decrease in visual acuity is mild to moderate. On ophthalmoscopy, the typical yellow-white flecks can be found scattered throughout the retina (fundus flavimaculatus) or are confined to the posterior pole with a central macular atrophic lesion. Technical and genetic examinations can support the diagnosis of intermediate-onset Stargardt.

3.3.1 Technical Examinations

Spectral-domain optical coherence tomography Focal central loss of photoreceptor appears as disruptions of the inner segment ellipsoid band. Subsequently, an empty lesion devoid of photoreceptors may be found (optical gap) and atrophy of the retinal pigment epithelium band thereafter [10].

Fundus autofluorescence The yellow-white flecks are clearly visible as hyperautofluorescent flecks with or without a central hypoautofluorescent atrophic lesion.

Fluorescein angiography The dark choroid sign is present in approximately 80 % of patients.

3.3.2 Natural Course

The yellow-white flecks, as well as the atrophic RPE lesions, centrifugally expand over time. However, the expansion is likely to be much slower than in early-onset Stargardt. Moreover, atrophic lesions may be limited to the macula for years and may not even reach a severe chorioretinal degeneration during lifetime.

Patients with intermediate-onset disease are therefore more likely to retain useful visual acuity for a long period of time

3.4 Late-Onset Stargardt

The mean age at onset of late-onset Stargardt is about 55 years. Patients generally present with either a mild decrease in visual acuity, metamorphopsia, oscillopsia, or visual field defects. Patients can be even asymptomatic and can coincidentally be found during ophthalmologic screening for other diseases. In most cases, ophthalmoscopy shows typical yellow-white flecks scattered throughout the retina or confined to the center of the macula. Atrophic RPE lesions may be seen in the macula but are not always present. When they are seen, the fovea is often spared from these atrophic lesions [5, 11, 12].

3.4.1 Technical Examination

Spectral-domain optical coherence tomography It may reveal relative central sparing of the photoreceptor layer, indicating foveal sparing of retinal damage.

Fundus autofluorescence The yellow-white flecks correspond with hyperautofluorescence. Sometimes, these flecks are surrounded by a halo of reduced autofluorescence. In most cases, a relatively preserved autofluorescence signal of the fovea is seen. The yellow-white flecks are clearly visible as hyperautofluorescent flecks with or without a central hypoautofluorescent atrophic lesion.

Full-field electroretinography Photopic and scotopic full-field ERG recordings are normal or relatively normal.

3.4.2 Natural Course

A distinctive characteristic of late-onset Stargardt is so-called foveal sparing. Although numerous yellow-white flecks can be found throughout the retina, the fovea is somehow not affected by atrophic lesions. Islands of sharply delineated atrophic RPE lesions appear around the fovea. These lesions interconnect, leaving only a single isthmus of RPE, thus resulting in a "peninsula-like" appearance, followed by a fovea that is completely surrounded by RPE atrophy. Foveal structure and function are relatively preserved, until the fovea eventually becomes affected by the increasing RPE atrophy.

If foveal sparing is seen, visual acuity is preserved for a long time. Due to the extensive surrounding RPE atrophy, patients switch between central fixation with a good visual acuity and far eccentric fixation. Eventually, loss of foveal sparing will result in a sudden decrease in visual acuity.

3.5 Molecular Genetics

Stargardt disease is caused by mutations in the *ABCA4* gene. *ABCA4* encodes for the adenosine triphosphate (ATP)-binding cassette transporter (ABCR) expressed specifically in the cones and rods of the retina. A dysfunctional ABCR results in inadequate handling of all-trans-retinal in outer segments of photoreceptor cells with the result that phototoxic bisretinoids of lipofuscin, including A2E, form in abundance. Disc shedding and subsequent phagocytosis of the outer segments by RPE cells lead to significant lysosomal accumulations of lipofuscin, ultimately causing RPE cell death and the subsequent loss of photoreceptors [13, 14]. There is considerable allelic heterogeneity, with more than 1000 variants in *ABCA4*, having been reported to date. Mutations of *ABCA4* have been linked to a spectrum of phenotypes ranging from age-related macular disease (AMD) to retinitis pigmentosa (RP) [15–17].

3.6 Differential Diagnosis

The main challenges in diagnosing Stargardt disease lie in the early-onset and late-onset spectrum.

Early-onset Stargardt If no yellow-white flecks are seen on ophthalmoscopy, patterns on full-field electroretinography may only point to a cone dystrophy, cone-rod dystrophy, or even rod-cone dystrophy. Early optic disc pallor, hyperpigmentations, and arteriolar attenuation indicate a cone-(rod) dystrophy but can also be found at later stages of early-onset Stargardt. Various genes underlie these descriptive and electrophysiological diagnoses (Table 3.1). These disorders are characterized by visual loss, abnormalities of color vision, visual field loss, and a variable degree of nystagmus, photophobia, and nyctalopia. Specific genetic testing for mutations on the *ABCA4* gene may therefore be the only approach to confirm the diagnosis of Stargardt disease.

Late-onset Stargardt The misunderstanding is that patients with an age at onset 50 years or above cannot have a retinal dystrophy and are thus most likely diagnosed with AMD.

Moreover, the clinical phenotype of foveal sparing is not exclusively found in late-onset Stargardt. Geographic atrophy in AMD, mitochondrial retinal dystrophy (MIDD) associated with the m.3243A>G mutation, central areolar choroidal dystrophy (CACD), and pseudo-Stargardt should also be considered and differentiated by genetic testing.

In addition, two autosomal dominant types of macular dystrophy exist that resemble STGD1:

- STGD3 caused by mutations in the *ELOVL4* gene [18]
- STGD4 associated with mutations in the *PROM1* gene [19]

Table 3.1 General electrophysiological abnormalities in Stargardt disease compared to cone and cone-rod dystrophies

	Photopic ERG	Scotopic ERG	Multifocal ERG
Stargardt	N/↓	N/↓	↓
Cone dystrophies	↓↓	N	↓↓
Cone-rod dystrophies	↓↓	↓	↓↓

3.7 Treatment

There is currently no treatment available for Stargardt disease. Gene replacement and stem cell therapy is under development.

Because of the pathogenesis of Stargardt disease (mutations in the *ABCA4* gene), sunlight protection by wearing sunglasses should be advised, as well as having a normal diet without inappropriate prescription of vitamin A supplements. These are the only preventive measures for slowing down the progression of disease. Regular ophthalmologic evaluations are recommended.

3.8 Remark

Due to the high clinical variability, prognosis depends on different parameters (in particular age at onset, severity of ABCA4 mutations, and electroretinographic findings) (Table 3.2) that may help the clinician provide the patient with an indication of the course of disease. Stargardt disease may progress rapidly over a few months rather than several years, leading to a severe decrease in visual acuity (Fig. 3.1). Peripheral

Table 3.2 Overview of types of Stargardt disease

Age at onset	Typical abnormalities at fundoscopy	Visual acuity decline	End-stage visual acuity (Snellen)	ERG abnormalities	ABCA4 mutations
Early (mean, 7 years)	None/bull's-eye/ central atrophy	Fast	Hand movement	Cone-rod	Severe–severe
Intermediate (mean, 23 years)	Yellowish flecks/ fundus flavimaculatus	Moderate	20/1200–20/200	Cone	Severe–mild
Late (mean, 55 years)	Foveal sparing	Slow	20/100–20/40	None	Mild–mild

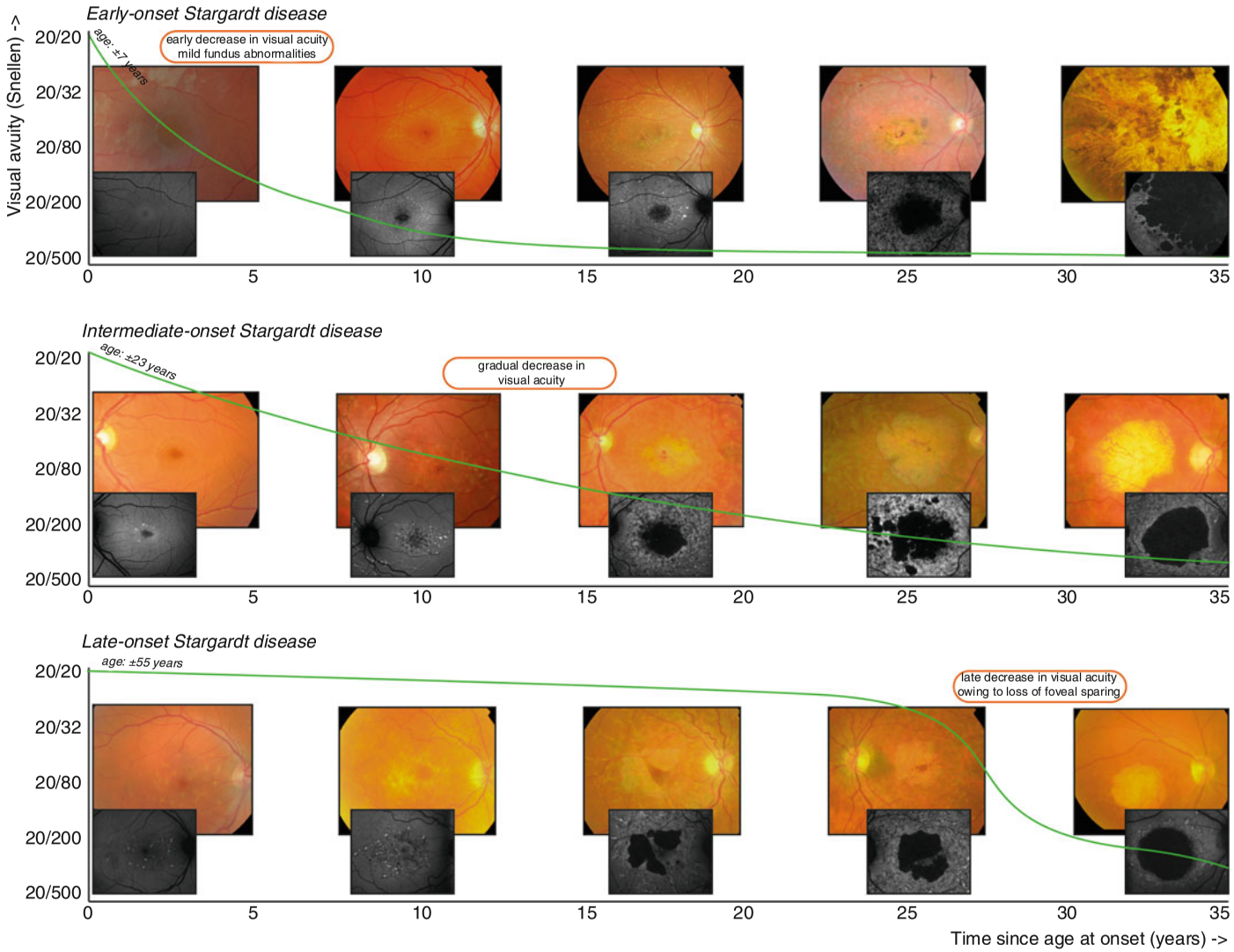

Fig. 3.1 Overview of disease progression in subtypes of Stargardt disease. Subtypes have distinctive disease onsets, indicating the severity of disease. The visual acuity decline is fast in early-onset Stargardt, whereas in late-onset Stargardt, visual acuity is affected only several years after disease onset

vision is not affected, even though some patients progress to a cone-rod phenotype that does affect the peripheral retinal function.

References

1. Stargardt K. Über familliäre, progressive Degeneration in der Maculagegend des Auges. Graefes Arch Clin Exp Ophthalmol. 1909;71:534–50.
2. Blacharski PA. Fundus flavimaculatus. In: Newsome, DA (ed): Retinal Dystrophies and Degenerations. New York: Raven Press. 1988; pp 135–59.
3. Allikmets R, Singh N, Sun H, Shroyer NF, Hitchinson A, Chidambaram A, et al. A photoreceptor cell-specific ATP-binding transporter gene (ABCR) is mutated in recessive Stargardt macular dystrophy. Nat Genet. 1997;15(3):236–46.
4. Franceschetti A. A special form of tapetoretinal degeneration: fundus flavimaculatus. Trans Am Acad Opthalmol Otolaryngol. 1965;69(6):1048–53.
5. van Huet RA, Bax NM, Westeneng-van Haaften SC, Muhamad M, Zonneveld-Vrieling MN, Hoefsloot LH, et al. Foveal sparing in Stargardt disease. Invest Ophthalmol Vis Sci. 2014;55(11):7467–78.
6. Rotenstreich Y, Fishman GA, Anderson RJ. Visual acuity loss and clinical observations in a large series of patients with Stargardt disease. Ophthalmology. 2003;110(6):1151–8.
7. Lambertus S, van Huet RA, Bax NM, Hoefsloot LH, Cremers FP, Boon CJ, et al. Early-onset Stargardt disease: phenotypic and genotypic characteristics. Ophthalmology. 2015;122(2):335–44.
8. Fujinami K, Zernant J, Chana RK, Wright GA, Tsunoda K, Ozawa Y, et al. Clinical and molecular characteristics of childhood-onset Stargardt disease. Ophthalmology. 2015;122(2):326–34.
9. Lee W, Noupuu K, Oll M, Duncker T, Burke T, Zemant J, et al. The external limiting membrane in early-onset Stargardt disease. Invest Ophthalmol Vis Sci. 2014;55(10):6139–49.
10. Nõupuu K, Lee W, Zernant J, Tsang SH, Allikmets R. Structural and genetic assessment of the *ABCA4*-associated optical gap phenotype. Invest Ophthalmol Vis Sci. 2014;55(11):7217–26.
11. Fujinami K, Sergouniotis PI, Davidson AE, Wright G, Chana RK, Tsunoda K, et al. Clinical and molecular analysis of Stargardt disease with preserved foveal structure and function. Am J Ophthalmol. 2013;156(3):487–501.e1.
12. Westeneng-van Haaften SC, Boon CJ, Cremers FP, Hoefsloot LH, den Hollander AI, Joyng CB. Clinical and genetic characteristics of late-onset Stargardt's disease. Ophthalmology. 2012;119(6):1199–210.
13. Weng J, Mata NL, Azarian SM, Tzekov RT, Birch DG, Travis GH. Insights into the function of Rim protein in photoreceptors and etiology of Stargardt's disease from the phenotype in abcr knockout mice. Cell. 1999;98(1):13–23.
14. Charbel Issa P, Barnard AR, Singh MS, Carter E, Jiang Z, Radu RA, et al. Fundus autofluorescence in the *Abca4*(−/−) mouse model of Stargardt disease—correlation with accumulation of A2E, retinal function, and histology. Invest Ophthalmol Vis Sci. 2013;54(8):5602–12.
15. Klevering BJ, Blankenagel A, Maugeri A, Cremers FP, Joyng CB, Rohrschneider K. Phenotypic spectrum of autosomal recessive cone-rod dystrophies caused by mutations in the *ABCA4* (ABCR) gene. Invest Ophthalmol Vis Sci. 2002;43(6):1980–5.
16. Klevering BJ, Deutman AF, Maugeri A, Cremers FP, Hoyng CB. The spectrum of retinal phenotypes caused by mutations in the *ABCA4* gene. Graefes Arch Clin Exp Ophthalmol. 2005;243(2):90–100.
17. van Driel MA, Maugeri A, Klevering BJ, Hoyng CB, Cremers FP. ABCR unites what ophthalmologists divide(s). Ophthalmic Genet. 1998;19(3):117–22.
18. Stone EM, Nichols BE, Kimura AE, Weingeist TA, Drack A, Sheffield VC. Clinical features of a Stargardt-like dominant progressive macular dystrophy with genetic linkage to chromosome 6q. Arch Ophthalmol. 1994;112(6):765–72.
19. Kniazeva M, Chiang MF, Morgan B, Anduze AL, Zack DJ, Han M, Zhang K. A new locus for autosomal dominant stargardt-like disease maps to chromosome 4. Am J Hum Genet. 1999;64(5):1394–9.

Macular Changes in Generalized Retinal Dystrophies and in Cone Dystrophies

4

Carel B. Hoyng and Ramon A.C. van Huet

Abstract

Macular changes in generalized retinal dystrophies may vary from slight pigmentary changes to atrophic lesions or bull's-eye retinopathy. However, often in the initial stage of the disease, no changes may be found in the posterior pole. Cystoid macular edema can lead to visual disturbance in the early phase of certain types of retinal dystrophies. Sometimes, they may respond to oral acetazolamide. In cone dystrophies, no clear abnormalities may be found in the macula in the early stages. Electrophysiological tests, like multifocal electroretinography and optical coherence tomography, are needed to make the diagnosis. Most frequent macular changes, however, are pigmentary changes and bull's-eye retinopathy.

Keywords

Macular • Dystrophy • Imaging • Retinitis pigmentosa • Cone dystrophy

4.1 Macular Changes in Generalized Retinal Dystrophies and in Cone Dystrophies

The most prevalent generalized retinal dystrophies are rod-cone dystrophies (retinitis pigmentosa, d.i. RP) with a prevalence of approximately 1 in 4,000 [1]. Cone-rod dystrophies (CRD) are more rare with a prevalence of approximately 1 in 30,000–40,000 [2]. Diagnosis is commonly made by the fundoscopic changes and full-field electroretinography (ffERG). In RP, the ffERG reveals changes in the rod-driven responses that precede changes in the cone-driven responses, while in CRD, the cones are initially affected, followed by the rods [2–5]. In later stages, both rod- and cone-driven responses may be equally affected. The initial examination of these patients not always takes place in the earliest stages of the disease, which often makes the differentiation between RP and CRD difficult, since fundoscopic changes overlap. Hence, one has to rely on the initial complaints of the patient. RP patients often experience nyctalopia with relatively good vision as the first symp-

C.B. Hoyng, MD, PhD (✉) • R.A.C. van Huet, MD
Department of Ophthalmology (400), Radboud University Medical Center, P.O. Box 9101, Nijmegen 6500 HB, The Netherlands
e-mail: Carel.Hoyng@Radboudumc.nl

G. Querques, E.H. Souied (eds.), *Macular Dystrophies*, DOI 10.1007/978-3-319-26621-3_4

tom, while CRD patients initially notice a fast decrease in vision and photophobia [4, 6].

Up to now, approximately 120 genes and 7 additional loci have been associated with RP, and 17 genes and some additional loci with CRD, including all Mendelian inheritance patterns (RetNet, available at https://sph.uth.edu/retnet/). Further elaboration on the genetic causes of generalized retinal dystrophies, either syndromic or nonsyndromic, is beyond the scope of this chapter.

Various macular changes occur in RP and CRD that vary from subtle pigment alterations to profound atrophy. Macular changes in RP and CRD often are dynamic processes and change over the course of the disease. We listed the most common macular abnormalities in RP and CRD.

4.2 Macular Changes in Generalized Retinal Dystrophies

4.2.1 No (Obvious) Abnormalities

RP often reveals no macular abnormalities on fundoscopy, fundus autofluorescence (FAF), and optical coherence tomography (OCT). A study on macular abnormalities in a large cohort of 518 Italian RP patients revealed no macular abnormalities in 56 % [7]. In absence of macular changes, early complaints of night blindness and subtle pigmentary changes in the peripheral retina, together with diminished responses on the scotopic ERG, may lead to the diagnosis. Family history is of additional value, especially in autosomal dominant or X-linked inheritance.

The first visual complaints in CRD may occur in absence of abnormalities in clinical and electrophysiological examination. CRD generally has an onset during childhood, and the first visual changes may be observed by coincidentally during routine screening programs. [8] In our own cohort of CRD patients with no ophthalmic abnormalities at young age, 50 % of them were suspected of conversion disorders or malingering and were referred for psychological or psychiatric examination. If no fundoscopic macular abnormalities are present, OCT may reveal subtle thickening of the external limiting membrane (ELM) and fundus autofluorescence (FAF) imaging may reveal subtle diffuse central hyperautofluorescence that is easily overlooked. However, these findings have been described in few cases with Stargardt disease and no large studies in RP or CRD cases have been performed yet [9–11].

4.2.2 Pigmentary Changes

Changes in the macular pigment epithelium are often present in CRD and less frequently in RP. Changes may vary from a granular aspect of the RPE to profound intraretinal pigmentation following RPE migration (Figs. 4.1 and 4.2). Subtle changes often precede further deterioration of the macular RPE, either in a bull's-eye pattern or in geographic atrophy of the posterior pole. Irregular pigmentations follow intraretinal migration of the RPE cells after photoreceptor cell death occurred and generally appear in end-stage disease.

4.2.3 Bull's-Eye Maculopathy

Fundoscopic Bull's-Eye Maculopathy Bull's-eye maculopathy (BEM) is a distinctive yet nonspecific macular phenotype characterized by annular atrophy or hypopigmentation of the reti-

Fig. 4.1 Parafoveal hyperpigmentation in a patient with retinitis pigmentosa

Fig. 4.2 Wide ring of hyperautofluorescence surrounding area of hypoautofluorescence in same patient as in Fig. 4.1

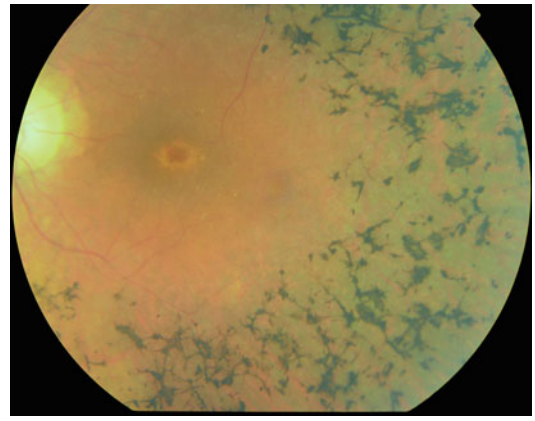

Fig. 4.3 Bull's-eye maculopathy in a patient with *IMPG2*-associated retinitis pigmentosa

Fig 4.4 Ring of hyperautofluorescence in retinitis pigmentosa

nal pigment epithelium (RPE) surrounding the fovea that occurs in various diseases affecting the bipolar cell layer, photoreceptor cell layer, or RPE [12]. BEM was initially described in association with chloroquine retinopathy [13], but now, BEM has also been associated with a heterogeneous group of inherited retinal disorders, including CRD and RP.

In CRD, BEM is often observed, although it often develops into profound macular atrophy over time [6]. In RP, BEM is far less common and has been described in specific forms, including (1) in syndromic RP such as Bardet-Biedl syndrome [14], (2) in nonsyndromic RP (e.g., *RPGR*-related and *IMPG2*-related RP) [15–17], and (3) in RP with Stargardt-like maculopathy (Fig. 4.3) [18]. A study in 41 patients with the p.R373C mutation in the *PROM1* gene revealed a BEM with large electrophysiological variance: 60 % had macular dystrophy, 36 % had CRD or RP, and 4 % had isolated cone dystrophy [17].

"Bull's-Eye" Ring on Fundus Autofluorescence The hyperautofluorescent ring found in RP patients is thought to represent the transitional zone between abnormal paracentral and normal central photoreceptor outer segment structure, which correlates and delineates the retinal region with visual field preservation (Fig. 4.4) [19–21]. The abnormal autofluorescence may suggest an anomalous high rate of photoreceptor phagocytosis and the changes in the RPE function may be a secondary phenomenon from increased metabolic load on the RPE because of photoreceptor apoptosis. The high load of lipofuscin that causes a maxi-

mum intensity of hyperautofluorescence would lead to the RPE atrophy with a subsequent loss of lipofuscin granules [19, 22]. Photoreceptor loss along with RPE atrophy is seen outside the ring and is represented by hypoautofluorescence.

4.2.4 Cystoid Macular Edema

Today, cystic macular edema (CME) represents a known pathologic complication in patients with hereditary retinal degenerations such as RP, X-linked retinoschisis, *NR2E3*-associated disease (including enhanced S-cone syndrome and Goldmann-Favre syndrome), choroideremia, and gyrate atrophy [23]. CME is characterized by a localized expansion of the macular intracellular and/or extracellular space. The reported prevalence of CME in RP patients varies historically between 8 % and 38 % [5, 7, 24–28]. OCT is highly sensitive for CME and useful for evaluating response to therapy and is more useful than fluorescein angiography (FA) because of a lack of intense fluorescein leakage [29, 30]. On OCT images, CME is represented by increased retinal thickness and the presence of intraretinal low reflectivity characterized as two distinct features: (1) outer retinal swelling represented by an ill-defined, widespread hyporeflective area of thickening and (2) cystic hyporeflective spaces, with high signal elements bridging the retinal layers (Fig. 4.5) [25, 31]. Vitreous traction, as well as epiretinal membranes, probably plays a contributing casual role in the development of CME in RP and other inherited retinal dystrophies [32]. Vitreous abnormalities are well documented in all stages of RP [33–35]. Tangential vitreous traction would potentially lead to a breakdown of the blood-retina barrier and promote the development of CME in retinal dystrophies [36]. In this event, a surgical approach might result in a reduction in CME [32].

Successful treatment of nontractional CME has been reported with carbonic anhydrase inhibitors (CAIs), which are thought to be effective through their action on the membrane-bound carbonic anhydrase (CA) IV receptors present on the RPE cells (Fig. 4.6) [31, 37, 38]. Moreover, other CAs in different retinal neurons also may play a role. CAIs act both on retinal and RPE cell function by acidifying the subretinal space, decreasing the standing potential, as well as increasing retinal adhesiveness. Retinal adhesiveness probably is enhanced by increasing RPE fluid transport. [39] CAIs therefore decrease the volume of the subretinal space. A significant effect on macular blood flow however has not been demonstrated [40].

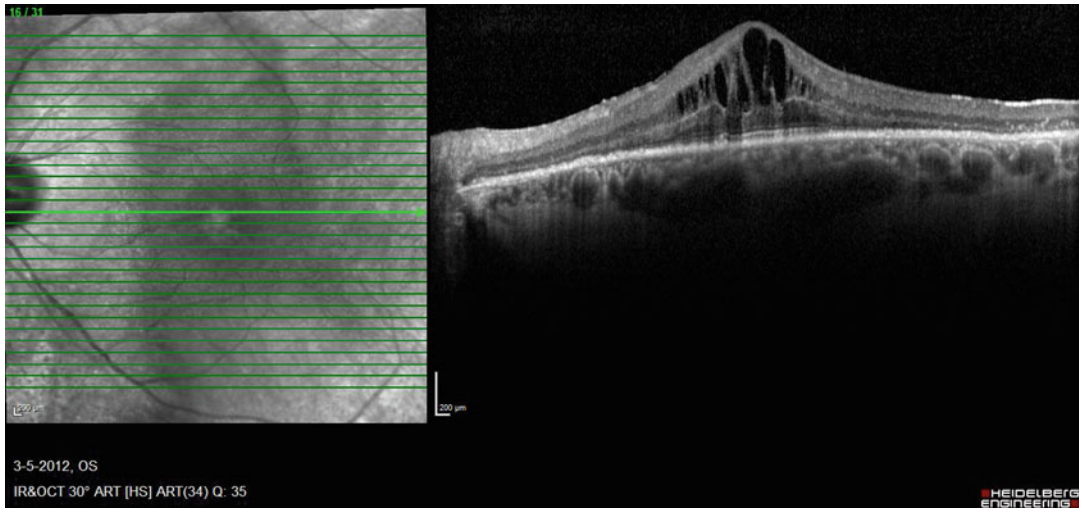

Fig. 4.5 Cystoid macular edema in a patient with retinitis pigmentosa type 17

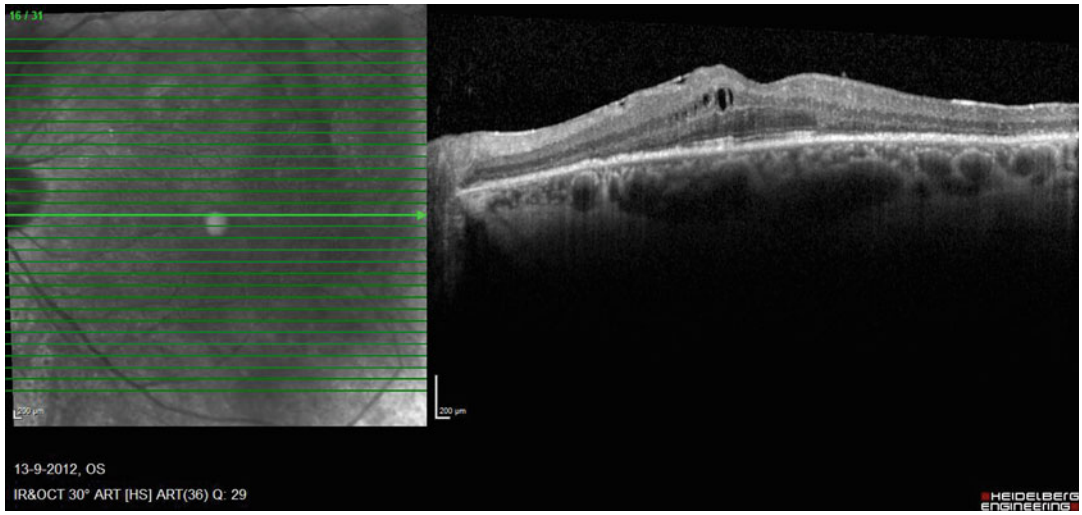

Fig. 4.6 Same patient as in Fig. 4.5 after oral treatment with acetazolamide 250 mg three times daily

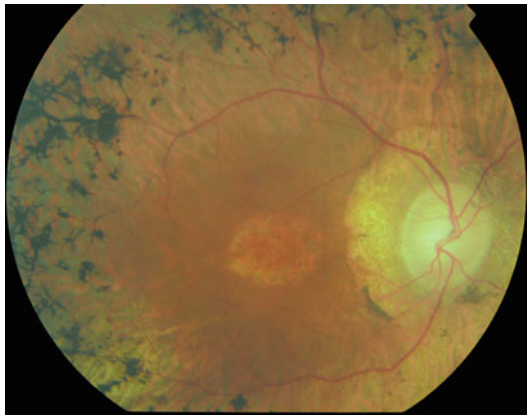

Fig. 4.7 Macular atrophy in a patient with retinitis pigmentosa due to *IMPG2* mutations

4.2.5 Epiretinal Membrane

Abnormalities of the vitreous-retinal interface frequently occur in retinal dystrophies [41]. Testa et al. reported 16 % epiretinal membranes in a large Italian cohort of RP patients [7]. ERM was defined as a membrane adherent to the inner retina, which presented as being globally or focally adherent. The diagnosis of ERM by OCT is based on the presence of a green line, with reddish tinges, that runs over the retinal surface, often together with underlying waves in the retinal surface layer due to tractional forces. Depending on the traction and anatomical disturbance of the underlying retinal layers, as well as the burden of symptoms caused by the ERM, there might be an indication for surgery [32].

4.2.6 Macular Atrophy

Macular geographic atrophy is the end-stage observation in CRD and in some forms of RP. In general, earlier and more subtle changes, as described above, precede the geographic atrophy (Fig. 4.7).

4.3 Macular Changes in Cone Dystrophy

4.3.1 No (Obvious) Macular Abnormalities

In cone dystrophy (CD), 10–20 % of the cases present with no obvious fundus abnormalities at first presentation. Often, the only abnormalities in clinical examination, apart from a decrease in visual acuity, are a reduction of cone potentials on the ERG or abnormal values in multifocal ERG.

However, fundus autofluorescence imaging may reveal subtle central hyperautofluorescence.

In case of achromatopsia (although it is stationary, it is often referred to as cone dysfunction), a small central "gap" in the photoreceptor outer segment layer may be apparent on the OCT. [8] New, high-resolution imaging such as adaptive optics may show abnormalities in patients without obvious fundoscopic changes [42].

4.3.2 Pigmentary Changes

Pigmentary changes can be seen in all kind of CD and vary from subtle alterations of the RPE to profound intraretinal pigment deposits due to RPE migration. In our cohort of 139 patients, about 50 % showed pigmentary changes. Most of the CD caused by mutations in the *ABCA4* gene show pigmentary changes and may additionally reveal a dark choroid on fluorescence angiography and even small hyperautofluorescent flecks on autofluorescence [11]. It is a matter of dispute whether this phenotype should not be called Stargardt disease. Most of these cases progress into a CRD.

4.3.3 Bull's-Eye Retinopathy and Macular Atrophy

Bull's-eye maculopathy represents a heterogeneous group of disorders. The clinical appearance is not helpful in assessing the degree of retinal dysfunction, and the ring of atrophy or hypopigmentation may vary in degrees of eccentricity from the fovea (Figs. 4.8 and 4.9). It is considered distinct from Stargardt maculopathy in which the atrophy is physically discontinuous, as best demonstrated by fundus autofluorescence imaging. The mechanisms by which the degeneration occurs in this striking distribution are not well understood [43]. The appearance may correspond to the pattern of lipofuscin accumulation in RPE cells, which in healthy subjects is highest at the posterior pole and shows a depression at the fovea, thus explaining the annular pattern and central sparing. Furthermore, the small area of central sparing was postulated as being due to a photoprotective effect of the high foveal concentration of luteal pigment.

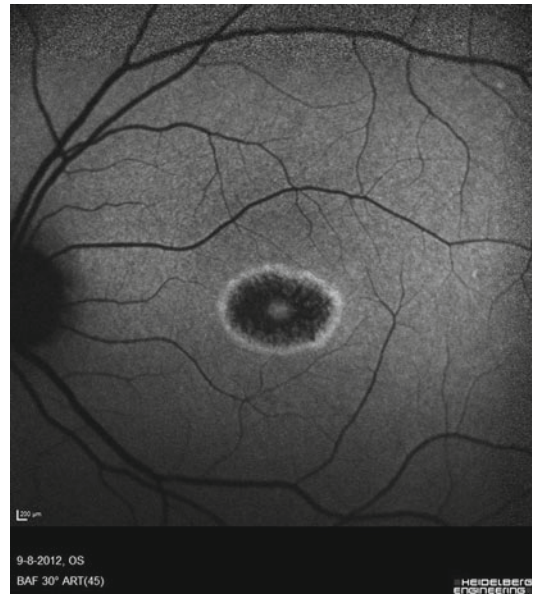

Fig. 4.8 Bull's-eye maculopathy in a patient with cone dystrophy

Fig. 4.9 Fluorescein angiography in same patient as in Fig. 4.8

The initially spared center usually becomes involved during the disease, at which point the diagnosis of bull's-eye maculopathy can no longer be made, and the atrophy is named geographic macular atrophy (Figs. 4.10 and 4.11).

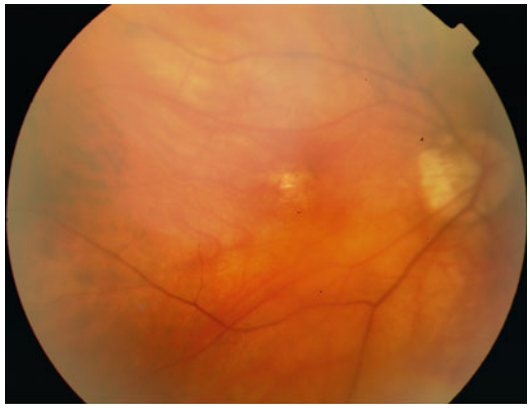

Fig. 4.10 Central atrophy in a patient with cone dystrophy due to a mutation in the *MFSD8* gene

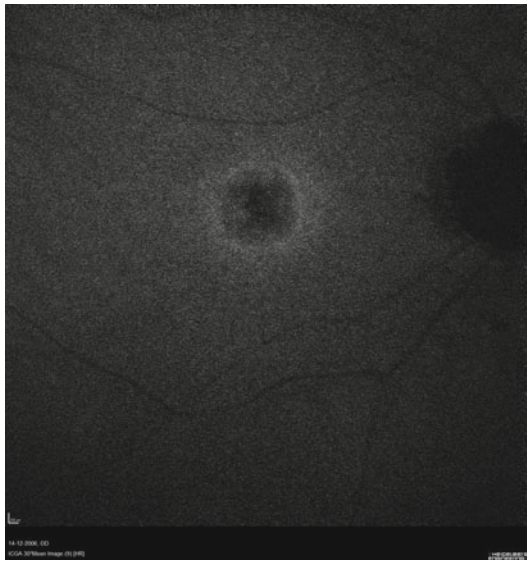

Fig. 4.11 Autofluorescence imaging in same patient as in Fig. 4.10 revealing foveal atrophy and parafoveal hyperautofluorescence

References

1. Bunker CH, Berson EL, Bromley WC, Hayes RP, Roderick TH. Prevalence of retinitis pigmentosa in Maine. Am J Ophthalmol. 1984;97(3):357–65.
2. Hamel CP. Cone rod dystrophies. Orphanet J Rare Dis. 2007;2:7.
3. Hamel C. Retinitis pigmentosa. Orphanet J Rare Dis. 2006;1:40.
4. Hartong DT, Berson EL, Dryja TP. Retinitis pigmentosa. Lancet. 2006;368(9549):1795–809.
5. Berson EL. Retinitis pigmentosa. The Friedenwald lecture. Invest Ophthalmol Vis Sci. 1993;34(5):1659–76.
6. Roosing S, Thiadens AA, Hoyng CB, Klaver CC, den Hollander AI, Cremers FP. Causes and consequences of inherited cone disorders. Prog Retin Eye Res. 2014;42:1–26.
7. Testa F, Rossi S, Colucci R, Gallo B, Di Iorio V, della Corte M, et al. Macular abnormalities in Italian patients with retinitis pigmentosa. Br J Ophthalmol. 2014;98(7):946–50.
8. Thiadens AA, Phan TM, Zekveld-Vroon RC, Leroy BP, van den Born LI, Hoyng CB, et al. Clinical course, genetic etiology, and visual outcome in cone and cone-rod dystrophy. Ophthalmology. 2012;119(4):819–26.
9. Burke TR, Yzer S, Zernant J, Smith RT, Tsang SH, Allikmets R. Abnormality in the external limiting membrane in early Stargardt disease. Ophthalmic Genet. 2013;34(1–2):75–7.
10. Lee W, Nõupuu K, Oll M, Duncker T, Burke T, Zernant J, et al. The external limiting membrane in early-onset Stargardt disease. Invest Ophthalmol Vis Sci. 2014;55(10):6139–49.
11. Lambertus S, van Huet RA, Bax NM, Hoefsloot LH, Cremers FP, Coon CJ, et al. Early-onset stargardt disease: phenotypic and genotypic characteristics. Ophthalmology. 2015;122(2):335–44.
12. Pinckers A, Cruysberg JR, de Kerk AL. Main types of bull's eye maculopathy. Functional classification. Doc Ophthalmol. 1984;58(3):257–67.
13. Hobbs HE, Sorsby A, Freedman A. Retinopathy following chloroquine therapy. Lancet. 1959;2(7101):478–80.
14. Campo RV, Aaberg TM. Ocular and systemic manifestations of the Bardet-Biedl syndrome. Am J Ophthalmol. 1982;94(6):750–6.
15. Koenekoop RK, Loyer M, Hand CK, Al Mahdi H, Dembinska O, Beneish R, et al. Novel RPGR mutations with distinct retinitis pigmentosa phenotypes in French-Canadian families. Am J Ophthalmol. 2003;136(4):678–87.
16. Kikawa E, Nakazawa M, Chida Y, Shiono T, Tamai M. A novel mutation (Asn244Lys) in the peripherin/RDS gene causing autosomal dominant retinitis pigmentosa associated with bull's-eye maculopathy detected by nonradioisotopic SSCP. Genomics. 1994;20(1):137–9.
17. Michaelides M, Gaillard MC, Escher P, Tiab L, Bedell M, Borruat FX, et al. The PROM1 mutation p.R373C causes an autosomal dominant bull's eye maculopathy associated with rod, rod-cone, and macular dystrophy. Invest Ophthalmol Vis Sci. 2010;51(9):4771–80.
18. Suzuki R, Hirose T. Bull's-eye macular dystrophy associated with peripheral involvement. Ophthalmol J Int Ophtalmol Int J Ophthalmol Z Augenheilkd. 1998;212(4):260–7.
19. Greenstein VC, Duncker T, Holopigian K, Carr RE, Greenberg JP, Tsang SH, Hood DC. Structural and functional changes associated with normal and

abnormal fundus autofluorescence in patients with retinitis pigmentosa. Retina. 2012;32(2):349–57.
20. Popovic P, Jarc-Vidmar M, Hawlina M. Abnormal fundus autofluorescence in relation to retinal function in patients with retinitis pigmentosa. Graefes Arch Clin Exp Ophthalmol. 2005;243(10):1018–27.
21. Lima LH, Cella W, Greenstein VC, Wang NK, Busuioc M, Smith RT, et al. Structural assessment of hyperautofluorescent ring in patients with retinitis pigmentosa. Retina. 2009;29(7):1025–31.
22. Delori FC, Dorey CK, Staurenghi G, Arend O, Goger DG, Weiter JJ. In vivo fluorescence of the ocular fundus exhibits retinal pigment epithelium lipofuscin characteristics. Invest Ophthalmol Vis Sci. 1995;36(3):718–29.
23. Ganesh A, Stroh E, Manayath GJ, Al-Zuhaibi S, Levin AV. Macular cysts in retinal dystrophy. Curr Opin Ophthalmol. 2011;22(5):332–9.
24. Newsome DA. Retinal fluorescein leakage in retinitis pigmentosa. Am J Ophthalmol. 1986;101(3):354–60.
25. Hirakawa H, Iijima H, Gohdo T, Tsukahara S. Optical coherence tomography of cystoid macular edema associated with retinitis pigmentosa. Am J Ophthalmol. 1999;128(2):185–91.
26. Fishman GA, Fishman M, Maggiano J. Macular lesions associated with retinitis pigmentosa. Arch Ophthalmol. 1977;95(5):798–803.
27. Fetkenhour CL, Choromokos E, Weinstein J, Shoch D. Cystoid macular edema in retinitis pigmentosa. Trans Am Acad Opthalmol Otolaryngol. 1977;83(3 Pt 1):OP515–21.
28. Walia S, Fishman GA, Hajali M. Prevalence of cystic macular lesions in patients with Usher II syndrome. Eye (Lond). 2009;23(5):1206–9.
29. Kim YJ, Joe SG, Lee DH, Lee JY, Kim JG, Yoon YH. Correlations between spectral-domain OCT measurements and visual acuity in cystoid macular edema associated with retinitis pigmentosa. Invest Ophthalmol Vis Sci. 2013;54(2):1303–9.
30. Stanga PE, Downes SM, Ahuja RM, Chong NH, Antcliff R, Reck AC, Bird AC. Comparison of optical coherence tomography and fluorescein angiography in assessing macular edema in retinal dystrophies: preliminary results. Int Ophthalmol. 2001;23(4–6):321–5.
31. Apushkin MA, Fishman GA, Janowicz MJ. Monitoring cystoid macular edema by optical coherence tomography in patients with retinitis pigmentosa. Ophthalmology. 2004;111(10):1899–904.
32. Hagiwara A, Yamamoto S, Ogata K, Sugawara T, Hiramatsu A, Shibata M, Mitamura Y. Macular abnormalities in patients with retinitis pigmentosa: prevalence on OCT examination and outcomes of vitreoretinal surgery. Acta Ophthalmol. 2011;89(2):e122–5.
33. Pruett RC. Retinitis pigmentosa: clinical observations and correlations. Trans Am Ophthalmol Soc. 1983;81:693–735.
34. Vingolo EM, Giusti C, Forte R, Onori P. Vitreal alterations in retinitis pigmentosa: biomicroscopic appearance and statistical evaluation. Ophthalmologica. 1996;210(2):104–7.
35. Yoshida N, Ikeda Y, Notomi S, Ishikawa K, Murakami Y, Hisatomi T, et al. Clinical evidence of sustained chronic inflammatory reaction in retinitis pigmentosa. Ophthalmology. 2013;120(1):100–5.
36. Takezawa M, Tetsuka S, Kakehashi A. Tangential vitreous traction: a possible mechanism of development of cystoid macular edema in retinitis pigmentosa. Clin Ophthalmol. 2011;5:245–8.
37. Salvatore S, Fishman GA, Genead MA. Treatment of cystic macular lesions in hereditary retinal dystrophies. Surv Ophthalmol. 2013;58(6):560–84.
38. Cox SN, Hay E, Bird AC. Treatment of chronic macular edema with acetazolamide. Acta Ophthalmol. 1988;106(9):1190–5.
39. Moldow B, Sander B, Larsen M, Engler C, Li B, Rosenberg T, Lund-Andersen H. The effect of acetazolamide on passive and active transport of fluorescein across the blood-retina barrier in retinitis pigmentosa complicated by macular oedema. Graefes Arch Clin Exp Ophthalmol. 1998;236(12):881–9.
40. Grunwald JE, Mathur S, DuPont J. Effects of dorzolamide hydrochloride 2% on the retinal circulation. Acta Ophthalmol Scand. 1997;75(3):236–8.
41. Triolo G, Pierro L, Parodi MB, De Bendedetto U, Gagliardi M, Manitto MP, Bandello F. Spectral domain optical coherence tomography findings in patients with retinitis pigmentosa. Ophthalmic Res. 2013;50(3):160–4.
42. Duncan JL, Zhang Y, Gandhi J, Nakanishi C, Othman M, Branham KE, et al. High-resolution imaging with adaptive optics in patients with inherited retinal degeneration. Invest Ophthalmol Vis Sci. 2007;48(7):3283–91.
43. Kurz-Levin MM, Halfyard AS, Bunce C, Bird AC, Holder GE. Clinical variations in assessment of bull's-eye maculopathy. Acta Ophthalmol. 2002;120(5):567–75.

Malattia Leventinese (Autosomal Dominant Drusen)

5

Veronika Vaclavik and Francis L. Munier

Abstract

Malattia Leventinese, also known as dominant radial drusen or Doyne honeycomb retinal dystrophy, was first described in patients living in the Leventine Valley in canton Ticino of southern Switzerland in 1925. A missense mutation (Arg345Trp) in the gene *EFEMP1* was discovered to be causative for both conditions. Malattia Leventinese is reported to be autosomal dominant with variable expressivity phenotype. Characteristic clinical findings consist of radial macular drusen, large confluent drusen, and juxtapapillary drusen, which can be an isolated finding. Early visual symptoms, typically starting at age of 30–50 years, include reduced central vision, photophobia, and metamorphopsia. The vision gradually deteriorates over many years. No curative treatment is available for ML; however, some prophylactic argon laser treatment has been promising in improving visual acuity and reducing the drusen volume. Anti-vascular endothelial growth (VEGF) treatment is efficient in stabilizing a choroidal neovascular membrane.

Keywords

Malattia Leventinese • Autosomal dominant drusen • Variable expressivity • Radial drusen • Autofluorescence • Mouse model

V. Vaclavik, MD
Oculogenetic Unit, Jules-Gonin Eye Hospital, Unviersity of Lausanne, Lausanne, Switzerland

Medical Retina, Hospital Cantonal Fribourg, Fribourg, Switzerland
e-mail: veronika.vaclavik@fa2.ch

F.L. Munier, MD (✉)
Retinoblastoma and Oculogenetic Units, Department of Ophthalmology, Jules-Gonin Eye Hospital, University of Lausanne, Lausanne, Switzerland
e-mail: francis.munier@fa2.ch

5.1 Introduction

Malattia Leventinese (ML), also known as dominant radial drusen (DRD) or Doyne honeycomb retinal dystrophy (DHRD) [1], is the first clinically and histopathologically described maculopathy of Mendelian inheritance. As the name indicates, ML first described in patients living in the Leventine Valley in canton Ticino of southern Switzerland in 1925 [2]. DRHD was first reported

G. Querques, E.H. Souied (eds.), *Macular Dystrophies*, DOI 10.1007/978-3-319-26621-3_5

in England by Doyne in 1899 [3]. In four sisters, he observed white deposits in a honeycomb pattern at the macula and nasally to the disc. He believed that these white spots were lesions due to exudates in the choroid and named the disease "honeycomb choroiditis." A few years later, Treacher Collins discovered that the choroid was completely normal and the white spots consisted of hyaline thickenings of Bruch's membrane [4]. Several years later, Waardenburg [5] and Forni and Babel [6] concluded, based on histopathological findings, that features of Leventinese disease are indistinguishable from those of Doyne honeycomb choroiditis. Although originally recognized in Switzerland and England, families affected with autosomal radial drusen have been identified in Czechoslovakia [7, 8] and the United States [9].

Both ML and DHRD were reported to be autosomal dominant with full penetrance [10, 11]. Both have different pattern of drusen [10]. In DHRD, drusen are an infrequent finding, and, even when present, are only a minor feature. In ML, they are said to be an invariable and abundant feature due to their phenotypic variability and previous histopathological findings [6]. ML and DHRD were considered separate entities until 1999, when a single missense mutation (Arg345Trp, R345W) in the gene *EFEMP1* (EGF-containing fibrillin-like extracellular matrix protein 1) was discovered to be causative for both conditions [12].

5.2 Clinical Features

Characteristic clinical findings include early-onset small radial drusen at the posterior pole and larger drusen at the posterior pole and also nasal to the optic nerve head (Figs. 5.1, 5.2, 5.3, 5.4, and 5.5). A distinct phenotypic feature with only juxtapapillary drusen as an isolated sign, with intact macula (see Fig. 5.3c), can be observed. The small drusen display a pathognomonic radial distribution converging toward the center of the macula [11, 13]. The radial distribution of drusen was an infrequent finding in DHRD [10, 14] and was originally used to distinguish ML from DHRD. Drusen can be first noticed in the asymptomatic teenager. They increase in number and size; some become soft and round and confluent and merge to form multiple solid plaques displaying a honeycomb pattern at the level of Bruch's membrane [6, 10, 11].

The onset of symptoms is typically at age of 30–50 years; however, childhood cases with severe visual loss have also been reported [10]. Good visual acuities in the seventh decade of life and one case of non-penetrance in a 62-year-old asymptomatic and mutation-positive patient with normal fundus appearance have been reported [15, 16], illustrating the variability of disease phenotypic expressivity. Disease severity varies with evidence of interocular, intrafamilial (see Figs. 5.1 and 5.3), and interfamilial variability in visual loss and natural history, as reported in more recent reports of British, Japanese, Chinese, and Indian pedigrees [15, 17–19].

Early visual symptoms include reduced central vision, photophobia, slow dark adaptation, paracentral scotomas, and metamorphopsias [15, 20, 21]. Color vision loss is a later finding [15]. Symptomatic patients report gradual deterioration over many years. Mild cases are characterized by normal visual acuity and the presence of small, discrete drusen at the macula (see Fig. 5.3); in some cases, the macula is normal and only some drusen deposited at the optic disc margin are observed [15, 19]. In the later stages of the disease and in severe cases, typically at the age of 50 years, central vision deteriorates and absolute scotomas develop predominantly as result of retinal pigment epithelium (RPE) atrophy [10, 22]. Subretinal neovascular membrane can develop (see Fig. 5.4a) but is a very uncommon complication [15, 18, 19, 23], sometimes associated with a subretinal hemorrhage as the presenting symptom of the disease [24]. A neovascular membrane can lead to a severe vision loss in younger patients in their 30–40s [19, 23, 25, 26] and can be bilateral [19]. In some cases, hyperplasia of the RPE and subretinal fibrous metaplasia can occur [26, 27].

Fig. 5.1 Family 1: two affected daughters, (**a**–**d**) mother (**e**, **f**), and their 64-year-old mother. (**a**) Fundus color the left eye (LE) of 36-year-old female: juxtapapillary drusen and some drusen around the fovea. Her visual acuity was 0.8; she was myopic (−10 D). Six years earlier, only the juxtapapillary drusen were visible. (**b**) Fundus autofluorescence (FAF) image LE of same patient: some macular and juxtapapillary drusen were hyperautofluorescent. (**c**) Fundus color LE of her 39-year-old sister: juxta- and peripapillary drusen, as well as confluent drusen at posterior pole with hyperpigmented area fibrosis and area of atrophy. The visual acuity: 0.1. (**d**) FAF LE of the same patient: hypofluorescence corresponding to atrophy and hyperautofluorescent dots corresponding to drusen. (**e**) Fundus color LE of their 64-year-old mother: some juxtapapillary drusen, confluent peripapillary, and around macula drusen; central atrophy. Visual acuity: hand movements. (**f**) FAF LE: hypofluorescence corresponding to atrophy, hyperautofluorescence corresponding to confluent and isolated drusen

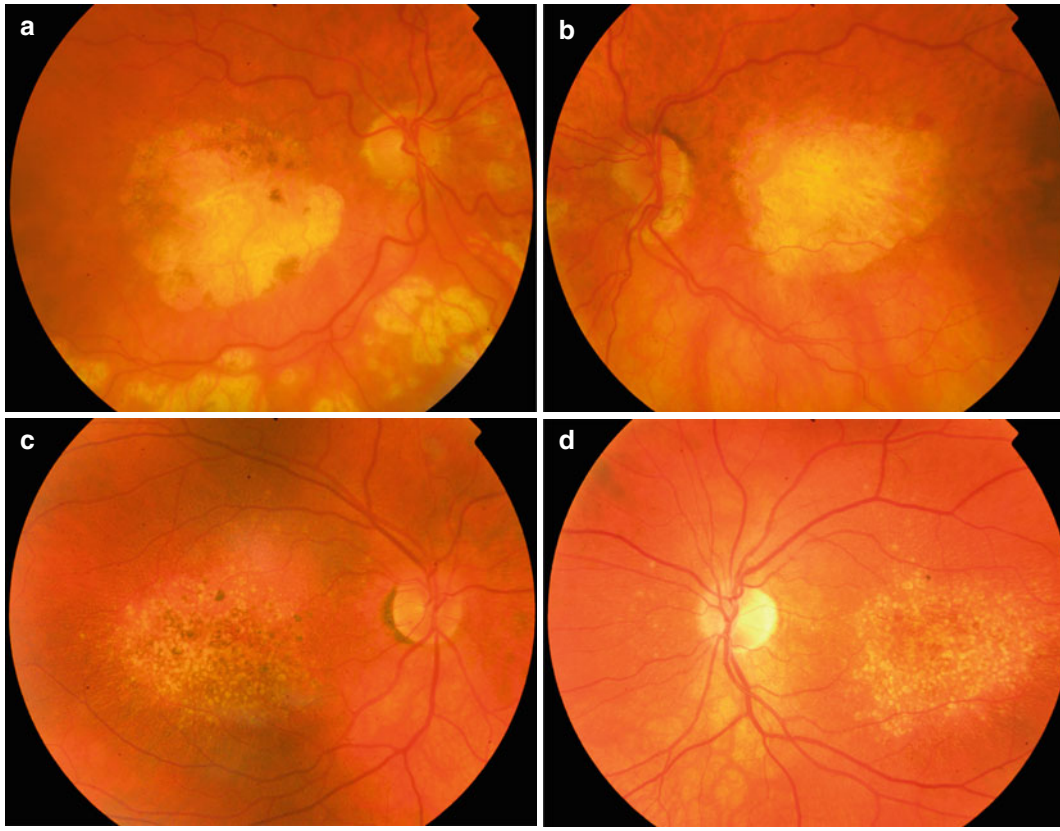

Fig. 5.2 Family 2: 79-year-old father (**a**, **b**) and his 49-year-old daughter (**c**, **d**). (**a**) Fundus color of the right eye (RE) of the father: central atrophy, optic nerve within normal limits, inferior of temporal artery scars post laser. Visual acuity: 0.1 corrected. (**b**) Fundus color of the left eye (LE) of the father: central atrophy, small hemorrhage at the superotemporal edge. Visual acuity: 0.16 corrected. (**c**) Fundus color of RE of the daughter: confluent large macular drusen, radial small drusen, and areas of hyperpigmentation. Visual acuity 1.0 corrected. (**d**) Fundus color of LE of the daughter: confluent large drusen and radial drusen at the macula, central atrophy, peripapillary drusen. Visual acuity 0.4 corrected

5.3 Paraclinic Testing and Their Use in the Diagnosis of Malattia Leventinese

Fundus autofluorescence (FAF) imaging allows the visualization of the RPE health by taking advantage of the fluorescent properties of lipofuscin [28]. The increased autofluorescence associated with drusen in monogenic macular dystrophies has been reported [29]. In recent report in patients with a confirmed fibulin-3 mutation status, all increased foci of autofluorescence correlated to drusen, but some drusen displayed reduced or absent autofluorescence. The autofluorescence was absent in areas of retinal atrophy, seen ophthalmoscopically, and reduced in some areas, suggesting widespread macular dysfunction [15]. Querques et al. [25] observed increased and intense autofluorescence only in large drusen, but not in small radial drusen. However, the main highlight of FAF imaging was to detect hyperfluorescent dots at the optic disc margin, confirming peripapillary drusen, which were not obvious on routine fundus examination [15, 19].

Time-domain and spectral-domain (SD) optical coherence tomography (OCT) have provided insight into structural retinal changes in patients with autosomal dominant drusen due to *EFEMP1* mutation. The first reports using a time-domain

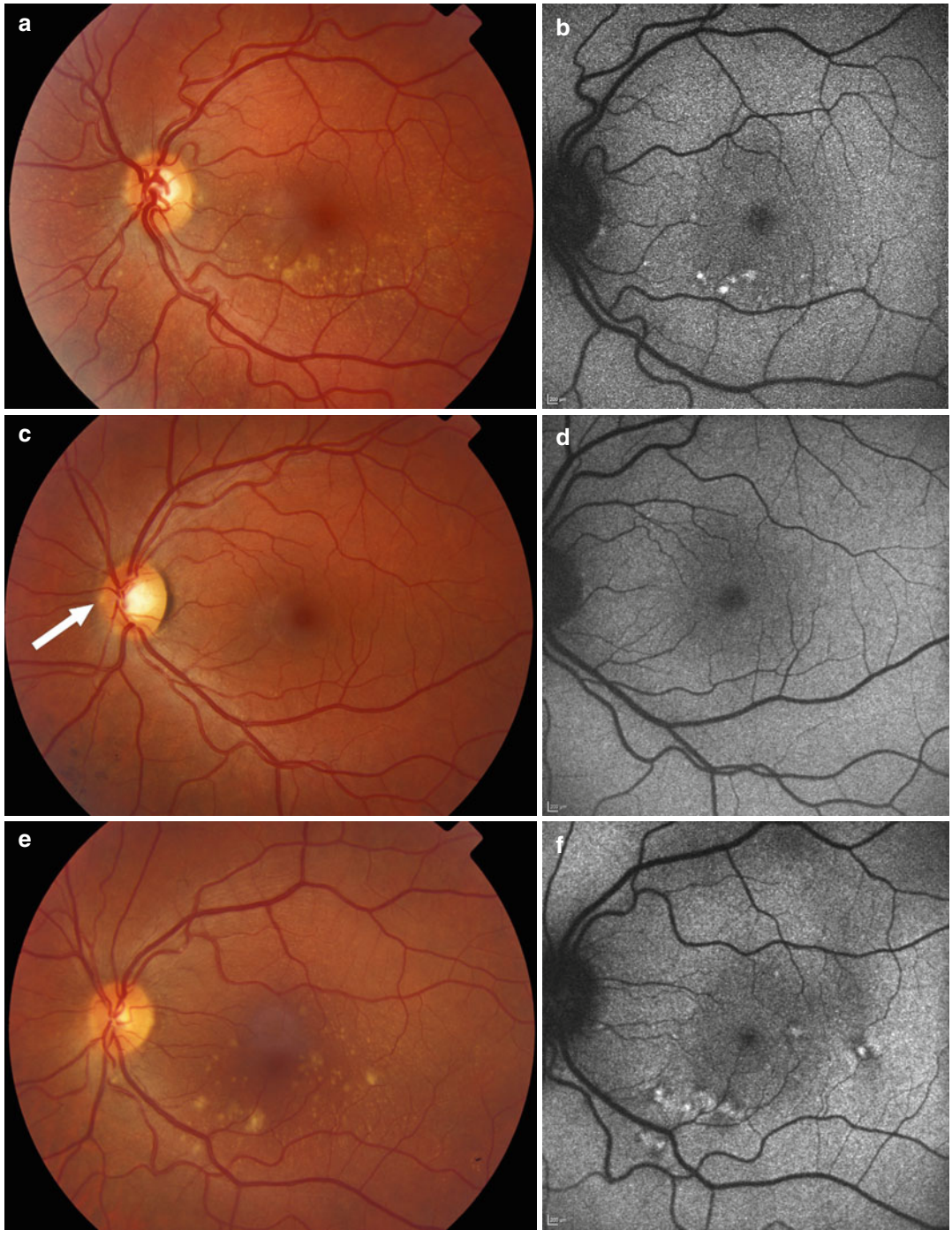

Fig. 5.3 Family 3: two affected daughters (30 and 32 years old) (**a**–**d**) and their 55-year-old mother (**e**, **f**). (**a**) Fundus color of the left eye (LE) of the 30-year-old affected daughter: juxtapapillary drusen and macular drusen, predominantly in the inferior part. Visual acuity 1.25. (**b**) Fundus autofluorescence (FAF) of the same patient: some macular drusen were hyperautofluorescent. (**c**) Fundus color of LE of the 32-year-old affected daughter: only nasal juxtapapillary drusen (*arrow*) are visible, absence of macular drusen. Visual acuity 1.25. (**d**) FAF of the same patient: absence of hyperautofluorescent areas at macula. (**e**) Fundus color of the 55-year-old affected mother: presence of drusen at the macula. Visual acuity 1.0. (**f**) FAF: some drusen were hyperautofluorescent

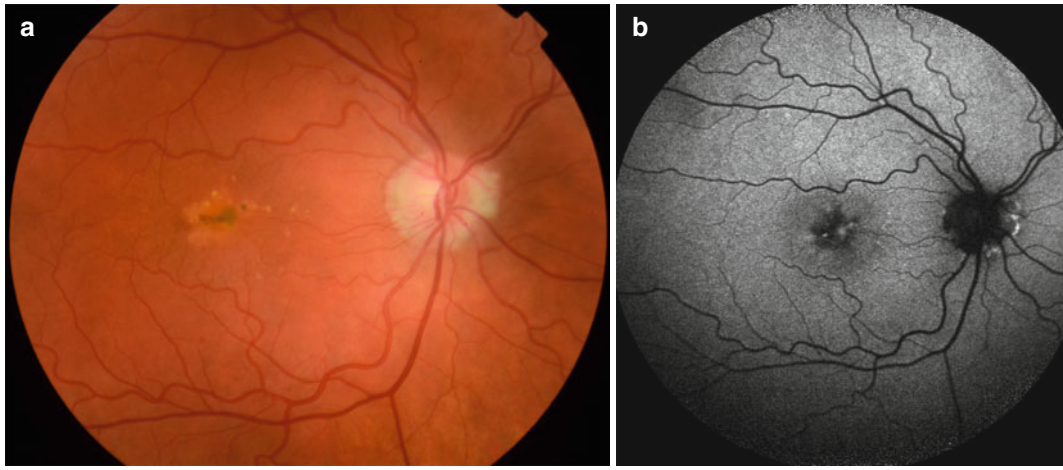

Fig. 5.4 Family 4: one patient (47 years old) from a large autosomal dominant pedigree. (**a**) Fundus color of the right eye: juxtapapillary drusen, some confluent drusen around fovea, central scar following neovascular membrane (previously treated with anti-VEGF), and small radial drusen. Visual acuity 0.9. (**b**) Fundus autofluorescence: hyperautofluorescence (corresponding to the drusen) and hypoautofluorescence (corresponding to the scar) around fovea. Hyperautofluorescent patches around optic nerve

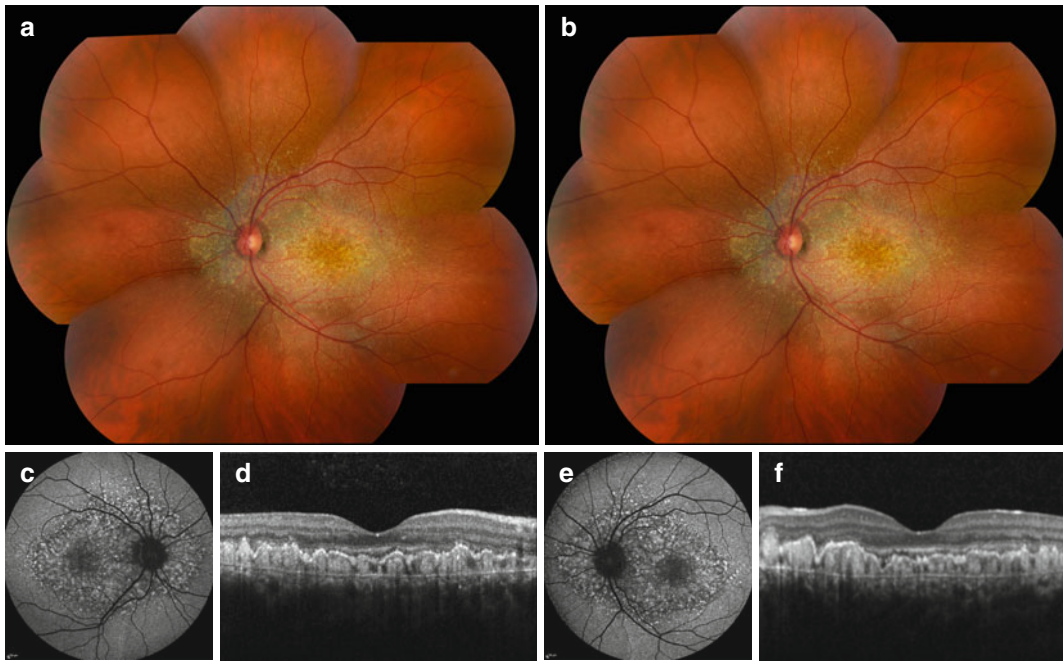

Fig. 5.5 Family 5: one patient (25 years old) with a de novo heterozygote R345W mutation in the *EFEMP1* gene. (**a**, **b**) Fundus color of the right eye (RE) and the left eye (LE): large, confluent drusen at posterior pole and nasal of the optic disc, small radial drusen. One juxtapapillary drusen RE, otherwise sparing (normal retina) around the optic discs. Visual acuity: 0.5 corrected, both eyes. (**c**–**e**) Fundus autofluorescence (FAF) images of RE and LE: hyperautofluorescence of drusen, area of hypofluorescence at the fovea in both eyes. (**d**–**f**) Spectral-domain optical coherence tomography of RE, LE: diffuse deposition of hyperreflective material underneath the retinal pigment epithelium (RPE) – diffuse, dome-shaped elevation of the RPE (large drusen). Hyperreflective sawtooth elevations (small drusen). Intact appearance of inner retina

OCT described a diffuse hyperreflective thickening of RPE–Bruch's membrane complex, associated with dome-shaped elevations, corresponding to large drusen [30, 31]. A remarkable preservation of the neurosensory retina was observed, both in perimacular and foveal areas [31]. Later reports, using an SD OCT, provided a better understanding of the two types of drusen: large round drusen appeared as diffuse or focal deposition of hyperreflective material underneath the RPE – determining a diffuse RPE elevation or a focal dome-shaped elevation. The small drusen, described as located above the RPE, had a sawtooth elevation appearance [25, 32]. The preservation of intact inner retina and preserved inner/outer segment junction was noted over small drusen, while the inner/outer segment junction was disrupted over large drusen [25]. In addition some intraretinal cyst and retinal tubulation were noted [25, 33]. Similarities between small, radial drusen in ML patients and cuticular drusen (also known as basolaminar drusen) have been reported [34, 35].

Additional insight into morphological and functional differences between the two types of drusen is given by reports of fluorescein angiography (FA) and indocyanine green angiography (ICG) features in ML. On both FA and ICG, large round drusen are hypofluorescent in early phases and turn into hyperfluorescent in late phase, with a dark halo on late ICG frames. The small drusen hyperfluoresce in early frames and decrease their fluorescence toward the later phase [25, 36]. Therefore, while small drusen share similitudes with cuticular drusen [35], the large drusen behave at FA and ICG more like age-related macular degeneration (AMD) drusen with a late hyperfluorescence [37].

Full-field electroretinogram (ERG), electrooculogram, and multifocal ERG data are available. The full-field ERG showed a normal rod b-wave responses, normal standard combined (mixed rod plus cone) response, and reduced 30-Hz flicker responses in both eyes in a 42-year-old patient from the Japanese pedigree [18]. Similar findings were described by the British group [21], who found that the scotopic sensitivity was reduced and dark adaptation kinetics were prolonged over the macular deposits only, but were normal elsewhere in patients affected by ML. Those findings were in keeping with a hypothesis that ML is a focal disease. A Swiss group [20] described "low-normal" amplitudes of the b-wave of rod and cone response, suggesting discrete but widespread functional abnormalities, while the b-wave amplitudes were subnormal in more advanced cases.

5.4 Molecular Genetics: Mapping

Linkage studies in families ML and DHRD mapped the disease locus to chromosome 2p16–21 [13, 22, 38, 39]. The first investigation was performed on 5 families (a large American kindred with 2 extensively affected branches and 3 kindreds from the Leventinese valley) with the ML phenotype with a total of 56 affected patients. They demonstrated linkage of ML to chromosome 2p. The maximum two-point LOD score observed in all families combined was 10.5 and was obtained with the marker D2S378. To further narrow the genetic interval containing the ML/DHRD gene, 63 members from a large nine-generation DHRD British pedigree, originally by O'Neill [1] and Pearce [14], were assessed for molecular genetic linkage study [13]. Two-point analysis showed a significant linkage of the DHRD to nine markers on the short arm of chromosome 2, a region overlapping the one recently reported to be linked to ML. A maximum LOD score of 7.29 was obtained at marker locus *D2S2251*. Haplotype analysis of recombination events localized the disease to a 5 cM interval between *D2S2316* and *D2S378*. These results established that DHRD maps to chromosome 2p16, a region included within the 14-kb region to which ML was recently mapped.

A combination of positional and candidate gene methods in 39 families from Switzerland, the United States, and Australia helped identifying a single nonconservative arginine 345 to tryptophan mutation (Arg345Trp) in the gene *EFEMP1* (EGF-containing fibrillin-like extracellular matrix protein 1) coding for fibulin-3 in all

families studied, inclusive of both phenotypes, ML and DHRD. The change was not present in 477 control individuals or in 494 patients with AMD [12]. In this original study, the authors found that among all families studied, there was a complete sharing of alleles of intragenic *EFEMP1* polymorphisms (SNPs). The same haplotype, and the absence of de novo R345W mutation in different ethnicities, was highly suggestive that the R345W mutation occurred only once in a common ancestor of every affected patient [12]. This study also confirmed that ML and DHRD are the same disorder.

A few years later, a genetic study revealed a novel disease haplotype with R345W mutation in an Indian pedigree, suggesting an independent origin [17]. A novel, different haplotype with the R345W mutation was identified in a Japanese pedigree [18], suggesting that the disease might have occurred independently in a common Japanese founder. In addition to those three different haplotypes, our group recently found a de novo R345W mutation in a young Portuguese patient with ML (unpublished data) with proven paternity, confirming that the *EFEMP1* R345W mutation is not a founder mutation, but more likely a hot spot mutation.

5.5 Histopathological Studies

Immunohistochemistry analysis, using monoclonal and polyclonal antibodies, of seven human donor eyes showed that, in normal retina, fibulin-3 is predominantly present in photoreceptor's inner and outer segment region and the nerve fiber layer, but not in the RPE, Bruch's membrane, or choroid [40]. In a donor eye from an 86-year-old ML patient carrying a homozygote R345W mutation, fibulin-3 was found to accumulate beneath the RPE, overlying drusen, and in Bruch's membrane, in addition to its presence in the interphotoreceptor matrix and the nerve fiber layer. *EFEMP1* accumulation was also detected within some RPE cells and a few drusen. The data suggested that *EFEMP1* was not a major component of drusen associated with ML [40].

In situ hybridization of human retinas was performed to study the pattern and level of expression of *EFEMP1* in ML donor eye and human control eyes [41]. An 80-year-old ML donor patient, heterozygote for R345W mutation in *EFEMP*1 gene, was available in that study. In normal eye, *EFEMP1* transcripts were localized mainly in the retinal ganglion cells, and the photoreceptor's outer segments showed very similar distribution to that of the ML eye. Even at the level of RPE, very similar patterning of *EFEMP1* expression was observed between a normal donor and ML eye. Surprisingly, in the ML eye, there was a 20-fold difference in *EFEMP*1 expression in the ciliary body, as compared to the *EFEMP1* expression in the RPE, while there was a complete lack of *EFEMP1* expression in ciliary body of normal donor. No histological abnormality was detected in the ciliary body of the ML donor. The robust upregulation of *EFEMP1* in the ciliary body is an ML-specific feature [42].

A recent morphologic and histochemical analysis of drusen in an ML donor and seven AMD donors showed that drusen from both diseases shared many major constituents. However, drusen from the ML donor had a unique onion-skin-like lamination and possessed collagen type IV, which was absent in age-related drusen [43].

5.6 Hypothesis on R345W Fibulin-3 Function

Human *EFEMP1* cDNA encodes a putative protein of 387–493 amino acids, with a predicted molecular mass of 43–54.6 kDa. *EFEMP1* gene consists of 12 exons and spans approximately 60 kb of genomic DNA [44]. There are five predicted splice variants, but only the shortest (43.1 kDa) and the longest (54.6 kDa) are expressed in substantial amounts at the protein level [45]. The *EFEMP1* protein is a broadly expressed extracellular matrix molecule: in tissues from adult mice, *EFEMP1* expression was abundant in the eye and lung and was moderate in the brain, heart, spleen, and kidney [12]. It is one of the seven members of the fibulin family of proteins. The protein sequence contains a signal

peptide, five to six calcium-binding epidermal growth factor (cbEGF) domains, a predicted N-glycosylation site at Asn249, and a highly hydrophobic C-terminal fibulin-type domain [45, 46]. The protein is highly conserved among humans and rodents, but its homology is restricted to the EGF-like domains. The single Arg-Trp mutation alters the last calcium-binding EGF-like domain of *EFEMP1* and is similar to the number of fibrillin mutations [47].

EFEMP1 has been renamed FIBULIN 3 (FBLN3) [48] and qualified to the family of fibulins, extracellular matrix proteins [49]. Six known members from mammalian species share an elongated structure and many calcium-binding sites and are hypothesized to function as intramolecular bridges that stabilize the structure of extracellular matrix [49].

A normal fibulin-3 interacts with several other proteins: a basement membrane protein (extracellular matrix protein-1), tissue inhibitor of metalloproteinase-3 (*TIMP3*), collagen XVIII/endostatin, hepatitis B virus-encoded X antigen, and elastin monomer tropoelastin. These interactions likely contribute to the integrity of basement membrane zone. Fibulin-3 colocalizes with fine elastic fibers and is involved in the formation of the extracellular matrix [50].

In vitro biochemical analysis indicates that mutant fibulin-3 protein containing the R345W mutation is misfolded. This change in conformation causes the mutant fibulin-3 to be secreted inefficiently and accumulate within cells [40]. In both ML and AMD eyes, fibulin-3 accumulates along drusen or other basal deposits [50]. Some cell culture studies suggested that mutant R345W fibulin-3 leads to macular degeneration through its misfolding and accumulation in the endoplasmic reticulum [51], causing cell death by activating the unfolded protein response [52]. However, the unfolded protein response has not been detected in in vivo studies [17]. A recent in vitro study suggested that R345W fibulin-3, but not the wild-type fibulin-3, required N-glycosylation to acquire a stable, native-like structure, enhancing the role of N-linked glycosylation in regulating the folding, secretion, and intracellular levels of fibulin-3 [53].

5.7 Animal Model

EFEMP1 –/– knockout mice, although appearing normal at birth, exhibited early-onset aging and developed multiple hernias, including inguinal hernias, pelvic prolapse, and protrusions of the xiphoid [54]. It showed reduced fertility and generalized fat, muscle, and organ atrophy. Histologic analysis revealed reduced and disrupted fine elastic fibers in fascia, adventitia, small blood vessels, and vaginal walls. There was no apparent retinal degeneration in the knockout mice [54].

EFEMP1 knock-in mouse model carrying the R345W mutation in the murine *EFEMP1* gene was generated, and some basal laminar deposits were histologically identified between the Bruch's membrane and the RPE as early as 4 months of age in both homozygote and heterozygote mice [17, 55]. Over time, these deposits increased in size and number. In older mice, membranous deposits were seen within the deposits and within Bruch's membrane, together with RPE and choroid abnormalities (degeneration, vacuolation, disruption of the RPE basal folding, choroidal atrophy). Fibulin-3 was found to accumulate in the sub-RPE deposits [55]. Some evidence of complement activation was detected in the RPE and Bruch's membrane of the mutant mice [17], concluding that the R345W mutation in *EFEMP1* is pathogenic and suggesting that alteration in the extracellular matrix may stimulate complement activation. This represents a potential connection between ML and AMD in macular degeneration.

The role of complement was further studied in a double-mutant mice: *EFEMP1* (R345W/R345W): C3 (–/–). In mice null for C3, the formation of basal deposits was inhibited, demonstrating that complement has an essential role in the formation of drusen-like basal deposits in *EFEMP1*–R345W knock-in mice and, perhaps, other macular degeneration [56].

5.8 Clinical Management/Treatment

As for many genetic retinal diseases, there is no specific treatment. However, ML has a close phenotypic similarity to AMD, where laser photoco-

agulation has been shown to lead to drusen reabsorption and has been tried as prophylactic treatment [57–60]. A meta-analysis of nine randomized controlled trials of laser treatment of AMD drusen confirmed that laser photocoagulation leads to drusen disappearance, but no evidence was found that it reduces vision loss, the risk of developing choroidal neovascular membrane (CNV), or geographic atrophy [61]. A recent study assessed the efficacy of laser photocoagulation as therapeutic approach for patients with ML and showed encouraging results. They treated 1 eye of 11 patients with genetically confirmed ML and found that treated eyes gained an average of 4.9 letters, while untreated eyes lost an average of 0.8 letters, over a 12-month period of the study. Some patients showed a significant improvement in retinal sensitivity in treated eyes. The mean drusen thickness increased in untreated eyes, but not in the treated eyes [33].

In later stages of the disease, subretinal neovascular membrane can occur and lead to severe vision loss [15, 18, 19, 23]. Because of phenotypic similarities to the CNV in AMD, some authors determined the effects of anti-VEGF (bevacizumab) intravitreal injections in two patients with ML. In both patients, the treatment leads to resolution of intraretinal fluid and improvement in visual acuity [23].

5.9 Differential Diagnosis

Several other monogenic macular dystrophies have been described and are principally characterized by posterior pole drusen, for which disease-causing mutations have been identified or chromosomal loci mapped. Sorsby fundus dystrophy [62] is caused by mutations in the tissue inhibitor of the *TIMP3* gene, and the clinical findings include drusen-like deposits at the level of Bruch's membrane and exudative or atrophic lesions of the macula [63]. The posterior pole drusen are also hallmark of North Carolina macular dystrophy [64]. The linkage studies mapped North Carolina dystrophy to a locus on chromosome 6q14–16 [65–67] and a locus on chromosome 5p13–p15 [68]. A similar condition, early-onset autosomal dominant dystrophy (*MCDR3*), and a North Carolina-like dystrophy with a hearing loss (*MCDR4*) [69] have been described and linked to chromosome 5p15–13 [70].

References

1. O'Neill MJF. Doyne honeycomb retinal dystrophy; DHRD. In: Online Mendelian inheritance in man. McKusick-Nathans Institute of Genetic Medicine. Johns Hopkins University. 2009. http://omim.org/entry/126600.Updated 1 Dec 2009. Accessed 16 Mar 2015.
2. Vogt A. Die Ophthalmoskopie im rotfreien Licht. In: Graefe A, Saemisch T, editors. Handbuch der gesammten Augenheilkunde. Untersuchungsmethoden. 3rd ed. Berlin: Verlag von Wilhelm Engelman; 1925. p. 1–118.
3. Doyne RW. Peculiar condition of choroiditis occurring in several members of the same family. Trans Ophthalmol Soc UK. 1899;19:71.
4. Collins E, Treacher A. A pathological report upon a case of Doyne's choroiditis ("honeycomb" or "family" choroiditis). Ophthalmoscope. 1913;11:537–8.
5. Waardenburg PJ. On recognizability of latent conductors of universal albinism and of ocular albinism. Ophthalmologica. 1948;115:126.
6. Forni S, Babel J. Etude clinique et histologique de la malattia leventinese. Affection appartenant au groupe des dégénérescences hyalines du pôle postérieur. Ophthalmologica. 1962;143:313–22.
7. Dusek J, Streicher T, Schmidt K. Hereditäre drusen der bruchschen membran. II. Untersuchung von semidünnschnitten und elektronenmikroskopischen ergebnissen. Klin Monbl Augenheilkd. 1982;181(8):79–83.
8. Streicher T, Krcméry K. Das fluoreszenzangiographische Bild der hereditären Drusen. Klin Monbl Augenheilkd. 1976;169:22–30.
9. Gass JDM, Agarwal A. Dominantly inherited radial basal laminar drusen (malattia leventinese, Doyne's honeycomb macular dystrophy). In: Gass' atlas of macular diseases, vol. 1. 5th ed. New York: Elsevier; 2012. p. 292–5.
10. Evans K, Gregory CY, Wijesuriya SD, Kermani S, Jay MR, Plant C, Bird AC. Assessment of the phenotypic range seen in Doyne honeycomb retinal dystrophy. Arch Ophthalmol. 1997;115(7):904–10.
11. Piguet B, Haimovici R, Bird AC. Dominantly inherited drusen represent more than one disorder: a historical review. Eye (Lond). 1995;9(Part 1):34–41.
12. Stone EM, Lotery AJ, Munier FL, Héon E, Piguet B, Guymer RH, et al. A single *EFEMP1* mutation associated with both Malattia Leventinese and Doyne honeycomb retinal dystrophy. Nat Genet. 1999;22(2):199–202.
13. Gregory CY, Evans K, Wijesuriya SD, Kermani S, Jay MR, Plant C, et al. The gene responsible for autosomal dominant Doyne's honeycomb retinal dystrophy

(DHRD) maps to chromosome 2p16. Hum Mol Genet. 1996;5(7):1055–9.
14. Pearce WG. Doyne's honeycomb retinal degeneration. Clinical and genetic features. Br J Ophthalmol. 1968;52(2):73–8.
15. Michaelides M, Jenkins SA, Brantley Jr MA, Andrews RM, Waseem N, Luong V, et al. Maculopathy due to the R345W substitution in fibulin-3: distinct clinical features, disease variability, and extent of retinal dysfunction. Invest Ophthalmol Vis Sci. 2006;47(7):3085–97.
16. Scarpatetti A, Forni S, Niemeyer G. Die Netzhautfunktion bei Malattia leventinese (dominant drusen). Klin Monbl Augenheilkd. 1978;172:590–7.
17. Fu L, Garland D, Yang Z, Shukia D, Rajendran A, Pearson E, et al. The R345W mutation in *EFEMP1* is pathogenic and causes AMD-like deposits in mice. Hum Mol Genet. 2007;16(20):2411–22.
18. Takeuchi T, Hayashi T, Bedell M, Zhang K, Yamada H, Tsuneoka H. A novel haplotype with the R345W mutation in the *EFEMP1* gene associated with autosomal dominant drusen in a Japanese family. Invest Ophthalmol Vis Sci. 2010;51(3):1643–50.
19. Zhang T, Xie X, Cao G, Jiang H, Wu S, Su Z, et al. Malattia leventinese/Doyne honeycomb retinal dystrophy in a Chinese family with mutation of the *EFEMP1* gene. Retina. 2014;34(12):2462–71.
20. Gerber DM, Munier FL, Niemeyer G. Cross-sectional study of visual acuity and electroretinogram in two types of dominant drusen. Invest Ophthalmol Vis Sci. 2003;44(2):493–6.
21. Haimovici R, Wroblewski J, Piguet B, Fitzke FW, Holder GE, Arden GB, Bird AC. Symptomatic abnormalities of dark adaptation in patients with *EFEMP1* retinal dystrophy (Malattia Leventinese/Doyne honeycomb retinal dystrophy). Eye (Lond). 2002;16(1):7–15.
22. Héon E, Piguet B, Munier F, Sneed SR, Morgan CM, Forni S, et al. Linkage of autosomal dominant radial drusen (malattia leventinese) to chromosome 2p16–21. Arch Ophthalmol. 1996;114(2):193–8.
23. Sohn EH, Patel PJ, MacLaren RE, Adatia FA, Pal B, Webster AR, Tufail A. Responsiveness of choroidal neovascular membranes in patients with R345W mutation in fibulin 3 (Doyne honeycomb retinal dystrophy) to anti-vascular endothelial growth factor therapy. Arch Ophthalmol. 2011;129(12):1626–8.
24. Pager CK, Sarin LK, Federman JL, Eagle R, Hagerman G, Rosenow J, Donoso LA. Malattia leventinese presenting with subretinal neovascular membrane and hemorrhage. Am J Ophthalmol. 2001;131(4):517–8.
25. Querques G, Guigui B, Leveziel N, Querques L, Bandello F, Souied EH. Multimodal morphological and functional characterization of Malattia Leventinese. Graefes Arch Clin Exp Ophthalmol. 2013;251(3):705–14.
26. Zech JC, Zaouche S, Mourier F, Placuchu H, Grange JD, Trepsat C. Macular dystrophy of malattia leventinese. A 25 year follow up. Br J Ophthalmol. 1999;83(10):1195–6.
27. Matsumoto M, Traboulsi EI. Dominant radial drusen and Arg345Trp *EFEMP1* mutation. Am J Ophthalmol. 2001;131(6):810–2.
28. von Rückmann A, Fitzke FW, Bird AC. Distribution of fundus autofluorescence with a scanning laser ophthalmoscope. Br J Ophthalmol. 1995;79(5):407–12.
29. von Rückmann A, Schmidt KG, Fitzke FW, Bird AC, Jacobi KW. Fundus-Autofluoreszenz bei Patienten mit vererbten Makuladystrophien, Malattia leventinese, familiar dominanten und altersbedingten Drusen. Klin Monbl Augenheilkd. 1998;213(2):81–6.
30. Gaillard MC, Wolfensberger TJ, Uffer S, Mantel I, Pournaras JA, Schorderet DF, Munier FL. Tomographie à cohérence optique dans la Malattia Leventinese. Klin Monbl Augenheilkd. 2005;222(3):180–5.
31. Souied EH, Leveziel N, Letien V, Darmon J, Coscas G, Soubrane G. Optical coherent tomography features of malattia leventinese. Am J Ophthalmol. 2006;141(2):404–7.
32. Zweifel SA, Maygar I, Berger W, Tschuor P, Becker M, Michels S. Multimodal imaging of autosomal dominant drusen. Klin Monbl Augenheilkd. 2012;229(4):399–402.
33. Lenassi E, Troeger E, Wilke R, Tufail A, Hawlina M, Jeffery G, Webster AR. Laser clearance of drusen deposit in patients with autosomal dominant drusen (p.Arg345Trp in *EFEMP1*). Am J Ophthalmol. 2013;155(1):190–8.
34. Leng T, Rosenfeld PJ, Gregori G, Puliafito CA, Punjabi OS. Spectral domain optical coherence tomography characteristics of cuticular drusen. Retina. 2009;29(7):988–93.
35. Querques G, Guigui B, Leveziel N, Querques L, Coscas G, Soubrane G, Souied EH. Insights into pathology of cuticular drusen from integrated confocal scanning laser ophthalmoscopy imaging and corresponding spectral domain optical coherence tomography. Graefes Arch Clin Exp Ophthalmol. 2011;249(11):1617–25.
36. Guigui B, Leveziel N, Martinet V, Massamba N, Sterkers M, Coscas G, Souied EH. Angiography features of early onset drusen. Br J Ophthalmol. 2011;95(2):238–44.
37. Arnold JJ, Quaranta M, Soubrane G, Sarks SH, Coscas G. Indocyanine green angiography of drusen. Am J Ophthalmol. 1997;124(3):344–56.
38. Kermani S, Gregory-Evans K, Tarttelin EE, Bellingham J, Plant C, Bird AC, et al. Refined genetic and physical positioning of the gene for Doyne honeycomb retinal dystrophy (DHRD). Hum Genet. 1999;104(1):77–82.
39. Taymans SE, Kirschner LS, Giatzakis C, Stratakis CA. Radiation hybrid mapping of chromosomal region 2p15–p16: integration of expressed and polymorphic sequences maps at the Carney complex (CNC) and Doyne honeycomb retinal dystrophy (DHRD) loci. Genomics. 1999;56(3):344–9.
40. Marmorstein LY, Munier FL, Arsenijevic Y, Schorderet DF, McLaughlin PJ, Chung D, et al.

Aberrant accumulation of *EFEMP1* underlies drusen formation in Malattia Leventinese and age-related macular degeneration. Proc Natl Acad Sci U S A. 2002;99(20):13067–72.
41. Kundzewicz A, Munier F, Matter JM. Expression and cell compartmentalization of *EFEMP1*, a protein associated with Malattia Leventinese. Adv Exp Med Biol. 2008;613:277–81.
42. Kundzewicz A. Role of ATH5 in the specification of retinal ganglion cells and expression and cell compartmentalization of *EFEMP1*, a protein associated with malattia leventinese Thesis of the University of Lausanne and University of Geneva, Lausanne. 2008.
43. Sohn EH, Wang K, Thompson, Riker MJ, Hoffmann JM, Stone EM, Mullins RF. Comparison of drusen and modifying genes in autosomal dominant radial drusen and age-related macular degeneration. Retina. 2015;35(1):48–57.
44. Blackburn J, Tarttelin EE, Gregory-Evans CY, Moosajee M, Gregory-Evans K. Transcriptional regulation and expression of the dominant drusen gene *FBLN3* (*EFEMP1*) in mammalian retina. Invest Ophthalmol Vis Sci. 2003;44(11):4613–21.
45. Lecka-Czernik B, Lumpkin Jr CK, Goldstein S. An overexpressed gene transcript in senescent and quiescent human fibroblasts encoding a novel protein in the epidermal growth factor-like repeat family stimulates DNA synthesis. Mol Cell Biol. 1995;15(1):120–8.
46. Timpl R, Sasaki T, Kostka G, Chu ML. Fibulins: a versatile family of extracellular matrix proteins. Nat Rev Mol Cell Biol. 2003;4(6):479–89.
47. Ikegawa S, Toda T, Okui K, Nakamura Y. Structure and chromosomal assignment of the human S1-5 gene (FBNL) that is highly homologous to fibrillin. Genomics. 1996;35(3):590–2.
48. Giltay R, Timpl R, Kostka G. Sequence, recombinant expression and tissue localization of two novel extracellular matrix proteins, fibulin-3 and fibulin-4. Matrix Biol. 1999;18(5):469–80.
49. Argraves WS, Greene LM, Cooley MA, Gallagher WM. Fibulins: physiological and disease perspectives. EMBO Rep. 2003;4(12):1127–31.
50. Zhang Y, Marmorstein LY. Focus on molecules: fibulin-3 (*EFEMP1*). Exp Eye Res. 2010;90(3):374–5.
51. Roybal CN, Marmorstein LY, Vander Jagt DL, Abcouwer SF. Aberrant accumulation of fibulin-3 in the endoplasmic reticulum leads to activation of the unfolded protein response and VEGF expression. Invest Ophthalmol Vis Sci. 2005;46(11):3973–9.
52. Blais JD, Addison CL, Edge R, Falls T, Zhao H, Wary K, et al. Perk-dependent translational regulation promotes tumor cell adaptation and angiogenesis in response to hypoxic stress. Mol Cell Biol. 2006;26(24):9517–32.
53. Hulleman JD, Kelly JW. Genetic ablation of N-linked glycosylation reveals two key folding pathways for R345W fibulin-3, a secreted protein associated with retinal degeneration. FASEB J. 2015;29(2):565–75.
54. McLaughlin PJ, Bakall B, Choi J, Liu Z, Sasaki T, Davis EC, et al. Lack of fibulin-3 causes early aging and herniation, but not macular degeneration in mice. Hum Mol Genet. 2007;16(24):3059–70.
55. Marmorstein LY, McLaughlin PJ, Peachey NS, Sasaki T, Mamorstein D. Formation and progression of subretinal pigment epithelium deposits in *EFEMP1* mutation knock-in mice: a model for the early pathogenic course of macular degeneration. Hum Mol Genet. 2007;16(20):2423–32.
56. Garland DL, Fernandez-Godino R, Kaur I, Speicher KD, Hamly JM, Lambris JD, et al. Mouse genetics and proteomic analyses demonstrate a critical role for complement in a model of DHRD/ML, an inherited macular degeneration. Hum Mol Genet. 2014;23:52–68.
57. Cleasby GW, Nakanishi AS, Norris JL. Prophylactic photocoagulation of the fellow eye in exudative senile maculopathy. A preliminary report. Mod Probl Ophthalmol. 1979;20:141–7.
58. Gass JD. Drusen and disciform macular detachment and degeneration. Arch Ophthalmol. 1973;90(3):206–17.
59. Gross-Jendroska M, Owens SL, Flaxel CJ, Guymer RH, Bird AC. Prophylactic laser treatment to fellow eyes of unilateral retinal pigment epithelial tears. Am J Ophthalmol. 1998;126(1):77–81.
60. Wetzig PC. Photocoagulation of drusen-related macular degeneration: a long-term outcome. Trans Am Ophthalmol Soc. 1994;92:299–303. discussion 303–6.
61. Parodi MB, Virgili G, Evans JR. Laser treatment of drusen to prevent progression to advanced age-related macular degeneration. Cochrane Database Syst Rev. 2009;3:CD006537.
62. Tiller GE. Fundus dystrophy, pseudoinflammatory, of Sorsby; SFD. In: Online Mendelian inheritance in man. McKusick-Nathans Institute of Genetic Medicine. Johns Hopkins University. http://omim.org/entry/136900. Updated 13 May 2009. Accessed 25 Feb 2015.
63. Weber BH, Vogt G, Pruett RC, Stöhr H, Felbor U. Mutations in the tissue inhibitor of metalloproteinases-3 (*TIMP3*) in patients with Sorsby's fundus dystrophy. Nat Genet. 1994;8(4):352–6.
64. Kelly J. Macular dystrophy, retinal, 1, North Carolina type, MCDR1. In: Online Mendelian inheritance in man. McKusick-Nathans Institute of Genetic Medicine. Johns Hopkins University. http://omim.org/entry/136550. Updated 26 Aug 2011. Accessed 25 Feb 2015.
65. Kiernan DF, Shah RJ, Hariprasad SM, Grassi MA, Small KW, Kiernan JP, Mieler WF. Thirty-year follow-up of an African American family with macular dystrophy of the retina, locus 1 (North Carolina macular dystrophy). Ophthalmology. 2011;118(7):1435–43.
66. Pauleikhoff D, Sauer CG, Müller CR, Radermacher M, Merz A, Weber BH. Clinical and genetic evidence for autosomal dominant North Carolina macular dystrophy in a German family. Am J Ophthalmol. 1997;124(3):412–5.

67. Small KW, Weber JL, Hung WY, Vance J, Roses A, Pericak-Vance M. North Carolina macular dystrophy: exclusion map using RFLPs and microsatellites. Genomics. 1991;11(3):763–6.
68. Rosenberg T, Roos B, Johnsen T, Bech N, Scheetz TE, Larsen M, et al. Clinical and genetic characterization of a Danish family with North Carolina macular dystrophy. Mol Vis. 2010;16:2659–68.
69. Reddy MA, Francis PJ, Berry V, Bradshaw K, Patel RJ, Maher ER, et al. A clinical and molecular genetic study of a rare dominantly inherited syndrome (MRCS) comprising of microcornea, rod-cone dystrophy, cataract, and posterior staphyloma. Br J Ophthalmol. 2003;87(2):197–202.
70. Michaelides M, Johnson S, Tekriwal AK, Holder GE, Bellmann C, Kinning E, et al. An early-onset autosomal dominant macular dystrophy (*MCDR3*) resembling North Carolina macular dystrophy maps to chromosome 5. Invest Ophthalmol Vis Sci. 2003;44(4):2178–83.

North Carolina Macular Dystrophy and North Carolina Macular Dystrophy-Like Disorders

6

Michel Michaelides and Anthony Moore

Abstract

The developmental macular disorders form part of a heterogeneous group of retinal disorders that are an important cause of visual impairment in children. The macular abnormality is present from birth and is usually nonprogressive, but rarely, visual loss may occur as a result of choroidal neovascularisation. Although there have been considerable advances made in recent years in our understanding of the clinical phenotypes, natural history and molecular genetics of these developmental disorders, many of the causative genes have yet to be identified. It is anticipated that new genetic technologies, such as next-generation sequencing, will soon lead to discovery of such genes; this new information will result in improved understanding of the biology of macular development and will be the first step in developing new therapies.

North Carolina macular dystrophy is the most common of these rare developmental macular disorders, and although the phenotype is well described, the molecular genetic basis remains unknown.

Keywords

Developmental • Macular • Dystrophy • Genetics • North Carolina

M. Michaelides, BSc, MBBS, MD, FRCOphth, FACS (✉)
Departments of Inherited Eye Disease, Medical Retina, and Paediatric Ophthalmology, Moorfields Eye Hospital, London, UK

Department of Genetics, UCL Institute of Ophthalmology, London, UK
e-mail: michel.michaelides@ucl.ac.uk

A. Moore, MA, FRCS, FRCOphth, FMedSci
Department of Ophthalmology, University of California School of Medicine, San Francisco, CA, USA

6.1 North Carolina Macular Dystrophy (MCDR1)

North Carolina macular dystrophy (NCMD) (*MCDR1*; macular dystrophy, retinal, 1) is an autosomal dominant disorder characterised by a variable macular phenotype and a nonprogressive natural history. The disorder shows complete penetrance but variable expressivity. Presentation is usually during the first decade, but mildly affected family members may remain asymptom-

G. Querques, E.H. Souied (eds.), *Macular Dystrophies*, DOI 10.1007/978-3-319-26621-3_6

atic and may only be identified at routine optometry review. The disorder is believed to represent a failure of macular development [1–7].

Bilaterally symmetrical fundus appearances in *MCDR1* range from a few small (less than 50 μm) yellow drusen-like lesions in the central macula (grade 1) to larger confluent lesions (grade 2) and well-demarcated macular chorioretinal atrophy (grade 3) (Fig. 6.1). Peripheral retinal drusen-like deposits have also been described but are uncommon. The severity of visual loss is dependant upon the grade of retinal phenotype, with vision being poorest in association with grade 3 lesions. Colour vision is usually normal. Occasionally, *MCDR1* is complicated by choroidal neovascular membrane (CNVM) formation at the macula. The electro-oculogram (EOG) and full-field electroretinogram (ERG) are normal, indicating that there is no generalised retinal dysfunction.

Histopathology is available of one patient with *MCDR1*, which showed accumulation of lipofuscin in the retinal pigment epithelium (RPE) within the atrophic macular lesion [3].

Linkage studies have mapped *MCDR1* to a locus on chromosome 6q16 [1]. To date, *MCDR1* has been described in various countries and no evidence of genetic heterogeneity has been reported [3–7]. The disease interval has been refined to 3 cM (1.8mb) between markers D6S1716 and D6S1671 [7]. All 11 annotated genes within the interval were analysed by mutation screening of coding regions, with no mutation identified [7]. There are several plausible explanations for the failure to identify the causative mutation in this

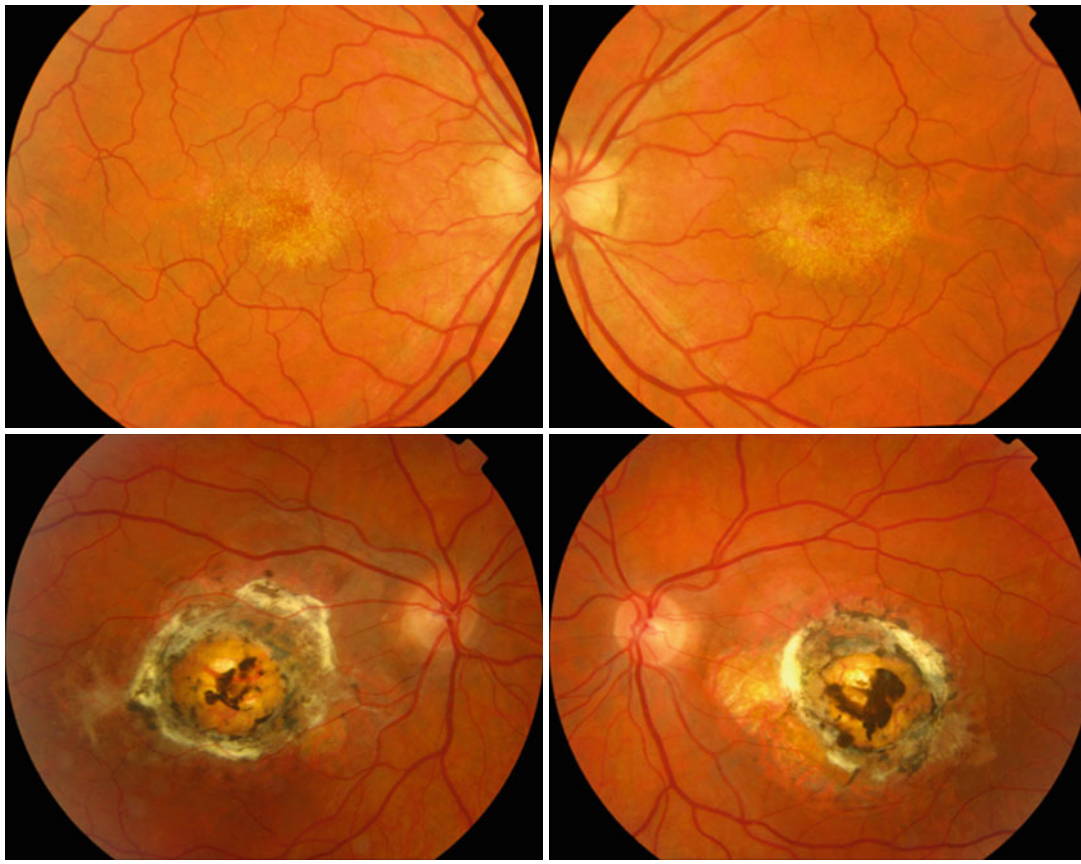

Fig. 6.1 North Carolina macular dystrophy (NCMD) (*MCDR1*). Colour fundus photographs showing both the typical drusen-associated phenotype that can be seen in NCMD (*above*) and the characteristic grade 3 pigmented atrophic lesion (*below*)

study. The mutation may have been missed and may be located in a non-coding or regulatory region, or in an as yet unrecognised exon of one of the identified positional candidate genes, or in an as yet unidentified gene. Alternatively, *MCDR1* may be caused by another mechanism such as copy number variation. The advent of next-generation sequencing should lead to the identification of the causative gene; this will improve our understanding of the pathogenesis of drusen and CNVM in *MCDR1* and will provide new insights into the biology of human macular development.

Stefko et al. have mapped a dominantly inherited macular dystrophy in a North American family to chromosome 6q14, adjacent to but likely distinct from the *MCDR1* locus [8, 9]. This macular dystrophy has a highly variable clinical phenotype, described as an autosomal dominant drusen disorder with macular degeneration (DD). Most young adults had fine macular drusen and good vision. Some affected individuals have congenital atrophic maculopathy and drusen and are symptomatic in infancy or early childhood.

Progressive bifocal chorioretinal atrophy (PBCRA) has also been linked to 6q14–q16.2 and the disease locus overlaps with the established *MCDR1* interval [10, 11]. These two autosomal dominant macular dystrophies have some phenotypic similarities and both are thought to result from a failure of normal macular development. However, PBCRA differs significantly from *MCDR1* in several important respects, including more severe visual loss, slow progression, abnormal colour vision, extensive nasal as well as macular atrophy and abnormal ERG and EOG. Therefore, if allelic, it is likely that different mutations are involved in their aetiology. An alternative explanation is that PBCRA and *MCDR1* are caused by mutations in two different adjacent developmental genes.

6.2 North Carolina Macular Dystrophy-Like Phenotypes

Three North Carolina macular dystrophy-like phenotypes mapping to different genetic loci than *MCDR1* have been described, suggesting further genetic heterogeneity in the *MCDR1* phenotype.

6.2.1 Autosomal Dominant Macular Dystrophy (MCDR3) Resembling North Carolina Macular Dystrophy

A British pedigree has been described with an early-onset autosomal dominant macular dystrophy (*MCDR3*) [12]. Visual acuity ranged from 6/5 to 6/60. The retinal changes were confined to the macular region and vary from mild RPE pigmentary change to atrophy. Drusen-like deposits were present to varying degrees and were characteristic of the phenotype (Fig. 6.2). Choroidal neovascular membrane formation was an established complication. The EOG and ERG were normal, indicating that there is no generalised retinal dysfunction. The only significant differences between this phenotype and *MCDR1* are that in *MCDR3*, colour vision is abnormal in the majority of affected individuals and there was evidence of disease progression, albeit in a single case.

A Danish family with a phenotype in keeping with *MCDR3* has also been reported [13]. Genetic linkage analysis in both the British and Danish families established linkage to chromosome 5p13.1–p15.33 and excluded the *MCDR1* locus [12, 13]. The gene has not to date been identified.

6.2.2 North Carolina-Like Macular Dystrophy and Progressive Sensorineural Hearing Loss (*MCDR4*)

A British family characterised by a nonprogressive *MCDR*1-like macular dystrophy in association with progressive sensorineural hearing loss has been reported (*MCDR4*) [14]. Visual acuity ranged from 6/9 to hand movements. In keeping with *MCDR1* and *MCDR3*, the EOG and full-field ERG were normal. Progressive sensorineural deafness was present in all affected individuals over the age of 20 years.

Genotyping excluded linkage to the *MCDR1* locus and established linkage to chromosome 14q.

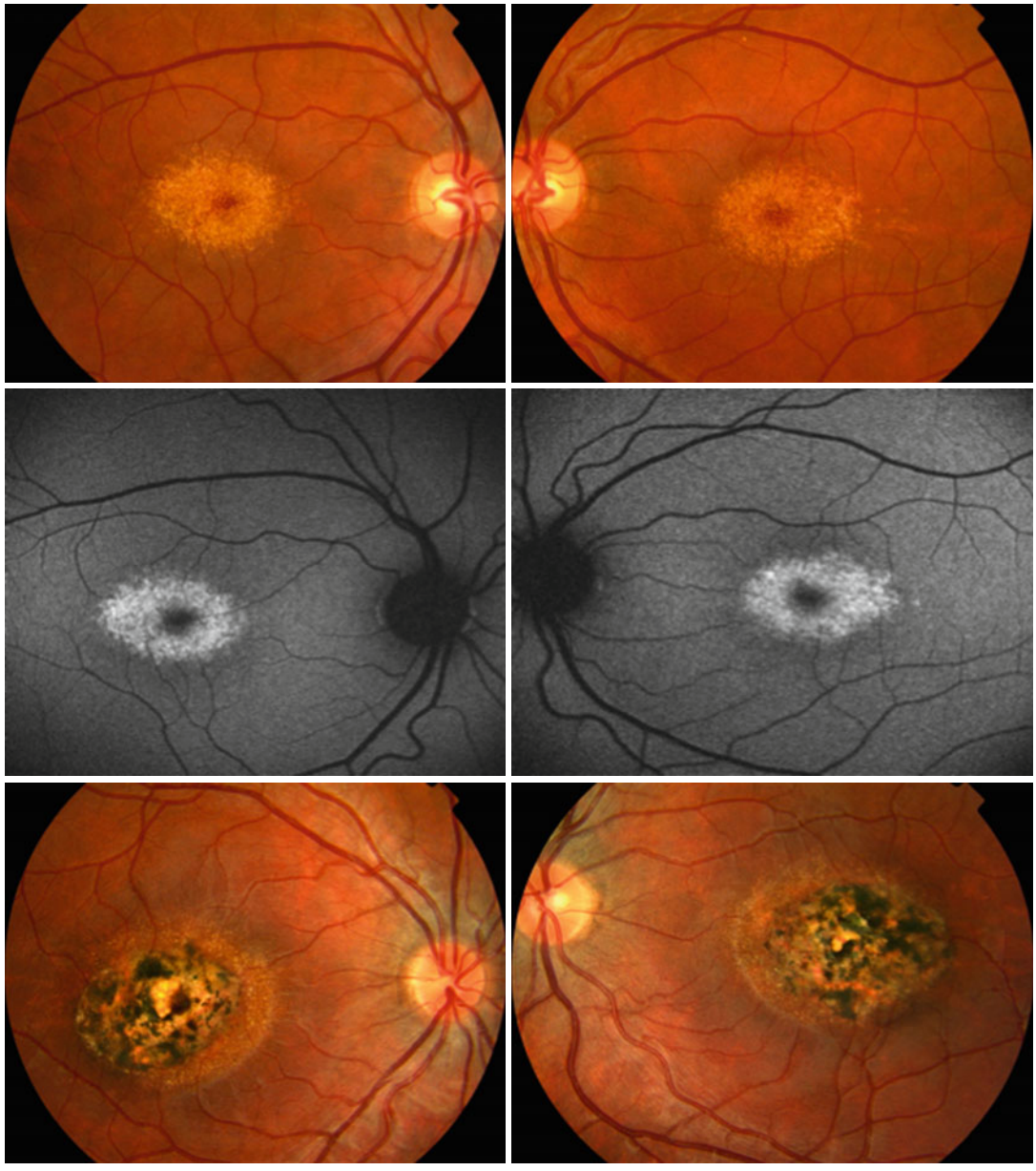

Fig. 6.2 Autosomal dominant macular dystrophy (*MCDR3*) resembling North Carolina macular dystrophy. Colour fundus photographs showing bilateral typical fine macular drusen-like deposits (*above*), which are associated with increased autofluorescence (*middle*), and bilateral macular RPE atrophy and pigment clumping, with surrounding drusen-like deposits (*below*)

6.2.3 North Carolina-Like Macular Dystrophy and Digital Anomalies (Sorsby Syndrome)

A British and a French family have been described with a dominantly inherited condition characterised by bilateral macular dysplasia in association with apical dystrophy or brachydactyly (Fig. 6.3) [15–17]. Visual acuity ranged from 6/12 to 4/60. The maculopathy was nonprogressive and variable in severity, ranging from mild RPE pigmentary changes to excavated chorioretinal atrophic lesions. There was no evidence of generalised retinal dysfunction.

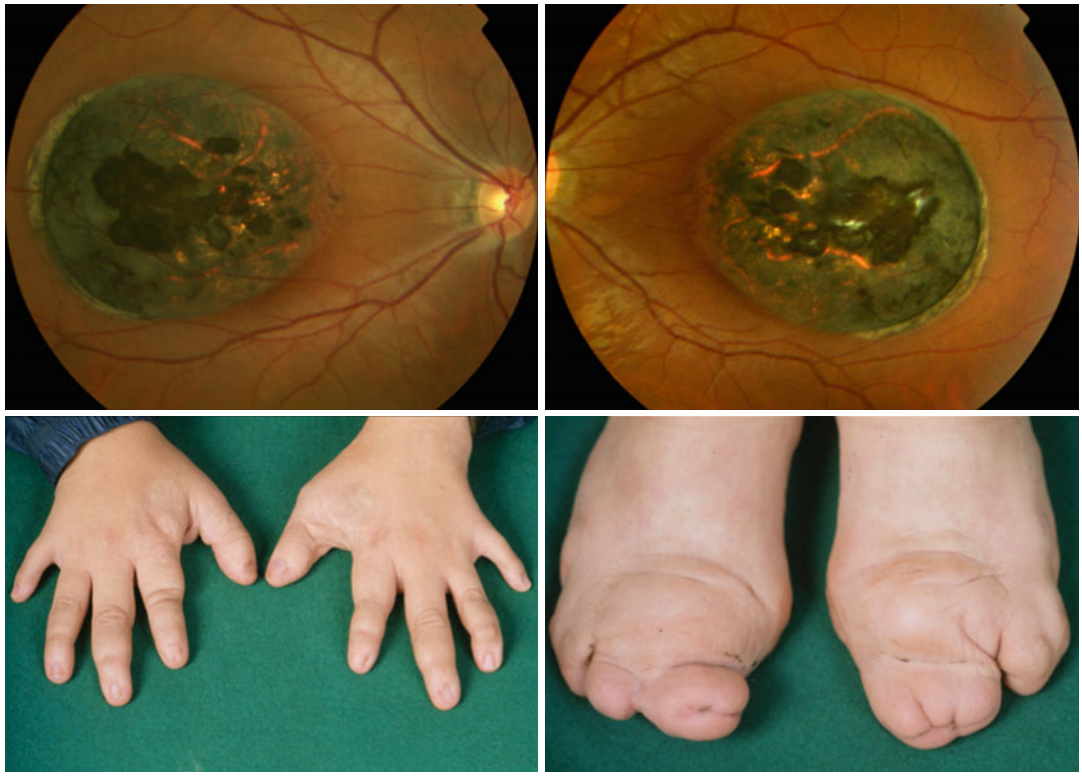

Fig. 6.3 North Carolina-like macular dystrophy and digital anomalies (Sorsby syndrome). Colour fundus photographs showing the typical bilateral macular dysplasia. In this individual, there is shortening and deformity of the fingers and toes due to aplasia and hypoplasia of middle and terminal phalanges. There is skin syndactyly in association with bifurcation of the terminal phalanx of the hallux causing severe deformity of the foot

The *MCDR1*, *MCDR3* and *MCDR4* loci have all been excluded in these two families on the basis of linkage, providing evidence of further genetic heterogeneity associated with the NCMD-like phenotype [17]. This is in keeping with the established heterogeneity in the genetic mechanisms underlying both split-hand and split-foot malformations (microdeletions being common) and the developmental macular dystrophies.

6.3 Management of Developmental Macular Disorders

There is currently no specific treatment for any of the developmental macular disorders. Nevertheless, it is important that the correct diagnosis is made at an early stage, in order to be able to provide accurate information on prognosis and to be able to offer informed genetic counselling. Molecular genetic diagnosis is currently restricted to foveal hypoplasia. It is anticipated that with modern deep sequencing methodologies, the genes underlying more of these disorders, especially those with established chromosomal loci (such as NCMD and associated disorders), will be identified in the near future.

Although there is no specific treatment available for this group of disorders, the provision of appropriate spectacle correction, low vision aids and educational support is also very important.

6.4 Concluding Remarks and Future Perspectives

The developmental macular dystrophies form part of a heterogeneous group of retinal disorders that are an important cause of blindness in children and

young adults. The molecular characterisation of these disorders remains an important goal, so that in the event of future-directed treatment options, it may thereby be possible to make a judgement as to whether particular patients are suitable for inclusion. Clearly in the first instance, the identification of the genetic defect will suggest potential mechanisms of disease and therapy.

References

1. Small KW, Weber JL, Roses A, Lennon F, Vance JM, Pericak-Vance MA. North Carolina macular dystrophy is assigned to chromosome 6. Genomics. 1992;13(3):681–5.
2. Small KW, Udar N, Yelchits S, Klein R, Garcia C, Gallardo G, et al. North Carolina macular dystrophy (*MCDR1*) locus: a fine resolution genetic map and haplotype analysis. Mol Vis. 1999;5:38–42.
3. Small KW, Voo I, Flannery J, Udar N, Glasgow BJ. North Carolina macular dystrophy: clinicopathologic correlation. Trans Am Ophthalmol Soc. 2001;99:233–7.
4. Reichel MB, Kelsell RE, Fan J, Gregory CY, Evans K, Moore AT, et al. Phenotype of a British North Carolina macular dystrophy family linked to chromosome 6q. Br J Ophthalmol. 1998;82(10):1162–8.
5. Szlyk JP, Paliga J, Seiple W, Rabb MF. Comprehensive functional vision assessment of patients with North Carolina macular dystrophy (MCDR1). Retina. 2005;25(4):489–97.
6. Khurana RN, Sun X, Pearson E, Yang Z, Harmon J, Goldberg MF, Zhang K. A reappraisal of the clinical spectrum of North Carolina macular dystrophy. Ophthalmology. 2009;116(10):1976–83.
7. Yang Z, Tong Z, Chorich LJ, Pearson E, Yang X, Moore A, et al. Clinical characterization and genetic mapping of North Carolina macular dystrophy. Vis Res. 2008;48(3):470–7.
8. Stefko ST, Zhang K, Gorin MB, Traboulsi EI. Clinical spectrum of chromosome 6-linked autosomal dominant drusen and macular degeneration. Am J Ophthalmol. 2000;130(2):203–8.
9. Kniazeva M, Traboulsi EI, Yu Z, Stefko ST, Gorin MB, Shugart YY, et al. A new locus for dominant drusen and macular degeneration maps to chromosome 6q14. Am J Ophthalmol. 2000;130(2):197–202.
10. Godley BF, Tiffin PA, Evans K, Keisell RE, Hunt DM, Bird AC. Clinical features of progressive bifocal chorioretinal atrophy: a retinal dystrophy linked to chromosome 6q. Ophthalmology. 1996;103(6):893–8.
11. Kelsell RE, Godley BF, Evans K, Tiffin PA, Gregory CY, Plant C, et al. Localization of the gene for progressive bifocal chorioretinal atrophy (PBCRA) to chromosome 6q. Hum Mol Genet. 1995;4(9):1653–6.
12. Michaelides M, Johnson S, Tekriwal AK, Holder GE, Bellmann C, Kinning E, et al. An early-onset autosomal dominant macular dystrophy (MCDR3) resembling North Carolina macular dystrophy maps to chromosome 5. Invest Ophthalmol Vis Sci. 2003;44(5):2178–83.
13. Rosenberg T, Roos B, Johnsen T, Bech N, Scheetz TE, Larsen M, et al. Clinical and genetic characterization of a Danish family with North Carolina macular dystrophy. Mol Vis. 2010;16:2659–68.
14. Francis PJ, Johnson S, Edmunds B, Kelsell RE, Sheridan E, Garrett C, et al. Genetic linkage analysis of a novel syndrome comprising North Carolina-like macular dystrophy and progressive sensorineural hearing loss. Br J Ophthalmol. 2003;87(7):893–8.
15. Sorsby A. Congenital coloboma of the macula, together with an account of the familial occurrence of bilateral macular coloboma in association with apical dystrophy of the hands and feet. Br J Ophthalmol. 1935;19(2):65–90.
16. Thompson EM, Baraitser M. Sorsby syndrome: a report on further generations of the original family. J Med Genet. 1988;25(5):313–21.
17. Kalhoro A, Puech V, Puech B, Webster AR, Michaelides M, Moore AT, Hunt DM. A molecular genetic investigation of two families with macular dysplasia in association with digit abnormalities (abstract). IOVS. 2008;49:E456.

Sorsby Fundus Dystrophy

7

Michel Michaelides and Anthony Moore

Abstract

The inherited macular dystrophies comprise a heterogeneous group of disorders characterised by central visual loss and encompass a wide range of clinical, psychophysical, imaging and histopathological findings. The majority of disease-causing genes have now been identified. There are a small group of these disorders, including Sorsby fundus dystrophy, autosomal dominant drusen and late-onset retinal macular dystrophy, that present in later adult life and may be complicated by choroidal neovascularisation or macular atrophic changes similar to those seen in age-related macular degeneration.

Keywords

Macula • Dystrophy • Sorsby • Choroidal neovascular membrane • Drusen

7.1 Introduction

The inherited macular dystrophies are characterised by bilateral visual loss and generally symmetrical macular abnormalities on ophthalmoscopy. The age of onset is variable, but most present in the first three decades of life. There is considerable clinical and genetic heterogeneity. Macular dystrophies showing autosomal dominant, autosomal recessive, X-linked recessive and mitochondrial inheritance have all been reported, with many of the disease-causing genes now identified.

7.2 Sorsby Fundus Dystrophy

Sorsby fundus dystrophy (SFD) is a rare, autosomal dominant macular dystrophy, characterised by early drusen-like deposition and later loss of central vision from macular atrophy or choroidal neovascular membrane (CNVM) by the fifth

M. Michaelides, BSc, MBBS, MD, FRCOphth, FACS (✉)
Departments of Inherited Eye Disease, Medical Retina, and Paediatric Ophthalmology, Moorfields Eye Hospital, London, UK

Department of Genetics, UCL Institute of Ophthalmology, London, UK
e-mail: michel.michaelides@ucl.ac.uk

A. Moore, MA, FRCS, FRCOphth, FMedSci
Department of Ophthalmology, University of California School of Medicine, San Francisco, CA, USA

G. Querques, E.H. Souied (eds.), *Macular Dystrophies*, DOI 10.1007/978-3-319-26621-3_7

decade (Figs. 7.1 and 7.2). Night blindness is an early symptom. A tritan colour defect has been previously suggested as an early sign in SFD [1]. Intravitreal bevacizumab and ranibizumab have both been shown to be effective in the treatment of CNVM associated with SFD [2, 3].

The differential diagnosis includes disorders with an autosomal dominant (AD) mode of inheritance associated with macular atrophy and/or CNVM, including autosomal dominant drusen and late-onset retinal macular dystrophy. The possibility of these disorders, including SFD, should also be considered in any family with an AD form of presumed 'age-related macular degeneration'.

The tissue inhibitor of metalloproteinase-3 (*TIMP3* gene on chromosome 22q) is implicated in SFD [4–6]. Most of the known mutations in *TIMP3*, including Ser181Cys [4], Ser156Cys [5] and Tyr172Cys [6], introduce potentially unpaired cysteine residues in the C-terminus of the protein, thereby resulting in inappropriate disulphide bond formation and an abnormal tertiary protein structure. This may alter *TIMP3*-mediated extracellular matrix turnover leading to the thickening of Bruch's membrane and the widespread accumulation of abnormal material beneath the retinal pigment epithelium (RPE) that is seen histologically [7–9]. The thickening of Bruch's membrane is likely to alter the flow of nutrients and growth factors across it, leading to RPE/photoreceptor dysfunction.

The finding that treatment with high doses of oral vitamin A reverses night blindness in this disorder [10] suggests that early retinal dysfunction may be due to a reduction in the permeability of Bruch's membrane, resulting in the hindrance of transport of vitamin A from the choriocapillaris to the photoreceptors by accumulated extracellular debris beneath the RPE. In addition, Majid et al. [11] have demonstrated that mutant *TIMP3* can induce apoptosis of RPE cells suggesting that apoptosis may be the final pathway for cell death in this disorder. Furthermore, *TIMP3* has been recently shown to be a potent inhibitor of angiogenesis, which may, in part, account for the complication of choroidal neovascularisation seen in SFD [12]. *TIMP3* inhibits vascular endothelial growth factor (VEGF)-mediated angiogenesis, most probably by blockade of VEGF-2 receptors [12].

Further insights into the pathophysiology of SFD may follow the development of a knock-in mouse carrying a disease-related Ser156Cys mutation in the orthologous murine *TIMP3* gene [13]. Immunolabelling studies and biochemical data from these mice suggested that site-specific excess rather than absence or deficiency of functional *TIMP3* may be the primary consequence of the known *TIMP3* mutations [13].

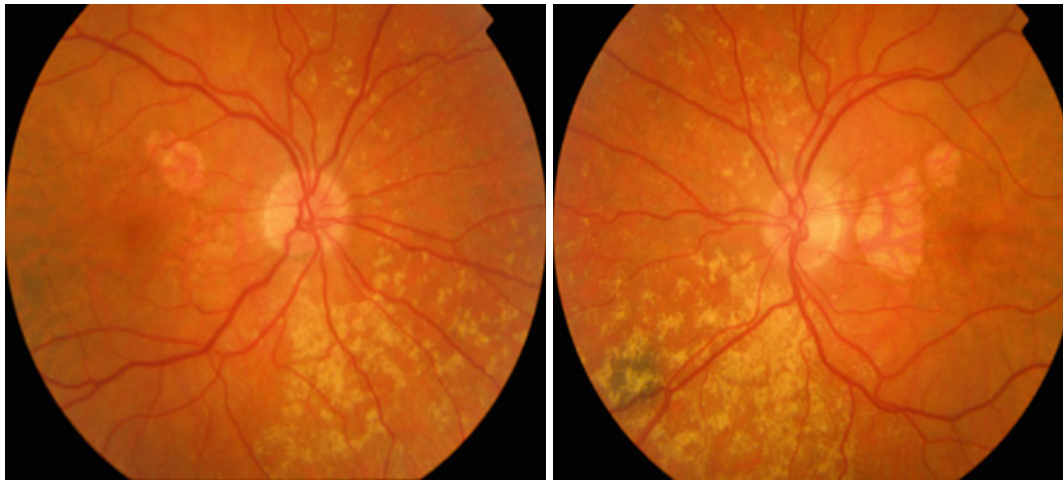

Fig. 7.1 Bilateral characteristic drusen-like deposits seen in Sorsby fundus dystrophy with areas of macular atrophy

Fig. 7.2 Choroidal neovascular membrane complicating Sorsby fundus dystrophy

7.3 Management

There is currently no established treatment for any of the inherited macular dystrophies. However, treatment trials have begun for Stargardt disease (STGD) and clinical trials in other disorders are anticipated over the next decade. In those macular dystrophies complicated by choroidal neovascularisation, anti-VEGF agents may be used and have been shown to be effective in Sorsby dystrophy [2, 3].

Despite the lack of effective treatment of the underlying disorder, early diagnosis, with molecular confirmation, is important for genetic counselling and also allows a more accurate prognosis. Affected family members can also be informed about potential environmental risk factors and be advised to avoid smoking and take steps to maintain a healthy diet and avoid obesity. Those patients with significant visual impairment should be referred for a low visual aid assessment.

Conclusions

The inherited macular dystrophies are a clinically and genetically heterogeneous group of disorders. Their phenotypes have now been well characterised and many causative genes have been identified. Establishing the diagnosis at an early stage can be helpful in enabling accurate prognosis and effective genetic counselling. At the present time, there is no effective treatment for these inherited macular dystrophies, although multiple avenues of research are beginning to result in early clinical trials and there is cautious optimism that further effective interventions will be available in the near future. However, intravitreal bevacizumab and ranibizumab have both been shown to be effective in the treatment of CNVM associated with SFD and other macular dystrophies [2, 3].

Although in some inherited macular dystrophies the disease appears to be confined to the macular region, in the majority of disorders, there is electrophysiological, psychophysical or histological evidence of widespread retinal dysfunction. Indeed, in the case of autosomal recessive STGD, the presence of widespread full-field ERG abnormalities can be used as an accurate indicator of a worse prognosis.

Improved knowledge of the pathomechanisms of inherited macular dystrophy and the underlying molecular genetics has not only raised the potential for future development of rational therapeutic regimens but has helped to refine diagnosis, disease classification and prognosis and improved genetic counselling.

References

1. Berninger TA, Polkinghorne PJ, Capon MR, Arden GB, Bird AC. Color vision defect. A early sign of Sorsby retinal dystrophy? Ophthalmologe. 1993;90(5):515–8 [article in German].
2. Kapoor KG, Bakri SJ. Intravitreal anti-vascular endothelial growth factor therapy for choroidal neovascularization due to Sorsby macular dystrophy. J Ocul Pharmacol Ther. 2013;29(4):444–7.
3. Balaskas K, Hovan M, Mahmood S, Bishop P. Ranibizumab for the management of Sorsby fundus dystrophy. Eye (Lond). 2013;27(1):101–2.
4. Weber BH, Vogt G, Pruett RC, Stohr H, Felbor U. Mutations in the tissue inhibitor of metalloproteinases-3 (*TIMP3*) in patients with Sorsby's fundus dystrophy. Nat Genet. 1994;8(4):352–6.
5. Felbor U, Stöhr H, Amann T, Schonherr U, Weber BH. A novel Ser156Cys mutation in the tissue inhibitor of metalloproteinases-3 (*TIMP3*) in Sorsby's fundus dystrophy with unusual clinical features. Hum Mol Genet. 1995;4(12):2415–6.

6. Jacobson SG, Cideciyan AV, Bennett J, Kingsley RM, Sheffield VC, Stone EM. Novel mutation in the *TIMP3* gene causes Sorsby fundus dystrophy. Arch Ophthalmol. 2002;120(3):376–9.
7. Chong NH, Alexander RA, Gin T, Bird AC, Lutert PJ. TIMP-3, collagen, and elastin immunohistochemistry and histopathology of Sorsby's fundus dystrophy. Invest Ophthalmol Vis Sci. 2000;41(3):898–902.
8. Capon MR, Marshall J, Krafft JI, Alexander RA, Hiscott PS, Bird AC. Sorsby's fundus dystrophy. A light and electron microscopic study. Ophthalmology. 1989;96(12):1769–77.
9. Stöhr H, Anand-Apte B. A review and update on the molecular basis of pathogenesis of Sorsby fundus dystrophy. Adv Exp Med Biol. 2012;723:261–7.
10. Jacobson SG, Cideciyan AV, Regunath G, Rodriguez FJ, Vandenburgh K, Sheffield VC, Stone EM. Night blindness in Sorsby's fundus dystrophy reversed by vitamin A. Nat Genet. 1995;11(1):27–32.
11. Majid MA, Smith VA, Easty DL, Baker AH, Newby AC. Sorsby's fundus dystrophy mutant tissue inhibitors of metalloproteinase-3 induce apoptosis of retinal pigment epithelial and MCF-7 cells. FEBS Lett. 2002;529(2–3):281–5.
12. Qi JH, Ebrahem Q, Moore N, Murphy G, Claesson-Welsh L, Bond M, et al. A novel function for tissue inhibitor of metalloproteinases-3 (*TIMP3*): inhibition of angiogenesis by blockage of VEGF binding to VEGF receptor-2. Nat Med. 2003;9(4):407–15.
13. Weber BH, Lin B, White K, Kohler K, Soboleva G, Herterich S, et al. A mouse model for Sorsby fundus dystrophy. Invest Ophthalmol Vis Sci. 2002;43(8):2732–40.

Mitochondrial Retinal Dystrophy Associated with the (m.3243A>G) Mutation

8

Camiel J.F. Boon and Pascale Massin

Abstract

Mitochondrial retinal dystrophy (MRD) is a maternally inherited, progressive retinal dystrophy caused by a mitochondrial mutation. MRD can be classified into four disease grades and is associated with systemic abnormalities such as maternally inherited diabetes and deafness, and mitochondrial encephalomyopathy, lactic acidosis, and stroke-like episodes (MELAS) syndrome. The fovea tends to be spared in MRD, with a relatively preserved visual acuity.

8.1 Background

Mitochondrial retinal dystrophy (MRD) is caused by an adenine-to-guanine mutation at position 3243 in the mitochondrial *MTTL1* gene encoding transfer (t) RNALEU(UUR) (m.3243A>G) [1]. The mutation is most well known for its association with the systemic conditions maternally inherited diabetes and deafness (MIDD) and mitochondrial encephalomyopathy, lactic acidosis, and stroke-like episodes (MELAS) syndrome. However, a marked intraindividual and interindividual variation in mitochondrial heteroplasmy causes wide spectrum of clinical symptoms and disease severity observed between family members who share the same mitochondrial mutation [2]. Cardiac, musculoskeletal, gastrointestinal, and renal involvement can also be seen, alone or in combination with the MIDD or MELAS syndrome phenotype.

The prevalence of the m.3243A>G mutation ranges from 7.6/100,000 in Northeast England to as high as 236/100,000 in Australia [3, 4]. The prevalence of the mutation among European and Japanese patients with adult-onset diabetes mellitus is approximately 0.8 % and 1.5 %, respectively [5]. However, the prevalence of the m.3243A>G mutation increases to more than 5 % in patients with adult-onset diabetes who also have deafness or a family history of deafness [5, 6].

C.J.F. Boon, MD, PhD, FEBOphth (✉)
Department of Ophthalmology, Leiden University Medical Center, Leiden, The Netherlands
e-mail: C.J.F.Boon@lumc.nl

P. Massin, MD, PhD
Department of Ophthalmology, Lariboisière Hospital, Paris, France
e-mail: Pascale.massin@aphp.fr

G. Querques, E.H. Souied (eds.), *Macular Dystrophies*, DOI 10.1007/978-3-319-26621-3_8

8.2 Clinical Findings

Patients with m.4343A>G-associated MRD can remain asymptomatic for a long time, and it is common for them to be identified during routine ophthalmological screening for diabetic retinopathy [2]. Fundus autofluorescence is the ophthalmic imaging modality of choice to identify retinal abnormalities that are typically associated with MRD. More than 85 % of m.3243A>G mutation carriers have retinal abnormalities, and MRD associated with the m.3243A>G mutation in the *MTTL1* gene has a fairly consistent phenotype [2, 7, 8]. This makes these retinal abnormalities one of the most prevalent and constant findings in the m.3243A>G-related disease spectrum. The spectrum of severity ranges from barely discernible pigmentary abnormalities in the outer retinal layers of the macula to profound chorioretinal atrophy in the macula. Retinal changes in MRD often also include the retina around the optic disc.

MRD associated with the m.3243A>G mutation can be classified into four grades, based on ophthalmoscopy and multimodal imaging including optical coherence tomography (OCT), fundus autofluorescence (FAF), and fluorescein angiography (Table 8.1) [2]. In every grade except grade 4, the structure and function of the fovea are relatively spared, resulting in a prolonged preservation of fairly good visual acuity. Even if the fovea is spared, considerable visual impairment can be present as a result of paracentral scotoma in cases of progressive atrophy around the fovea in grade 3 disease.

Patients with grade 1 MRD have discrete pigmentary abnormalities in the central fundus (Fig. 8.1a–d, Table 8.1) [2] that are also barely visible on autofluorescence and fluorescein angiography. Without prior knowledge of the underlying m.3243A>G mutation, these changes can be easily overlooked. The visual acuity in this early grade MRD is excellent.

In grade 2 MRD, isolated or multifocal faint white-yellowish or hyperpigmented subretinal deposits are present in the posterior pole (Fig. 8.1e, f) [2]. These deposits are visible in addition to the extremely fine pigment changes in grade 1 MRD. Few deposits can be present in early grade 2 disease, but the pigment changes involve the entire macula and sometimes encircle the optic disc in advanced grade 2 MRD. Fundus autofluorescence in grade 2 MRD shows granular changes and/or irregular flecks of increased and decreased autofluorescence. Fluorescein angiography shows mainly hyperfluorescence due to moderate RPE atrophy, except in areas of hyperpigmentation blocking background fluorescence. In all of these imaging modalities, the foveal aspect appears relatively spared, with a correspondingly preserved visual acuity.

Grade 3 MRD is characterized by the appearance of one or more areas of well-delineated areas of chorioretinal ("geographic") atrophy outside of the fovea (Fig. 8.2a–d) [2]. In grade 3 MRD, the area of geographic atrophy does not involve the central fovea in contrast to grade 4 disease, again explaining the relatively preserved visual acuity in this advanced disease stage. On FAF and OCT, the central foveal structure is relatively preserved compared with the surrounding atrophic zone (see Fig. 8.2a, b, d). Patients with MRD do not have typical drusen on ophthalmoscopy, FAF, or OCT, and choroidal neovascularization is extremely uncommon.

In grade 4 MRD, the profound chorioretinal atrophy also affects the fovea (Fig. 8.2e–g), resulting in marked central vision loss (Table 8.1; see Fig. 8.1) [2]. The visual acuity of patients in stage 4 disease can decrease to finger counting.

Due to the mitochondrial nature of the disease, a certain degree of ocular myopathy and myogenic ptosis can also be seen [2, 9]. Up to 86 % of patients with m.3243A>G-associated MIDD have evidence of retinal dystrophy [9]. As a result of the marked clinical variability, up to 17 % of patients are diagnosed as carriers of the m.3243A>G mutation purely based on an ophthalmological examination, for instance, at routine screening for diabetic retinopathy [2]. Thus, the establishment of the diagnosis of m.3243A>G mitochondrial retinal dystrophy should also depend on a high index of suspicion in patients who present with typical macular lesions.

The peripheral visual field is usually normal in MRD, and full-field electroretinography and the electro-oculogram are generally unaffected.

Table 8.1 The four grades of mitochondrial retinal dystrophy associated with the m.3243A>G mutation

Grade	Mean visual acuity	Ophthalmoscopy	Fundus autofluorescence (FAF)	Optical coherence tomography	Fluorescein angiography (FA)
1	20/20 (range, 20/25–20/16)	Mild pigmentary abnormalities in the central fundus (Fig. 8.1a)	Mild hypoautofluorescent mottling (Fig. 8.1b)	No obvious abnormalities (Fig. 8.1d)	Small hyperfluorescent spots (Fig. 8.1c)
2	20/20 (range, 20/63–20/12.5)	Isolated or multifocal faintly white-yellowish and/or hyperpigmented subretinal deposits in posterior pole (Fig. 8.1e)	Yellow-white spots/flecks correspond to mostly increased FAF; decreased FAF in mildly atrophic areas (Fig. 8.1f)	Irregular thickening and/or attenuation of the line corresponding to the photoreceptor inner/outer segment (ellipsoid) area; underlying retinal pigment epithelium (RPE) somewhat attenuated and irregular	Hypofluorescence of spots/flecks on FA due to blockage of background fluorescence; hyperfluorescent window defects in mildly atrophic zones
3	20/25 (range, 20/40–20/16)	Appearance of one or more areas of well-delineated, profound chorioretinal ("geographic") atrophy outside the fovea, in addition to grade 2 abnormalities (Fig. 8.2a)	Well-defined areas of absent autofluorescence due to atrophy of the lipofuscin-containing RPE in deeply atrophic areas (Figs. 8.2b)	Attenuated RPE cell layer as well as a markedly attenuated photoreceptor layer and external limiting membrane in areas of chorioretinal atrophy (Fig. 8.2d)	RPE window defects with visibility of the underlying larger choroidal vasculature and atrophy of the choriocapillaris
4	20/80 (range, 20/630–20/40)	Central fovea affected by profound chorioretinal atrophy (Fig. 8.2e)	Area of absent autofluorescence involving the fovea (Fig. 8.2f)	Atrophy of the outer retinal layers (Fig. 8.2g)	RPE window defect and atrophy of choriocapillaris in area of geographic atrophy

FA fluorescein angiography, *FAF* fundus autofluorescence, *RPE* retinal pigment epithelium

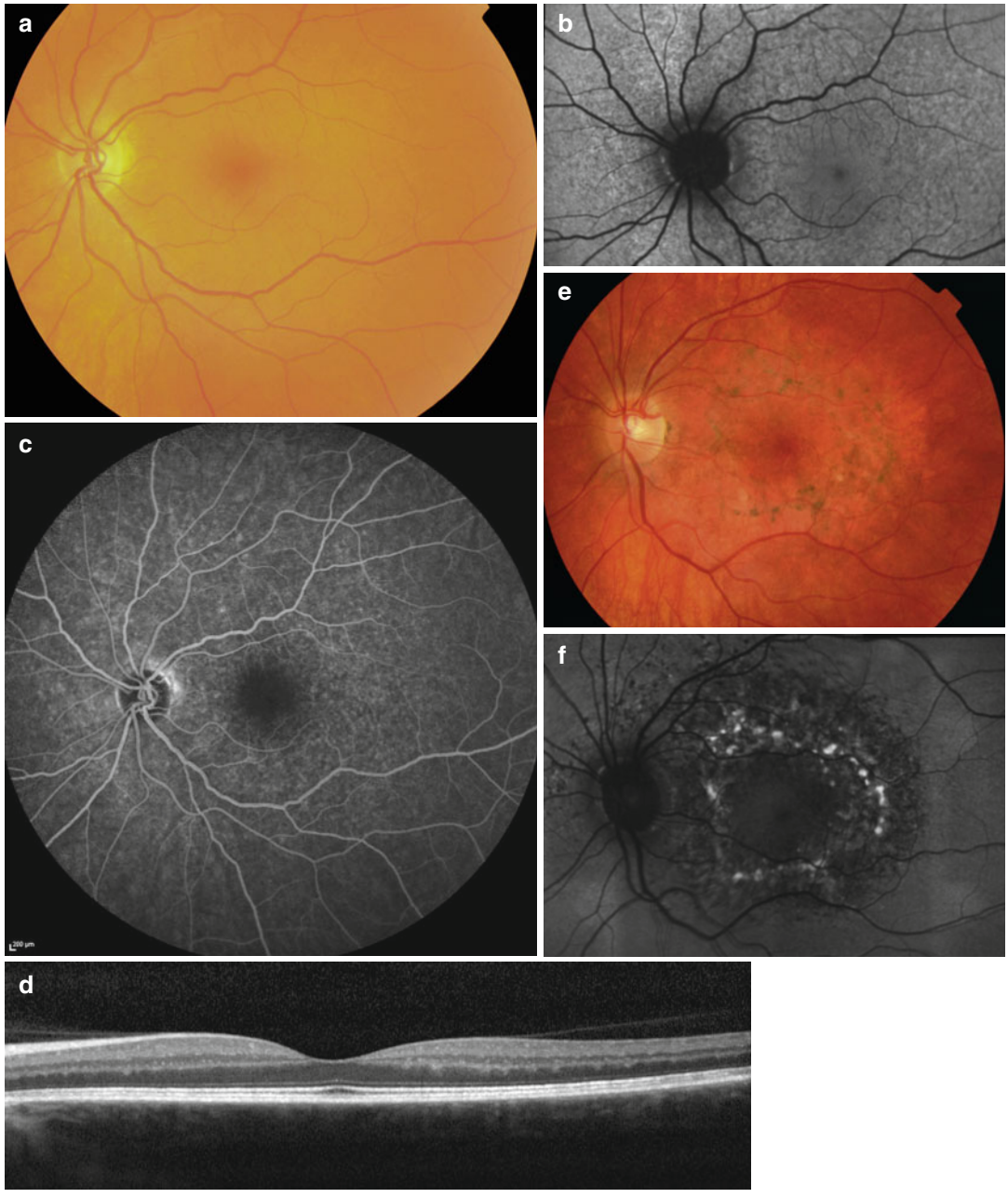

Fig. 8.1 Grade 1 and 2 mitochondrial retinal dystrophy (MRD). (**a**) Color fundus photograph of grade 1 MRD in an asymptomatic 42-year-old patient with a visual acuity of 20/20. (**b**) On detailed ophthalmoscopy, discrete pigmentary changes could be observed in the macula, which corresponded to mild but clearly visible mottled fundus autofluorescence (FAF) changes in the macula and peripapillary region. (**c**) Fluorescein angiography showed mild mottled hyperfluorescent abnormalities. (**d**) Optical coherence tomography in grade 1 MRD shows no obvious abnormalities. (**e**) Color fundus photograph of grade 2 MRD in a 27-year-old patient carrying the m.3243A>G (visual acuity: 20/20) showing an oval area of mottled hypopigmentation and hyperpigmented spots in the macula and around the optic disc. (**f**) FAF imaging shows mottled autofluorescence changes, with relative preservation of the foveal autofluorescence which is seen in many MRD cases

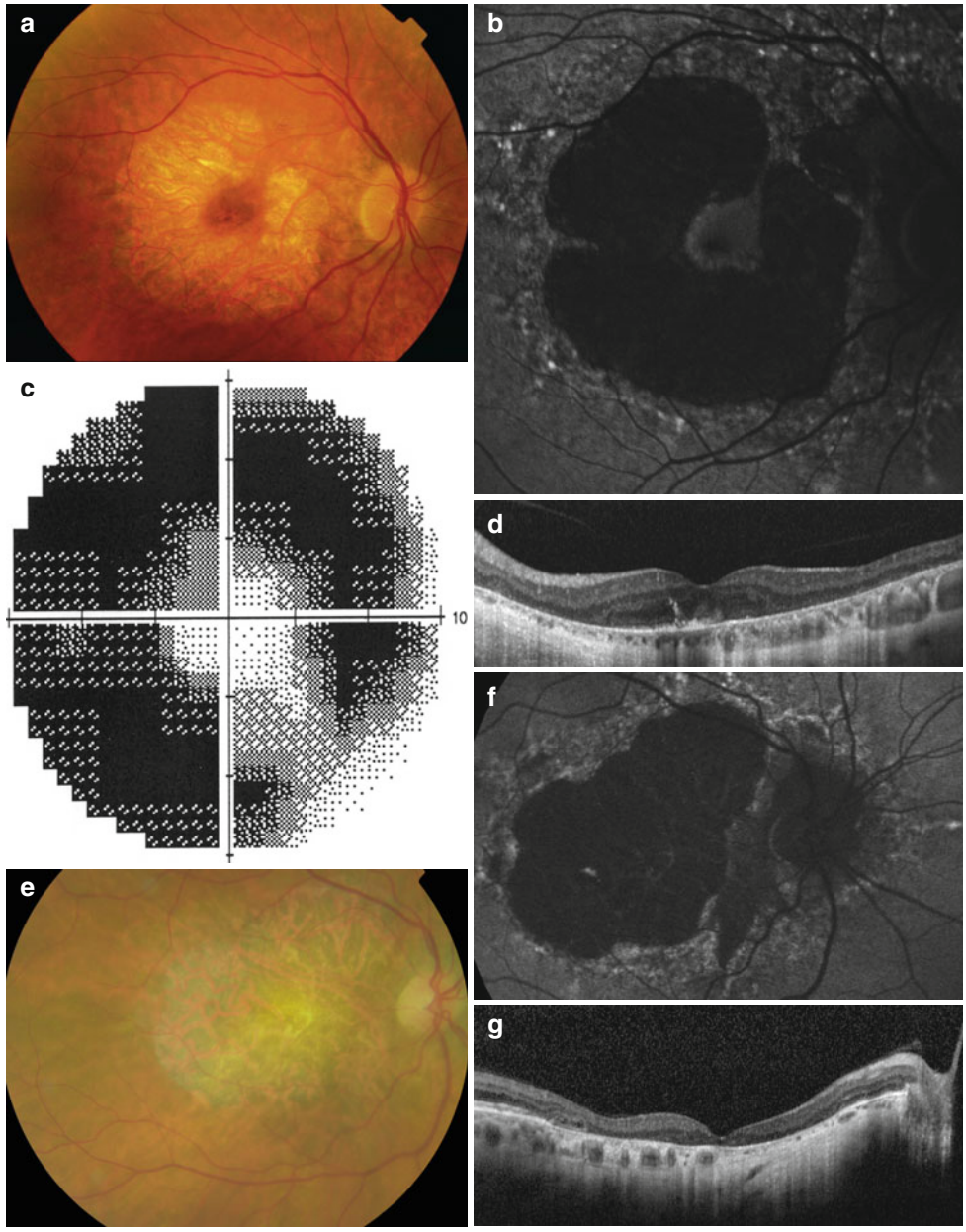

Fig. 8.2 Grade 3 and 4 mitochondrial retinal dystrophy (MRD). (**a**) Color fundus photograph of grade 3 MRD of a 43-year-old patient (visual acuity: 20/20) showing areas of more profound chorioretinal (geographic) atrophy in the macula with relative foveal sparing. (**b**) Fundus autofluorescence (FAF) in this patient showed a large dark area of absent FAF in the macula and adjacent to the optic disc corresponding to profound atrophy of the retinal pigment epithelium (RPE), which is also visible in (**a**). In addition, spots of highly increased FAF were visible throughout the posterior pole. (**c**) The foveal structure is relatively spared, which also correlates to relative functional sparing on central visual field testing. (**d**) Optical coherence tomography (OCT) scan (left eye of same patient, horizontal scan) shows some structural sparing of the outer retinal (photoreceptor) structures as compared to the surrounding atrophic areas. (**e**) Color fundus photograph of grade 4 MRD in a 57-year-old patient who also had mitochondrial encephalomyopathy, lactic acidosis, and stroke-like episodes (MELAS) syndrome, insulin-dependent diabetes mellitus, and deafness due to the m.3243A>G mutation. Marked chorioretinal atrophy in the macula was present since at least 5 years, with a corresponding visual acuity of 20/630. (**f**) FAF imaging in this patient showed a black area of RPE atrophy in the macula and around the optic disc, bordered by irregular autofluorescence changes. (**g**) OCT of grade 4 MRD shows profound outer retinal atrophy that includes the fovea

8.3 Disease Course

In stage 2 MRD, it usually takes many years to progress to geographic atrophy with vision loss [2, 10]. However, the evolution differs from one patient to the other, and the dystrophy may remain stable for years, without evolution toward atrophy. In stage 3 MRD cases in which the remaining foveal island is surrounded by profound atrophy, the foveal structure and visual acuity can remain be relatively spared for at least 5 years. In atypical cases with a central vitelliform lesion, progression to central atrophy and vision loss may occur faster, within 3 years.

8.4 Differential Diagnosis

Mitochondrial mutations are inherited maternally, so all offspring of an affected female should also carry the mutation. Nevertheless, the diagnosis of MRD can be challenging, because the maternal inheritance pattern can be masked due to non-penetrance resulting from a low degree of heteroplasmy. In addition, mutation analysis in blood has a 15 % false-negative rate, so additional DNA analysis of urine may be indicated in cases of a negative blood analysis with a typical MRD phenotype [11].

Most carriers of the m.3243A>G mutation have associated systemic diseases, and the clinical constellation of symptoms and diseases encompasses a broad and variable clinical spectrum besides typical MIDD or MELAS syndrome. As many as 17 % of patients are diagnosed as carriers of the m.3243A>G mutation based solely on the findings of an ophthalmological examination [2]. The identification of MRD therefore also depends on a high index of suspicion in patients who present with a typical phenotype.

Patients with *ABCA4*-associated late-onset Stargardt disease can have somewhat similar retinal lesions and also frequently have relative sparing of the fovea [12]. However, most late-onset Stargardt disease patients have a dark choroid on fluorescein angiography, and the peripapillary retina tends to be spared in contrast to MRD cases. Pseudo-Stargardt pattern dystrophy (see Chap. 3) and central areolar choroidal dystrophy (see Chap. 10), caused by autosomal dominant *PRPH2* gene mutations, should also be considered [13–15]. Another important differential diagnostic option is atrophic age-related macular degeneration (AMD), not only because it is the most common form of macular degeneration but also because both diabetes mellitus and deafness are common among the elderly. However, most patients with atrophic AMD have drusen on ophthalmoscopy and OCT, which are not present in MRD, and the lesions in AMD are usually less autofluorescent than in MRD. Finally, desferrioxamine maculopathy and pseudoxanthoma elasticum maculopathy may also be considered.

Conclusion

MRD is retinal dystrophy that mainly affects the macula and peripapillary retina, caused by the m.3243A>G mutation in the mitochondrial DNA. MRD is associated with a broad range of systemic associations, including maternally inherited diabetes and deafness (MIDD) and MELAS syndrome. A certain degree of ptosis and/or external ophthalmoplegia may also be present. The visual acuity in MRD is usually relatively preserved until grade 4 disease is reached, because of prolonged anatomical and functional sparing of the fovea.

References

1. Goto Y, Nonaka I, Horai S. A mutation in the tRNA(Leu)(UUR) gene associated with the MELAS subgroup of mitochondrial encephalomyopathies. Nature. 1990;348(6302):651–3.
2. de Laat P, Smeitink JA, Janssen MC, Keunen J, Boon CJ. Mitochondrial retinal dystrophy associated with the m.3243A>G mutation. Ophthalmology. 2013;120(12):2684–96.
3. Chinnery PF, Johnson MA, Wardell TM, Singh-Kler R, Hayes C, Brown DT, et al. The epidemiology of pathogenic mitochondrial DNA mutations. Ann Neurol. 2000;48(2):188–93.
4. Manwaring N, Jones MM, Wang JJ, Rochtchina E, Howard C, Mitchell P, Sue CM. Population prevalence of the MELAS A3243G mutation. Mitochondrion. 2007;7(3):230–3.

5. Murphy R, Turnbull DM, Walker M, Hattersley AT. Clinical features, diagnosis and management of maternally inherited diabetes and deafness (MIDD) associated with the 3243A>G mitochondrial point mutation. Diabet Med. 2008;25(4):383–99.
6. Guillausseau PJ, Massin P, Dubois-LaForgue D, Timsit J, Virally M, Gin H, et al. Maternally inherited diabetes and deafness: a multicenter study. Ann Intern Med. 2001;134(9 Pt 1):721–8.
7. Massin P, Guillausseau PJ, Vialettes B, Paquis V, Orsini F, Grimaldi AD, Gaudric A. Macular pattern dystrophy associated with a mutation of mitochondrial DNA. Am J Ophthalmol. 1995;120(2):247–8.
8. Rath PP, Jenkins S, Michaelides M, Smith A, Sweeney MG, Davis MB, et al. Characterisation of the macular dystrophy in patients with the A3243G mitochondrial DNA point mutation with fundus autofluorescence. Br J Ophthalmol. 2008;92(5):623–9.
9. Massin P, Virally-Monod M, Vialettes B, Paques M, Gin H, Porokhov B, et al. Prevalence of macular pattern dystrophy in maternally inherited diabetes and deafness. GEDIAM group. Ophthalmology. 1999;106(9):1821–7.
10. Ambonville C, Meas T, Lecleire-Collet A, Laloi-Michelin M, Virall M, Kevorkian JP, et al. Macular pattern dystrophy in MIDD: long-term follow-up. Diabetes Metab. 2008;34(4 Pt 1):389–91.
11. de Laat P, Koene S, van den Heuvel LP, Rodenburg RJ, Janssen MC, Smeitink JA. Clinical features and heteroplasmy in blood, urine and saliva in 34 Dutch families carrying the m.3243A>G mutation. J Inherit Metab Dis. 2012;35(6):1059–69.
12. Westeneng-van Haaften SC, Boon CJ, Cremers FP, Hoefsloot LH, den Hollander AI, Hoyng CB. Clinical and genetic characteristics of late-onset Stargardt's disease. Ophthalmology. 2012;119(6):1199–210.
13. Boon CJ, den Hollander AI, Hoyng CB, Cremers FP, Klevering BJ, Keunen JE. The spectrum of retinal dystrophies caused by mutations in the peripherin/RDS gene. Prog Retin Eye Res. 2008;27(2):213–35.
14. Boon CJ, Klevering BJ, Cremers FP, Zonneveld-Vrieling MN, Theelen T, Den Hollander AI, Hoyng CB. Central areolar choroidal dystrophy. Ophthalmology. 2009;116:771–82. 782.e1.
15. Boon CJ, van Schooneveld MJ, den Hollander AI, van Lith-Verhoeven JJ, Zonneveld-Vrieling MN, Theelen T, et al. Mutations in the peripherin/RDS gene are an important cause of multifocal pattern dystrophy simulating STGD1/fundus flavimaculatus. Br J Ophthalmol. 2007;91(11):1504–11.

X-Linked Retinoschisis

9

Isabelle Audo, José-Alain Sahel, Saddek Mohand-Saïd, Graham Holder, and Anthony Moore

Abstract

X-linked retinoschisis (MIM#312700) is linked to mutations in *RS1* encoding retinoschisin a protein critical for cell-cell adhesion and intercellular matrix interactions. It is a rare inherited disorder with a prevalence estimated between 1/5,000 and 1/20,000, affecting male subjects with female carriers being asymptomatic with only few reports of subtle changes. Age of onset can be as early as pre-school screening. Clinical manifestations are variable even within the same family with little phenotype/genotype correlation. Macular abnormalities are present in virtually all cases, the most typical picture being the classic spoke-wheel appearance of macular cysts. Atrophic lesions will develop in later stages. The full-field electroretinogram is critical for the diagnosis especially in case of atypical presentation or in late stages. It typically reveals an electronegative waveform in response to a standard or bright flash under scotopic

I. Audo, MD, PhD (✉)
Département de génétique, Institut de la Vision, Paris, France

Institut de la Vision, Sorbonne Universités, UPMC University Paris 06, UMR_S 968, Paris, France

Centre Hospitalier National d'Ophtalmologie des Quinze-Vingts, DHU View Maintain, INSERM-DHOS CIC 1423, Paris, France

INSERM, U968, Paris, France

CNRS, UMR_7210, Paris, France

University College of London Institute of Ophthalmology, London, UK
e-mail: isabelle.audo@inserm.fr

J.-A. Sahel, MD • S. Mohand-Saïd, MD, PhD
Institut de la Vision, Sorbonne Universités, UPMC University Paris 06, UMR_S 968, Paris, France

Centre Hospitalier National d'Ophtalmologie des Quinze-Vingts, DHU View Maintain, INSERM-DHOS CIC 1423, Paris, France

INSERM, U968, Paris, France

CNRS, UMR_7210, Paris, France
e-mail: j.sahel@gmail.fr; saddekms@gmail.com

G. Holder, PhD
Moorfields Eye Hospital, University College London Institute of Ophthalmology, London, UK
e-mail: Graham.Holder@moorfields.nhs.uk

A. Moore, MA, FRCS, FRCOphth, FMedSci
Department of Ophthalmology, University of California School of Medicine, San Francisco, CA, USA
e-mail: tony.moore@ucsf.edu

G. Querques, E.H. Souied (eds.), *Macular Dystrophies*, DOI 10.1007/978-3-319-26621-3_9

conditions with a reduced b/a ratio in keeping with generalized inner retinal dysfunction. The diagnosis can be molecularly confirmed by identifying mutations in *RS1*. Management will include a careful refraction, low vision aids, school support and anhydrase carbonic inhibitors. Gene therapy trials are underway.

Keywords
X-linked retinoschisis • Retinoschisis • Retinoschisin • RS1 • Electronegative electroretinogram • Intraretinal cysts

Often classified within the macular dystrophies, *X-linked retinoschisis* (XLRS, MIM #312700) pathogenesis however involves more than the macular area and it should be regarded more as a generalized retinal disease with inner retinal dysfunction. It is linked to mutations in the *RS1* gene located on Xp22 [1].

Haas was the first to report two affected male patients with the typical radiating cystic maculopathy [2]. The X-linked pattern of inheritance was suggested by Pagenstecher in 1913 [3]. The term "retinoschisis" was first proposed by Wilczek in 1935 to reflect the splitting of the neural retina characterizing this disorder [4]. The disorder is present worldwide with an estimated prevalence of between 1/5,000 and 1/20,000 [5]. It is, however, higher in Finland (about 1/14,000) due to three founder mutations [6].

The clinical manifestations of XLRS are highly variable in affected males even within the same family; there is no clear phenotype/genotype correlation. Female carriers generally have a normal eye examination, but may occasionally show subtle abnormalities. There have been a few reports of affected females with homozygous *RS1* mutations in families with parental consanguinity [7, 8].

9.1 Clinical Presentation

XLRS shows a complete penetrance in affected males with marked phenotypic variability. The *initial presentation* is usually with decreased vision often detected during pre-school vision screening around 3 or 4 years of age. Children who are not detected during screening usually present with vision problems at school or with convergent strabismus. Such children are often hyperopic, but the visual acuity does not improve to normal with refractive correction. Spontaneous vitreous haemorrhage occurring in a male child or adolescent is another mode of presentation, and XLRS is the most common cause of spontaneous vitreous haemorrhage in a young male. Rarely XLRS can present as severe bullous schisis in infancy [5]; if unilateral, this may present as an early-onset strabismus or, if bilateral, with nystagmus. There may be associated vitreous haemorrhage. There is often an associated pigment line at the edge of the schisis. The bullous schisis cavity may flatten with time.

Visual acuity can vary between 20/25 and 20/400 or worse. The worst visual acuity is seen in case of extensive schisis that involve the central retina. Vision in most affected males is usually relatively stable until middle age when progressive macular atrophy may develop.

Peripheral visual field test is usually normal except in areas of the visual field corresponding to peripheral schisis where there may be an absolute scotoma. *Colour vision* is usually normal or may show a tritan defect in relation with secondary macular cone dysfunction.

Fundus examination shows macular abnormalities in virtually all cases, and these changes may be the only findings. Foveal schisis are seen as microcystic spaces radiating from the fovea (classic spoke-wheel appearance) (Fig. 9.1) [9] and are usually associated with a relatively preserved visual acuity. With time, the cysts collapse, giving way to non-specific macular atrophic changes associated with decreased

Fig. 9.1 (**a**) Colour fundus photographs; (**b**) fundus autofluorescence; (**c**) foveal horizontal scan for SD-OCT (Adapted from Audo et al. [9] with the kind permission of Springer Science + Business Media)

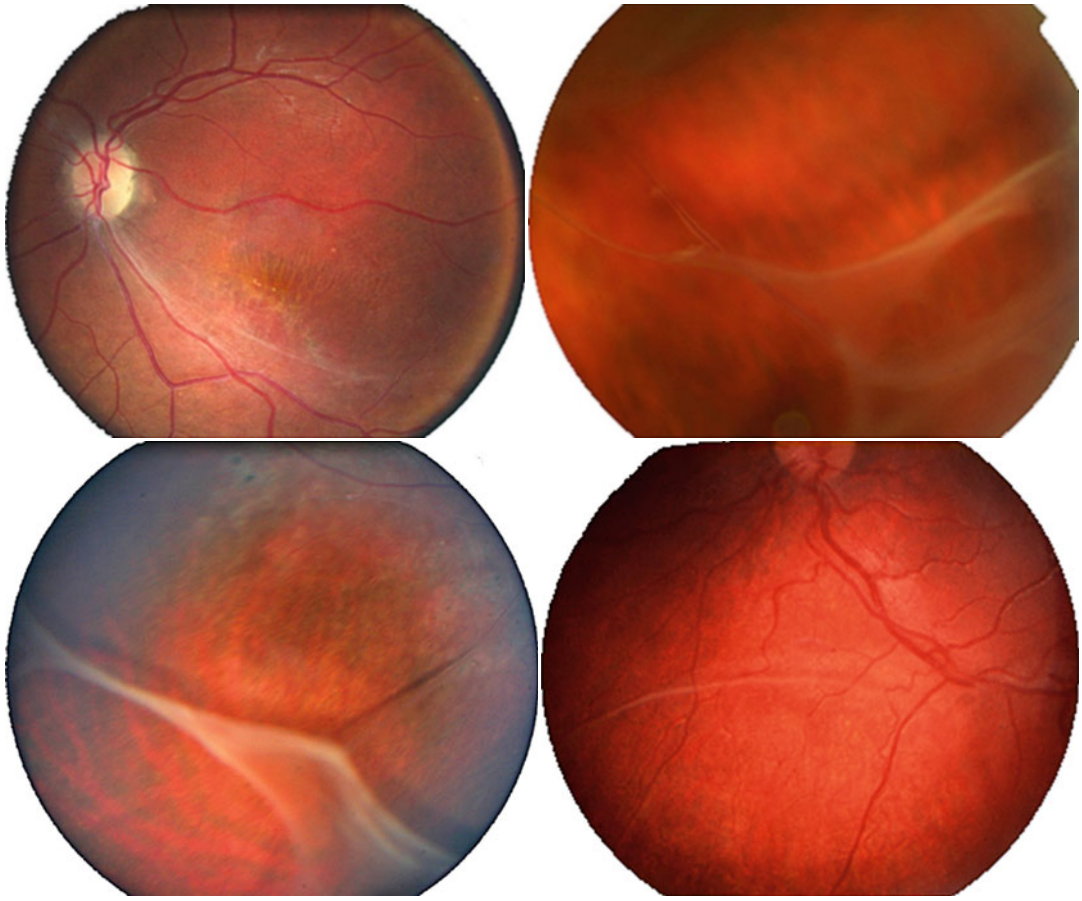

Fig. 9.2 Peripheral schisis (Adapted from Audo et al. [9] with the kind permission of Springer Science + Business Media)

visual acuity. Peripheral retinal schisis are seen in 50–70 % of patients and most commonly involve the inferotemporal quadrant (Fig. 9.2). Pigmented peripheral retinal scars can appear after spontaneous involution of peripheral cysts (Fig. 9.3).

Other less common peripheral abnormalities include inner retinal sheen or glistening resembling the Mizuo phenomenon (Fig. 9.4) [10–12], vascular sheathing and closure, peripheral pigment clumping, neovascularisation in the peripheral retina or of the optic disc [13], pseudopapillitis, and exudative retinal detachment with retinal telangiectasia [14]. Neovascular glaucoma has also been reported and may occur secondary to retinal vascular closure [15].

Another atypical manifestation of XLRS includes fundus albipunctatus-like or crystalline appearance of the posterior pole (Fig. 9.5) and widespread inner retinal sheen without foveal schisis [16–18]. In these difficult cases, electrophysiological assessment and molecular genetic testing will direct the diagnosis.

Fundus abnormalities in *female carriers* of XLRS are very uncommon with only few reports of macular cysts and an electronegative electroretinogram (ERG) response [19, 20] or subtle changes on multifocal ERG testing [21]. Retinal abnormalities similar to the affected male have been reported in females from consanguineous unions found to carry homozygous pathogenic changes on *RS1* [7, 22].

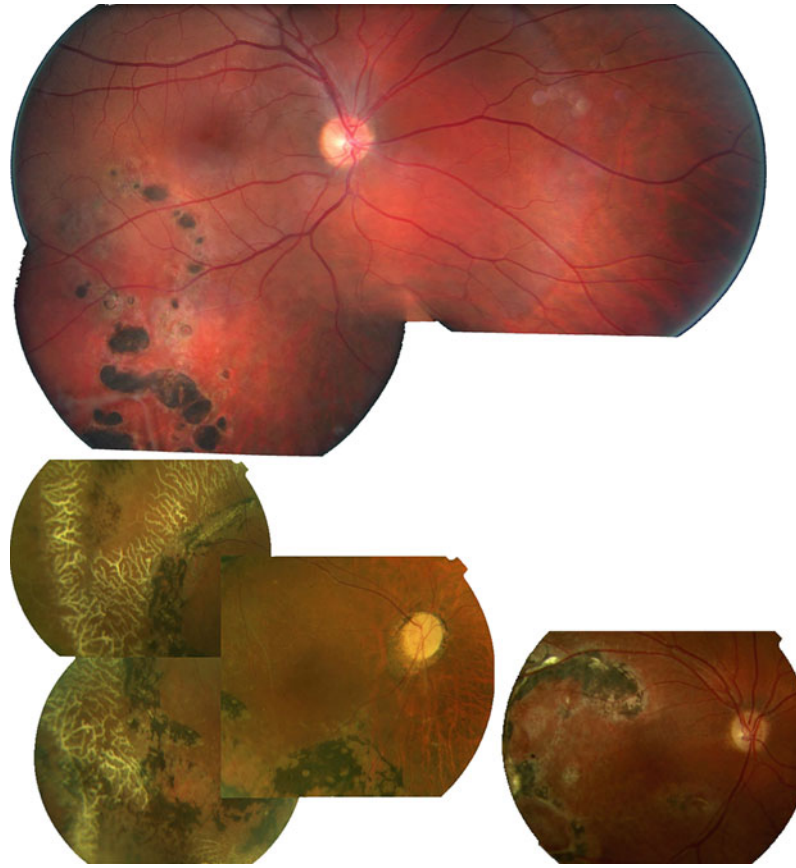

Fig. 9.3 Pigmentary changes in long-standing schisis (Adapted from Audo et al. [9] with the kind permission of Springer Science + Business Media)

Fundus autofluorescence can be of help when fundus changes are minimally detectable. It shows modification of foveolar autofluorescence with irregular or radial abnormalities when foveal schisis is present [23] (see Fig. 9.1). These changes are most likely in keeping with altered light transmission. Central hypo-autofluorescence is correlated with atrophic changes.

Spectral Domain Optical Coherence Tomography (SD-OCT) (See Fig. 9.1) This non-invasive tool has changed the diagnostic approach to XLRS: Cystic changes may be present in any layer of the retina and extend beyond visible fundus abnormalities [24–26]. In older patients, SD-OCT can detect macular thinning corresponding to atrophy.

Fluorescein angiography is not indicated for the diagnosis of X-linked retinoschisis, ERG in combination with OCT being the most helpful diagnostic tools with confirmation by molecular genetic testing. At the spoke-wheel stage, there is typically cyst pooling of the dye with no leakage allowing differential diagnosis with macular oedema. Late stages with macular atrophy of the retinal pigment epithelium will manifest with window defects.

9.2 Histopathology

Histological reports initially suggested splitting within the neurosensory retina, predominantly the nerve fiber layer differing from senile retinoschisis in which splitting occurs in the middle layers [27–29]. A more recent study of a specimen with neovascular glaucoma reports splitting within the outer plexiform layer both in peripheral and macular schisis [15]. Focal retinal pigment epithelium degeneration and photoreceptor disruption may occur as a secondary change.

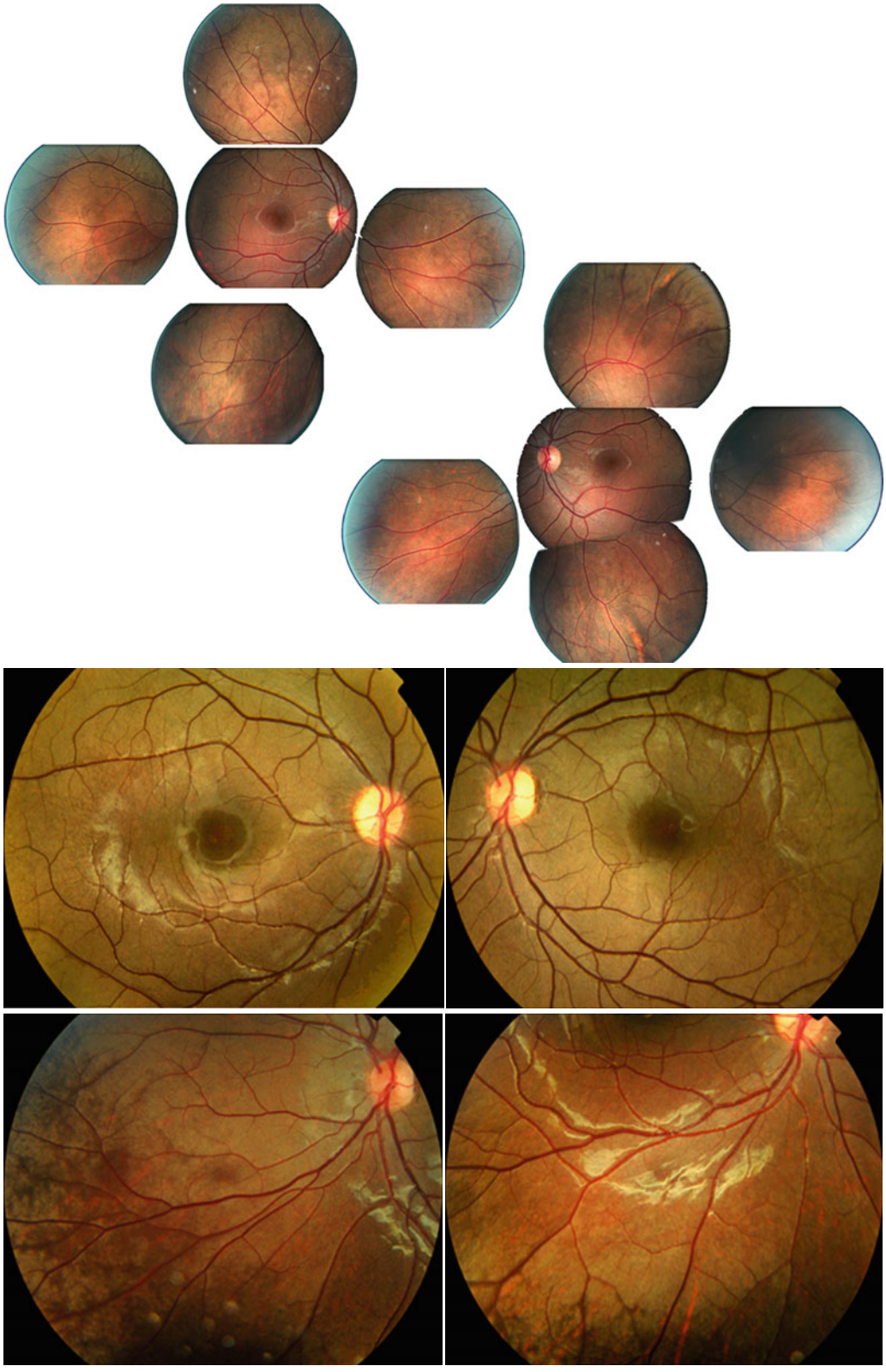

Fig. 9.4 Unusual form of XLRS with tapetal-like reflex (Adapted from Audo et al. [9] with the kind permission of Springer Science + Business Media)

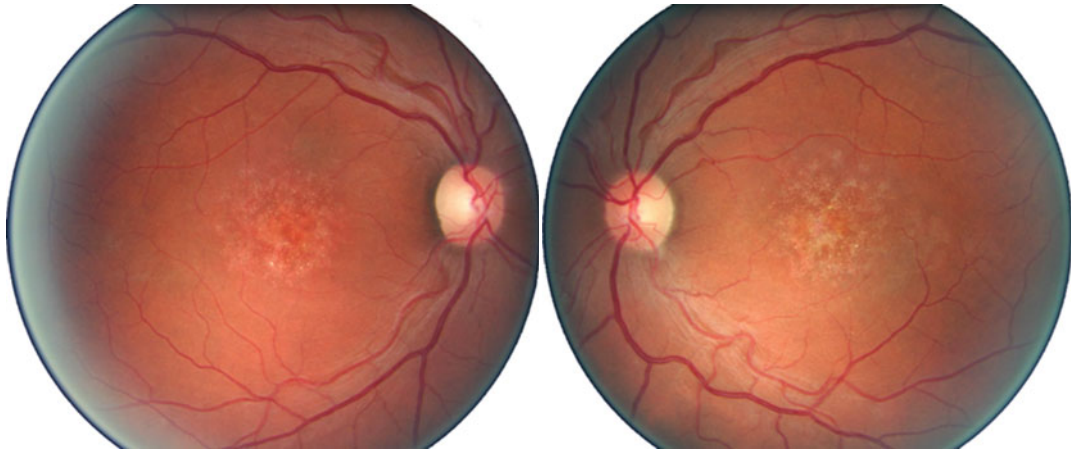

Fig. 9.5 Unusual XLRS manifestation with white-dot appearance (From Audo et al. [9] with the kind permission of Springer Science + Business Media)

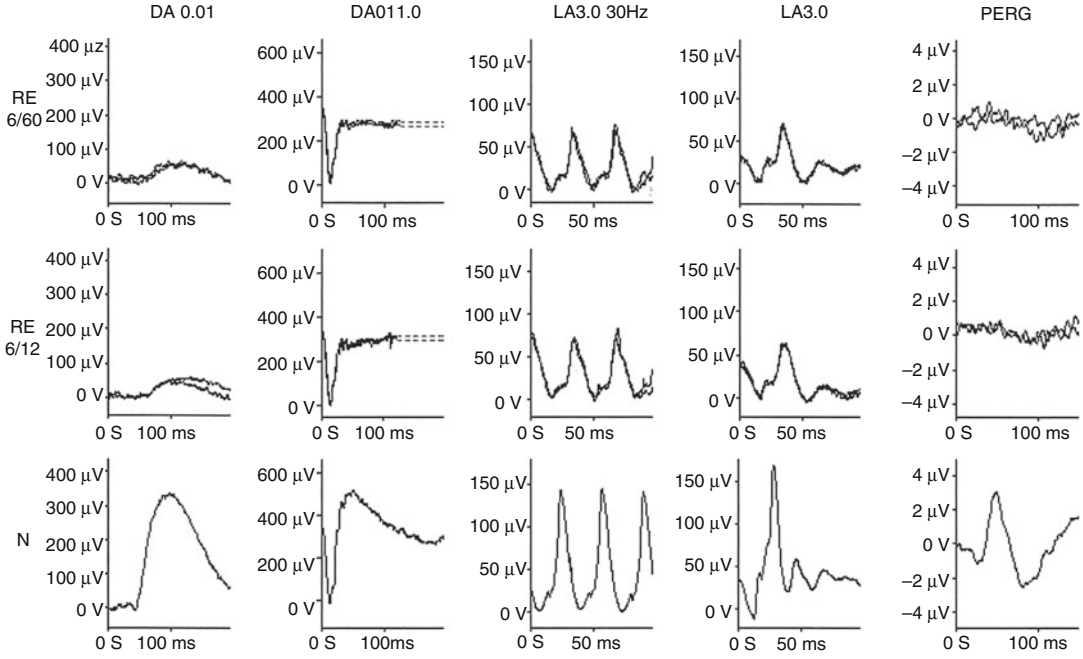

Fig. 9.6 ERG abnormalities in XLRS: the rod-specific ERG (DA 0.01) is bilaterally subnormal; the bright flash dark-adapted ERGs (DA 11.0) are bilaterally electronegative, the b-wave amplitudes being smaller than the a-waves; the 30-Hz flicker ERGs are bilaterally delayed and also decreased in amplitude; the LA 3.0 responses revealed a reduced b/a ratio; pattern ERGs (*PERGs*) are markedly subnormal in keeping with macular dysfunction (From Audo et al. [9] with the kind permission of Springer Science + Business Media)

9.3 Electrophysiology and Psychophysics

Full-field electroretinogram (ffERG) is critical for the clinical diagnosis of XLRS, especially in atypical cases: the ffERG typically shows an electronegative waveform in response to a bright flash under dark-adapted conditions (Fig. 9.6). There is a normal, or nearly normal, a-wave, reflecting normal photoreceptor function, and a severely reduced b-wave in keeping with post-photoreceptor transmission defect [30, 31]. There

is also a reduced b/a ratio in response to a single flash in photopic condition as well as reduced 30 Hz flicker amplitude. These findings are consistent with inner retinal dysfunction affecting both rod and cone pathways. There is predominant dysfunction of the ON pathway, with the OFF pathway being less variably affected [23, 31–33]. Positive correlations both between mutation severity and decreased b-wave amplitude as well as age and decreased b-wave amplitude have been reported [34, 35]. ERG abnormalities are, however, variable: an a-wave amplitude reduction has been reported [36], in particular if XLRS is complicated with retinal detachment. Relative b-wave preservation has also been reported in few cases [35, 36], outlining the importance of familial history, clinical examination, and mutations screening for the proper diagnosis in atypical cases.

9.4 Differential Diagnosis

The clinical diagnosis of XLRS is based on fundus examination, ERG findings of an electronegative waveform to the dark-adapted maximal response, and the typical cystic changes on OCT. The diagnosis can be confirmed by the identification of pathogenic mutations in the *RS1* gene.

Differential diagnosis will include other causes of *foveal cystic changes* and peripheral schisis. Foveal cystic changes may be seen in rare autosomal recessive or dominant schisis [37, 38], but in these disorders there are usually normal full-field ERG responses. Other causes of foveal schisis include cystoid macular oedema in rod-cone dystrophies, the enhanced S-cone syndrome, autosomal recessive bestrophinopathy, and nicotinic acid maculopathy. These disorders can usually be easily distinguished from XLRS on the basis of family history, electrophysiological testing, imaging, and molecular diagnosis.

Other forms of peripheral schisis include senile/degenerative schisis and the retinal schisis of high myopia. Senile schisis affects both males and females after 50 years of age, is usually bilateral, and is predominantly localized in the inferotemporal quadrant. In both senile schisis and the peripheral schisis of high myopia, the full-field ERG is normal.

Differential diagnosis will also include other causes of electronegative ERG [39].

9.5 Genetics and Pathophysiology

XLRS is due to mutations in *RS1* located on Xp22.1 [1]. The gene spans a genomic region of 32.4 kb with six exons encoding a signal peptide, characteristic secreted proteins (exons 1 and 2), a retinoschisin domain (exon 3), and the well-conserved discoidin domain motif (exon 4–6) implicated in cell adhesion [40, 41]. The resulting protein, a 224-amino acid protein, is called retinoschisin (RS1). In the adult retina, RS1 is expressed in photoreceptors and bipolar cells and is secreted in the extracellular matrix. It plays a critical role in cell-cell adhesion and cell-matrix interaction important for retinal lamination and synaptic structure relevant for the proper retinal function, in particular at the photoreceptor presynaptic terminals and at the dendritic tips of bipolar cells [41–44].

More than 190 mutations have been reported in patients with XLRS (see the LOVD – Leiden Open Variation Database; http://databases.lovd.nl/shared/genes/RS1), the majority of which are missense mutations localized within the discoidin domain leading to misfolding, misrouting, or functional loss of the protein and suggesting an important function role for this domain. Other mutations include deletions, insertions, and splice site mutations leading to loss of functional protein production [45].

9.6 Management

There is no current specific treatment for XLRS. A careful refraction, the detection of amblyopia and appropriate management, and the provision of low vision aids when needed can improve residual visual performance. In children, it is essential to provide adequate educational

support at school. Patients should avoid high contact sports, and protective goggles may be advised for ball sports. Families should be offered genetic counselling.

Carbonic anhydrase inhibitors, either topically (dorzolamide three times a day) or orally, have shown to reduce intraretinal cysts with some improvement in visual acuity, although the response may take several months of treatment [46–48]. If the acuity worsens with treatment, discontinuation with retreatment has shown some benefit [49]. Although the long-term effect of such treatment is not known, it seems sensible to recommend a treatment trial for at least 3 month for patients who are keen to improve their vision and are able to tolerate the side effects.

Surgical treatment is indicated when XLRS is complicated by rhegmatogenous retinal detachment or persistent vitreous haemorrhage. Retinal detachment surgery has a higher risk of developing proliferative vitreoretinopathy and may have limited effect on visual outcome [5, 50].

Proof of principal for gene replacement therapy on mouse models has now been achieved for both for structural and functional recovery [44, 51–55] and the first gene therapy trial is now undertaken in the group of Dr Paul Sieving (ClinicalTrials.gov: NCT02317887) with other planned trials in the United States (ClinicalTrials.gov: NCT02416622).

References

1. Sauer CG, Gehrig A, Warneke-Wittstock R, Marquardt A, Ewing CC, Gibson A, et al. Positional cloning of the gene associated with X-linked juvenile retinoschisis. Nat Genet. 1997;17(2):164–70.
2. Haas J. Ueber das Zusammenvorkommen von Veranderungen der Retina und Chorioidea. Arch Augenheilkd. 1898;37:343–8.
3. Pagenstecher H. Ueber eine unter dem Bilde der Netzhautablosung verlaufende, erbliche Erkrankung der Retina. Graefes Arch Ophthalmol. 1913;86(3):457–62.
4. Wilczek M. Ein Fall der Netzhautspaltung (Retinoschisi) mit einer öffnung. Zeit Augenheilkd. 1935;85(2–3):108–16.
5. George ND, Yates JR, Bradshaw K, Moore AT. Infantile presentation of X linked retinoschisis. Br J Ophthalmol. 1995;79(7):653–7.
6. Huopaniemi L, Rantala A, Forsius H, Somer M, de la Chapelle A, Alitalo T. Three widespread founder mutations contribute to high incidence of X-linked juvenile retinoschisis in Finland. Eur J Hum Genet. 1999;7(3):368–76.
7. Ali A, Feroze AH, Rizvi ZH, Rehman TU. Consanguineous marriage resulting in homozygous occurrence of X-linked retinoschisis in girls. Am J Ophthalmol. 2003;136(4):767–9.
8. Saleheen D, Ali A, Khanum S, Ozair MZ, Zaidi M, Sethi MJ, et al. Molecular analysis of the XLRS1 gene in 4 females affected with X-linked juvenile retinoschisis. Can J Ophthalmol. 2008;43(5):596–9.
9. Audo I, Mohand-Saïd M, Sahel J-A, Holder GE, Moore AT. Inherited chorioretinal dystrophies. In: Puech B, De Laey JJ, Holder GE, editors. X-linked retinoschisis. Heidelberg: Springer; 2014. p. 383–92.
10. de Jong PT, Zrenner E, van Meel GJ, Keunen JE, van Norren D. Mizuo phenomenon in X-linked retinoschisis. Pathogenesis of the Mizuo phenomenon. Arch Ophthalmol. 1991;109(8):1104–8.
11. Robson AG, Mengher LS, Tan MH, Moore AT. An unusual fundus phenotype of inner retinal sheen in X-linked retinoschisis. Eye. 2009;23(9):1876–8.
12. Iannaccone A, Mura M, Dyka FM, Ciccarelli ML, Yashar BM, Ayyagari R, et al. An unusual X-linked retinoschisis phenotype and biochemical characterization of the W112C RS1 mutation. Vision Res. 2006;46(22):3845–52.
13. Pearson R, Jagger J. Sex linked juvenile retinoschisis with optic disc and peripheral retinal neovascularisation. Br J Ophthalmol. 1989;73(4):311–3.
14. Greven CM, Moreno RJ, Tasman W. Unusual manifestations of X-linked retinoschisis. Trans Am Ophthalmol Soc. 1990;88:211–25; discussion 226–8.
15. Ando A, Takahashi K, Sho K, Matsushima M, Okamura A, Uyama M. Histopathological findings of X-linked retinoschisis with neovascular glaucoma. Graefes Arch Clin Exp Ophthalmol. 2000;238(1):1–7.
16. van Schooneveld MJ, Miyake Y. Fundus albipunctatus-like lesions in juvenile retinoschisis. Br J Ophthalmol. 1994;78(8):659–61.
17. Hotta Y, Nakamura M, Okamoto Y, Nomura R, Terasaki H, Miyake Y. Different mutation of the XLRS1 gene causes juvenile retinoschisis with retinal white flecks. Br J Ophthalmol. 2001;85(2):238–9.
18. Tsang SH, Vaclavik V, Bird AC, Robson AG, Holder GE. Novel phenotypic and genotypic findings in X-linked retinoschisis. Arch Ophthalmol. 2007;125(2):259–67.
19. Gieser EP, Falls HF. Hereditary retinoschisis. Am J Ophthalmol. 1961;51:1193–200.
20. Wu G, Cotlier E, Brodie S. A carrier state of X-linked juvenile retinoschisis. Ophthalmic Paediatr Genet. 1985;5(1–2):13–7.
21. Kim LS, Seiple W, Fishman GA, Szlyk JP. Multifocal ERG findings in carriers of X-linked retinoschisis. Doc Ophthalmol. 2007;114(1):21–6.
22. Rodriguez FJ, Rodriguez A, Mendoza-Londono R, Tamayo ML. X-linked retinoschisis in three females

from the same family: a phenotype-genotype correlation. Retina. 2005;25(1):69–74.
23. Renner AB, Kellner U, Fiebig B, Cropp E, Foerster MH, Weber BH. ERG variability in X-linked congenital retinoschisis patients with mutations in the RS1 gene and the diagnostic importance of fundus autofluorescence and OCT. Doc Ophthalmol. 2008;116(2):97–109.
24. Gerth C, Zawadzki RJ, Werner JS, Heon E. Retinal morphological changes of patients with X-linked retinoschisis evaluated by Fourier-domain optical coherence tomography. Arch Ophthalmol. 2008;126(6):807–11.
25. Gregori NZ, Berrocal AM, Gregori G, Murray TG, Knighton RW, Flynn Jr HW, et al. Macular spectral-domain optical coherence tomography in patients with X linked retinoschisis. Br J Ophthalmol. 2009;93(3):373–8.
26. Yu J, Ni Y, Keane PA, Jiang C, Wang W, Xu G. Foveomacular schisis in juvenile X-linked retinoschisis: an optical coherence tomography study. Am J Ophthalmol. 2010;149(6):973–8 e2.
27. Yanoff M, Kertesz Rahn E, Zimmerman LE. Histopathology of juvenile retinoschisis. Arch Ophthalmol. 1968;79(1):49–53.
28. Manschot WA. Pathology of hereditary juvenile retinoschisis. Arch Ophthalmol. 1972;88(2):131–8.
29. Condon GP, Brownstein S, Wang NS, Kearns JA, Ewing CC. Congenital hereditary (juvenile X-linked) retinoschisis. Histopathologic and ultrastructural findings in three eyes. Arch Ophthalmol. 1986;104(4):576–83.
30. Peachey NS, Fishman GA, Derlacki DJ, Brigell MG. Psychophysical and electroretinographic findings in X-linked juvenile retinoschisis. Arch Ophthalmol. 1987;105(4):513–6.
31. Khan NW, Jamison JA, Kemp JA, Sieving PA. Analysis of photoreceptor function and inner retinal activity in juvenile X-linked retinoschisis. Vision Res. 2001;41(28):3931–42.
32. Alexander KR, Barnes CS, Fishman GA. High-frequency attenuation of the cone ERG and ON-response deficits in X-linked retinoschisis. Invest Ophthalmol Vis Sci. 2001;42(9):2094–101.
33. Shinoda K, Ohde H, Mashima Y, Inoue R, Ishida S, Inoue M, et al. On- and off-responses of the photopic electroretinograms in X-linked juvenile retinoschisis. Am J Ophthalmol. 2001;131(4):489–94.
34. Sergeev YV, Caruso RC, Meltzer MR, Smaoui N, MacDonald IM, Sieving PA. Molecular modeling of retinoschisin with functional analysis of pathogenic mutations from human X-linked retinoschisis. Hum Mol Genet. 2010;19(7):1302–13.
35. Bowles K, Cukras C, Turriff A, Sergeev Y, Vitale S, Bush RA, Sieving PA. X-linked retinoschisis: RS1 mutation severity and age affect the ERG phenotype in a cohort of 68 affected male subjects. Invest Ophthalmol Vis Sci. 2011;52(12):9250–6.
36. Bradshaw K, George N, Moore A, Trump D. Mutations of the XLRS1 gene cause abnormalities of photoreceptor as well as inner retinal responses of the ERG. Doc Ophthalmol. 1999;98(2):153–73.
37. Yassur Y, Nissenkorn I, Ben-Sira I, Kaffe S, Goodman RM. Autosomal dominant inheritance of retinoschisis. Am J Ophthalmol. 1982;94(3):338–43.
38. Lewis RA, Lee GB, Martonyi CL, Barnett JM, Falls HF. Familial foveal retinoschisis. Arch Ophthalmol. 1977;95(7):1190–6.
39. Audo I, Robson AG, Holder GE, Moore AT. The negative ERG: clinical phenotypes and disease mechanisms of inner retinal dysfunction. Surv Ophthalmol. 2008;53(1):16–40.
40. Gehrig AE, Warneke-Wittstock R, Sauer CG, Weber BH. Isolation and characterization of the murine X-linked juvenile retinoschisis (Rs1h) gene. Mamm Genome. 1999;10(3):303–7.
41. Weber BH, Schrewe H, Molday LL, Gehrig A, White KL, Seeliger MW, et al. Inactivation of the murine X-linked juvenile retinoschisis gene, Rs1h, suggests a role of retinoschisin in retinal cell layer organization and synaptic structure. Proc Natl Acad Sci U S A. 2002;99(9):6222–7.
42. Molday LL, Hicks D, Sauer CG, Weber BH, Molday RS. Expression of X-linked retinoschisis protein RS1 in photoreceptor and bipolar cells. Invest Ophthalmol Vis Sci. 2001;42(3):816–25.
43. Grayson C, Reid SN, Ellis JA, Rutherford A, Sowden JC, Yates JR, et al. Retinoschisin, the X-linked retinoschisis protein, is a secreted photoreceptor protein, and is expressed and released by Weri-Rb1 cells. Hum Mol Genet. 2000;9(12):1873–9.
44. Ou J, Vijayasarathy C, Ziccardi L, Chen S, Zeng Y, Marangoni D, et al. Synaptic pathology and therapeutic repair in adult retinoschisis mouse by AAV-RS1 transfer. J Clin Invest. 2015;125(7):2891–903.
45. Functional implications of the spectrum of mutations found in 234 cases with X-linked juvenile retinoschisis. The Retinoschisis Consortium. Hum Mol Genet. 1998;7(7):1185–92.
46. Genead MA, Fishman GA, Walia S. Efficacy of sustained topical dorzolamide therapy for cystic macular lesions in patients with X-linked retinoschisis. Arch Ophthalmol. 2010;128(2):190–7.
47. Ghajarnia M, Gorin MB. Acetazolamide in the treatment of X-linked retinoschisis maculopathy. Arch Ophthalmol. 2007;125(4):571–3.
48. Apushkin MA, Fishman GA. Use of dorzolamide for patients with X-linked retinoschisis. Retina. 2006;26(7):741–5.
49. Thobani A, Fishman GA. The use of carbonic anhydrase inhibitors in the retreatment of cystic macular lesions in retinitis pigmentosa and X-linked retinoschisis. Retina. 2011;31(2):312–5.
50. Rosenfeld PJ, Flynn Jr HW, McDonald HR, Rubsamen PE, Smiddy WE, Sipperley JO, et al. Outcomes of vitreoretinal surgery in patients with X-linked retinoschisis. Ophthal Surg Lasers. 1998;29(3):190–7.
51. Min SH, Molday LL, Seeliger MW, Dinculescu A, Timmers AM, Janssen A, et al. Prolonged recovery of retinal structure/function after gene therapy in an

Rs1h-deficient mouse model of x-linked juvenile retinoschisis. Mol Ther. 2005;12(4):644–51.
52. Zeng Y, Takada Y, Kjellstrom S, Hiriyanna K, Tanikawa A, Wawrousek E, et al. RS-1 Gene delivery to an adult Rs1h knockout mouse model restores ERG b-Wave with reversal of the electronegative waveform of X-linked retinoschisis. Invest Ophthalmol Vis Sci. 2004;45(9):3279–85.
53. Janssen A, Min SH, Molday LL, Tanimoto N, Seeliger MW, Hauswirth WW, et al. Effect of late-stage therapy on disease progression in AAV-mediated rescue of photoreceptor cells in the retinoschisin-deficient mouse. Mol Ther. 2008;16(6):1010–7.
54. Kjellstrom S, Bush RA, Zeng Y, Takada Y, Sieving PA. Retinoschisin gene therapy and natural history in the Rs1h-KO mouse: long-term rescue from retinal degeneration. Invest Ophthalmol Vis Sci. 2007;48(8):3837–45.
55. Takada Y, Fariss RN, Muller M, Bush RA, Rushing EJ, Sieving PA. Retinoschisin expression and localization in rodent and human pineal and consequences of mouse RS1 gene knockout. Mol Vis. 2006;12:1108–16.

Miscellaneous Rare Macular Dystrophies

10

M. Dominik Fischer and Camiel J. F. Boon

Abstract

There are several very rare macular dystrophies that do not fall into the categories described elsewhere in this atlas. One of those, central areolar choroidal dystrophy (CACD) generally is a purely macular dystrophy caused by dominantly inherited *PRPH2* gene mutations. Dominant cystoid macular dystrophy is an intriguing progressive retinal dystrophy that presents with early-onset cystoid fluid collections in the macula as characteristic and primary clinical feature. Juvenile macular dystrophy and hypotrichosis due to recessive *CDH3* mutations combines a cone-rod dystrophy macular phenotype with general ectodermal changes such as abnormal hair growth, digital changes, and partial anodontia. The autosomal-dominant late-onset retinal degeneration (L-ORD), caused by *C1QTNF5* gene mutations, shows typical retinal abnormalities that can extend beyond the macula, and patients can report night blindness in addition to central vision loss. Interestingly, L-ORD patients can have long anteriorly inserted lens zonules and loss of iris pigment.

Keywords

Central areolar choroidal dystrophy (CACD) • Dominant cystoid macular dystrophy (DCMD) • Juvenile macular dystrophy and hypotrichosis • Late-onset retinal degeneration (L-ORD) • *PRPH2* gene • *CDH3* gene • *C1QTNF5* gene

10.1 Introduction

In this chapter, four major rare macular dystrophies are described. These macular dystrophies do not share clinically or genetic characteristics, except that they are all well-defined clinical entities that primarily affect the macula and do not fall into one of the disease categories described in the other chapters.

M.D. Fischer, MD, FEBO
Department of Ophthalmology, Centre for Ophthalmology Tubingen, University Eye Hospital Tubingen, Tubingen, Germany

C.J.F. Boon, MD, PhD, FEBOphth (✉)
Department of Ophthalmology, Leiden University Medical Center, Albinusdreef 2, 2333, ZA Leiden, The Netherlands
e-mail: C.J.F.Boon@lumc.nl

G. Querques, E.H. Souied (eds.), *Macular Dystrophies*, DOI 10.1007/978-3-319-26621-3_10

10.2 Central Areolar Choroidal Dystrophy

10.2.1 Background

Central areolar choroidal dystrophy (CACD) in multiple generations was first described by the Dutch ophthalmologist De Haas in 1931, and the phenotype was further delineated by Sorsby. Although the disease name suggests a primary abnormality in the choroid, CACD primarily affects the photoreceptors. Most cases are inherited autosomal dominantly due to a mutation in the *PRPH2* gene, although the disease is genetically heterogeneous. The *PRPH2* gene encodes a protein that is important for photoreceptor outer segment structure and function [1]. Mutations in the *PRPH2* gene can cause a wide range of retinal dystrophies besides CACD, including pseudo-Stargardt pattern dystrophy (see Chap. 3) and retinitis pigmentosa [1].

10.2.2 Clinical Findings

A certain degree of genotype-phenotype correlation exists in CACD, as the mean age at onset depends on the underlying *PRPH2* mutation. For example, in the phenotype caused by the p.Arg172Trp mutation and the p.Arg195Leu mutation in *PRPH2*, the age at onset is relatively early – in the third to fourth decade – whereas the p.Arg142Trp mutation generally has a later onset in the fifth to sixth decade [1–3]. Patients with CACD present with mild central visual loss, metamorphopsia, and, occasionally, mild photophobia [4]. Central scotomas can be noted in more advanced cases.

Fundus abnormalities in CACD can be classified into four stages (Fig. 10.1) [1, 4]. In stage 1, slight parafoveal pigmentary changes of the retinal pigment epithelium (RPE) are seen (Fig. 10.1a). Stage 2 is characterized by a round to oval, mildly atrophic hypopigmented area of up to five disc diameters in size (Fig. 10.1d). In stage 3, one or more areas of profound, well-demarcated chorioretinal atrophy appear outside the fovea (Fig. 10.1g). CACD reaches stage 4 when the fovea is also included in this area of chorioretinal atrophy (Fig. 10.1j). Visual acuity often decreases to less than 20/200 in this advanced stage. CACD is only rarely associated with drusen. Some patients develop more extensive atrophic pigmentary abnormalities beyond the vascular arcades, and chorioretinal atrophy can also be centered around the optic disc.

Fig. 10.1 Clinical stages of central areolar choroidal dystrophy (*CACD*). (**a**) Fundoscopy of stage 1 CACD reveals slight parafoveal hypopigmentation. (**b**) This area of hypopigmentation on ophthalmoscopy corresponds with an area increased fundus autofluorescence (*FAF*). (**c**) Fluorescein angiography (*FA*) in stage 1 CACD shows hyperfluorescent parafoveal changes. (**d**) In stage 2 CACD, a round to oval area of hypopigmentation is visible in the macula. (**e**) This area corresponds to speckled changes of increased and decreased FAF. With time, initially increased FAF evolves to decreased FAF changes as the lesion enlarges and atrophy of the retinal pigment epithelium (*RPE*) progresses. (**f**) FA in stage 2 CACD shows speckled hyperfluorescence of the lesion, due to partial RPE atrophy. (**g**) Stage 3 CACD shows one or more patches of well-circumscribed chorioretinal atrophy, appearing outside the central fovea, within the area of slight hypopigmentation. (**h**) These areas of chorioretinal atrophy correspond to severely decreased to absent FAF. (**i**) In stage 4 CACD, the well-defined area of chorioretinal atrophy involves the fovea, with a corresponding severe decrease in visual acuity. (**j**) This area corresponds with a round to oval zone of absent FAF involving the fovea in late stage 4 CACD, bordered by a small residual band of increased FAF. (**k**) End-stage CACD also shows a well-demarcated area of chorioretinal atrophy on the fluorescein angiogram, with enhanced visibility of the residual underlying choroidal vessels. (**l**) Patient with early stage 3 CACD, showing a small, round, black area of profound RPE atrophy (thus making it stage 3 CACD) in addition to the speckled FAF changes. (**m**) Spectral-domain optical coherence tomography image (*SD-OCT*) through the deeply atrophic area shows more marked atrophy of the outer retina (external limiting membrane and ellipsoid) and RPE, surrounded by more discrete outer retinal changes. (**n**) SD-OCT section taken through the fovea, showing mainly an attenuated outer retina with a hyperreflective ellipsoid line that is absent in the central macula, but with a relatively preserved external limiting membrane

Fluorescein angiography shows progressive hyperfluorescence due to window defects as a result of progressive RPE atrophy in advancing CACD stages (Fig. 10.1c, f i, k,; Table 10.1).

Fundus autofluorescence in early CACD shows speckled changes of increased and decreased FAF, whereas in stage 3 and 4 CACD, a black "punched-out" lesion due to profound RPE atrophy is seen in the posterior pole,

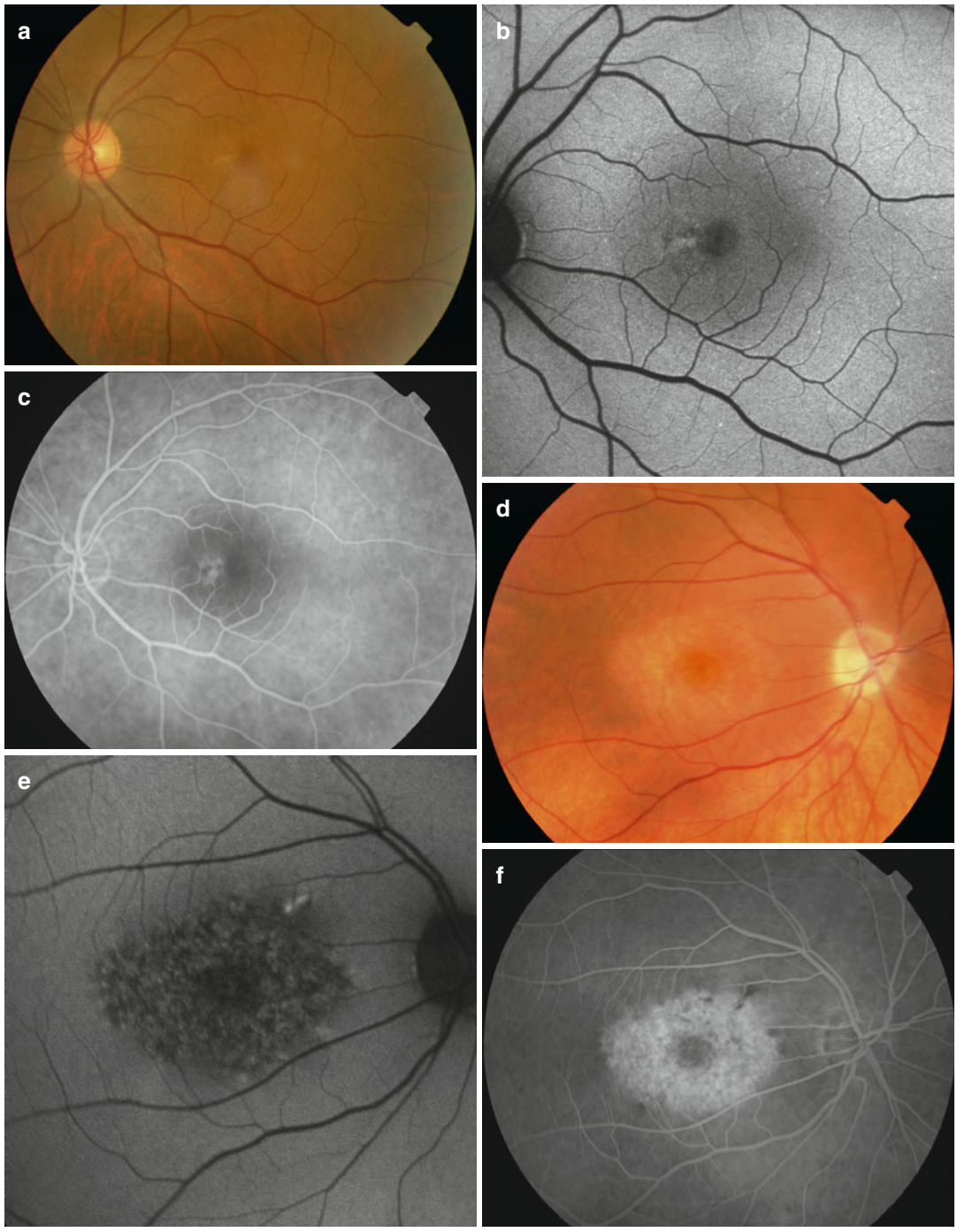

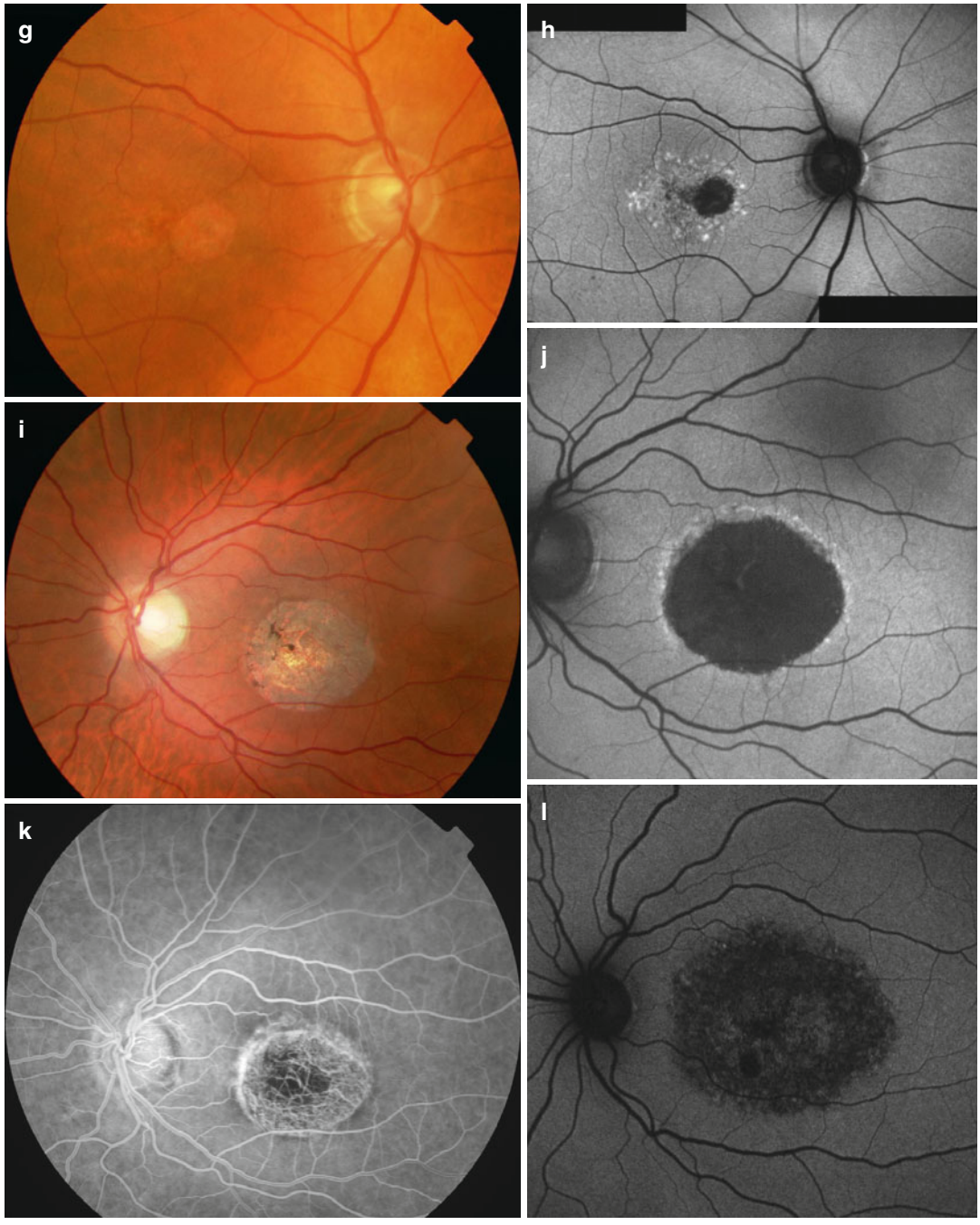

Fig. 10.1 (continued)

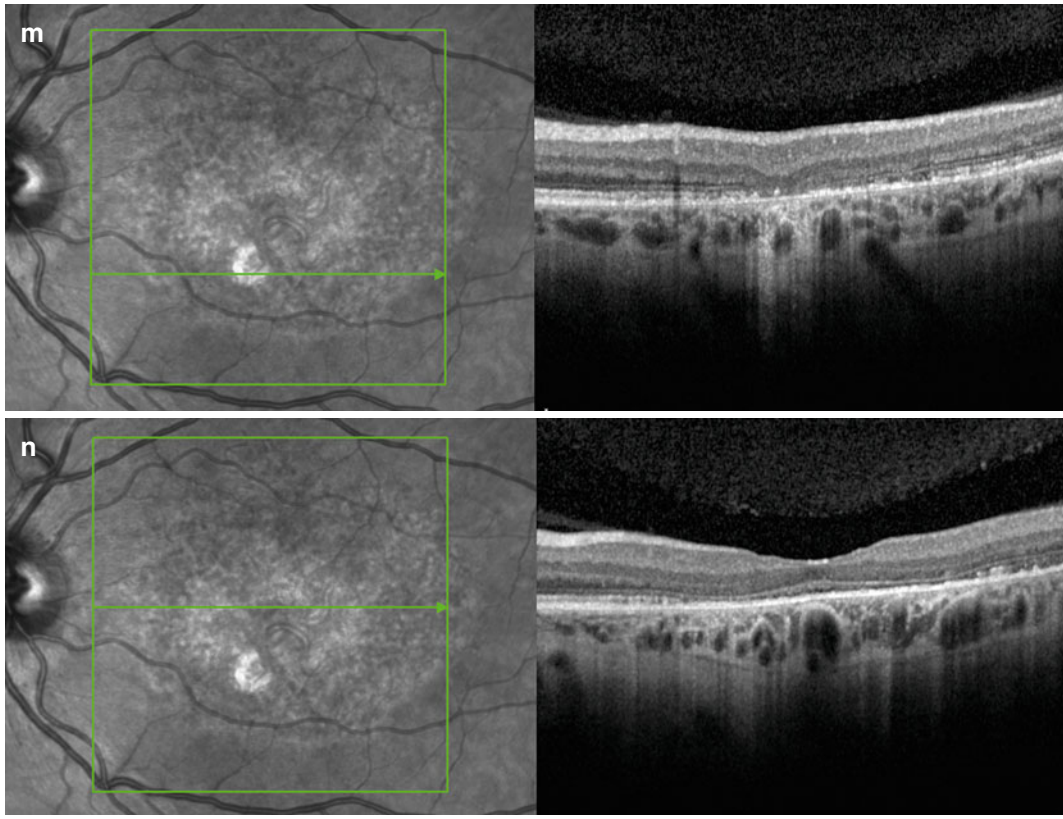

Fig. 10.1 (continued)

bordered by a small residual band of increased autofluorescence (Figs. 10.1b, e, h, k) [4]. On optical coherence tomography (OCT), mildly atrophic lesions in stage 1, 2, and 3 central areolar choroidal dystrophy correspond to variable alterations in the reflectivity of the outer retina, generally without drusen (Figs. 10.1l, m). In the profoundly atrophic areas in stage 3 and 4, the outer retinal layers are markedly attenuated (Fig. 10.1m, n).

The photopic and scotopic full-field electroretinography (ERG) is generally normal in CACD, but panretinal cone or cone-rod dysfunction can develop in advanced CACD [1]. The pattern ERG is usually reduced or extinguished, and the multifocal ERG often shows markedly decreased (para-)central responses [3, 4]. The electro-oculography (EOG) is normal.

10.2.3 Disease Course

As in all *PRPH2*-associated retinal dystrophies, the disease severity in patients with an identical *PRPH2* mutation may be highly variable, even in mutation carriers from the same family [1]. Nonpenetrance has been observed in up to 21 % of patients [4]. Therefore, cases can appear sporadic or automal recessive. The visual prognosis of *PRPH2*-related CACD roughly depends on the underlying mutation [1]. Visual acuity can be relatively preserved for many years, as it can take more than 20 years for CACD to progress from stage 2 to stage 4. Choroidal neovascularization is very rare and can be seen in patients with concurrent high myopia. Retinal atrophic changes in CACD can predispose to effects of vitreomacular traction and macular hole formation.

Table 10.1 Summary of clinical characteristics of central areolar choroidal dystrophy (CACD)

CACD stage	Mean visual acuity (range)	Ophthalmoscopy	Optical coherence tomography (OCT)	Fundus autofluorescence (FAF)	Fluorescein angiography	Electroretinography
Stage 1	20/20 (20/33 – 20/20)	Slight parafoveal pigment changes	Mild irregular reflectivity changes of outer photoreceptor – retinal pigment epithelium (RPE) complex	Increased parafoveal FAF	Mild parafoveal hyperfluorescence	Normal
Stage 2	20/23 (20/80 – 20/16)	Round to oval mildly atrophic hypopigmented area	Irregular reflectivity changes of outer photoreceptor – RPE complex	Speckled increased and decreased FAF	Speckled hyperfluorescence (mild RPE window defect)	Normal
Stage 3	20/27 (20/100 – 20/16)	Appearance of profound chorioretinal atrophy outside fovea	Marked thinning of outer photoreceptor structures in atrophic zone; relative sparing of fovea	Well-defined atrophic area of absent FAF outside fovea	Visible remaining hyperfluorescent choroidal vessels in atrophic area	Normal or cone/cone-rod dysfunction
Stage 4	20/182 (20/400 – 20/33)	Profound chorioretinal (geographic) atrophy affecting fovea	Marked thinning of outer photoreceptor structures in atrophic zone including fovea	Well-defined atrophic area of absent FAF affecting fovea	Like stage 3	Normal or cone/cone-rod dysfunction

10.2.4 Differential Diagnosis

Early CACD should be differentiated from atrophic age-related macular degeneration, mitochondrial retinal dystrophy caused by the m.3243A>G mutation (for instance, in association with maternally inherited diabetes and deafness; see Chap. 8), North Carolina macular dystrophy, malattia leventinese/Doyne honeycomb retinal dystrophy, Sorsby fundus dystrophy, Stargardt disease, and cone(-rod) dystrophy [5]. Stage 3 and 4 CACD can be similar to all macular diseases with advanced chorioretinal atrophy.

10.2.5 Conclusion

CACD is an autosomal-dominantly inherited macular dystrophy with a relatively late onset, caused by mutations in the *PRPH2* gene.

10.3 Dominant Cystoid Macular Dystrophy

10.3.1 Background

Dominant cystoid macular dystrophy was first described by Deutman and colleagues in 1976 [6, 7]. This peculiar autosomal-dominant dystrophy is characterized by early-onset macular cystoid fluid collections (possibly edema). The gene locus is linked to the interval 7p15.3, but the exact gene and pathogenesis are currently unknown [8, 9].

10.3.2 Clinical Findings

Patients start to experience a slowly progressive loss of visual acuity in childhood. Most patients are moderately to highly hyperopic. DCMD can be classified into three stages, based on characteristics on ophthalmoscopy, fundus autofluorescence, fluorescein angiography, OCT, as well as electrophysiological characteristics (Table 10.2, Fig. 10.2) [9]. The staging system correlates with age and visual acuity. In stage 1, DCMD patients are younger than 20 years and have cystoid fluid collections (CFCs) in the macula with fine folding of the internal limiting membrane and mild pigment changes (Fig. 10.2a–e). In stage 2 DCMD, the CFCs decrease in size, and moderate macular chorioretinal atrophy develops. Patients with stage 3 DCMD are older than 50 years and show profound chorioretinal atrophy and coarse hyperpigmented deposits in the posterior pole.

In early DCMD, the fluorescein angiogram shows dilated, telangiectatic capillaries in the central macula, with profuse leakage into the CFCs in the late angiographic phase (Fig. 10.2b). In patients with advanced DCMD, window defects are seen on the angiogram due to RPE atrophy, together with some residual diffuse fluorescein leakage extending beyond the posterior pole (Fig. 10.2f). Fundus autofluorescence shows mildly increased fundus autofluorescence (FAF) in the early stage, and with advancing chorioretinal atrophy, FAF decreases progressively (Fig. 10.2g, j). On OCT, CFCs are visible in the neuroretina that do not appear clearly different from the cystoid macular edema that can be seen in numerous other retinal diseases. In early DCMD, small round CFCs are mainly situated in the inner and outer nuclear layer (Fig. 10.2e). These CFCs become more extensive and pronounced with time. In stage 2 and 3 DCMD, the CFCs diminish, whereas retinal and RPE attenuation increases (Fig. 10.2h, k). Visual field testing and electrophysiology characteristics in DCMD are depicted in Table 10.2.

The clinical characteristics and a histopathological study of DCMD suggest a marked disorganization of the inner nuclear layer associated with retinal cystoid changes and suggest that DCMD may primarily be a disease of the Müller cells [9, 10].

10.3.3 Disease Course

In the first decade, the visual acuity generally is higher than 20/40. In the second and third decade, the visual acuity generally does not exceed 20/30. After the age of 30, considerable interindividual

Table 10.2 Summary of clinical characteristics of dominant cystoid macular dystrophy (DCMD)

Disease stage	Mean age [range]	Mean VA [range]	Fundoscopy	Optical coherence tomography (OCT)	Fundus autofluorescence (FAF)	Fluorescein angiography	Electrooculography	Electroretinography	Goldmann visual field
Stage 1	13 [0–32]	20/37 [20/15 – 20/200]	Fine folding of inner limiting membrane Cystoid fluid collections (CFCs) Mild granular pigment changes in macula	CFCs	Mildly increased FAF in the macula	Hyperfluorescent CFCs Perifoveal capillary dilation	Normal Mildly reduced	Normal	Normal
Stage 2	38 [21–50]	20/54 [20/20 – CF]	Mild but visible chorioretinal macular atrophy CFCs	Mild retinal atrophy Small CFCs	Moderately decreased FAF in macula	Hyperfluorescent CFCs	Normal to mildly – severely reduced (68 %)	Normal, minority (<20 %) subnormal cone and rod function	Peripheral visual field constriction in 25 % of patients
Stage 3	61 [44–90]	20/212 [20/40- HM]	Profound chorioretinal atrophy in macula Coarse hyperpigmentations Attenuated arterioles	Profound chorioretinal atrophy No CFCs	Large area of decreased FAF corresponding to profound RPE atrophy	Early hypofluorescence with late staining of atrophic area, surrounded by hyperfluorescence	Severely reduced	Abnormal cone and rod function	Peripheral visual field constriction in 63 % of patients

Age age at moment of examination in years, *VA* visual acuity, *OCT* optical coherence tomography, *FAF* fundus autofluorescence, *FA* fluorescein angiography, *EOG* electrooculography, *ERG* electroretinograophy, *CFCs* cystoid fluid collections, *CF* counting fingers, *RPE* retinal pigment epithelium, *HM* hand movements

variability in visual acuity is seen, with a slow decline to 20/200 or less in most patients in the fourth and fifth decade. After the age of 60, many DCMD patients are legally blind. Choroidal neovascularization does not occur, but on rare occasions, peripheral vascular dilations with leakage of exudates may develop. The CFCs may decrease in response to topical or oral treatment with carbonic anhydrase inhibitors.[4]

10.3.4 Differential Diagnosis

DCMD should be differentiated from X-linked juvenile retinoschisis (XLRS). Apart from the different mode of inheritance, the "cystoid" schisis cavities in XLRS are often more confluent, with eventually only small strands of tissue bordering these spaces. On fluorescein angiography, no leakage is seen into the schisis spaces in XLRS. Fundus autofluorescence and red-free photography show a typical radial pattern of abnormalities in the fovea in XLRS, in contrast to DCMD. Other differential diagnostic entities include retinitis pigmentosa with cystoid macular edema and other conditions that can be associated with cystoid macular edema, such as uveitis, idiopathic parafoveal telangiectasia, and diabetic retinopathy.

10.3.5 Conclusion

DCMD is an autosomal-dominantly inherited dystrophy characterized by bilateral early-onset CFCs in the macula, which distinguishes this disorder from other retinal dystrophies. With time, progressive chorioretinal atrophy and pigmentary changes develop in the posterior pole.

10.4 Juvenile Macular Dystrophy and Hypotrichosis

10.4.1 Background

Juvenile macular dystrophy and hypotrichosis is caused by autosomal recessive mutations in *CDH3* on chromosome 16q22 and was first described by Wagner in 1935 [11]. *CDH3* encodes for P-cadherin, a protein linked to hair and retinal development [12]. As visual deficits are suspected to arise already in early childhood, some authors suggested "hypotrichosis with cone-rod dystrophy" to be a more fitting name [13].

10.4.2 Clinical Findings

Alopecia develops shortly after birth with partial and short regrowth of hair during puberty (Fig. 10.3a). Visual function is reduced from childhood onwards with progressive degeneration extending beyond the macular region. ERG testing shows progressive cone and rod system dysfunction.

The macula typically appears with nummular patterns of atrophic and hyperpigmented patches (Fig. 10.3b). Demarcation lines clearly divide affected and intact retina but sometimes can be obscured by diffuse pigmentary changes and white-yellowish flecks.

10.4.3 Disease Course

Visual function is affected already in school age with visual acuity ranging from 20/32 to 20/200. Fundoscopy reveals first signs of a macular dystrophy, and ERG responses indicate both rod and cone system dysfunction. Fundoscopic changes and functional deficits are slowly progressive but are not known to develop into complete blindness.

10.4.4 Differential Diagnosis

Ectodermal dysplasia, ectrodactyly, and macular dystrophy syndrome can also result from *CDH3* mutations and features hypotrichosis with concomitant macula dystrophy. However, it also includes digital abnormalities, sparse and short eyebrows and eyelashes, and partial anodontia [14].

10.4.5 Conclusion

Juvenile macular dystrophy and hypotrichosis is caused by autosomal recessive mutations in the *CDH3* gene and should be called "hypotrichosis with cone-rod dystrophy."

10.5 Late-Onset Retinal Degeneration (L-ORD)

10.5.1 Background

Late-onset retinal degeneration (L-ORD) was first described as a disease entity by Kuntz et al. in 1996, with histopathologic evidence of a retina-wide layer of extracellular material of 20–40 μm thickness between the RPE and Bruch's membrane [15]. An autosomal-dominant founder mutation (p.Ser163Arg) in the complement 1q tumor necrosis factor 5 gene (*C1QTNF5*) was identified as causative, which can be traced back to a single ancestor from southeast Scotland. *C1QTNF5* is co-expressed in the RPE with the membrane frizzled-related protein MFRP, which is mutated in autosomal recessive nanophthalmos. L-ORD has been termed differently across the literature with autosomal-dominant hemorrhagic macular dystrophy, late-onset macular degeneration, and late-onset retinal macular degeneration all pointing towards the clinically significant involvement of the macula.

10.5.2 Clinical Findings

The most consistent finding associated with L-ORD is a thick layer of extracellular sub-RPE deposit evident on spectral-domain optical coherence tomography (SD-OCT) imaging. This layer is often thicker in the macula but extends to the extreme retinal periphery. Other clinical findings depend on the stage of the disease and can include anomalies in the anterior segment, such as long anteriorly inserted zonules (which may complicate capsulorhexis cataract surgery), iris atrophy, and trabecular pigment deposition (Fig. 10.4) [16, 17]. The posterior segment can demonstrate signs of retinal atrophy such as midperipheral bone spicules with well-demarcated lines between viable and atrophic areas of retina. Hallmark features of the macula are perimacular yellow dots and choroidal neovascularization.

10.5.3 Disease Course

As the name suggests, patients rarely become symptomatic before age of 40 in this progressive disorder (Table 10.3). The only finding in this asymptomatic first stage may be long anteriorly inserted lens zonules, iris atrophy, and trabecular pigment deposition, which in some cases may evolve into secondary glaucoma.

Stage 2 is characterized by the first primary symptoms such as difficulties with dark adapta-

Fig. 10.2 Clinical classification of dominant cystoid macular dystrophy (*DCMD*) into three stages: (**a**–**d**) stage 1 DCMD, (**e**–**h**) stage 2 DCMD, and (**i**–**k**) stage 3 DCMD. (**a**) Color fundus photograph of a 15-year-old patient with stage 1 DCMD showing wrinkling of the inner limiting membrane, cystoid fluid collections (*CFCs*) and fine pigment changes in the macula. (**b**) Fluorescein angiogram (late phase) showing hyperfluorescent CFCs in the fovea and more diffuse hyperfluorescent intraretinal edema in the posterior pole. (**c**) Fundus autofluorescence image showing areas of punctiform mildly increased autofluorescence and mild diffuse hyperautofluorescence in the macula. (**d**) Optical coherence tomography (*OCT*) scan through the fovea showing CFCs in the inner and outer nuclear layer. (**e**) Color fundus photograph of a patient with stage 2 DCMD showing atrophic pigment changes in the macula. (**f**) Fluorescein angiogram showing central hyperfluorescence caused by the atrophic retinal pigment epithelium (*RPE*) window defect and residual hyperfluorescent cystoid edema, surrounded by mild, indistinct hyperfluorescence. (**g**) Fundus autofluorescence image showing moderately decreased autofluorescence in the central macula. (**h**) OCT scan showing mild diffuse retinal edema and some small residual CFCs, irregularity of the outer photoreceptor structures, but an RPE layer that seemed largely intact. (**i**) Color fundus photograph of stage 3 DCMD, displaying profound chorioretinal atrophy in the macula with attenuated arterioles and coarse hyperpigmentations. (**j**) Fundus autofluorescence image showing a large area of markedly decreased autofluorescence due to RPE atrophy. (**k**) OCT scan showing chorioretinal atrophy and a mild epiretinal membrane

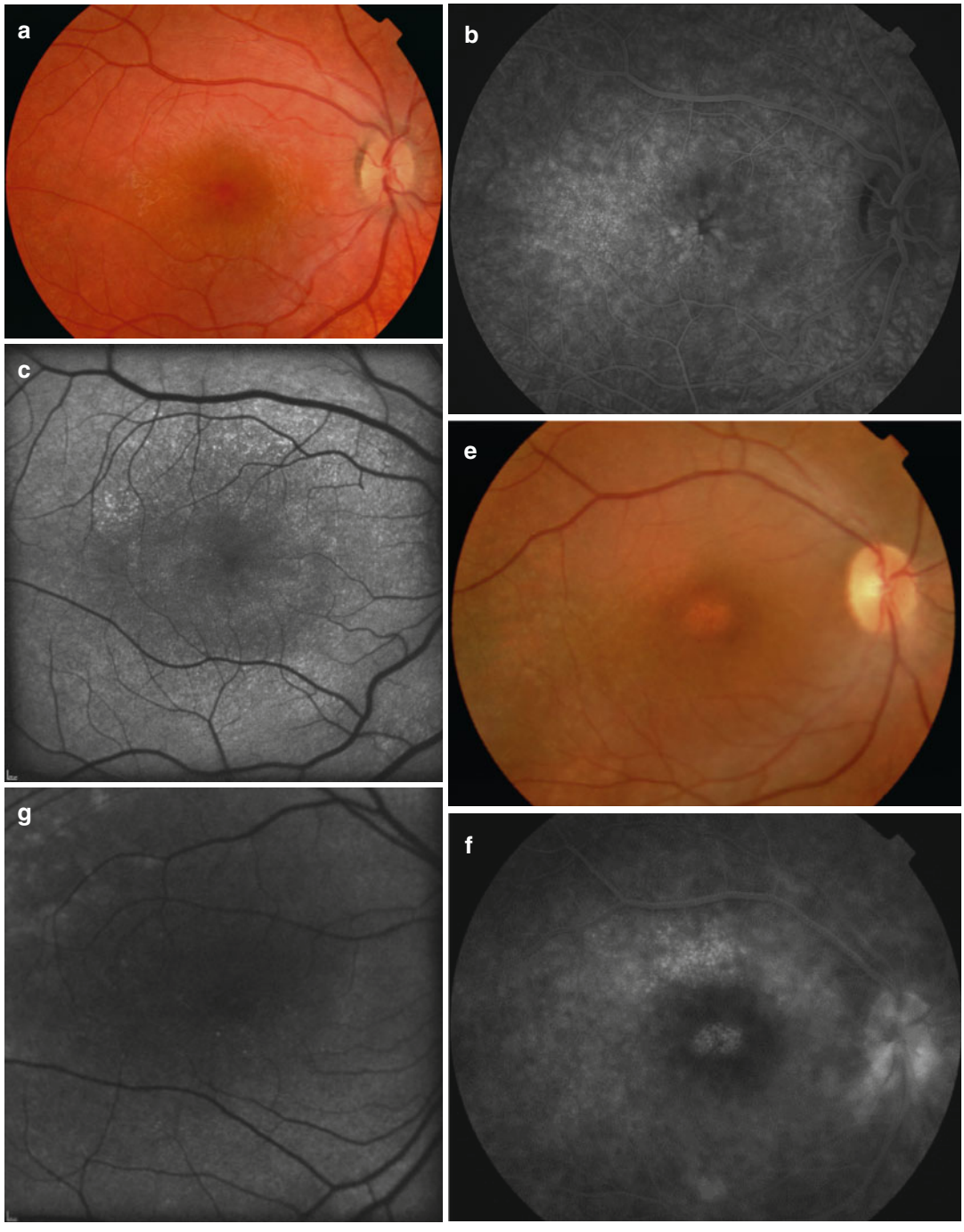
a
b
c
e
g
f

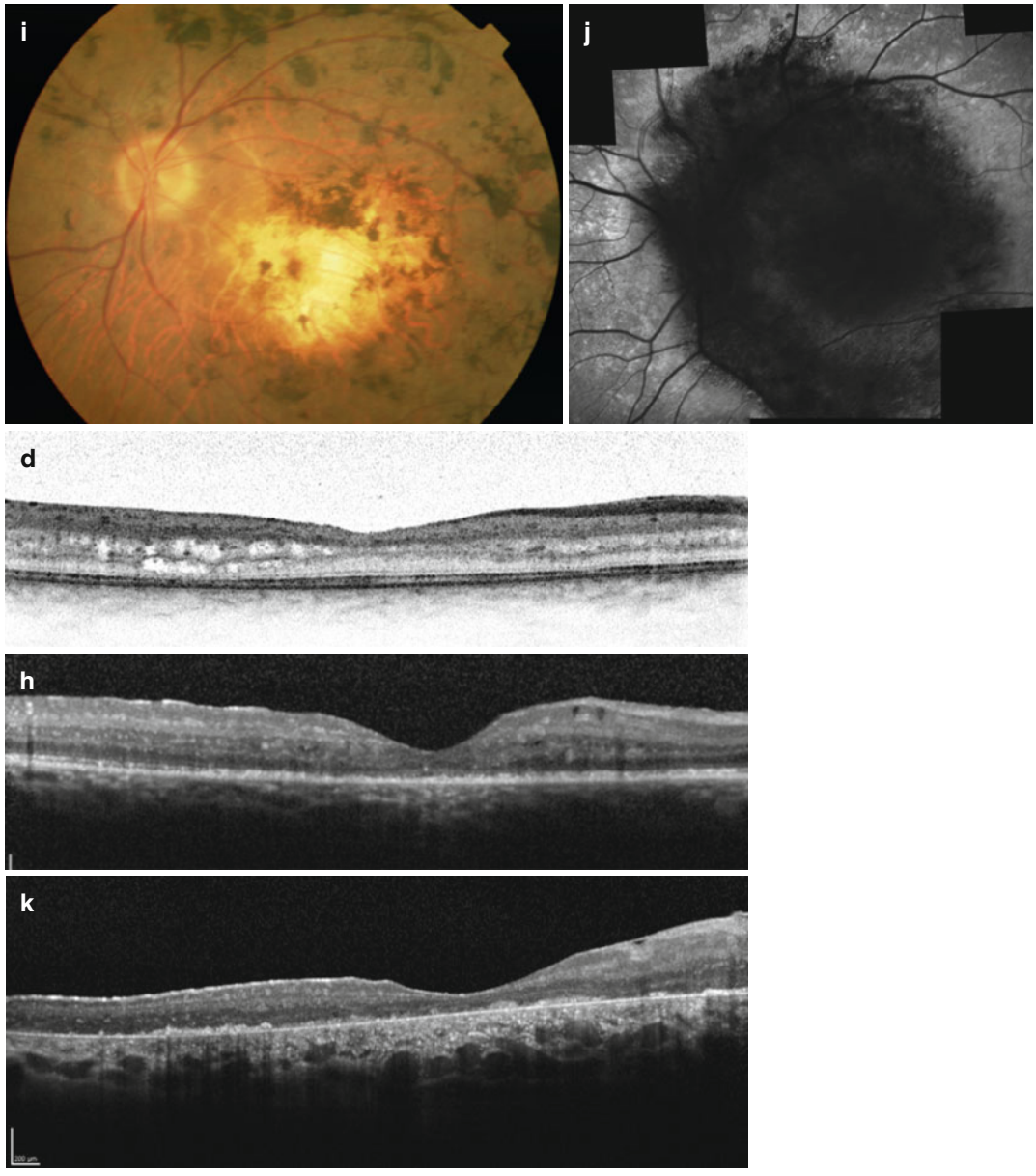

Fig. 10.2 (continued)

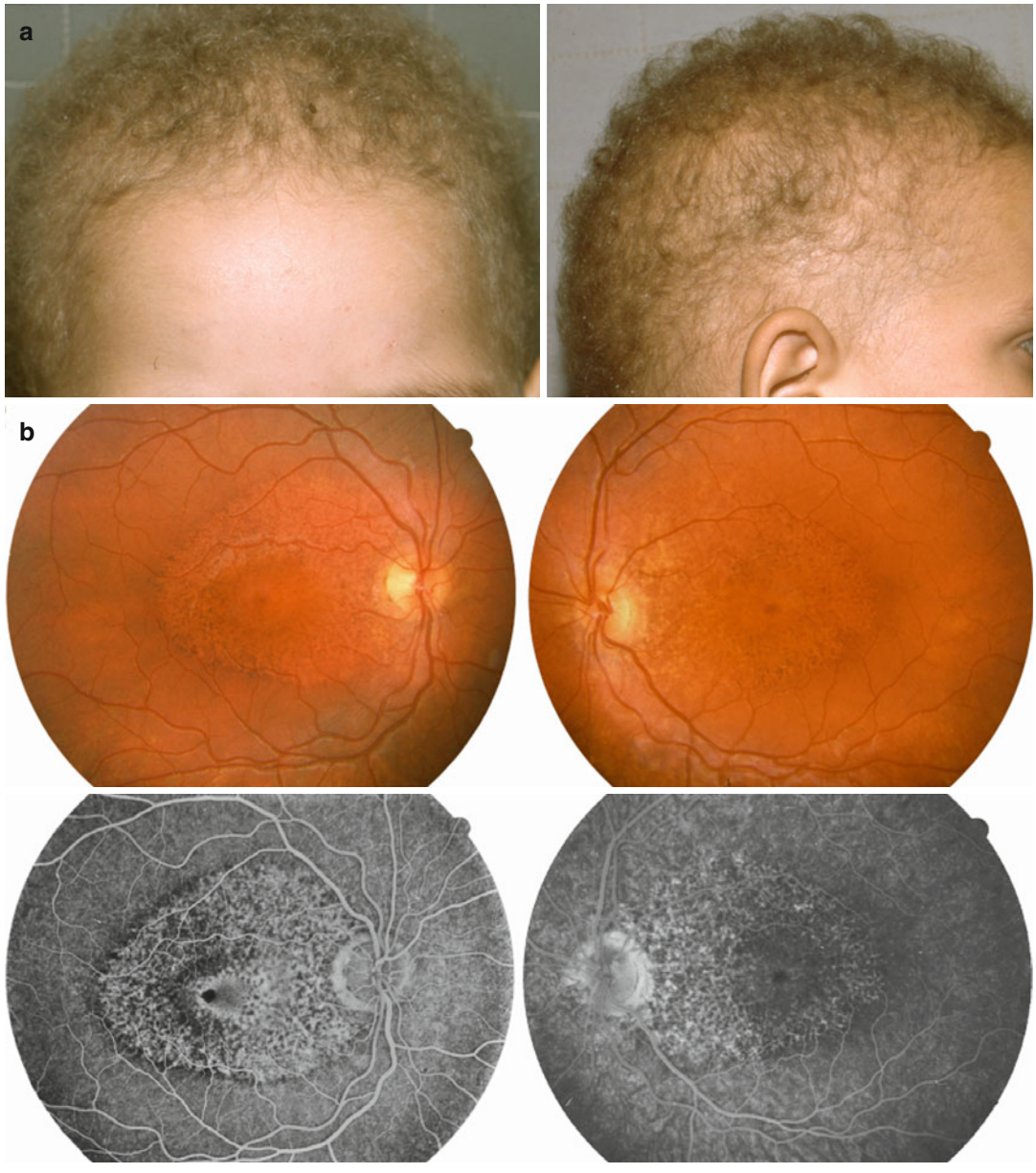

Fig. 10.3 (**a**) Hypotrichosis due to *CDH3* mutations. (**b**) Macular dystrophy due to *CDH3* mutations

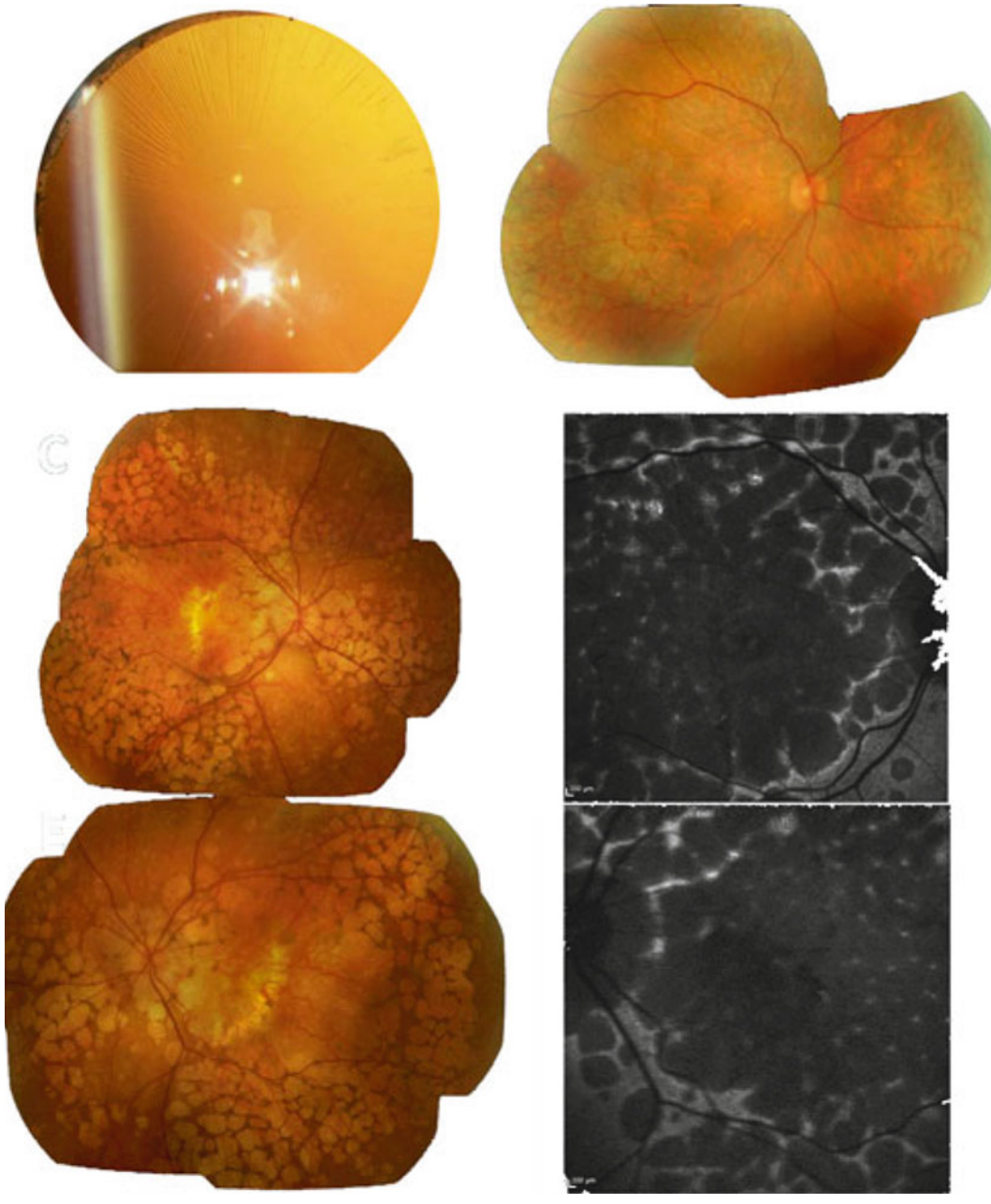

Fig. 10.4 Ocular features of late-onset retinal dystrophy (*L-ORD*). The anterior segment photograph (*upper left*) shows peripupillary iris atrophy and abnormally long, anteriorly inserted lens zonules. Fundus images show areas of retinal pigment epithelial (*RPE*) atrophy in the midperipheral retina together with marked atrophy in the posterior pole (patients in second-fourth row). The fundus photograph of the fourth L-ORD patient (*bottom row*) shows a large area of macular atrophy with scalloped borders, without atrophy in the midperipheral retina (*bottom*). Fundus autofluorescence imaging confirms black areas of marked RPE atrophy (From Holder [16] with the kind permission of Springer Science + Business Media; adapted from Soumplis et al. [17])

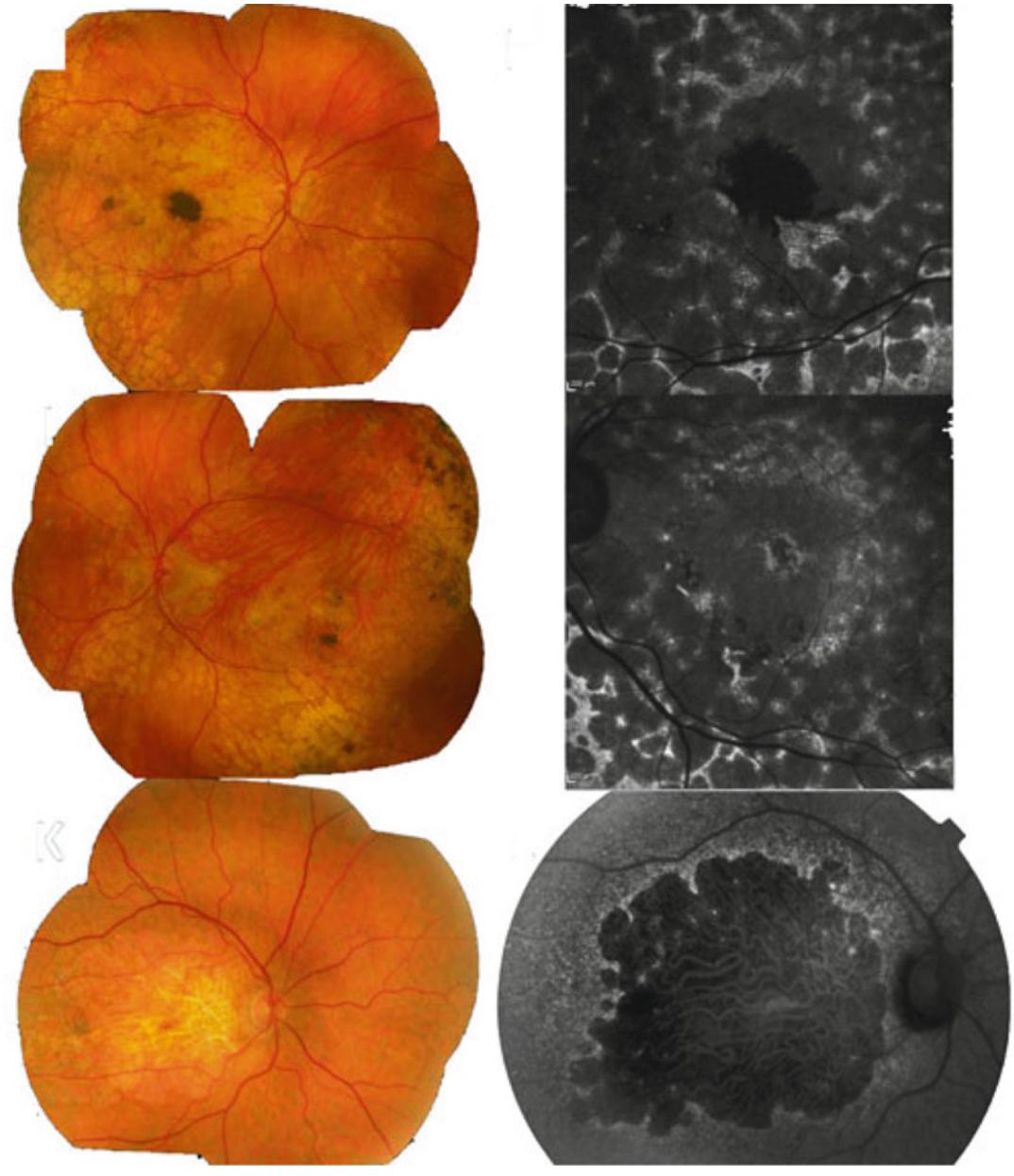

Fig. 10.4 (continued)

Table 10.3 Summary of clinical characteristics of late-onset retinal degeneration (L-ORD)

L-ORD stage	Mean visual acuity (range)	Ophthalmoscopy	OCT	Fundus autofluorescence (FAF)	Fluorescein angiography	Electroretinography
Stage 1	20/20 (20/33 – 20/20)	Slight parafoveal pigment changes	Normal	Normal	Normal	Normal
Stage 2	20/23 (20/80 – 20/16)	Pigment changes in midperiphery, early perimacular yellow dots	Extracellular sub-RPE deposits	Heterogenous FAF in midperiphery	Areas of speckled hyperfluorescence in midperiphery (mild RPE window defect)	Normal
Stage 3	20/27 (20/100 – 20/16)	Mid-peripheral bone spicules with well-demarcated atrophic areas, perimacular yellow dots, macular choroidal neovascularization	Increased thickness of extracellular sub-RPE deposits; marked thinning of outer retina in atrophic areas	Well-defined atrophic areas of absent FAF in midperiphery	Areas of hyperfluorescence in midperiphery (RPE window defect); macular choroidal neovascularization	Reduced rod response

tion and nyctalopia, which are accompanied by changes in the midperiphery and early perimacular yellow dots. It is important to note that fundus changes might precede or follow onset of symptoms, which contributes to the frequent misdiagnosis of the condition. Visual acuity, kinetic and static perimetry, color vision, and ERG are typically still normal. Dark-adaptometry may be abnormal at this stage and correlates with thickness of the extracellular sub-RPE deposits.

Stage 3 can be expected at age 60 and older and typically involves rapid deterioration of visual acuity due to choroidal neovascularization. Other fundus changes also become more pronounced and typically feature well-demarcated lines between viable and atrophic areas of retina with midperipheral bone spicules. The frequent findings of annular scotoma formation between 10 and 40° eccentricity and predominant reduction in rod-derived ERG responses all point towards a leading effect on rod function with accompanying macular neovascular pathology.

10.5.4 Differential Diagnosis

L-ORD shares features of retinitis pigmentosa, age-related macular degeneration, choroideremia, gyrate atrophy, and Sorsby fundus dystrophy and is often misdiagnosed.

10.5.5 Conclusion

L-ORD is an autosomal-dominantly inherited macular dystrophy with a relatively late onset, caused by mutations in the *C1QTNF5* gene.

References

1. Boon CJ, den Hollander AI, Hoyng CB, Cremers FP, Klevering BJ, Keunen JE. The spectrum of retinal dystrophies caused by mutations in the peripherin/RDS gene. Prog Retin Eye Res. 2008;27(2):213–35.
2. Downes SM, Fitzke FW, Holder GE, Payne AM, Bessant DA, Bhattacharya SS, Bird AC. Clinical features of codon 172 RDS macular dystrophy: similar phenotype in 12 families. Arch Ophthalmol. 1999;117(10):1373–83.
3. Michaelides M, Holder GE, Bradshaw K, Hunt DM, Moore AT. Cone-rod dystrophy, intrafamilial variability, and incomplete penetrance associated with the *R172W* mutation in the peripherin/RDS gene. Ophthalmology. 2005;112(9):1592–8.
4. Boon CJ, Klevering BJ, Cremers FP, Zonneveld-Vrieling MN, Theelen T, Den Hollander AI, Hoyng CB. Central areolar choroidal dystrophy. Ophthalmology. 2009;116(4):771–82.
5. Saksens NT, Fleckenstein M, Schmitz-Valckenberg S, Holz FG, den Hollander AI, Keunen JE, et al. Macular dystrophies mimicking age-related macular degeneration. Prog Retin Eye Res. 2014;39:23–57.
6. Deutman AF, Pinckers AJ, Aan de Kerk AL. Dominantly inherited cystoid macular edema. Am J Ophthalmol. 1976;82(4):540–8.
7. Notting JG, Pinckers JL. Dominant cystoid macular dystrophy. Am J Ophthalmol. 1977;83(2):234–41.
8. Kremer H, Pinckers A, van den Helm B, Deutman AF, Ropers HH, Mariman EC. Localization of the gene for dominant cystoid macular dystrophy on chromosome 7p. Hum Mol Genet. 1994;3(2):299–302.
9. Saksens NT, van Huet RA, van Lith-Verhoeven JJ, den Hollander AI, Hoyng CB, Boon CJ. Dominant cystoid macular dystrophy. Ophthalmology. 2015;122(1):180–91.
10. Loeffler KU, Li ZL, Fishman GA, Tso MO. Dominantly inherited cystoid macular edema. A histopathologic study. Ophthalmology. 1992;99(9):1385–92.
11. Wagner H. Maculaaffektion, vergesellschaftet mit Haarabnormität von Lanugotypus, beide vielleicht angeboren bei zwei Geschwistern. Graefes Arch Ophthalmol. 1935;134(1):74–81.
12. Sprecher E, Bergman R, Richard G, Lurie R, Shalev S, Petronius D, et al. Hypotrichosis with juvenile macular dystrophy is caused by a mutation in *CDH3*, encoding P-cadherin. Nat Genet. 2001;29(2):134–6.
13. Leibu R, Jermans A, Hatim G, Miller B, Sprecher E, Perlman I. Hypotrichosis with juvenile macular dystrophy: clinical and electrophysiological assessment of visual function. Ophthalmology. 2006;113(5):841–7.
14. Kjaer KW, Hansen L, Schwabe GC, Marques-de-Faria AP, Eiberg H, Mundlos S. Distinct *CDH3* mutations cause ectodermal dysplasia, ectrodactyly, macular dystrophy (EEM syndrome). J Med Genet 2005;42(4):292–8.
15. Kuntz CA, Jacobson SG, Cideciyan AV, Li ZY, Stone EM, Possin D, Milam AH. Sub-retinal pigment epithelial deposits in a dominant late-onset retinal degeneration. Invest Ophthalmol Vis Sci. 1996;37(9):1772–82.
16. Holder GE. Late-onset retinal dystrophy (LORD). In: Puech B, De Laey JJ, Holder GE, editors. Inherited chorioretinal dystrophies. Berlin: Springer; 2014. p. 181–4.
17. Soumplis V, Sergouniotis PI, Robson AG, Michaelides M, Moore AT, Holder GE, Webster AR. Phenotypic findings in *C1QTNF5* retinopathy (late-onset retinal degeneration). Acta Ophthalmol. 2013;91:e191–5.

Macular Dystrophies: Management and Interventions

11

Katia Marazova and José-Alain Sahel

Abstract

Inherited macular dystrophies comprise a highly heterogeneous group of diseases characterized by irreversible loss of central vision as a result of atrophy of the macula and underlying retinal pigment epithelium. Despite significant progress in understanding molecular bases of these diseases, there are still no preventive or curative treatments. This chapter discusses vision restoration strategies and focuses on innovative therapies for inherited macular diseases that are currently under development and evaluation, e.g., gene therapy, retinal prosthesis, and optogenetics.

Keywords

Inherited macular dystrophies • Gene therapy • Neuroprotection • Retinal implants • Optogenetics • Cell therapy • Sensory substitution device

11.1 General Recommendations

Currently, there is no effective treatment to prevent, stop, or reverse the course of inherited macular diseases. Vision impairment associated with these diseases inevitably leads to difficulties in performing daily activities, including working, driving, reading, writing, and watching TV, and carries increased health risks related to falls, bone fractures, depression, and social isolation. In general, management of visual disability comprises supportive measures to maintain the activities of daily living and improve quality of life, such as orientation and mobility training, educational support, physical and occupational therapy, and psychosocial interventions. Low vision rehabilitation (including provision of low vision aids

K. Marazova, PhD
Institut de la Vision, Sorbonne Universités,
UPMC University Paris 06, UMR_S 968,
INSERM U968, CNRS UMR_7210,
17 rue Moreau, Paris 75012, France

J.-A. Sahel, MD (✉)
Institut de la Vision, Sorbonne Universités,
UPMC University Paris 06, UMR_S 968,
INSERM U968, CNRS UMR_7210,
17 rue Moreau, Paris 75012, France

Centre Hospitalier National d'Ophtalmologie
des Quinze-Vingts, DHU Sight Again,
INSERM-DHOS CIC 1423, Paris, France
e-mail: j.sahel@gmail.fr

G. Querques, E.H. Souied (eds.), *Macular Dystrophies*, DOI 10.1007/978-3-319-26621-3_11

and training in their use) combined with optical (e.g., appropriate spectacles, high-intensity lamps, contrast-enhancing filters, near and far magnification devices, glare reduction and contrast-enhancing devices) and nonoptical (e.g., writing guides, bold-lined paper, high-contrast watches, large print items) corrective interventions is proposed in an individually tailored manner, depending on the degree of visual impairment and the disease prognosis.

Over the last 10 years, significant progress in technologies for low vision enhancement and mobility assisting has been made (reviewed in [1]). These include global positioning system (GPS)-based navigation system, talking signs, auditory signals at street crossings, and bar coding for labeling locations and objects. Magnified text, text-to-speech, and speech-to-text software and other accessibility requirements of the World Wide Web Consortium for equal access to Web content for people with disabilities are available today on most computers. Refreshable tactile graphics systems provide access to digital content (e.g., cell phones, keyboards). Innovative head-mounted electronic low vision devices that have been designed to provide a virtual field of view (field compensation), in addition to magnification, are currently under evaluation.

A growing body of evidence suggests that visible light and, more specifically, the blue spectral range may induce retinal damage and worsen the course of retinal degenerative disorders [2, 3]. Patients with macular dystrophy are advised to avoid sunlight exposure and to wear lower wavelength-blocking glasses outdoors during the day. For maximum protection, the filtering glasses should absorb all of the blue, violet, and UVA radiation and filter out 97–99 % of the spectral and ultraviolet energy below 550 nm wavelength. A recent report suggested that filtering light in a band from 415 to 455 nm may be sufficient to prevent or limit the retinotoxic effects of the light [3]. This more precise phototoxic action spectrum could be advantageously valued in selective photoprotection ophthalmic filters without disrupting essential visual and nonvisual functions of the eye [3]. Avoiding smoking is highly advisable [4].

The most relevant recommendations on nutritional supplements for patients with macular degenerative diseases come from the results of the largest studies sponsored by the National Eye Institute, the Age-Related Eye Disease Study (AREDS), published in October 2001 and its follow-up study (AREDS2) published in May 2013. It has been reported that oral supplementation with the AREDS formulation (vitamins C and E, beta-carotene, zinc, and copper) reduces the risk of progression to advanced age-related macular degeneration (AMD) [5]. AREDS2 examined whether or not addition of the carotenoids lutein and zeaxanthin or the omega-3 long-chain polyunsaturated fatty acids docosahexaenoic acid (DHA) + eicosapentaenoic acid (EPA) or both might further improve the results of the original AREDS formula. Further reduction of the risk of progression to advanced AMD was not observed, but lutein + zeaxanthin was suggested as an appropriate carotenoid substitute in the AREDS formulation [6].

Prevention and treatment of macular dystrophies and vision restoration in retinal degenerative diseases are of paramount importance for public health. The general recommendations mentioned above may slow down, to some extent, the disease course and help patients better cope with the disease. However, there is still no curative treatment for inherited macular dystrophies. Innovative therapies aiming to efficiently stop disease progression or restore some visual perception are currently under development and evaluation.

11.2 Gene Therapy

Inherited macular dystrophies refer to a large clinically and genetically heterogeneous group of disorders associated with various forms of stationary or progressive visual impairment. In the human retina, cone photoreceptors enable visual acuity, spatial resolution, and color vision and play an essential role in daily living activities, such as reading and facial recognition. Cone photoreceptors are concentrated in the fovea, the central part of the macula. Decreased central vision

and reduced color vision are typical features of diseases associated with cone degeneration alone, cone degeneration followed by rod degeneration, and associated defects of retinal pigment epithelium (RPE), underlying the macula. Genes implicated in the pathogenesis of inherited macular dystrophies can in principle be targets for gene corrective therapies (reviewed in Sahel and Roska [7]).

The past two decades have been marked by rapidly evolving understanding of the retinal biology and pathophysiology and identifying genes and mutations underlying retinal degeneration. Significant progress of gene therapy for eye disorders, in particular for retinal disorders, has been achieved not only in animal models but also in humans. Most gene-mediated therapies developed today use viral vectors, e.g., adenovirus (Ad)-, adeno-associated virus (AAV)-, or lentivirus-based vectors. Among them, AAV-derived vectors have been the vector of choice due to several key features, such as efficient gene delivery, low immunogenicity, and stable transgene expression.

There are a variety of different AAV serotypes possessing distinct properties: For example, subretinal injection of serotype 4 specifically targets RPE, serotypes 7 and 8 are more specific for photoreceptors, and serotype 5 can target both layers with equivalent efficacy; intravitreal injection of AAV2 or 8 results in transduction of retinal ganglion cells (RGCs) [8]. Additional specificity in the locus of gene expression can be achieved by choosing cell-specific promoters. To date, the most common way for gene delivery to photoreceptors and RPE cells is the subretinal administration. However, it is technically more challenging than intravitreal injection and could be associated with postsurgical complications, such as retinal detachment. A new AAV variant (7m8) able to ensure efficient pan-retinal delivery of the therapeutic gene from the vitreous was recently developed [9], offering clinically relevant implications for further gene therapy development.

Replacing defective gene with a correct sequence is a therapeutic approach particularly suitable for monogenic recessive disorders that are, in general, associated with loss-of-function gene mutations. Numerous successful preclinical studies moved proof-of-concept gene therapies in ophthalmology from bench to bedside.

11.2.1 Leber Congenital Amaurosis

The most notable gene replacement treatment was demonstrated by the team of Jean Bennett in the Swedish Briard dog, a canine model of Leber congenital amaurosis (LCA), in which a long-term and sustained restoration of visual function was documented after single subretinal injection of AAV2.RPE65 [10, 11]. *RPE65* encodes protein involved in the production of 11-cis retinal and in visual pigment regeneration. Characterized by profound impairment of the retina and poor visual function in infancy and early childhood, LCA is one of the most severe retinal degenerative diseases. In addition to *RPE65*, the disease is caused by mutations in at least other 20 genes (RetNet: https://sph.uth.edu/retnet), coding for proteins that regulate different cell functions, including phototransduction (*GUCY2D*), retinal development (*CRB1*, *OTX2*, *CRX*), NAD biosynthesis (*NMNAT1*), retinoid cycle (*LRAT*, *RPE65*, *RDH12*), cell maintenance (*AIPL1*, *TULP1*, *RD3*), and ciliary function (*CEP290*, *IQCB1*, *LCA5*, *RPGRIP1*). Some of the genes implicated in the pathogenesis of LCA (*RPE65*, *SPATA7*, *RPGRIP1*, *CRB1*, *CEP290*, *LRAT*, *CRX*, *RDH12*) play a causative role also in retinitis pigmentosa and cone-rod dystrophy [12].

The first clinical trials of rAAV-mediated gene therapy for patients with LCA2 demonstrated safety and efficacy, with a stable and durable functional gain for at least 3 years [13–15]. Readministration of *RPE65* gene-based treatment to the contralateral eye of adult patients with LCA was reported to evoke significantly greater responses in the second eye, supporting the feasibility and benefits of repeated gene therapy in retinal degenerative diseases [16]. The initial positive results from LCA gene therapy studies were recently challenged by new findings. In 2013, Cideciyan and coworkers reported that the visual improvements in *RPE65*-treated

LCA patients persisted up to 3 years, but the retinal degeneration continued to progress [17]. This observation was recently confirmed by Jacobson and coworkers who described sustained initial improvement in visual function (1–3 years after gene therapy), followed by progressive decline 4.5–6 years after treatment [18]. At present, the transient nature of the gene therapy effects remains unclear and needs further investigation.

Following the promising results of the gene therapy with AAV2.RPE65, several groups focus today on development of gene replacement therapy for LCA associated with mutations in the *GUCY2D* and *CEP290* genes. *GUCY2D* is one of the most frequently mutated genes and responsible for approximately 12 % of all LCA cases (LCA1) [19]. *GUCY2D* is expressed specifically in the retina (nuclei and inner segments of rod and cone photoreceptors) and encodes photoreceptor-specific retinal guanylate cyclase-1 (RetGC1) involved in the resynthesis of cGMP required for the recovery of the dark state after phototransduction [19]. Recent investigations provided evidence that AAV-mediated delivery of *Gucy2e* results in restoration of cone function and preservation of cone photoreceptors over the lifetime of the RetGC1 gene knockout mouse, a model exhibiting loss of cones only [20, 21]. In the RetGC1/RetGC2 double knockout mouse that exhibits loss of both rod and cone structure and function, the AAV-mediated RetGC1 expression following subretinal injection was able to preserve the morphology of both photoreceptors and to restore the retinal function [22]. These results suggest that gene replacement therapy for people with LCA caused by mutations in the *GUCY2D* gene would be feasible in principle.

Very recently, the European Commission granted orphan designation (EMA/COMP/97253/2014) for development of AAV vector serotype 8 containing the human *GUCY2D* gene for treatment of LCA. As mutations in *GUCY2D* are also associated with autosomal recessive and dominant forms of cone-rod dystrophy [22], this gene replacement therapy may offer vision restoration to a larger group of people with retinal dystrophy. Mutations in the *CEP290* gene (encoding a centrosomal protein involved in ciliary assembly and ciliary trafficking) contribute to up to 20 % of all LCA cases [23, 24]. This is why strategies for development of proof-of-concept studies for gene therapy in *CEP290*-associated LCA are under consideration. A recent report provided evidence that the *CEP290* disease-specific cellular phenotype can be corrected in patient-derived fibroblasts by lentiviral vector expressing full-length human *CEP290* [25]. These very preliminary results mark an initial step toward gene therapy for LCA10, but they need significant further research before extending to clinic.

Alternative to gene therapy, phase 1b study (ClinicalTrials.gov: NCT01014052) recently reported that the oral retinoid intermediate QLT091001 was well tolerated and able to improve visual function (as measured by visual field and visual acuity) in some subjects with LCA or retinitis pigmentosa caused by mutations in the *RPE65* and *LRAT* genes [26]. QLT091001 was administered orally for 7 days and followed for up to 2.2 years for safety outcomes and visual function end points.

11.2.2 Stargardt Disease

Stargardt disease (STGD1) is the most common hereditary macular dystrophy and the most common cause of central visual loss in young people. It is characterized by bilateral atrophy of the macula and underlying RPE. Ninety to 95 % of all cases of Stargardt disease are inherited in an autosomal recessive manner and associated with mutations in the photoreceptor-specific *ABCA4* gene [27]. The encoded ATP-binding transmembrane protein is specifically expressed in the rims of rod and cone outer segment disks [28] and is involved in the transport of all-trans-retinal conjugates across the disk membranes. As dysfunctional protein cannot perform its transport function, lipofuscin pigments accumulate in the RPE and trigger RPE cell death and secondary photoreceptor degeneration.

The proof-of-concept results toward development of gene therapy for Stargardt disease were achieved in the *Abca4*$^{-/-}$ mice, the only available

at present animal model [29]. The vector of choice was the lentiviral vector that can accommodate the *ABCA4* cDNA of 6.8 kb and deliver long-term gene expression. It has been demonstrated that single subretinal injection of equine anemia virus-based lentiviral gene therapy (EIAV-CMV-ABCA4) (1) ensured high transduction efficiency of both rod and cone photoreceptors in the mouse model of Stargardt disease and (2) substantially reduced the disease-associated A2E accumulation at 6 and 12 months after vector delivery (although functional phenotypes were not evaluated in this study) [29].

The same group recently reported results of safety and biodistribution study assessing the effects of subretinally delivered StarGen (trademark of Oxford BioMedica, now SAR422459) in macaques and rabbits [30]. The drug is a nonreplicating nonhuman recombinant lentiviral vector based on EIAV aimed at introducing the normal human *ABCA4* gene to the retina cells. It has been demonstrated that EIAV-CMV-GFP reporter vector efficiently transduced both rod and cone photoreceptors in addition to the RPE and that the vector DNA sequences were confined to the ocular tissues of the drug-injected eye [30]. Single subretinal injection was well tolerated, with only slight and transient cellular inflammatory response in the target eye. These preclinical data provided support for the initiation of a clinical trial of gene therapy for Stargardt disease (approval for phase 1/2A trials, 2011), with positive interim results in eight patients treated at dose level 1 (no serious adverse events related to the drug or its method of administration up to 12 months posttreatment) [31]. The first escalation safety study of subretinally injected SAR422459 to patients with Stargardt macular degeneration (ClinicalTrials.gov: NCT01367444) is currently under way at the Casey Eye Institute, Oregon Health & Science University, United States, and the Centre Hospitalier National d'Ophtalmologie des Quinze-Vingts, Paris, France. The study will enroll 28 patients and will evaluate three doses of SAR422459 to confirm the highest dose that is safe and well tolerated.

Nonviral DNA nanoparticles can provide an alternative way to accommodate and deliver the large-size *ABCA4* gene. Using an optimized DNA nanoparticle technology for subretinal delivery of *ABCA4*, a persistent transgene expression was observed in the *Abca4*$^{-/-}$ mice, together with significant correction of the functional (recovery of dark adaptation) and structural (reduced lipofuscin granules) STGD1 phenotypes in treated animals [32]. These results suggest that nanoparticles may become a clinically relevant approach for delivery of the *ABCA4* gene and other genes that are too large for traditional viral vectors.

Mutations in *ABCA4* are associated not only with the autosomal recessive form of Stargardt disease but also with autosomal recessive cone-rod dystrophy, autosomal recessive retinitis pigmentosa, and increased susceptibility to AMD. *ABCA4* gene replacement therapy currently evaluated for Stargardt disease may in the future offer a therapeutic option for these other retinal dystrophies.

In recent years, several pharmacological approaches targeting pathways implicated in the pathogenesis of Stargardt disease have been investigated. One of them addresses the accumulation of lipofuscin within the RPE cells, an event known to be associated with compromised lysosomal function and reduced phagocytic activity and antioxidant capacities of the RPE cells. Centrophenoxine (meclofenoxate) was reported to reduce lipofuscin deposit, retard the accumulation of lipofuscin, and even remove lipofuscin from aging cells and tissues [33], possibly by elevating the activity of the antioxidant enzymes [34]. A significant removal of lipofuscin from RPE cells was reported in monkeys treated with the reversible inhibitor of the H,K ATPase Remofuscin (Altana Chemical Research, Konstanz, Germany), a small molecule belonging to the tetrahydropyridoethers class. Although the exact mechanism of this effect remains unknown, these findings indicate that Remofuscin has potential in the treatment of Stargardt disease and the dry AMD [33]. Another compound able to remove lipofuscin from RPE (breakup and degradation of the deposits) is the potassium-competitive H,K-ATPase blocker soraprazan. Soraprazan received orphan designation from the

European Commission by the end of 2013 (EU/3/13/1208). Ramiprilat, an angiotensin-converting enzyme (ACE) inhibitor that may reduce the formation of toxic free radicals recently received orphan designation (EU/3/13/1117) for treatment of Stargardt disease. Reduced intraneuronal deposition of lipofuscin and antioxidant properties in animal models was reported for L-carnitine [35, 36]. In patients with AMD, acetyl-L-carnitine alone [36] or in combination with Q10 and omega-3 fatty acids improved and stabilized the visual function as measured by visual field mean defect, visual acuity, and foveal sensitivity [37]. These findings appear promising for therapeutic development in macular degenerative conditions. Better understanding of the complex metabolic and intracellular signaling pathways implicated in Stargardt disease-associated retinal degeneration (e.g., GPCRs, PLC/IP3/Ca2+ signaling, NADPH oxidase-mediated ROS production) continues to identify potential drug targets [38].

11.2.3 Vitelliform Macular Dystrophies

Juvenile vitelliform macular dystrophy (Best vitelliform macular dystrophy (BVMD), Best disease) is the second most common cause of inherited maculopathy, after Stargardt disease [39]. It is a slowly progressive disease occurring in childhood and adolescence and resulting in progressive and irreversible central vision loss. Diagnosis is based on positive family history for autosomal dominant inheritance, presence of a vitelliform lesion in the macular area on ophthalmoscopy, and a moderately to severely decreased light peak on electrooculography [40]. BVMD is caused by mutations in the *BEST1* gene that encodes bestrophin-1, a protein localized to the basolateral plasma membrane of RPE [41, 42]. More than 260 mutations have been identified within *BEST1*, and 86 % of these have been associated with BVMD and other retinopathies, including adult vitelliform macular dystrophy (AVMD) (up to 25 % of cases), autosomal recessive bestrophinopathy, cone-rod dystrophy, and autosomal dominant vitreoretinochoroidopathy (reviewed in [39, 40]); however, the exact function of bestrophin 1 still remains unclear. AVMD, which predominantly affects middle-aged individuals, shows significant phenotypic overlap with BVMD [43]. AVMD is caused by mutations in the *PRPH2* gene encoding the protein peripherin 2 found in the outer segment of rod and cone photoreceptors. *PRPH2* mutations are also associated with a variety of retinal dystrophies, including other macular dystrophies, cone and cone-rod dystrophies, and retinitis pigmentosa [39]. However, many cases of vitelliform macular dystrophies do not harbor mutations in either *BEST1* or *PRPH2*.

Two factors would be crucial for development of successful treatments for vitelliform macular dystrophies: understanding the pathophysiology of these diseases and availability of relevant animal models. Recently, reversal of pathological lesions in *cmr* dogs (a spontaneous animal model of *BEST1*-associated retinopathies) was achieved by rAAV2-mediated *BEST1* gene augmentation therapy [44]. Although very preliminary, these results provide hope that vitelliform macular dystrophies may be amenable to gene substitution therapy.

In cases of vitelliform macular dystrophies complicated by choroidal neovascularization, anti-VEGF agents (e.g., ranibizumab) [45], photodynamic therapy, and thermic photocoagulation have shown efficacy [46].

11.2.4 Other Examples of Gene Therapies for Retinal Diseases

Many preclinical studies are currently under way to prepare for future gene therapy trials. One of the targeted disorders is **achromatopsia**, an early-onset, usually stationary, cone dystrophy. In more than 90 % of cases, the disease is caused by mutations in five genes of the cone phototransduction cascade, *CNGA3* and *CNGB3* being the most frequently mutated genes. A recent study in naturally occurring canine models of a *CNGB3* defect showed rescue of cone photoreceptor function after a single subretinal injection

of rAAV5-mediated gene replacement therapy using different forms of the human red cone opsin promoter [47]. The rescued cone function was documented by cone-specific electroretinogram, and recovery of day vision was sustained for over 2 years, suggesting that the correction was stable and probably permanent. In 2013, rAAV vector containing the human *CNGB3* gene received orphan drug designation (EU/3/13/1099) for treatment of achromatopsia. **X-linked retinoschisis** is a leading cause of macular degeneration in young males [48]. It is characterized by a splitting of the inner layers of the neurosensory retina, resulting in characteristic foveal schisis and vision loss. The disease is caused by mutations in the *RS1* gene encoding retinoschisin, an important protein for cell adhesion [49]. Recent studies demonstrated that AAV-mediated *RS1* delivery can promote long-term rescue of retinal structure and function in a mouse model of X-linked retinoschisis [50–53]. Very encouraging results consisting in substantial improvements in rod and cone photoreceptor-mediated visual function and synaptic transmission in mice and nonhuman primates were reported using intravitreal administration of 7m8-RS1 [9]. These preclinical studies provide evidence that gene replacement therapy can be considered as a potential treatment for X-linked retinoschisis.

Choroideremia, which is a recessive, monogenic retinal disorder without extraocular manifestations, could be considered an "ideal" target for gene augmentation therapy. It is caused by mutations in the *CHM* gene on the X chromosome (encoding human Rab escort protein 1) and leads to progressive retinal degeneration and blindness in men by their fourth decade. After successful morphological and functional rescue in animal models of choroideremia, the first clinical trial has been undertaken in Oxford University (open-label, dose-escalation phase I). It aims at assessing the safety and tolerability of the AAV2.REP1 vector administered at two different doses to the retina in 12 choroideremia patients (ClinicalTrials.gov: NCT01461213; PI: Robert McLaren). So far, six patients have been included with no major safety issues [54].

Some inherited maculopathies involve genes that cause phenotypically different disorders, e.g., *PRPH2* plays a causative role in autosomal dominant central areolar choroidal dystrophy, "pseudo-Stargardt pattern dystrophy," and pattern dystrophies like butterfly-shaped pigment dystrophy and adult-onset foveomacular vitelliform dystrophy (but also in autosomal dominant retinitis pigmentosa) [55]. Other maculopathies are monogenic, such as autosomal dominant Doyne honeycomb retinal degeneration and occult macular degeneration, caused by mutations in *EFEMP1* and *RP1L1*, respectively; Sorsby's fundus dystrophy, which is caused by mutations in the *TIMP-3* gene [55]; and North Carolina macular dystrophy (*MCDR1* on chromosome 6q16) [56]. Genetic heterogeneity of inherited maculopathies and the complex cause-function interactions represent a significant challenge for development of gene therapy today, together with other factors such as availability of relevant animal models and disease markers, prevalence of the disorder and its natural history, function and risks associated with the transgene product, and cost. Mutation-independent strategies could offer alternative therapeutic potential.

11.3 Neuroprotection

A significant body of evidence has shown that neurotrophic factors slow retinal degeneration in a number of animal models. Ciliary neurotrophic factor (CNTF) is one of the best studied factors for neuroprotection in the retina [57]. Protective effects of CNTF have been demonstrated in a variety of animal models of retinal degeneration (transgenic, naturally occurring, or light-induced) and across several species (mice, rats, cats, dogs). Protection of cone photoreceptors from degeneration and promotion of regeneration of outer segments in degenerating cones [58] are features that make CNTF specifically suitable for treatment of macular degenerative diseases. Indeed, CNTF delivered by intraocular encapsulated cell technology (NT-501 implant, Neurotech USA) was evaluated in phase 1 and 2 clinical trials and reported safe for the human retina over short

(6 months) and long (2 years) periods in patients with advanced retinitis pigmentosa, Usher syndrome type 2, and geographic atrophy in AMD [59–61]. Functional rescue in these human retinal diseases is yet to be demonstrated. A phase 1–2 clinical trial with the NT-501 intraocular implant releasing CNTF to the retina of patients affected with *CNGB3* achromatopsia is currently under way (ClinicalTrials.gov: NCT01648452).

Preventing cone degeneration may allow for treatment of a wide range of inherited retinal diseases, also including cone-rod dystrophies in which rod degeneration precedes cone degeneration (retinitis pigmentosa). Rod-derived cone viability factor (RdCVF) was demonstrated to induce cone survival and functional rescue in animal models of recessive and dominant retinitis pigmentosa [62, 63], in a manner independent from either the mechanisms or extent of rod degeneration (Fig. 11.1). RdCVF is now considered not only as an autocrine- and paracrine-acting neuroprotective agent but also as a physiological signal involved in the maintenance of photoreceptors, of importance during both aging and exposure to oxidative stress [64]. The rescue of cone photoreceptors is important not only to treat macular diseases with predominant cone dysfunction but will also be crucial in maintaining vision in rod-cone dystrophies, e.g., retinitis pigmentosa.

11.4 Retinal Prosthesis

In macular dystrophies, similarly to numerous inherited retinal degenerative diseases, parts of the inner retina survive, even after complete degeneration of the retinal photosensitive layer, and remain responsive to electrical stimulation. Retinal prosthesis uses this morphological paradigm to activate the remaining inner retinal network and to restore visual function. Different groups worldwide are currently working on retinal implant devices. The most important clinical follow-up data today are reported for the epiretinal implant Argus II (Second Sight Medical Products, Sylmar, California, United States). This device is surgically positioned on the surface of the retina to communicate directly with the ganglion and bipolar cells. It receives light signals from an external camera system that includes a video real-time processing unit (Fig. 11.2). These signals are transmitted wirelessly to an antenna in the implant and then to the 60-electrode array to send information to the brain via the optic nerve. Long-term results of multicenter clinical study demonstrated that fitted with Argus II patients with profound visual loss (29 subjects with retinitis pigmentosa and one with choroideremia) performed better on visual tasks, including object localization, motion and oriented grating discrimination, identification

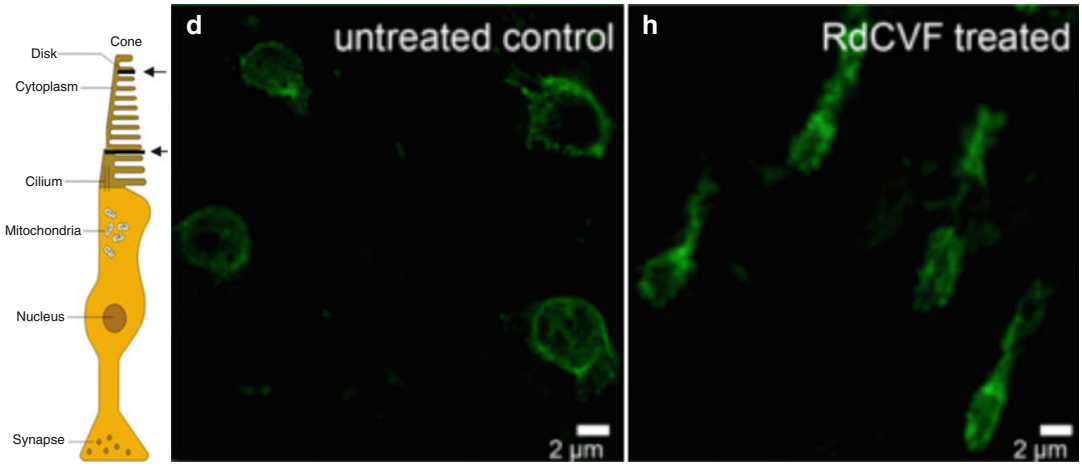

Fig. 11.1 RdCVF preserves the morphology of the cone outer segment in P23H rat: (**d**) untreated control retina and (**h**) RdCVF-treated retina (Modified from Yang et al. [63])

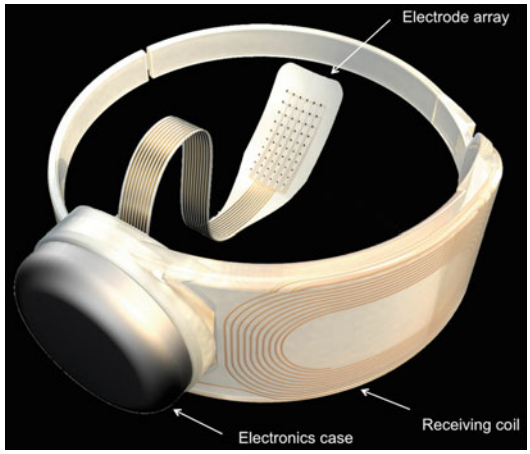

Fig. 11.2 Argus II epiretinal prosthesis: electrode array, electronic case, receiving coil (Courtesy of Second Sight Medical Products, Lausanne, Switzerland)

of letters and words, and even reading short sentences [65, 66]. Argus II can also simulate visual braille as a sensory substitute for reading [67]. Argus II received the commercial use approval of the European regulators (2011) and the US Food and Drug Administration (2013) for patients with profound visual loss.

An innovative vision restoration system, IRIS® (Pixium Vision SA, France), is currently being tested in several centers in Europe (ClinicalTrials.gov: NCT01864486). IRIS® is an epiretinal system that consists of three technical components: an implant (with an array of approximately 50 electrodes), a visual interface, and a pocket computer.

Subretinal implants are positioned in close proximity to the surviving neurons in the visual pathway (between the retina and the choroids) and receive light directly from the environment [68]. In theory, this approach may offer better inherent mechanical stability and may possibly require less current for effective stimulation, but it remains challenging from a surgical point of view. Clinical trial data (NCT01024803) obtained with the subretinal device made by Retina Implant AG, Germany, (the wirelessly powered subretinal implant Alpha IMS) in profoundly blind patients with retinitis pigmentosa demonstrated stable visual percepts, restoration of useful vision in daily life, and even identification of objects and letters [69, 70]. The Retina Implant AG subretinal implant technology received CE marking in 2013. Despite the much larger number of pixels (1,500), however, the resulting visual acuity was similar to the 60-electrode Argus II implant (approximately 20/1200).

Researchers at Stanford University are currently developing with Pixium Vision a wirelessly powered photovoltaic prosthesis [71] in which each pixel of the subretinal array directly converts patterned pulsed near-infrared light projected from video goggles into local electric current to stimulate the nearby retinal neurons. Full integration of the photovoltaic retinal prosthesis and high-resolution stimulation of the RGC have been demonstrated in normal and degenerate (RCS) rat retinas [72]. Implants with pixel sizes of 280, 140, and 70 μm implanted in the subretinal space in normal and RCS rats were able to elicit robust cortical responses upon stimulation with pulsed near-infrared light [73], providing evidence that the visual information generated by the implant in the retina arrives at the visual cortex. Several advantageous features—the surgical procedure appears simple, all pixels function independently, the external camera operates over a wide range of ambient illumination, and the natural link between eye movements and image perception is preserved—make the photovoltaic prosthesis promising for vision restoration in retinal degenerative diseases.

Despite the great technical progress, the quality of the images achieved with retinal prosthetic devices remains a challenge. New electrode designs and new materials aiming at improving visual resolution and safety profiles are currently under investigation.

11.5 Optogenetics

Optogenetics combines genetic strategies to target light-sensitive proteins within the cells and optical stimulation to activate these selectively targeted proteins. For vision restoration, optogenetics aims at converting strategically important retinal cell types into "artificial photoreceptors." This is possible, first, because many cone

photoreceptors survive even in advanced stages of retinal disease and maintain their cell body for extended periods of time [74, 75] and, second, because of the discovery of genes that inserted into cells encode membrane proteins responsive to light and able to turn the neurons ON or OFF [76, 77]. Several groups have demonstrated that spared inner retinal neurons are sensitized to light using channelrhodopsin-2 (ChR2), a microbial-type rhodopsin found in the green algae *Chlamydomonas reinhardtii* [78, 79], and halorhodopsin (NpHR), an archaebacterial protein from *Natronomonas pharaonis* [80] (Fig. 11.3).

ChR2 delivered by rAAV was shown to establish targeted, robust, and long-term transgene expression in ON bipolar cells of the retina, leading to electrophysiological and behavioral improvements in visual function in animal models of blindness; *rd1*, *rd10*, and *rd16* mouse models [81–83]; and RCS rat [84]. Recent studies have shown that NpHR introduced to surviving cone cell bodies in two mouse models of retinitis pigmentosa (RP) reactivated retinal ON and OFF pathways, as well as the retinal circuitry, and enabled RP mice to perform visually guided behaviors [85]. Moreover, NpHR targeted to human postmortem photoreceptors with no measurable intrinsic rod- or cone-mediated photosensitivity restored light responses in photoreceptor cells, clearly demonstrating that reactivation of the surviving retinal structures and phototransduction cascade required for vision is possible [85]. These preclinical data hold promise that legally blind or severely visually impaired patients with no visual field, but with a preserved layer of cone bodies (visible on optical coherent tomography), could be eligible for optogenetic functional restoration of cones.

Optogenetic stimulation of the remaining RGCs or bipolar cells in retinal degenerative disorders provides an alternative approach to vision restoration. Optogenetics has some advantages, including minimally invasive neuronal stimulation, independence of the nature of the retinal degeneration, and resemblance of the artificially stimulated retinal activity to the normal activity of retinal circuits. Different strategies for optogenetic vision restoration, including their advantages and possible combination with other methods to slow retinal degeneration and/or restore vision, were recently reviewed [7].

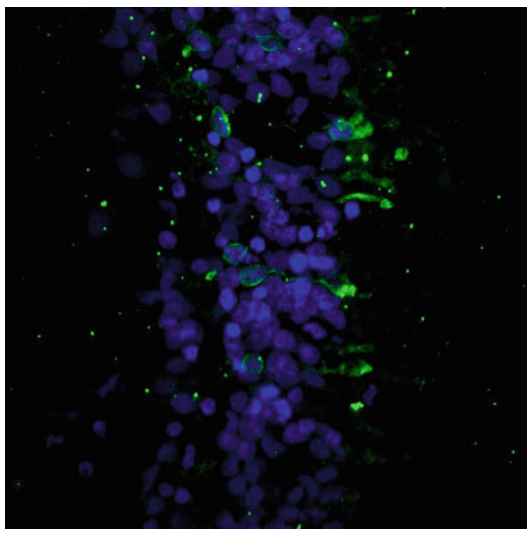

Fig. 11.3 Human retina section: targeted expression of halorhodopsin in cone cell bodies (GFP-immunostained photoreceptors) (Courtesy of Institut de la Vision)

11.6 Cellular Therapy

Transplantation of retinal cells or photoreceptor precursor cells is another potential strategy to restore vision in patients with macular dystrophies. At present, the most promising options considered for retinal transplantations are embryonic stem cells (ESCs) that can be isolated from developing embryos and induced pluripotent stem cells (iPSCs) that can be generated from adult differentiated somatic cells, e.g., fibroblasts, via overexpression of a set of transcription factors Oct4, Sox2, Klf4, and c-Myc [86]. Initial data demonstrated that transplanted progenitor or precursor cells isolated at the correct ontogenetic stage from the developing retina can integrate into the host retina and differentiate into rod photoreceptors [87].

Recent findings confirmed the survival and differentiation of some photoreceptors derived from three-dimensional ESC cultures: ESC-derived

photoreceptor cell precursors were able to integrate and mature and to form outer segments and some synaptic connections after transplantation into the degenerate adult mouse retina [88]. Whether similar integration and functional improvement can be achieved using human cells remains to be established. In all cases, translation to clinical studies will require validated disease models, robust methods, and standardized protocols to control cell maturation and cell fate specification and relevant cell-manufacturing strategies. A recent study reported in vitro recreation of key structural and functional features of the native retina, in particular the presence of photoreceptors with outer segment disks and photosensitivity [89]. An innovative approach to produce retinal cells for regenerative medicine and drug-screening purposes was recently proposed [90]. It is based on confluent human iPSC, bypassing embryoid body formation and the use of exogenous molecules, coating, or Matrigel. This new retinal differentiation process allows simultaneous generation of both RPE cells and self-forming neural retina-like structures containing retinal progenitor cells (RPCs) within 2 weeks. When switched to floating cultures, structures containing RPCs can differentiate into all retinal cell types, including RGCs and precursors of photoreceptors, needed for therapeutic applications.

The main advantages of cell therapies as a source for regenerative therapy is that: (1) they are gene-independent, thus applicable to a broad range of retinal diseases, and (2) can be expanded indefinitely in culture and used as an unlimited source of retinal cells for treatment of retinal degenerative diseases. The first ever safety and tolerability prospective clinical trial to evaluate subretinal injection of hESC-derived RPE cells in patients with advanced dry AMD and Stargardt macular dystrophy is currently under way (ClinicalTrials.gov: NCT01344993; NCT01345006). Very early results suggest graft survival, biological activity, and no major safety concern (no signs of hyperproliferation, tumorigenicity, ectopic tissue formation, or apparent rejection after 4 months) [91, 92]. As hiPSCs can be obtained directly from the patient, they have the advantage of being autologous and therefore less immunogenic. Retinal cells derived from hiPSCs have been generated by different laboratories worldwide, and some groups are currently setting up human clinical trials with hiPSC-derived RPE for treatment of AMD, e.g., pilot clinical study to assess the safety and feasibility of the transplantation of autologous iPSCs in patients with exudative AMD started in Japan in 2013 [93]. There is no safety report so far. Recently, this pioneering clinical study has been suspended with the decision of the RIKEN Center for Developmental Biology not to treat the second patient [94]. Advances in research into iPSC applications for treatment of retinal degeneration were recently reviewed in detail by Cramer and MacLaren [95–97].

11.7 Sensory Substitution Devices

Technologies transforming auditory or tactile information into visual sensory information are currently under clinical evaluation. Using a visual-to-auditory sensory substitution device called "The vOICe", blind and blindfolded participants were able to locate and identify objects through images encoded by sound [98, 99]. Even congenitally fully blind adults could be taught to read and recognize complex images using "soundscapes," sounds topographically representing images [100, 101]. A device that translates information from a digital video camera to the tongue, BrainPort®, helps blind individuals to recognize high-contrast objects, their location and movement, and some aspects of perspective and depth [102]. Sensory substitution devices are noninvasive and cheap and usually require training in a scale of hours [101]. By providing a visual-like experience, they can compensate for some effects of early or lifelong blindness and serve as aids in daily visual tasks.

11.8 Concluding Remarks

Identifying patients who can benefit from these emerging therapeutic strategies is crucial for selecting appropriate therapy. High-resolution

imaging techniques (e.g., optical coherence tomography and adaptive optics) and functional studies (e.g., microperimetry) are essential for patient selection and establishing the benefit of these novel therapies. Standardized mobility and task-related tests are needed for assessment of the subjective visual handicap and for a reliable evaluation of the actual benefit for the patient. Development of new rehabilitation programs and devices, especially those that take advantage of visual plasticity (persisting even in old age), should be of paramount importance. Novel nano-sized materials and systems developed in recent years provide novel tools for drug, gene, and trophic factor delivery in ophthalmology and offer, in principle, low risk of immunogenicity, high transfection efficiency, relatively low cost, and, possibly, greater ease of production compared with viral vectors. In addition, they can accommodate large genes, unlike traditional viral vectors. Recent papers have reviewed nonviral vectors and nanotechnology for vision restoration [103, 104].

Further investigations on genetics and genotype-phenotype correlations would unravel new insights into disease causes and specific therapeutic targets for macular dystrophies. Despite the improved vision after *RPE65* gene augmentation therapy, photoreceptor degeneration was shown to progress both in the canine model and in humans [17, 18]. These findings emphasize the need of (1) slowing the retinal degeneration process in long term, in addition to improving the retinal function, and (2) evaluation of combination therapies in the treatment of retinal dystrophies [17]. What would be particularly important is to transfer the knowledge of rare macular dystrophies toward generation of effective therapies that could potentially be applicable in very common macular diseases such as AMD.

References

1. The National Eye Institute. Vision research: needs, gaps, and opportunities. https://nei.nih.gov/strategicplanning. Accessed 18 Aug 2015.
2. Young RW. Solar radiation and age-related macular degeneration. Surv Ophthalmol. 1988;32(4):252–69.
3. Arnault E, Barrau C, Nanteau C, Gondouin P, Bigot K, Vienot F, et al. Phototoxic action spectrum on a retinal pigment epithelium model of age-related macular degeneration exposed to sunlight normalized conditions. PLoS ONE. 2013;8(8), e71398.
4. Thornton J, Edwards R, Mitchell P, Harrison RA, Buchan I, Kelly SP. Smoking and age-related macular degeneration: a review of association. Eye (Lond). 2005;19(9):935–44.
5. Age-Related Eye Disease Study Research Group. A randomized, placebo-controlled, clinical trial of high-dose supplementation with vitamins C and E, beta carotene, and zinc for age-related macular degeneration and vision loss: AREDS report no. 8. Arch Ophthalmol. 2001;119(10):1417–36.
6. Age-Related Eye Disease Study 2 Research Group. Lutein + zeaxanthin and omega-3 fatty acids for age-related macular degeneration: the Age-Related Eye Disease Study 2 (AREDS2) randomized clinical trial. JAMA. 2013;309(19):2005–15.
7. Sahel JA, Roska B. Gene therapy for blindness. Annu Rev Neurosci. 2013;36:467–88.
8. Colella P, Auricchio A. AAV-mediated gene supply for treatment of degenerative and neovascular retinal diseases. Curr Gene Ther. 2010;10(5):371–80.
9. Dalkara D, Byrne LC, Klimczak RR, Visel M, Yin L, Merigan WH, et al. In vivo-directed evolution of a new adeno-associated virus for therapeutic outer retinal gene delivery from the vitreous. Sci Transl Med. 2013;5(189):189ra76.
10. Acland GM, Aguirre GD, Ray J, Zhang Q, Aleman TS, Cideciyan AV, et al. Gene therapy restores vision in a canine model of childhood blindness. Nat Genet. 2001;28(1):92–5.
11. Acland GM, Aguirre GD, Bennett J, Aleman TS, Cideciyan AV, Bennicelli J, et al. Long-term restoration of rod and cone vision by single dose rAAV-mediated gene transfer to the retina in a canine model of childhood blindness. Mol Ther. 2005;12(6):1072–82.
12. Asai-Coakwell M, March L, Dai XH, Duval M, Lopez I, French CR, et al. Contribution of growth differentiation factor 6-dependent cell survival to early-onset retinal dystrophies. Hum Mol Genet. 2013;22(7):1432–42.
13. Maguire AM, Simonelli F, Pierce EA, Pugh Jr EN, Mingozzi F, Bennicelli J, et al. Safety and efficacy of gene transfer for Leber's congenital amaurosis. N Engl J Med. 2008;358(21):2240–8.
14. Bainbridge JW, Smith AJ, Barker SS, Robbie S, Henderson R, Balaggan K, et al. Effect of gene therapy on visual function in Leber's congenital amaurosis. N Engl J Med. 2008;358(21):2231–9.
15. Jacobson SG, Cideciyan AV, Ratnakaram R, Heon E, Schwartz SB, Roman AJ, et al. Gene therapy for leber congenital amaurosis caused by RPE65 mutations: safety and efficacy in 15 children and adults followed up to 3 years. Arch Ophthalmol. 2012;130(1):9–24.
16. Bennett J, Ashtari M, Wellman J, Marshall KA, Cyckowski LL, Chung DC, et al. AAV2 gene therapy

readministration in three adults with congenital blindness. Sci Transl Med. 2012;4(120):120ra15.
17. Cideciyan AV, Jacobson SG, Beltran WA, Sumaroka A, Swider M, Iwabe S, et al. Human retinal gene therapy for Leber congenital amaurosis shows advancing retinal degeneration despite enduring visual improvement. Proc Natl Acad Sci U S A. 2013;110(6):E517–25.
18. Jacobson SG, Cideciyan AV, Roman AJ, Sumaroka A, Schwartz SB, Heon E, Hauswirth WW. Improvement and decline in vision with gene therapy in childhood blindness. N Engl J Med. 2015;372(20):1920–6.
19. den Hollander AI, Roepman R, Koenekoop RK, Cremers FP. Leber congenital amaurosis: genes, proteins and disease mechanisms. Prog Retin Eye Res. 2008;27(4):391–419.
20. Boye SE, Boye SL, Pang J, Ryals R, Everhart D, Umino Y, et al. Functional and behavioral restoration of vision by gene therapy in the guanylate cyclase-1 (GC1) knockout mouse. PLoS ONE. 2010;5(6), e11306.
21. Mihelec M, Pearson RA, Robbie SJ, Buch PK, Azam SA, Bainbridge JW, et al. Long-term preservation of cones and improvement in visual function following gene therapy in a mouse model of leber congenital amaurosis caused by guanylate cyclase-1 deficiency. Hum Gene Ther. 2011;22(10):1179–90.
22. Boye SL, Peshenko IV, Huang WC, Min SH, McDoom I, Kay CN, et al. AAV-mediated gene therapy in the guanylate cyclase (RetGC1/RetGC2) double knockout mouse model of Leber congenital amaurosis. Hum Gene Ther. 2013;24(2):189–202.
23. den Hollander AI, Koenekoop RK, Yzer S, Lopez I, Arends ML, Voesenek KE, et al. Mutations in the CEP290 (NPHP6) gene are a frequent cause of Leber congenital amaurosis. Am J Hum Genet. 2006;79(3):556–61.
24. Perrault I, Delphin N, Hanein S, Gerber S, Dufier JL, Roche O, et al. Spectrum of NPHP6/CEP290 mutations in Leber congenital amaurosis and delineation of the associated phenotype. Hum Mutat. 2007;28(4):416.
25. Burnight ER, Wiley LA, Drack AV, Braun TA, Anfinson KR, Kaalberg EE, et al. CEP290 gene transfer rescues Leber congenital amaurosis cellular phenotype. Gene Ther. 2014;21(7):662–72.
26. Koenekoop RK, Sui R, Sallum J, van den Born LI, Ajlan R, Khan A, et al. Oral 9-cis retinoid for childhood blindness due to Leber congenital amaurosis caused by RPE65 or LRAT mutations: an open-label phase 1b trial. Lancet. 2014;384(9953):1513–20.
27. Allikmets R, Singh N, Sun H, Shroyer NF, Hutchinson A, Chidambaram A, et al. A photoreceptor cell-specific ATP-binding transporter gene (ABCR) is mutated in recessive Stargardt macular dystrophy. Nat Genet. 1997;15(3):236–46.
28. Molday LL, Rabin AR, Molday RS. ABCR expression in foveal cone photoreceptors and its role in Stargardt macular dystrophy. Nat Genet. 2000;25(3):257–8.
29. Kong J, Kim SR, Binley K, Pata I, Doi K, Mannik J, et al. Correction of the disease phenotype in the mouse model of Stargardt disease by lentiviral gene therapy. Gene Ther. 2008;15(19):1311–20.
30. Binley K, Widdowson P, Loader J, Kelleher M, Iqball S, Ferrige G, et al. Transduction of photoreceptors with equine infectious anemia virus lentiviral vectors: safety and biodistribution of StarGen for Stargardt disease. Invest Ophthalmol Vis Sci. 2013;54(6):4061–71.
31. Oxford Biomedica. Oxford BioMedica Announces Positive DSMB Review of Ongoing RetinoStat® and StarGen™ Clinical Studies. www.oxfordbiomedica.co.uk/press-releases/oxford-biomedica-announces-positive-dsmb-review-of-ongoing-retinostat-r-and-stargen-clinical-studies/. Accessed 12 Aug 2015.
32. Han Z, Conley SM, Makkia RS, Cooper MJ, Naash MI. DNA nanoparticle-mediated ABCA4 delivery rescues Stargardt dystrophy in mice. J Clin Invest. 2012;122(9):3221–6.
33. Julien S, Schraermeyer U. Lipofuscin can be eliminated from the retinal pigment epithelium of monkeys. Neurobiol Aging. 2012;33(10):2390–7.
34. Roy D, Pathak DN, Singh R. Effect of centrophenoxine on the antioxidative enzymes in various regions of the aging rat brain. Exp Gerontol. 1983;18(3):185–97.
35. Amenta F, Ferrante F, Lucreziotti R, Ricci A, Ramacci MT. Reduced lipofuscin accumulation in senescent rat brain by long-term acetyl-L-carnitine treatment. Arch Gerontol Geriatr. 1989;9(2):147–53.
36. Pescosolido N, Imperatrice B, Karavitis P. The aging eye and the role of L-carnitine and its derivatives. Drugs R D. 2008;9 Suppl 1:3–14.
37. Feher J, Kovacs B, Kovacs I, Schveoller M, Papale A, Balacco GC. Improvement of visual functions and fundus alterations in early age-related macular degeneration treated with a combination of acetyl-L-carnitine, n-3 fatty acids, and coenzyme Q10. Ophthalmologica. 2005;219(3):154–66.
38. Chen Y, Palczewska G, Mustafi D, Golczak M, Dong Z, Sawada O, et al. Systems pharmacology identifies drug targets for Stargardt disease-associated retinal degeneration. J Clin Invest. 2013;123(12):5119–34.
39. Meunier I, Senechal A, Dhaenens CM, Arndt C, Puech B, Defoort-Dhellemmes S, et al. Systematic screening of BEST1 and PRPH2 in juvenile and adult vitelliform macular dystrophies: a rationale for molecular analysis. Ophthalmology. 2011;118(6):1130–6.
40. Pasquay C, Wang LF, Lorenz B, Preising MN. Bestrophin 1 – phenotypes and functional aspects in bestrophinopathies. Ophthalmic Genet. 2015;36(3):193–212.
41. Marquardt A, Stohr H, Passmore LA, Kramer F, Rivera A, Weber BH. Mutations in a novel gene, VMD2, encoding a protein of unknown properties cause juvenile-onset vitelliform macular dystrophy (Best's disease). Hum Mol Genet. 1998;7(9):1517–25.

42. Petrukhin K, Koisti MJ, Bakall B, Li W, Xie G, Marknell T, Sandgren O, Forsman K, Holmgren G, Andreasson S, et al. Identification of the gene responsible for Best macular dystrophy. Nat Genet. 1998;19(3):241–7.
43. MacDonald IM, Lee T. Best vitelliform macular dystrophy. In: Pagon RA, Adam MP, Ardinger HH, Wallace SE, Amemiya A, Bean LJH, et al. GeneReviews [Internet]. Seattle: University of Washington, Seattle; 1993–2015. 30 Sep 2003 [updated 12 Dec 2013]. Available from http://www.ncbi.nlm.nih.gov/books/NBK1167/. Accessed 14 Aug 2015.
44. Guziewicz KE, Komaromy AM, Iwabe S, Cideciyan AV, Dutrow EV, Zangerl B, et al. Sustained therapeutic reversal of canine bestrophinopathy with gene therapy using recombinant AAV2 (abstract). Invest Opthalmol Vis Sci. 2013;54(15):5965.
45. Mimoun G, Caillaux V, Querques G, Rothschild PR, Puche N, Souied EH. Ranibizumab for choroidal neovascularization associated with adult-onset foveomacular vitelliform dystrophy: one-year results. Retina. 2013;33(3):513–21.
46. Querques G, Zerbib J, Santacroce R, Margaglione M, Delphin N, Rozet JM, et al. Functional and clinical data of Best vitelliform macular dystrophy patients with mutations in the BEST1 gene. Mol Vis. 2009;15:2960–72.
47. Komaromy AM, Alexander JJ, Rowlan JS, Garcia MM, Chiodo VA, Kaya A, et al. Gene therapy rescues cone function in congenital achromatopsia. Hum Mol Genet. 2010;19(13):2581–93.
48. George ND, Yates JR, Moore AT. X linked retinoschisis. Br J Ophthalmol. 1995;79(7):697–702.
49. Sauer CG, Gehrig A, Warneke-Wittstock R, Marquardt A, Ewing CC, Gibson A, et al. Positional cloning of the gene associated with X-linked juvenile retinoschisis. Nat Genet. 1997;17(2):164–70.
50. Zeng Y, Takada Y, Kjellstrom S, Hiriyanna K, Tanikawa A, Wawrousek E, et al. RS-1 gene delivery to an adult Rs1h knockout mouse model restores ERG b-wave with reversal of the electronegative waveform of X-linked retinoschisis. Invest Ophthalmol Vis Sci. 2004;45(9):3279–85.
51. Kjellstrom S, Bush RA, Zeng Y, Takada Y, Sieving PA. Retinoschisin gene therapy and natural history in the Rs1h-KO mouse: long-term rescue from retinal degeneration. Invest Ophthalmol Vis Sci. 2007;48(8):3837–45.
52. Janssen A, Min SH, Molday LL, Tanimoto N, Seeliger MW, Hauswirth WW, et al. Effect of late-stage therapy on disease progression in AAV-mediated rescue of photoreceptor cells in the retinoschisin-deficient mouse. Mol Ther. 2008;16(6):1010–7.
53. Park TK, Wu Z, Kjellstrom S, Zeng Y, Bush RA, Sieving PA, Colosi P. Intravitreal delivery of AAV8 retinoschisin results in cell type-specific gene expression and retinal rescue in the Rs1-KO mouse. Gene Ther. 2009;16(7):916–26.
54. MacLaren RE, Groppe M, Barnard AR, Cottriall CL, Tolmachova T, Seymour L, Clark KR, During MJ, Cremers FP, Black GC, et al. Retinal gene therapy in patients with choroideremia: initial findings from a phase 1/2 clinical trial. Lancet. 2014;383(9923):1129–37.
55. Roosing S, Thiadens AA, Hoyng CB, Klaver CC, den Hollander AI, Cremers FP. Causes and consequences of inherited cone disorders. Prog Retin Eye Res. 2014;42:1–26.
56. Small KW, Hermsen V, Gurney N, Fetkenhour CL, Folk JC. North Carolina macular dystrophy and central areolar pigment epithelial dystrophy. One family, one disease. Arch Ophthalmol. 1992;110(4):515–8.
57. Wen R, Tao W, Li Y, Sieving PA. CNTF and retina. Prog Retin Eye Res. 2012;31(2):136–51.
58. Li Y, Tao W, Luo L, Huang D, Kauper K, Stabila P, et al. CNTF induces regeneration of cone outer segments in a rat model of retinal degeneration. PLoS ONE. 2010;5(3), e9495.
59. Sieving PA, Caruso RC, Tao W, Coleman HR, Thompson DJ, Fullmer KR, Bush RA. Ciliary neurotrophic factor (CNTF) for human retinal degeneration: phase I trial of CNTF delivered by encapsulated cell intraocular implants. Proc Natl Acad Sci U S A. 2006;103(10):3896–901.
60. Kauper K, McGovern C, Sherman S, Heatherton P, Rapoza R, Stabila P, et al. Two-year intraocular delivery of ciliary neurotrophic factor by encapsulated cell technology implants in patients with chronic retinal degenerative diseases. Invest Ophthalmol Vis Sci. 2012;53(12):7484–91.
61. Talcott KE, Ratnam K, Sundquist SM, Lucero AS, Lujan BJ, Tao W, et al. Longitudinal study of cone photoreceptors during retinal degeneration and in response to ciliary neurotrophic factor treatment. Invest Ophthalmol Vis Sci. 2011;52(5):2219–26.
62. Leveillard T, Mohand-Said S, Lorentz O, Hicks D, Fintz AC, Clerin E, et al. Identification and characterization of rod-derived cone viability factor. Nat Genet. 2004;36(7):755–9.
63. Yang Y, Mohand-Said S, Danan A, Simonutti M, Fontaine V, Clerin E, et al. Functional cone rescue by RdCVF protein in a dominant model of retinitis pigmentosa. Mol Ther. 2009;17(5):787–95.
64. Leveillard T, Sahel JA. Rod-derived cone viability factor for treating blinding diseases: from clinic to redox signaling. Sci Transl Med. 2010;2(26):26ps16.
65. Humayun MS, Dorn JD, da Cruz L, Dagnelie G, Sahel JA, Stanga PE, et al. Interim results from the international trial of Second Sight's visual prosthesis. Ophthalmology. 2012;119(4):779–88.
66. da Cruz L, Coley BF, Dorn J, Merlini F, Filley E, Christopher P, et al. The Argus II epiretinal prosthesis system allows letter and word reading and long-term function in patients with profound vision loss. Br J Ophthalmol. 2013;97(5):632–6.
67. Lauritzen TZ, Harris J, Mohand-Said S, Sahel JA, Dorn JD, McClure K, Greenberg RJ. Reading visual

braille with a retinal prosthesis. Front Neurosci. 2012;6(168):1–7.
68. Zrenner E. Will retinal implants restore vision? Science. 2002;295(5557):1022–5.
69. Zrenner E, Bartz-Schmidt KU, Benav H, Besch D, Bruckmann A, Gabel VP, et al. Subretinal electronic chips allow blind patients to read letters and combine them to words. Proc Biol Sci. 2011;278(1711):1489–97.
70. Stingl K, Bartz-Schmidt KU, Besch D, Braun A, Bruckmann A, Gekeler F, et al. Artificial vision with wirelessly powered subretinal electronic implant alpha-IMS. Proc Biol Sci. 2013;280(1757):20130077.
71. Wang L, Mathieson K, Kamins TI, Loudin JD, Galambos L, Goetz G, et al. Photovoltaic retinal prosthesis: implant fabrication and performance. J Neural Eng. 2012;9(4):046014.
72. Mathieson K, Loudin J, Goetz G, Huie P, Wang L, Kamins TI, et al. Photovoltaic retinal prosthesis with high pixel density. Nat Photonics. 2012;6(6):391–7.
73. Mandel Y, Goetz G, Lavinsky D, Huie P, Mathieson K, Wang L, et al. Cortical responses elicited by photovoltaic subretinal prostheses exhibit similarities to visually evoked potentials. Nat Commun. 2013;4:1980.
74. Li ZY, Kljavin IJ, Milam AH. Rod photoreceptor neurite sprouting in retinitis pigmentosa. J Neurosci. 1995;15(8):5429–38.
75. Lin B, Masland RH, Strettoi E. Remodeling of cone photoreceptor cells after rod degeneration in rd mice. Exp Eye Res. 2009;88(3):589–99.
76. Bi A, Cui J, Ma YP, Olshevskaya E, Pu M, Dizhoor AM, Pan ZH. Ectopic expression of a microbial-type rhodopsin restores visual responses in mice with photoreceptor degeneration. Neuron. 2006;50(1):23–33.
77. Zhang Y, Ivanova E, Bi A, Pan ZH. Ectopic expression of multiple microbial rhodopsins restores ON and OFF light responses in retinas with photoreceptor degeneration. J Neurosci. 2009;29(29):9186–96.
78. Nagel G, Ollig D, Fuhrmann M, Kateriya S, Musti AM, Bamberg E, Hegemann P. Channelrhodopsin-1: a light-gated proton channel in green algae. Science. 2002;296(5577):2395–8.
79. Boyden ES, Zhang F, Bamberg E, Nagel G, Deisseroth K. Millisecond-timescale, genetically targeted optical control of neural activity. Nat Neurosci. 2005;8(9):1263–8.
80. Zhang F, Wang LP, Brauner M, Liewald JF, Kay K, Watzke N, et al. Multimodal fast optical interrogation of neural circuitry. Nature. 2007;446(7136):633–9.
81. Lagali PS, Balya D, Awatramani GB, Munch TA, Kim DS, Busskamp V, et al. Light-activated channels targeted to ON bipolar cells restore visual function in retinal degeneration. Nat Neurosci. 2008;11(6):667–75.
82. Doroudchi MM, Greenberg KP, Liu J, Silka KA, Boyden ES, Lockridge JA, et al. Virally delivered channelrhodopsin-2 safely and effectively restores visual function in multiple mouse models of blindness. Mol Ther. 2011;19(7):1220–9.
83. Macé E, Caplette R, Marre O, Sengupta A, Chaffiol A, Barbe P, et al. Targeting channelrhodopsin-2 to ON-bipolar cells with vitreally administered AAV restores ON and OFF visual responses in blind mice. Mol Ther. 2015;23(1):7–16.
84. Tomita H, Sugano E, Isago H, Hiroi T, Wang Z, Ohta E, Tamai M. Channelrhodopsin-2 gene transduced into retinal ganglion cells restores functional vision in genetically blind rats. Exp Eye Res. 2010;90(3):429–36.
85. Busskamp V, Duebel J, Balya D, Fradot M, Viney TJ, Siegert S, et al. Genetic reactivation of cone photoreceptors restores visual responses in retinitis pigmentosa. Science. 2010;329(5990):413–7.
86. Takahashi K, Yamanaka S. Induction of pluripotent stem cells from mouse embryonic and adult fibroblast cultures by defined factors. Cell. 2006;126(4):663–76.
87. MacLaren RE, Pearson RA, MacNeil A, Douglas RH, Salt TE, Akimoto M, et al. Retinal repair by transplantation of photoreceptor precursors. Nature. 2006;444(7116):203–7.
88. Gonzalez-Cordero A, West EL, Pearson RA, Duran Y, Carvalho LS, Chu CJ, et al. Photoreceptor precursors derived from three-dimensional embryonic stem cell cultures integrate and mature within adult degenerate retina. Nat Biotechnol. 2013;31(8):741–7.
89. Zhong X, Gutierrez C, Xue T, Hampton C, Vergara MN, Cao LH, et al. Generation of three-dimensional retinal tissue with functional photoreceptors from human iPSCs. Nat Commun. 2014;5:4047.
90. Reichman S, Terray A, Slembrouck A, Nanteau C, Orieux G, Habeler W, et al. From confluent human iPS cells to self-forming neural retina and retinal pigmented epithelium. Proc Natl Acad Sci U S A. 2014;111(23):8518–23.
91. Schwartz SD, Hubschman JP, Heilwell G, Franco-Cardenas V, Pan CK, Ostrick RM, et al. Embryonic stem cell trials for macular degeneration: a preliminary report. Lancet. 2013;379(9817):713–20.
92. Schwartz SD, Regillo CD, Lam BL, Eliott D, Rosenfeld PJ, Gregori NZ, et al. Human embryonic stem cell-derived retinal pigment epithelium in patients with age-related macular degeneration and Stargardt's macular dystrophy: follow-up of two open-label phase 1/2 studies. Lancet. 2015;385(9967):509–16.
93. RIKEN. Pilot clinical study into iPS cell therapy for eye disease starts in Japan. . http://www.riken.jp/en/pr/press/2013/20130730_1/. Accessed 12 Aug 2015.
94. Garber K. RIKEN suspends first clinical trial involving induced pluripotent stem cells. Nat Biotechnol. 2015;33(9):890–1.
95. Cramer AO, MacLaren RE. Translating induced pluripotent stem cells from bench to bedside: application to retinal diseases. Curr Gene Ther. 2013;13(2):139–51.

96. Nazari H, Zhang L, Zhu D, Chader GJ, Falabella P, Stefanini F, et al. Stem cell based therapies for age-related macular degeneration: the promises and the challenges. Prog Retin Eye Res. 2015;48:1–39.
97. Jayakody SA, Gonzalez-Cordero A, Ali RR, Pearson RA. Cellular strategies for retinal repair by photoreceptor replacement. Prog Retin Eye Res. 2015;46:31–66.
98. Auvray M, Hanneton S, O'Regan JK. Learning to perceive with a visuo-auditory substitution system: localisation and object recognition with 'the vOICe'. Perception. 2007;36(3):416–30.
99. Merabet LB, Battelli L, Obretenova S, Maguire S, Meijer P, Pascual-Leone A. Functional recruitment of visual cortex for sound encoded object identification in the blind. Neuroreport. 2009;20(2):132–8.
100. Striem-Amit E, Cohen L, Dehaene S, Amedi A. Reading with sounds: sensory substitution selectively activates the visual word form area in the blind. Neuron. 2012;76(3):640–52.
101. Striem-Amit E, Guendelman M, Amedi A. 'Visual' acuity of the congenitally blind using visual-to-auditory sensory substitution. PLoS ONE. 2012;7(3):e33136.
102. Sampaio E, Maris S, Bach-y-Rita P. Brain plasticity: 'visual' acuity of blind persons via the tongue. Brain Res. 2001;908(2):204–7.
103. Yin H, Kanasty RL, Eltoukhy AA, Vegas AJ, Dorkin JR, Anderson DG. Non-viral vectors for gene-based therapy. Nat Rev Genet. 2014;15(8):541–55.
104. Zarbin MA, Arlow T, Ritch R. Regenerative nanomedicine for vision restoration. Mayo Clin Proc. 2013;88(12):1480–90.

Index

A
Achromatopsia, 36, 106–108
Adeno-associated virus (AAV), 103, 104, 107
Adenosine triphosphate (ATP)-binding cassette transporter (ABCR), 27
Adult-onset foveomacular vitelliform dystrophy (AFVD)
  autosomal-dominant trait, 12
  differential diagnosis, 14–15
  disease course, 14
  PRPH2, BEST1, and *IMPG1* and *IMPG2* genes, 12
  RPE-photoreceptor complex function, 12
  vitelliform lesions, 12–14
Adult vitelliform macular dystrophy (AVMD), 106
AFVD See Adult-onset foveomacular vitelliform dystrophy (AFVD)
Age-Related Eye Disease Study (AREDS), 102
Age-related macular disease (AMD), 47
  AFVD, 14
  late-onset Stargardt, 28
  MRD, 68
Autosomal dominant drusen. S*ee* Malattia Leventinese (ML)

B
Best disease. S*ee* Vitelliform macular dystrophy (VMD)
Bestrophinopathy, 2, 7, 9
Binimetinib treatment, 15
BPD. S*ee* Butterfly-shaped pigment dystrophy (BPD)
Bull's-eye maculopathy (BEM)
  CRD, 36
  generalized retinal dystrophies, 32–34
Butterfly-shaped pigment dystrophy (BPD)
  autosomal-dominantly inherited macular dystrophy, 15
  clinical findings, 15, 16
  differential diagnosis, 16
  disease course, 15
  PRPH2 mutations, 15

C
Carbonic anhydrase inhibitors (CAIs), 34, 79
Central areolar choroidal dystrophy (CACD), 28
  clinical characteristics of, 85, 88
  differential diagnosis, 89
  disease course, 87
  ERG, 87
  fluorescein angiography, 85, 86
  fundus abnormalities, 84–86
  fundus autofluorescence, 85–87
  genotype-phenotype correlation, 84
  OCT, 87
  PRPH2 gene, 84
Channelrhodopsin-2 (ChR2), 110
Choroidal neovascularization (CNV), 8
  AFVD, 13, 14
  AMD, 48
  BPD, 15
  CACD, 87
  ML, 48
  vitelliform macular dystrophies, 106
Choroidal neovascular membrane (CNVM)
  MCDR1, 54
  SFD, 59–61
Choroideremia, 34, 107
Complement 1q tumor necrosis factor 5 gene *(C1QTNF5)* gene, 92, 99
Cone-rod dystrophies (CRD)
  Bull's-eye maculopathy, 36
  ffERG, 36
  macular atrophy, 36, 37
  no obvious fundus abnormalities, 35
  pigmentary changes, 36
  prevalence of, 31
Cystic macular edema (CME), 34
Cystoid fluid collections (CFCs), 89, 92, 93

D
Desferrioxamine-related retinopathy, 15
Dominant cystoid macular dystrophy (DCMD)
  clinical classification of, 89, 90, 92–94
  differential diagnosis, 91
  visual acuity, 89, 91
Dominant radial drusen (DRD). S*ee* Malattia Leventinese (ML)
Doyne honeycomb retinal dystrophy (DHRD). S*ee* Malattia Leventinese (ML)
Dystrophia reticularis laminae pigmentosae retinae. S*ee* Reticular pattern dystrophy

G. Querques, E.H. Souied (eds.), *Macular Dystrophies*, DOI 10.1007/978-3-319-26621-3

E
Early-onset Stargardt
differential diagnosis, 28
fluorescein angiography, 26
fundus autofluorescence, 26
indication of, 28
multifocal electroretinography, 26
SD-OCT , 26
visual acuity, 28, 29
Electro-oculogram (EOG)
AFVD, 13
BPD, 15
NCMD, 54
VMD, 6
Electroretinogram (ERG)
CACD, 87
Malattia Leventinese (ML), 45
NCMD, 54
XLRS, 74
Ellipsoid zone (EZ)
atrophic lesions, 4
previtelliform stage, 2, 3
vitelliruptive lesions, 4, 8
Embryonic stem cells (ESCs), 110
Epiretinal membrane (ERM), 35

F
FIBULIN 3 (FBLN3), 47
Fluorescein angiography (FA)
CACD, 85, 86
CME, 34
early-onset stargardt, 26
intermediate-onset Stargardt, 27
Malattia Leventinese (ML), 45
VMD, 2–3
XLRS, 75
Full-field electroretinography (ffERG), 31
CACD, 87
CRD, 36
late-onset Stargardt, 27
XLRS, 77–78
Fundus autofluorescence (FAF)
Bull's-eye ring, 33–34
early-onset stargardt, 26
intermediate-onset Stargardt, 26
late-onset Stargardt, 27
Malattia Leventinese (ML), 42
multimodal imaging, 6
previtelliform lesion, 3
pseudohypopyon lesion, 4, 6
vitelliform stage, 2–4
VMD
multimodal imaging, 6
previtelliform lesion, 3
pseudohypopyon lesion, 4, 6
vitelliform stage, 2–4
XLRS, 73, 75
Fundus pulverulentus
autosomal-dominant inheritance pattern, 20
clinical findings, 20–21
differential diagnosis, 21
disease course, 21
PRPH2 gene mutation, 20

G
Generalized retinal dystrophies
BEM, 32–34
CME, 34
epiretinal membrane, 35
macular atrophy, 35
no macular abnormalities, 32
pigmentary changes, 32, 33

I
Inherited macular dystrophies
cellular therapy, 110–111
gene therapy
AAV, 103
achromatopsia, 106–107
BVMD, 106
choroideremia, 107
LCA, 103–104
replacing defective gene, 103
STGD1, 104–106
X-linked retinoschisis, 107
low vision rehabilitation, 101–102
neuroprotection, 107–108
nutritional supplements, patients, 102
optogenetics, 109–110
prevention and treatment, 102
retinal prosthesis, 108–109
sensory substitution devices, 111
vision impairment, 101
Intermediate-onset Stargardt
fluorescein angiography, 27
fundus autofluorescence, 26
indication of, 28
SD-OCT, 26
visual acuity, 28, 29

J
Juvenile macular dystrophy and hypotrichosis, 91–92, 95

K
Kearns-Sayre syndrome, 15

L
Late-onset retinal degeneration (L-ORD)
clinical characteristics, 92, 98
C1QTNF5 gene, 92
differential diagnosis, 99
ocular features of, 92, 96, 97
SD-OCT imaging, 92

Late-onset Stargardt, 27
differential diagnosis, 28
full-field electroretinography, 27
fundus autofluorescence, 27
indication of, 28
spectral-domain optical coherence tomography, 27
visual acuity, 28, 29
Leber congenital amaurosis (LCA), 103–104
L-ORD. S*ee* Late-onset retinal degeneration (L-ORD)

M
Macular dystrophy, retinal 1 *(MCDR1)*. S*ee* North Carolina macular dystrophy (NCMD)
Malattia Leventinese (ML)
animal model, 47
clinical features, 40–44
clinical management/treatment, 47–48
differential diagnosis, 48
*EFEMP*1 gene, 45–47
ERG, 45
FAF imaging, 42
fluorescein angiography (FA), 45
indocyanine green angiography (ICG) features, 45
SD-OCT, 42, 45
Maternally inherited diabetes and deafness (MIDD), 63
Mitochondrial encephalomyopathy, lactic acidosis, and stroke like episodes (MELAS) syndrome, 63
Mitochondrial retinal dystrophy (MRD), m.3243A>G mutation
chorioretinal (geographic) atrophy, 64, 65, 67
differential diagnosis, 68
discrete pigmentary abnormalities, 64–66
disease course, 68
hyperpigmented subretinal deposits, 64–66
MIDD/MELAS syndrome, 63
peripheral visual field, 64
prevalence of, 63
retinal changes, 64
Mizuo phenomenon, 74, 76
Multifocal electroretinography, 26

N
Night blindness, 17, 32, 60
North Carolina macular dystrophy (NCMD)
clinical presentation, 53–54
CNVM, 54
copy number variation, 55
developmental macular disorders, 57
EOG and ERG, 54
histopathology, 54
PBCRA, 55
phenotypes mapping
MCDR3, 55, 56
MCDR4, 55
Sorsby syndrome, 56–57

O
Optical coherence tomography (OCT), 13
CACD, 87
CME, 33
SD-OCT (*see* Spectral-domain optical coherence tomography (SD-OCT))
Outer limiting membrane (OLM), 20

P
Pattern dystrophies (PD)
AFVD (*see* Adult-onset foveomacular vitelliform dystrophy (AFVD))
BPD (*see* Butterfly-shaped pigment dystrophy (BPD))
fundus pulverulentus
autosomal-dominant inheritance pattern, 20
clinical findings, 20–21
differential diagnosis, 21
disease course, 21
PRPH2 gene mutation, 20
multifocal pattern dystrophy simulating Stargardt disease/fundus flavimaculatus (*see* Pseudo-Stargardt pattern dystrophy)
reticular pattern dystrophy, 19–20
Peculiar foveomacular dystrophy. S*ee* Adult-onset foveomacular vitelliform dystrophy (AFVD)
Progressive bifocal chorioretinal atrophy (PBCRA), 55
Pseudo-Stargardt pattern dystrophy
clinical findings, 17–19
differential diagnosis, 19
disease course, 18, 19
PRPH2 gene, 17

R
Reticular pattern dystrophy, 19–20
Retinal guanylate cyclase-1 (RetGC1), 104
Retinal pigment epithelium (RPE)
AFVD, 12, 13
AMD, 111
atrophic lesions, 4
BPD patients, 15
CACD, 84, 85
C1QTNF5, 92
DCMD, 89
early-onset Stargardt, 26
fundus pulverulentus, 20
generalized retinal dystrophies, 32
late-onset Stargardt, 27
MCDR3, 55
MRD, 64
reticular pattern dystrophy, 20
VMD
atrophic lesions, 4
previtelliform stage, 2, 3
vitelliruptive lesions, 4, 8
Rod-derived cone viability factor (RdCVF), 108
R345W fibulin-3 function, 46–47

S
Sorsby fundus dystrophy (SFD)
clinical management, 61
CNVM, 59–61
differential diagnosis, 60
early drusen-like deposition, 59
night blindness, 60
TIMP3 gene, 60
Sorsby syndrome, 56–57
Spectral-domain optical coherence tomography (SD-OCT)
ABCA4 gene, 27
AFVD, 14
early-onset stargardt, 26
intermediate-onset stargardt, 26
late-onset Stargardt, 27
L-ORD, 92
Malattia Leventinese (ML), 42, 45
VMD patients
atrophic lesions, 4, 8
fibrotic lesion, 4, 6, 8
multimodal imaging, 6
previtelliform stage, 3, 4
pseudohypopyon stage, 3, 5, 6
vitelliform stage, 3, 4
vitelliruptive lesions, 7
XLRS, 73, 75
Sporadic AFVD, 12
Stargardt disease
ABCA4 gene, 25
clinical diagnosis, 25–26
early-onset (*see* Early-onset Stargardt)
inherited macular dystrophies, 104–106
intermediate-onset (*see* Intermediate-onset Stargardt)
late-onset (*see* Late-onset Stargardt)
peripheral vision, 25
photophobia, 25
prevalence, 25
retinal dystrophy, 25
symptoms, 25
treatment, 25

T
Tissue inhibitor of metalloproteinase-3 (*TIMP3* gene), 60

V
Visual-to-auditory sensory substitution device, 111
Vitelliform macular dystrophy (VMD)
bestrophinopathy, 9
choroidal neovascularization, 8
clinical description, 2
differential diagnosis, 8–9
electrophysiology, 6–7
FAF
multimodal imaging, 6
previtelliform lesion, 3
pseudohypopyon lesion, 4, 6
vitelliform stage, 2–4
fluorescein angiography, 2–3
genetics, 2
genotype-phenotype correlations, 8
heterogeneous and pleomorphic disease, 1
indocyanine green angiography, 3
inherited macular dystrophies, 106
SD-OCT
atrophic lesions, 4, 8
fibrotic lesion, 4, 6, 8
multimodal imaging, 6
previtelliform stage, 3, 4
pseudohypopyon stage, 3, 5, 6
vitelliform stage, 3, 4
vitelliruptive lesions, 7

X
X-linked retinoschisis (XLRS)
clinical management, 78–79
clinical manifestations of, 72
clinical presentation
colour vision, 72
female carriers, 74
fluorescein angiography, 75
foveal schisis, 72–74
fundus albipunctatus-like/crystalline appearance, 74, 77
fundus autofluorescence, 73, 75
initial presentation, 72
Mizuo phenomenon, 74, 76
peripheral schisis, 74
peripheral visual field test, 72
pigmented peripheral retinal scars, 74, 75
SD-OCT, 73, 75
spontaneous vitreous haemorrhage, 72
visual acuity, 72
differential diagnosis, 78
ffERG, 77–78
genetics and pathophysiology, 78
histopathology, 75